

https://dspace.org/

Investigating 2-hydroxypropyl--cyclodextrin (HPCD) as a novel therapeutic agent for breast cancer

Saha, Sourav Taru

2019
University of the Witwatersrand, Johannesburg
https://hdl.handle.net/10539/43921

Saha, Sourav Taru . (2019). Investigating 2-hydroxypropyl--cyclodextrin (HPCD) as a novel therapeutic agent for breast cancer [PhD thesis, University of the Witwatersrand, Johannesburg].WireDSpace.https://hdl.handle.net/10539/43921

Downloaded from a DSpace repository. https://dspace.org/



Investigating 2-hydroxypropyl-β-cyclodextrin (HPβCD) as a novel therapeutic agent for breast cancer

by

Sourav Taru Saha

1575707

Thesis

Submitted in fulfilment of the requirements for the degree

Philosophiae Doctor (PhD.)
in

Molecular and Cell Biology

in the Faculty of Science, University of the Witwatersrand, Johannesburg, South Africa

Supervisor: Professor Mandeep Kaur

June

2019

DECLARATION

I, Sourav Taru Saha (**1575707**), registered for the degree: Doctor of Philosophy (PhD.) by dissertation in the academic year 2016 at the University of the Witwatersrand, declare the following:

- I am aware that plagiarism (the use of someone else's work without their permission and/or without acknowledging the original source) is wrong.
- I confirm that the work submitted for assessment for the above degree is my own unaided work except where explicitly indicated otherwise and acknowledged.
- I have not submitted this work before for any other degree or examination at this or any other University.
- The information used in the thesis HAS NOT been obtained by me while employed by, or working under the aegis of, any person or organisation other than the University.
- I have followed the required conventions in referencing the thoughts and ideas of others.
- I understand that the University of the Witwatersrand may take disciplinary action against me if there is a belief that this is not my own unaided work or that I have failed to acknowledge the source of the ideas or words in my writing.
- The entire work was carried out solely by me.

NRF Declaration

The financial assistance of the National Research Foundation (NRF) towards this research is hereby acknowledged (NRF-TWAS). UID No. 99742.

Opinions expressed and conclusions arrived at, are those of the author and are not necessarily to be contributed to the NRF.

Signature: Sourav Taru Saha Date: 20.06.19

ACKNOWLEDGEMENTS

This research would not have been possible without the support and assistance of the following people and institutions:

The deepest of thanks to my supervisor, Professor Mandeep Kaur, for her continuous guidance, motivation and mentorship of this project as well as all the encouragement, advice and motivation throughout the course of my PhD.

My heartfelt thanks to all members of Gate House 527 for their assistance and advice.

I would also like to acknowledge the University of the Witwatersrand (Postgraduate Merit Award) and the National Research Foundation (NRF) for financial assistance during my study period.

Finally I would like to thank my close friends and family who have supported and encouraged me to finish my research.

.

LIST OF ABBREVIATIONS

5-FU	5- Fluorouracil
27 HC	27-hydroxycholesterol
7-AAD	7-Aminoactinomycin D
ABCA1	ATP-binding cassette transporter
ACAT1	Acetyl-coenzyme A acetyltransferase 1
ADP	Adenosine 5'-diphosphate protein
AIs	Aromatase inhibitors
AIF	Apoptosis inducing factor
AP	Acetyl Plumbagin
APS	Ammonium persulfate
ALT	Alanine aminotransferase
AMP	5' adenosine monophosphate-activated protein
AMPK	AMP-activated protein kinase
AST	Aspartate aminotransferase
ATCC	American Type Cell Culture Collection
BC	Breast cancer
BCA	Bicinchoninic acid
Bcl-X_L	B-cell lymphoma-extra-large
BER	Base excision repair
BSA	Bovine serum albumin
CANSA	The Cancer Association of South Africa
CaMKKβ	Calmodulin-subordinate protein kinase-beta
Cav-1	Caveolin-1
CEs	Cholesterol esters
CETP	Cholesteryl ester transfer protein
CO_2	Carbon dioxide
CRE	Cholesterol response element
CyD	Cyclodextrin

Cu^{2+}	Copper cation
DC FBS	Dextran charcoal stripped foetal bovine serum
DEN	Dentatin
dH_2O	Distilled water
DMEM	Dulbecco's Modified Eagle's Medium
DMSO	Dimethyl sulfoxide
DNA	Deoxyribonucleic acid
DCF	2', 7' –dichlorofluorescein
DCFDA	2', 7' –dichlorofluorescin diacetate
DR	Death receptor
E_2	Estradiol
ECACC	The European Collection of Authenticated Cell Cultures
EDTA	Ethylenediaminetetraacetic acid
EE	Environmental enrichment
EGFR	Epidermal growth factor receptor
EMA	European Medicines Agency
EMS	Effects on metabolic syndrome
EMT	Epithelial-mesenchymal transition
ER	Estrogen receptor
ER+	Estrogen receptor- positive
TNBC	Estrogen receptor- negative
ERK	Extracellular signal-regulated kinases
FAS	Fatty acid synthase
FBS	Foetal bovine serum
FDA	US Food and Drug Administration
Fig.	Figure
FITC	Fluorescein
GPI	Glycosylphosphatidylinisotol
GPCR	G-protein coupled receptors
GPER	G protein-coupled estrogen receptor 1

GPR	G protein-coupled receptor
GLOBOCAN	Global cancer statistics
GUV	Giant unilamellar vesicles
H_2O_2	Hydrogen peroxide
HeLa	Henrietta Lacks cervical cancer cell line
HPαCD	Hydroxypropyl-alpha CyD
HPβCD	2-hydroxypropyl-β-cyclodextrin
HCl	Hydrochloric acid
HDL	High-density lipoprotein
HER2	Human epidermal growth factor receptor 2
HH	Hedgehog
HMG-CoA	Hydroxy-methyl glutaryl-coenzyme A
HMGCR	Hydroxymethylglutaryl coenzyme A reductase
H&E	Hematoxylin and eosin
HEK-293	Human embryonic kidney
HGT	Human Gastric Cancer
HRP	Horseradish peroxidase
hrs	Hours
IGF1-R	Insulin-like growth factor receptor
IP	Intraperitoneally
JAK-STAT	Janus kinases - Signal Transducer and Activator of Transcription proteins
JC-1	5, 5′, 6, 6′-tetrachloro-1, 1′, 3, 3′-tetraethylbenzimi-dazolylcarbocyanine iodide

KB Cells	KERATIN-forming tumour *cell* line *HeLa*
KPO_4	Potassium phosphate buffer
LCAT	Lecithin-cholesterol acyltransferase
LDL	Low-density lipoprotein
LDLR	Low-density lipoprotein receptor
LKB1	Liver kinase B1
LNCaP	Androgen-sensitive human prostate adenocarcinoma
LXR	Liver X receptor
MAPK	Mitogen-activated protein kinase
MβCD	Methyl-β-cyclodextrin
MαCD	2, 6-di-*O*-methyl-α cyclodextrin
MCF7	Michigan Cancer Foundation-7
MDR	Multidrug resistance
MHRA	UK Medicines & Healthcare products Regulatory Agency
MMR	Mismatch repair
MRC-5	Medical Research Council cell strain 5
miRNA	MircoRNA
min	Minutes
MOMP	Mitochondrial outer membrane potential
mTOR	Mammalian target of rapamycin
mTORC1	Mammalian target of rapamycin complex 1
MTT	3-(4, 5-Dimethylthiazol-z-yl)-2,5diphenyltetrazolium bromide
MUC1	Mucin-1
NaCl	Sodium chloride
NAD+	Nicotinamide adenine dinucleotide
NER	Nucleotide excision repair
NIH	National Institutes of Health
NP-40	Nonidet P-40

NPC	Niemann Pick type C
OD	Optical density
PARP	Poly ADP ribose polymerase
PBS	Phosphate buffered saline
PC	Phosphatidylcholine
PCR	Polymerase chain reaction
PC12	Pheochromocytoma of the rat adrenal medulla
PCSK9	Proprotein convertase subtilisin/kextin type- 9
P-gp	P-glycoprotein
PI3K	Phosphoinositide 3-kinase
PUFA	Polyunsaturated fatty acids
PL	Plumbagin
PR	Progesterone receptor
P-S	Penicillin-streptomycin
PS	Phosphatidylserine
PTCH1	Protein patched homolog 1
PVDF	Polyvinylidene fluoride
RCT	Reverse cholesterol transport
Refs.	References
RIPA	Radio immunoprecipitation assay
RNA	Ribonucleic acid
ROS	Reactive oxygen species
RT	Room temperature
RXR	Retinoid X receptor
SCAP	SREBP cleavage activating protein
S.D	Standard deviation
SDS	Sodium dodecyl sulfate
SDS-PAGE	Sodium dodecyl sulfate polyacrylamide gel electrophoresis
SERMs	Selective estrogen receptor response modulators
SHH	Sonic Hedgehog

SMO	Smoothened
SRE	Sterol regulatory element
SOD	Superoxide dismutases
SR-B1	Scavenger receptor class B type 1
SREBF1	Sterol Regulatory Element Binding Transcription Factor 1
SREBF2	Sterol Regulatory Element Binding Transcription Factor 2
SREBP	Sterol regulatory element-binding protein
STR	Short Tandem Repeat
Tam	Tamoxifen
TBS	Tris-buffered saline
TBST	Tris-buffered saline with Tween-20
TEMED	Tetramethylethylenediamine
TGF-β	Transforming growth factor beta
TNBC	Triple Negative Breast Cancer
TNF	Tumour necrosis factor
TRND	Therapeutics for Rare and Neglected Diseases
V	Volts
VLDL	Very low-density lipoproteins
WHO	World health organization
WT	Wild-type

LIST OF SYMBOLS

β	Beta
©	Copyright
°C	Degrees Celsius
g	Grams
kDa	Kilodaltons
µ	Micro
µg	Micrograms
µL	Microlitres
µM	Micromolar
µm	Micrometer
mg	Milligrams
mL	Millilitres
mm	Millimetres
mol/L	Moles per litre
nm	Nanometres
nM	Nanomolar
pg	Picograms
®	Registered
™	Trademark
U/mL	Unit per millilitre
x *g*	Centrifugal force

LIST OF FIGURES

Fig. 1: GLOBOCAN 2018 statistics:.....2
Fig. 2: BC distribution based on receptors:.....4
Fig. 3: Shows that apoptosis works through two main pathways: 10
Fig. 4: Shows the chemical structure of cholesterol:.....11
Fig 5: Cholesterol synthesis via the Mevalonate pathway, intracellular and extracellular regulation of cholesterol:. 12
Fig. 6: The mevalonate pathway: 14
Fig. 7: Intracellular and Extracellular transportation of cholesterol.....16
Fig. 8: Cholesterol is involved in stimulation of various BC signalling pathways. 21
Fig. 9: Mode of action for statins:. 25
Fig. 10: Proposed Mechanism of β CyD induced cholesterol-depletion:.....28
Fig 11: Proposed mode of action of HPβCD:.....29
Fig. 12: The mode of action of the Cell-APOPercentage dye.....40
Fig. 13: The mechanism of action of the JC-1 dye.....41
Fig. 14: The mechanism of ROS. 43
Fig. 15: The mechanism of Caspase-3/7 assay. 44
Fig. 16: Principle of cholesterol quantification assay. 46
Fig. 17: A representative cholesterol standard curve. 48
Fig. 18: A representative BSA protein standard curve.....51
Fig. 19: Groups of mice used in the study.....54
Fig. 20: Graph comparing the percentage growth inhibition of MCF7 cells at selected concentrations of HPβCD 61
Fig. 21: Graph comparing the percentage growth inhibition of MDA-MB-231 cells at selected concentrations of HPβCD 62
Fig. 22: Graph comparing the percentage growth inhibition of MRC-5 cells at selected concentrations of HPβCD 63
Fig. 23: Graph comparing the percentage growth inhibition of HEK-293 cells at selected concentrations of HPβCD 64
Fig. 24: Graph comparing the percentage of apoptosis in MCF7 cells at selected concentrations of HPβCD 66

Fig. 25: Light microscope images showing the amount of apoptosis in MCF7 cells at selected concentrations of HPβCD 67
Fig. 26: Graph comparing the percentage of apoptosis in MDA-MB-231 cells at selected concentrations HPβCD 68
Fig. 27: Light microscope images showing the amount of apoptosis in MDA-MB-231cells at selected concentrations of HPβCD. 69
Fig. 28: Graph comparing the percentage of apoptosis in MRC-5 cells at selected concentrations of HPβCD 70
Fig. 29: Light microscope images showing the amount of apoptosis in MRC-5 cells at selected concentrations of HPβCD 71
Fig. 30: Graph comparing the percentage of apoptosis in HEK-293 cells at selected concentrations of HPβCD 72
Fig. 31: Light microscope images showing the amount of apoptosis in HEK-293 cells at selected concentrations of HPβCD 73
Fig. 32: MOMP plots for MCF7 cells. 75
Fig. 33: MOMP plots for MDA-MB-231 cells. 76
Fig. 34: MOMP plots for MRC-5 cells. 77
Fig. 35: ROS generation in MCF7 cells. 79
Fig. 36: ROS generation in MDA-MB-231 cells. 80
Fig. 37: ROS generation in MRC-5 cells. 81
Fig. 38: Caspase-3/7 profile in MCF cells.....83
Fig. 39: Caspase-3/7 profile in MDA-MB-231 cells.....84
Fig. 40: Caspase-3/7 profile in HEK-293 cells. 85
Fig. 41: Graph comparing the total, free and esterified cholesterol levels in MCF7 cells at selected concentrations of HPβCD 87
Fig. 42: Graph comparing the total, free and esterified cholesterol levels in MDA-MB-231 cells at selected concentrations of HPβCD. 88
Fig. 43: Graph comparing the total, free and esterified cholesterol levels in MRC-5 cells at selected concentrations of HPβCD 89
Fig. 44: Pictures taken on fluorescent microscope (The FLoid® cell imaging station) after Filipin staining, comparing the overall cholesterol levels in MCF7 cells. 91
Fig. 45: Pictures taken on fluorescent microscope (The FLoid® cell imaging station) after Filipin staining, comparing the overall cholesterol levels in MDA-MB-231 cells.....92

Fig. 46: Graph comparing fold change in depletion of fluorescence intensity (FU) as compared to untreated cells. 93
Fig. 47: Western blot assay to detect protein expression of SREBP-1 in MCF7 cells.....95
Fig. 48: Western blot assay to detect protein expression of SREBP-1 in MDA-MB-231 cells. 95
Fig. 49: Western blot assay to detect protein expression of SREBP-1 in MRC-5 cells.....95
Fig. 50: Mice images post euthanization showing tumour sizes in untreated group at a late stage, injected with MDA-MB-231 cells. 97
Fig. 51: Mice images post euthanization showing tumour sizes in treated group at a late stage, injected with MDA-MB-231 cells and treated with HPβCD (3000 mg/kg b.w.) for 10 doses.....97
Fig. 52: Mice images post euthanization showing tumour sizes in treated group at an intermediate stage, injected with MDA-MB-231 cells and treated with HPβCD (3000 mg/kg b.w.) for 10 doses. 98
Fig. 53: Mice images showing tumour sizes in untreated group at an early stage, injected with MDA-MB-231 cells. 99
Fig. 54: Mice images showing tumour sizes in treated group at an early stage, injected with MDA-MB-231 cells and treated with HPβCD (3000 mg/kg b.w.) for 10 doses. 101
Fig. 55: All three healed mice (No. 12, 13 and 14) tested for relapse of TNBC tumour for a period of 4 weeks. 102
Fig. 56: Weight change in all 14 mice across the study. 103
Fig. 57: Graphical representation of ALT/AST levels in all 14 mice across the study.....104

LIST OF TABLES

Table 1: List of anti-cancer drugs complexed with CyDs for better results. **Error! Bookmark not defined.**

Table 2: List of diseases till date responsive to direct HPβCD treatment without complexation. ..... **Error! Bookmark not defined.**

Table 3: Cell lines used for the study. 35

Table 4: Components for Reagent A per well 47

Table 5: Lysis buffer components. ..... **Error! Bookmark not defined.**

Table 6: SDS-PAGE gel (10%, 1 mm) components. 52

Table 7: SDS-PAGE buffer components. ..... **Error! Bookmark not defined.**

Table 8: Shows IC_{50} values for MCF7, MDA-MB-231, MRC-5 and HEK-293 cells. 64

LIST OF OUTPUTS

Provisional patent has been filed by WITS Enterprise entitled

"HPβCD for use in the treatment of breast cancer" **(P1194P)** on 31st January 2019.

Publication- "Targeting cellular cholesterol for anticancer therapy"
(Authors: Liang Gu, # Sourav Taru Saha, # Jodie Thomas and Mandeep Kaur*, # joint first author) manuscript accepted in Febs Journal. I.F. - 4.53

Oral presentation
Title of Conference: 9th Cross Faculty Graduate Symposium, 2018
Title of Contribution: "KS-01: The answer to breast cancer???"
All Authors in Order Appearing on Output: Sourav Taru Saha and Mandeep Kaur*
City/Country: Johannesburg, South Africa

Oral presentation
Title of Conference: Title of Conference: 18th International Congress of Endocrinology, 53rd SEMDSA Congress, 2018.
Title of Contribution: "KS-01: A novel therapeutic strategy in treating breast cancer."
All Authors in Order Appearing on Output: Sourav Taru Saha and Mandeep Kaur*
City/Country: Cape Town, South Africa

Oral presentation
Title of Conference: 8th Cross Faculty Graduate Symposium, 2017
Title of Contribution: "KS-01: A novel therapeutic approach in treating breast cancer".
All Authors in Order Appearing on Output: Sourav Taru Saha and Mandeep Kaur*
City/Country: Johannesburg, South Africa

Poster presentation
Title of Conference: Molecular Biology Research Thrust (MBRT), 2018
Title of Contribution: "A Comprehensive study of KS-01 both *in vitro* and *in vivo* as a potential anti-breast cancer agent".
All Authors in Order Appearing on Output: Sourav Taru Saha and Mandeep Kaur*
City/Country: Johannesburg, South Africa

Poster presentation
Title of Conference: Molecular Biology Research Thrust (MBRT), 2017
Title of Contribution: "Investigating the apoptosis inducing potential of KS-01 *in vitro* in breast cancer cell lines".
All Authors in Order Appearing on Output: Sourav Taru Saha and Mandeep Kaur*
City/Country: Johannesburg, South Africa

TABLE OF CONTENTS

1. ABSTRACT 1

2. INTRODUCTION 2

2.1 Epidemiology and prevalence of Breast cancer (BC) 2

2.2 Hormones involved in BC and classification 3

2.3 Treatment options for BC 5

2.4 Biology behind BC 6

2.5 Apoptosis and Cancer 8

2.6 Cholesterol and cancer 10

2.6.1 Cellular cholesterol biosynthesis 13

2.6.2 Cellular control of cholesterol homeostasis 15

2.6.3 Cellular regulation of cholesterol content 19

2.7 Ceasing cholesterol synthesis vs depletion of excess cholesterol 23

2.7.1 Cholesterol-synthesis blocking as anti-cancer therapy 24

2.7.2 Cholesterol-depletors as anti-cancer agents 26

3. AIM and OBJECTIVES 33

3.1 Aim 33

3.2 Objectives 33

4. WORKFLOW 34

5. MATERIALS AND METHODS 35

5.1 CELL CULTURING 35

5.1.1 MCF7 cell line 35

5.1.2 MDA-MB-231 cell line 36

5.1.3 MRC-5 cell line 36

5.1.4 HEK-293 cell line 36

5.2 SUB-CULTURING OF CELLS 36

5.2.1 MCF7, MDA-MB-231, MRC-5 and HEK-293 cell lines....36
5.3 CELL STOCKS....37
5.3.1 Revival of stocks....37
5.4 CELL COUNTING WITH TRYPAN BLUE EXCLUSION ASSAY....37
5.5 PLATING OF CELLS....38
5.5.1 MCF7, MDA-MB-231, MRC-5 and HEK-293 cell lines....38
5.6 *IN VITRO* AND *IN VIVO* TREATMENTS....38
5.6.1 MCF7, MDA-MB-231, MRC-5 and HEK-293 cell lines....38
5.7 GROWTH INHIBITION ASSAYS....39
5.7.1 MTT (3-(4, 5-dimethylthiazol-2-yl)-2, 5-diphenyltetrazolium bromide) ASSAY....39
5.7.2 Cell-APOPercentage APOPTOSIS ASSAY....39
5.7.3. MITOCHONDRIAL OUTER MEMBRANE POTENTIAL (MOMP) ASSAY....41
5.7.4. REACTIVE OXYGEN SPECIES (ROS) ASSAY....42
5.7.5 CASPASE-3/7 ASSAY....44
5.8 CHOLESTEROL ASSAYS....45
5.8.1 CHOLESTEROL QUANTIFICATION ASSAY....45
5.8.2 CHOLESTEROL STAINING WITH FILIPIN....48
5.8.3 WESTERN BLOTTING and SDS-PAGE....49
5.9 XENOGRAFT STUDY....53
5.9.1 Inoculation....55
5.9.2 Anaesthetization....55
5.9.3 Measurements and observations made on animals....55
5.9.4 Terminal procedures....56
5.9.5 Alanine transaminase/aspartate transaminase (ALT/AST) tests....56
5.9.6 Surgical procedures with recovery....56
5.9.7 Body fluid sampling....57
5.9.8 Biochemistry....57

5.9.10 Animal welfare and reduction of suffering, if any 57
5.9.11 Housing conditions 58
5.9.12 Transport of animals 59
5.10 Statistical analysis 59
6. RESULTS 60
6.1 GROWTH INHIBITION ASSAYS 60
6.1.1 MTT ASSAY 60
6.1.2 Cell-APOPercentage APOPTOSIS ASSAY 65
6.1.3 MITOCHONDRIAL OUTER MEMBRANE POTENTIAL ASSAY (MOMP) 74
6.1.4 ROS ASSAY (Reactive Oxygen Species) 78
6.1.5 CASPASE-3/7 ASSAY 82
6.2 CHOLESTEROL ASSAYS 86
6.2.1 CHOLESTEROL QUANTIFICATION ASSAY 86
6.2.2 CHOLESTEROL STAINING 90
6.2.3 WESTERN BLOTTING 94
6.3 *IN VIVO* STUDIES (MICE XENOGRAFTS) 96
7. DISCUSSION 105
8. CONCLUSIONS 116
9. FUTURE STUDIES 116
10. TROUBLESHOOTING 118
11. REFERENCES 119

1. ABSTRACT

Cancer cells have an increased need for cholesterol, which is required for cell membrane integrity. Cholesterol accumulation has been described in various malignancies including breast cancer. Cholesterol has also been known to be the precursor of estrogen and vitamin D, both of which play a key role in the histology of breast cancer. Elevated cholesterol levels have been linked to breast cancer therefore depleting cholesterol levels in cancer cells can be a viable strategy for treatment. 2-hydroxypropyl-β-cyclodextrin (HPβCD) is a cholesterol depleting compound which is a cyclic amylose oligomer composed of glucose units. It solubilizes cholesterol and is proven to be toxicologically benign in humans. This led us to hypothesise that it might deplete cholesterol from cancer cells and may prove to be a clinically useful compound. Our work provides experimental evidences to support this hypothesis. We identified the potency of HPβCD *in vitro* against two breast cancer cell lines: MCF7 (Estrogen positive, ER+), MDA-MB-231 [Triple negative breast cancer (TNBC)], and compared the results against two normal cell lines: MRC-5 (Normal Human Lung Fibroblasts) and HEK-293 (Human embryonic kidney) using cytotoxic, apoptosis and cholesterol based assays. HPβCD treatment reduced intracellular cholesterol resulting in significant breast cancer cell growth inhibition through apoptosis. The results hold true for both ER+ and TNBC. We have also tested HPβCD *in vivo* in MF-1 mice xenograft model and obtained 73.9%, 94% and 100% reduction in tumour size for late, intermediate and early stage TNBC. These data suggest that HPβCD can prevent cholesterol accumulation in breast cancer cells and is a promising anti-cancer agent.

2. INTRODUCTION

2.1 Epidemiology and prevalence of Breast cancer (BC)

Breast cancer (BC) is one of the most commonly occurring malignancies in women around the world. As per the world health organization's (WHO) latest report in 2018, BC impacts almost 2.1 million women each year and also is the leading cause for the greatest number of cancer related deaths in women. In 2018 alone, 627,000 women died from BC **(Fig. 1)** which is approximately 15% of all cancer related deaths among women. Africa and Asia have the least number of BC survivors as compared to Northern America and Europe (Ferlay, Soerjomataram et al. 2015). GLOBOCAN 2018 estimates that almost half of all cancer related deaths occurs in Asia, mostly because almost 60% of the global population lives there. Europe had about 23.4% of the total number of global cases and about 20.3% of cancer related mortality, but that constitutes to only 9% of the world's population. The United States accounts for 21% of cancer incidence and 14.4% of related mortality. Cancer deaths in Asia and Africa are much higher than the incidence because of overall distribution of the different cancer types and elevated fatality rates (https://www.medscape.org/viewarticle/902643).

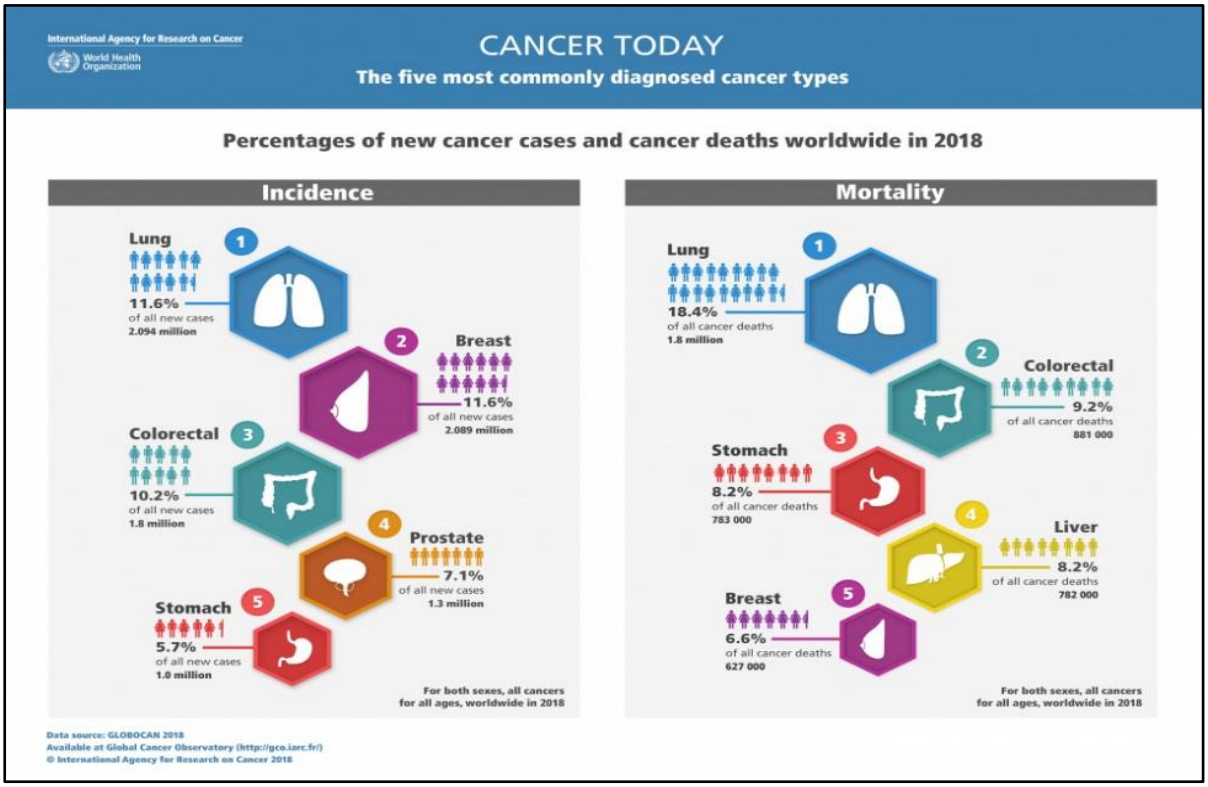


Fig. 1: GLOBOCAN 2018 statistics: *BC is positioned 2nd in terms of cancer incidence and 5th in mortality rates with almost 2.089 million new cases [Image adopted from: [https://www.uicc.org/new-global-cancerdata-globocan-2018, Accessed 12.01.19].*

With every passing year there seems to be a growing incidence of BC in Africa (Adeloye, Sowunmi et al. 2018). South Africa is positioned 50th on the World Growth Research Asset's rundown of nations with the most prevalent BC predominance rates. Lifetime dangers of having BC growth vary from one in 81 amongst black African women to a one in 13 among white women (Vorobiof, Sitas et al. 2001). As per CANSA's (The Cancer Association of South Africa) list distributed on 27th June 2014 in light of South African Therapeutic Exploration Committee, BC Positions 4th in all cancer related deaths and 2nd in women (http://www.cansa.org.za). A report published by the medical journal Lancet predicts that South Africa might see an 85% increase in the number of cancer cases by the year 2030 (Morhason-Bello, Odedina et al. 2013). Therefore, it is quite evident that there is a pertinent need to research and enhance the current medications in cancer.

2.2 Hormones involved in BC and classification

Steroid hormones have been observed to be a noteworthy determinant of BC. The functions of steroid hormones are mediated by their individual receptors, which function as transcription factors. Among the steroid receptors, estrogen receptor (ER) and the progesterone receptor (PR) are of exceptional interest in light of the fact that their protein levels are hoisted in malignant and premalignant breast tumour as compared to normal tissue (Lange and Yee 2008). BC's with ER's are known as estrogen positive (or ER+), while those containing PR's are referred to as PR-positive (or PR+). Other types are human epidermal growth factor receptor 2 (HER2 +), Triple - (TNBC) and Triple + BC (http://www.breastcancer.org).

Around 70-80 percent of BC's are ER+ and are most frequent in women undergoing menopause. ER+ BC's are frequently treated with a mix of drugs, some of which block the effects of estrogen. Estrogen drives the development of ER+ breast tumours by its capacity to promote both multiplication and BC cells' survival (Stanculescu, Bembinster et al. 2010). HER2+ cancers on the other hand, have increased numbers of HER2 growth-promoting receptors (Hart, Migliaccio et al. 2015). They're treated with therapies that target HER2. As indicated by the American Cancer Society, around 15 to 20 percent of BC's are HER2+ (http://www.cancer.org). TNBC is described by tumours that do not express ER, PR or HER2 receptors and these cancers are non-responsive to endocrine therapy. The potential for metastasis in TNBC is quite similar to that of other BC's but these tumours have shorter median times for death and relapse (Hudis and Gianni 2011). Around 10 to 20 percent of BC's are TNBC and are typically treated with chemotherapy drugs, radiation, surgery and other drugs.

A pie chart showing BC distribution based on receptors is shown in **Fig. 2**.Yet another type of BC is Triple+, they are cancers that are HER2+ and ER/PR+. They can be treated with medications that block estrogen and also HER2 targeted therapies.

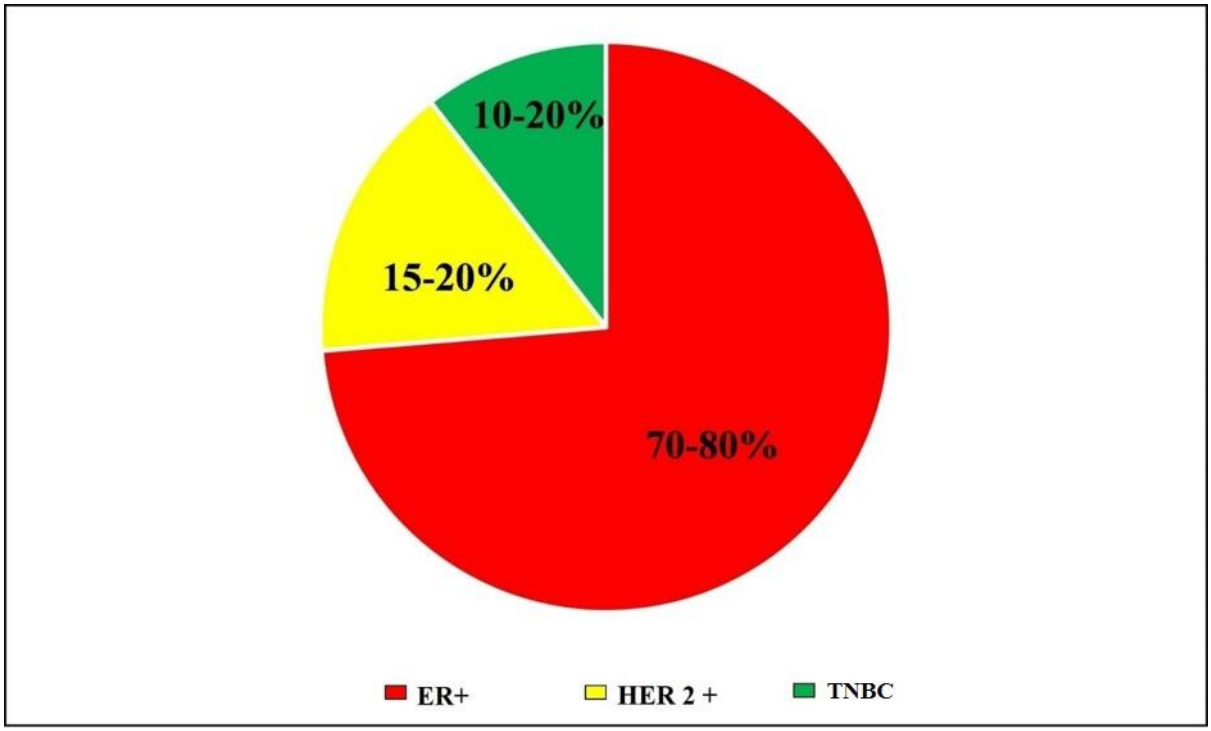


Fig. 2: BC distribution based on receptors: *Almost 70-80% cases are ER+, 15-20% HER2+ and 10-20% TNBC.*

The exact mechanisms whereby estrogen impacts BC malignancy is yet to be comprehensively understood. The most broadly acknowledged hypothesis, backed with experimental evidences (Hewitt and Korach 2000; Yue, Wang et al. 2010) holds that estrogen, acting through ERα, initiates cellular replication and starts transformations that occur as a component of errors in DNA replication. This effect of estrogen then abets the mutated cells, which keeps on accumulating until malignancy occurs. The development of BC involves the overall exposure to estrogen as well as several other genetic factors. ER was first discovered in the 1950s by Dr. Elwood V. Jensen (Jensen and Jordan 2003; O'Malley and Khan 2013). To date, three types of ER have been identified- ERα, ERβ, and GPR-30 (G protein-coupled *receptor* 30) (Carmeci, Thompson et al. 1997; Filardo, Quinn et al. 2002; Hewitt and Korach 2002; Filardo and Thomas 2005). ERα is encoded by the gene ESR1 located on chromosome 6, ERβ on the other hand is encoded by ESR2 located on chromosome 14 and GPR-30 is encoded by the GPER gene (G protein-coupled estrogen receptor 1) located on chromosome 7. While ERα and ERβ are hormone receptors, GPR-30 isn't. It is rather a G-

protein coupled receptor that has been appeared to interact with estrogen (Prossnitz, Arterburn et al. 2008; Prossnitz, Oprea et al. 2008).

Despite the fact that both ERα and ERβ are expressed in the breast tissue whilst interacting to estrogen with comparable affinities (Speirs, Skliris et al. 2002), studies have shown that just ERα is vital for normal breast development (Platet, Cathiard et al. 2004; Mehta, Hawthorne et al. 2014) driving researchers to scrutinize the capacity of ERβ in a typical breast tissue. Numerous examinations have likewise detailed that expression of ERβ subdues ERα's expression and capacity (Saji, Jensen et al. 2000; Stope, Popp et al. 2010). Unlike ERα, ERβ exists as different isoforms-ERβ1, ERβ1 "short structure", ERβ2/cx, ERβ3, ERβ4, and ERβ5 (Ogawa, Inoue et al. 1998; Omoto, Eguchi et al. 2003; Poola, Abraham et al. 2005; Leung, Mak et al. 2006). Most are because of the splicing of exons 7 and 8 (Moore, McKee et al. 1998; Skliris, Leygue et al. 2006). Among all the isoforms, just ERβ1 contains the ligand-binding domain (Leygue and Murphy 2013). To date, quite a bit of what we think about the connection among ER and BC malignancy focuses essentially on one specific receptor-ERα. It was thus established that, it is either the presence or absence of ERα that decides if a patient's malignancy can be classified as either ER+ or negative, respectively. ERα-negative BC may express other hormone receptors for example, PR and even ERβ, yet they are regularly non-receptive to estrogen. Of all BC subtypes, ERα-positive BC is the most pervasive, representing roughly 75% of BC malignancies in women (http://www.cancer.org). Reports have demonstrated that patients with ERα-positive BC have superior prognosis in light of the fact that these tumours will in general have less aggressive phenotypes. Patients with metastatic tumours having elevated ERα levels had essentially better survival results in contrast with patients with ERα-negative tumours (Ali and Coombes 2000) and this is in all probability because of the way that most patients with ERα-positive tumours additionally had an increased probability of reacting to the existing endocrine treatments (Ali and Coombes 2000).

2.3 Treatment options for BC

Five different stages of BC has been classified: a) Stage 0- is described as non-invasive tumours, the cancer cells do not break out of the site of origin b) Stage I- describes invasive BC, the cancer cells break out and invade the normal surrounding breast tissue c) Stage II- is described as tumour size being 2-5 cms and could have spread to the axillary lymph nodes d) Stage III- is described as the cancer cells migrating to 4 -9 axillary lymph nodes and the tumour is larger than 5 cms and e) Stage IV- describes invasive BC that has spread beyond the breast

and nearby lymph nodes and also to distant organs of the body, usually referred to as "metastatic"(Devitt 1967). Several treatment options are currently available for the treatment of these stages in BC. Surgery and chemotherapy are generally utilised if detected at an early stage. However, chemotherapy medications (doxorubicin, paclitaxel, 5-fluorouracil, Cyclophosphamide and Carboplatin) have several shortcomings like affecting cells in the bone marrow, hair follicles, mouth, digestive tract and reproductive system. It can likewise bring down the white blood cell count which results in neutropenia. Another strategy is the hormone treatment which includes utilization of Selective Estrogen Receptor Modulator (SERM) drugs. They hinder the attachment of estrogen to ER in cancer cells, thereby slowing the growth of tumour and eventually killing them. SERMs include tamoxifen (a gold standard drug), raloxifene and toremifene (Maughan, Lutterbie et al. 2010). However, they too have their own side effects like development of uterine cancer, cataracts, blood clots and heart attack (http://www.breastcancer.org). The hormone treatment is viable in both pre- and post-menopausal ER+ BC but despite enhanced survival, numerous patients relapse, especially at later times. Moreover, after relapse the disease is not curable even with other available therapies (aromatase inhibitors) and numerous patients die (Hess, Pusztai et al. 2003). For HER2+ BC, HER2 targeted therapy is generally used (Herceptin, Tykerb) (Dent, Oyan et al. 2013). However, resistance to all these aforesaid drugs still hinders the treatment of cancer patients (Perl and Carroll 2011; O'hare, Zabriskie et al. 2012). Therefore, alternative therapeutic approaches need to be investigated for successful cancer treatment.

2.4 Biology behind BC

Cancer is a progression of pathological changes characterized by deregulation of the cell cycle thus bringing about uncontrolled multiplication of cells mostly leading to metastasis (Teicher, Linehan et al. 2012) with most common sites being the lobular cells or the conduits. BC is a malignant (cancerous) development that starts in the tissues of the breast. The tumour is carcinogenic if the cells can intrude surrounding tissues or metastasize to distant areas of the body. Less frequently, BC can start in the stromal tissues, which incorporate the connective tissues of the breast (http://www.breastcancer.org). It has been established that BC emerges through genetic and epigenetic changes in cancerous genes (Campoy, Laurito et al. 2016). It has been suggested that cancer phenotype is portrayed by a couple of natural abilities gained amid a multistep procedure of carcinogenesis, i.e. supported proliferative signalling, evasive measures from growth suppressors, resistance to cell death, enhanced angiogenesis and initiation of intrusion and metastasis (Hanahan and Weinberg 2000). Other authors have linked

cancer development with “instability of the genome and mutation” and “tumour-advancing inflammation” (Dai, Xiang et al. 2016). Moreover, both receptors (ER and PR) have been proven to be significant prognostic variables in the clinical administration of the disease (Cui and Rohan 2006). Thus, inhibition of ER has become one of the major strategies for the aversion and treatment of BC (Arpino, Weiss et al. 2005). The ERs are ligand-dependent transcription factors which mediate articulation of target genes through direct or indirect binding of DNA or to the other transcription factors respectively (Bjornstrom and Sjoberg 2005). In BC, the genes and transcriptional mechanisms for ER mediated cell multiplication have been explicitly depicted (Doisneau-Sixou, Sergio et al. 2003), but the pro-survival systems in the breast are less clear. While ERs play a crucial part in the maintenance of mitochondrial membrane integrity like B-cell lymphoma-extra-large (Bcl-xL) and Bcl-2 (Gompel, Somaï et al. 2000). Profiling the gene expression has uncovered a more extensive scope for cell survival targets that are primarily dependent on ERs, including anti-apoptotic and pro-apoptotic factors (Frasor, Danes et al. 2003). Cancer occurs when the qualities of normal cells transform. Each human cell have about 35,000 genes. Transformation in a single gene does not cause malignant growth; rather, it happens when changes occur in key genes that are sorted into three groups, i.e., 1) tumour suppressor genes 2) DNA repair genes 3) proto-oncogenes. Development and multiplication of the cells are controlled through the cell cycle. The set of genes controlling the cell cycle are mentioned below:

a) *Tumour suppressor genes*

p53 is the most extensively researched tumour suppressor gene and the most well-known genetic mutations are found in BC cells (Ingvarsson 1999). If damaged, with impaired function, cells with the damaged DNA will proceed to multiply and will create progressively mutated cells (Ingvarsson 1999; Mirmalek, Hajilou et al. 2014). The p53 also has a role in controlling the cell cycle. If the cell can't fix its DNA damage, p53 gives the suicide or apoptosis signal to abrogate further passage of damaged cells. p53 occurs in 1% of sporadic BC cases. Genetic BC malignancy incorporate just 5– 10% of cases and it doesn't generally leads to cancer (Gralow 2006). In 1994, a research lead to the discovery of BRCA1 gene (Miki, Swensen et al. 1994), and later in the year another gene named BRCA2 was discovered (Wooster, Neuhausen et al. 1994), which was linked to BC. 40% and 30% of all the BC cases have mutations in BRCA1 and BRCA2 respectively.

b) DNA repair genes

Two different types of DNA repair machineries exist. The first one essentially repairs DNA damage occurring from UV light, ionizing rays, DNA damage and oxidative stress. The base excision repair (BER) pathway, the nucleotide excision repair (NER) pathway and the direct reversal of DNA damage comes into play for this type of DNA damage. The other machinery for repair deals with the errors made during DNA replication. This mechanism includes factors involved in Mismatch repair (MMR), DNA helicases, homologous recombination, editing and processing nucleases and other genes, which are seen to be defective in diseases associated with the sensitivity to DNA damaging agents (Jackson and Bartek 2009).

c) Proto-oncogenes and oncogenes

Proto-oncogenes are normal non-mutated genes that control the cell division. They keep the cells in the cell cycle and signals them to undergo division. The most commonly known proto-oncogenes are human epidermal development factor receptor-2 (HER2), c-myc, and Cyclin D.

2.5 Apoptosis and Cancer

Apoptosis is a well-known programmed cell death mechanism that has been linked with cancer for several decades now. There are two main apoptotic pathways a) the extrinsic (death receptor) pathway and b) the intrinsic (mitochondrial pathway) **(Fig 3.)**.

The extrinsic signalling pathway is mediated by transmembrane receptor ligands. These include members of the tumour necrosis factor (TNF) family (Locksley, Killeen et al. 2001). They are known to consist of a domain of around 80 amino acids called the "death domain" (Ashkenazi and Dixit 1998). To date, the most profoundly described death receptors (DR's) incorporate DR3, DR4 & DR5 as well as FasL and TNF-α (Chicheportiche, Bourdon et al. 1997). The intrinsic signalling pathway includes changes in the inner mitochondrial membrane in response to stimuli which leads to a loss of the mitochondrial transmembrane potential (MMP) and release pro-apoptotic proteins, cytochrome c & AIF (apoptosis inducing factor) (Saelens, Festjens et al. 2004). Deciphering the signalling pathways triggering the apoptotic cascade has revealed how apoptosis is initiated in light of different physiological stresses over the span of tumourigenesis or as a consequence of anti-cancer treatment. Current research has uncovered how apoptosis is evaded in the tumours that are successful in advancing to conditions of severe resistance to therapies and malignancy (Lowe, Cepero et al. 2004; Adams and Cory 2007). As of now, the intrinsic signalling pathway is more broadly implicated as a barrier to malignancy in cancer. The fact that programmed cell death by apoptosis is a primary

barrier to cancer development has been established by studies conducted over the last two decades (Lowe, Cepero et al. 2004; Adams and Cory 2007). Investigations of the signalling machinery has revealed how apoptosis is initiated under various physiological stresses as mentioned before. This includes signalling imbalances from high levels of oncogene signalling and hyper proliferation linked DNA damage. Some research has however revealed how apoptotic activity has reduced in those tumours that succeed in progressing to states of extreme malignancy and resistance to therapy (Lowe, Cepero et al. 2004; Adams and Cory 2007).

Both the pathways ultimately activates proteases like caspases-8 and 9 and in turn initiates a series of proteolytic steps involving the effector caspases which are responsible for the final execution of apoptosis. The cell is then disintegrated and engulfed by phagocytosis. The initiation and trigger of apoptosis that mediates the signals between the regulators and effectors is regulated by the anti-apoptotic and pro-apoptotic members of the Bcl-2 family (Adams and Cory 2007). Bcl-2, along with Mcl-1, A1, Bcl-xL and Bcl-w are inhibitors of apoptosis which act by suppressing pro-apoptotic proteins like Bax and Bak. Bak proteins are usually encapsulated in the mitochondrial outer membrane. Both Bax and Bak are responsible for the disruption of the integral outer mitochondrial membrane thereby leading to the release of cytochrome c to the cytosol **(Fig. 3)**. Once cytochrome c is released, it in turn activates a series of caspases that act through proteolysis and leads to significant cellular changes linked with apoptosis. Tumour cells tend to employ a myriad of strategies in order to thwart apoptosis. The most common phenomena is the potential loss of function in the p53 tumour suppressor gene. In many cases tumours may start to increase the expression of anti-apoptotic regulators like Bcl-2 and Bcl-xL by simultaneously downregulating pro-apoptotic factors like Bax, Bim and Puma or by completely evading the extrinsic pathway. The most significant advances till now has confirmed the scope of ‘‘apoptosis’’ as a barrier to cancer.

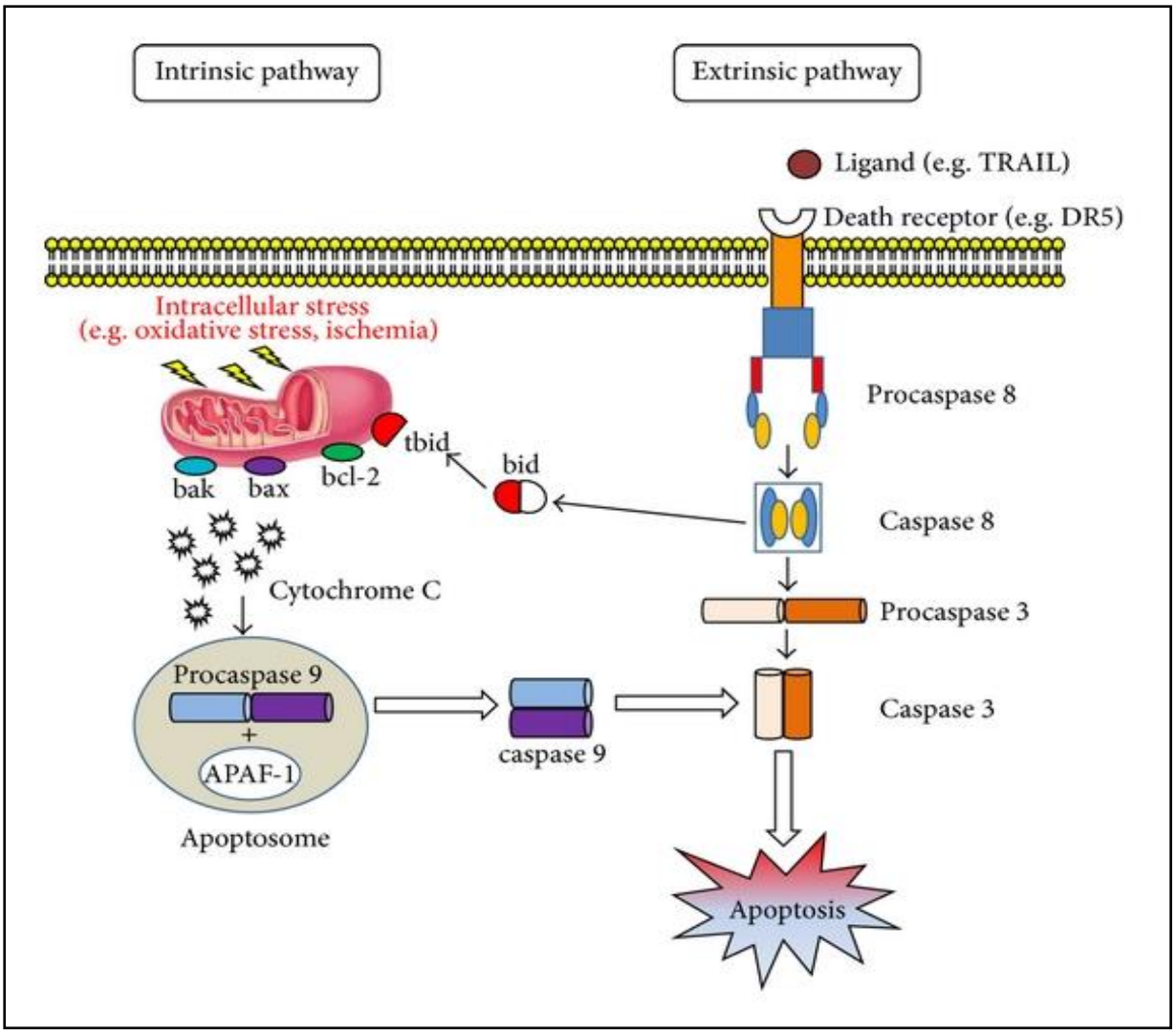


Fig. 3: Shows that apoptosis works through two main pathways: *death receptor-mediated (or extrinsic) and mitochondria-dependent (or intrinsic) [Image adopted from (Loreto, La Rocca et al. 2014), Accessed on: 12.01.19]*.

2.6 Cholesterol and cancer

Cholesterol exists either as the free form or as an ester with a single fatty acid of 10-20 carbons in length, which is attached covalently to the hydroxyl group at position 3 of the cholesterol ring in the body with a molecular formula as $C_{27}H_{46}O$ **(Fig. 4)**. It serves as a critical component of cell membranes that is vital for association of lipid bilayers to maintain membrane integrity and cell signalling. Cholesterol orchestrated *de novo* and the dietary cholesterol are transported through lipoproteins i.e., HDLs (High density lipoproteins) & LDLs (Low density Lipoproteins). Similar mechanism is valid for cholesteryl esters (CEs), the form in which cholesterol is stored in cells. Cholesterol is transported in the plasma transcendently as CEs connected to lipoproteins. Dietary cholesterol is regulated from the intestine to the liver.

The liver orchestrates Very Low Density Lipoproteins (VLDL's) **(Fig. 5)** which are later changed over to LDL's. The plasma membrane cholesterol are extracted by HDLs and subsequently esterified by lecithin-cholesterol acyltransferase (LCAT). Reverse cholesterol transport allows peripheral cholesterol to come back into the liver via LDLs. Finally, free cholesterol is formed which are discharged in the bile as salts. Over the years, cholesterol metabolites have been reported to be associated with several types of cancer malignancies (Lin, Huo et al. 2013; McDonnell, Park et al. 2014). The mitochondrial cytochrome P450 family catalysts utilise cholesterol to synthesise steroids and oxysterols. Estrogen, is one such steroid well studied in malignancy development (Fox, Andrade et al. 2009). Another example is oxysterols, crucial in cholesterol homeostasis. These metabolites predominantly inhibits the synthesis of cholesterol thereby enhancing the export of nuclear liver X receptors (LXRs) (Dufour, Viennois et al. 2012; York and Bensinger 2013). Most of the oxysterols have anti-proliferative effects in different malignant growth types (Lin, Huo et al. 2013). 27-hydroxycholesterol (27-HC) has lately been shown to be an ER agonist in BC, initiating tumour development and metastasis (McDonnell, Park et al. 2014). In BC, 27-HC accumulation is triggered when mutations in CYP7B1 occur (Wu, Ishikawa et al. 2013).

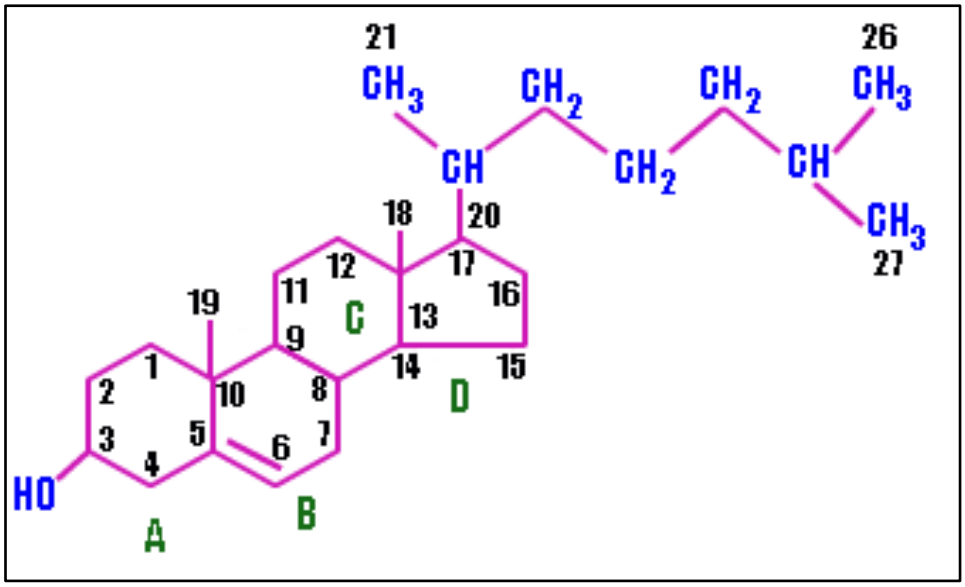


Fig. 4: Shows the chemical structure of cholesterol: *It consists of steroid rings comprising 10-20 carbons with a hydroxyl group, two methyl groups and a hydrogen tail [Image adapted from https://chemistry.tutorvista.com, Accessed 12.01.19].*

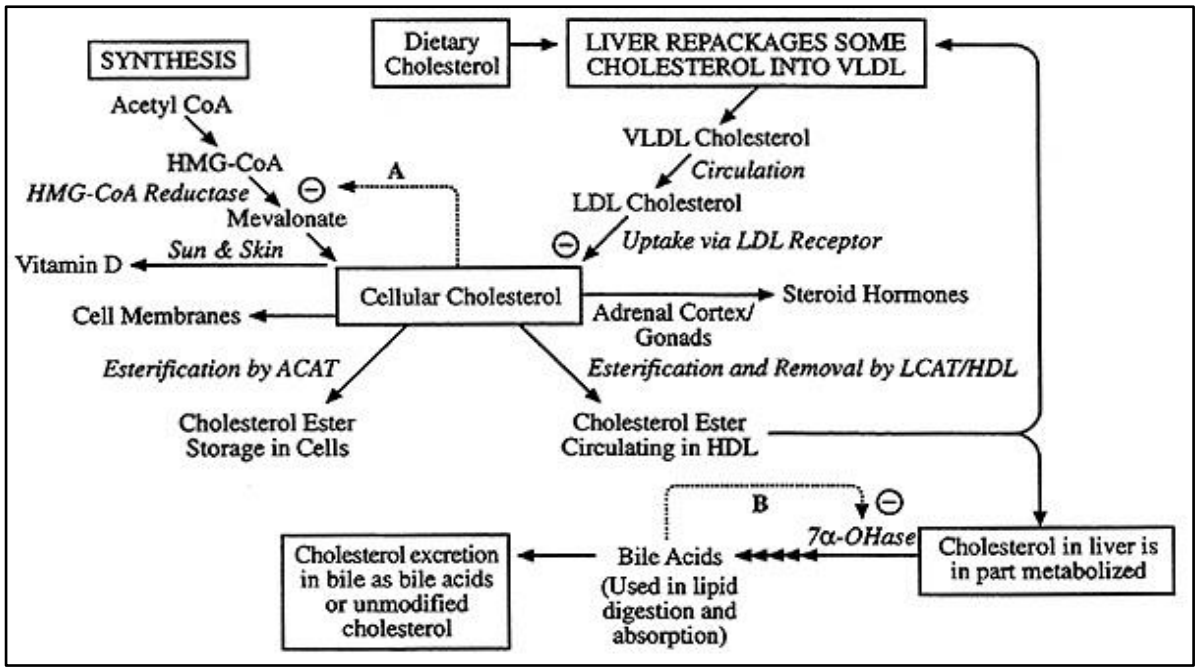


Fig 5. Cholesterol synthesis via the Mevalonate pathway, intracellular and extracellular regulation of cholesterol: *The liver orchestrates VLDL's, which are later changed over to LDL's. Cholesterol in the plasma membrane are extracted by HDLs and subsequently esterified by LCAT. [Image adapted from http://www2.csudh.edu/nsturm/CHE450/16_Cholesterol.htm, Accessed 12.01.19].*

The role of cholesterol metabolites in BC malignancy still needs further investigations. Focusing on the synthesis, transport or metabolites of the cholesterol homeostasis pathways are possibilities for controlling malignant growth development.

The detailed mechanisms involved in transforming normal cholesterol metabolism to malignancy still needs to be comprehended. However, experimental discoveries propose a clear need for higher level of cholesterol accumulation and biosynthesis in malignant cells (Mo and Elson 2004; Murtola, Syvälä et al. 2012). Limiting cholesterol biosynthesis at various steps from lanosterol results in the hindrance of cell cycle movement, apoptosis and tumour differentiation (Silvente-Poirot and Poirot 2012). Several studies have demonstrated a connection between obesity and diet with increased cancer development risks. Both have been shown to be associated with changes in lipid profiles, particularly an abatement in HDL cholesterol levels (Kim, Park et al. 2009). Nonetheless, cholesterol's role as a major player in BC is still ambiguous. Cancer cells in general needs elevated levels of cholesterol because of cell proliferation and due to cholesterol's role in maintenance of membrane rigidity and synthesis as well as formation of lipid rafts. For instance, breast and prostate cancer cell lines

have been shown to contain higher levels of cholesterol and were seen to be sensitive to cholesterol-depletion mediated cell death (Hager, Solomon et al. 2006; Li, Park et al. 2006). Likewise, cholesterol is a known precursor of vitamin D and estrogen, both of which play a key role in the histology of BC (Cui and Rohan 2006). Lately, hydroxymethylglutaryl coenzyme A reductase (HMGCR) and the mevalonate pathway **(Fig. 6)** were also cited to have a distinct role in cancer (Clendening and Penn 2012).

Over the last fifteen years the role of cholesterol in cancer growth has been elucidated in a broader way (Clendening and Penn 2012) and the correlation has been backed up by several studies including monitoring the levels of HDL and LDL in cancer patients (Furberg, Jasienska et al. 2005; Liu, Qian et al. 2011), enhanced cholesterol synthesis in cancer cells (Mo and Elson 2004; Clendening and Penn 2012; Ginestier, Monville et al. 2012), regulation of apoptosis and cell cycle signalling (Zhuang, Lin et al. 2002; Danilo and Frank 2012), metastasis (Murai 2012), steroidogenesis in cancer cells (Dillard, Lin et al. 2008; Mostaghel, Solomon et al. 2012), increased concentration of oxysterols (Silvente-Poirot and Poirot 2012), overexpression of cholesterol transport receptors: HDL and LDL (Danilo and Frank 2012) and more recently the active role of the cholesterol metabolite 27-HC (Nelson, Wardell et al. 2013; Wu, Ishikawa et al. 2013; Nelson, Chang et al. 2014). Thus, the precedent has been set for developing cholesterol-modulating anti-cancer agents (Mohammad, Malvi et al. 2014; Warita, Warita et al. 2014). Certain types of cancer cells are known to accumulate cholesterol to keep up rapid cell division; in this way, depriving cancer cells of abundant cholesterol has been conceived as an effective anti-cancer system. Dietary cholesterol (Llaverias, Danilo et al. 2011), especially lipoproteins (LDL and HDL) have been reported to fuel the development of BC (Danilo and Frank 2012; dos Santos, Domingues et al. 2014).

2.6.1 Cellular cholesterol biosynthesis

A plethora of literature has been published on cholesterol biosynthesis pathway. Briefly, the biochemical synthesis of cholesterol involves a cascade of 21 enzymatic steps (Silvente-Poirot and Poirot 2014) known as the mevalonate pathway. The mevalonate pathway begins with the precursor: acetyl-CoA produced during glycolysis **(Fig.6)**, which is converted to hydroxyl-methyl glutaryl-coenzyme A (HMG-CoA) (Buhaescu and Izzedine 2007; Martín, Pfrieger et al. 2014), and further into cholesterol (Sharpe and Brown 2013). Testosterone, derived from cholesterol, is then converted into E_2 (estrogen sex hormone, estradiol) through aromatase enzyme (Markov, Gutierrez-Mazariegos et al. 2017). The aromatase enzyme activity or levels

of aromatase enzyme are found to be significantly higher in BC (mainly in ER+) compared to normal breast tissue (Brueggemeier, Quinn et al. 1999; Díaz-Cruz, Shapiro et al. 2005), thus establishing basis for the use of aromatase inhibitors to decrease the synthesis of E_2 and thereby reducing cancer growth (Lonning 2004; Macedo, Sabnis et al. 2009). Since several cellular and biological processes are dependent on cholesterol, therefore, it is essential to scrutinise that whether blocking the cholesterol synthesis is a good strategy to treat cancers in the long-run, especially when patients will be using the drug for longer periods of time or, reducing the level of intracellular cholesterol using cholesterol-depleting agents may prove to be a better approach. To ensure the success of cholesterol-based therapeutic approach, it is critical to understand the complex processes involved in maintaining cholesterol homeostasis both intracellularly and extracellularly. Disruption of cholesterol homeostasis may cause undesirable biological effects such as cancer (Simons and Ikonen 2000; Cruz, Mo et al. 2013) and drug resistance (Debry, Nash et al. 1997; Garrigues, Escargueil et al. 2002).

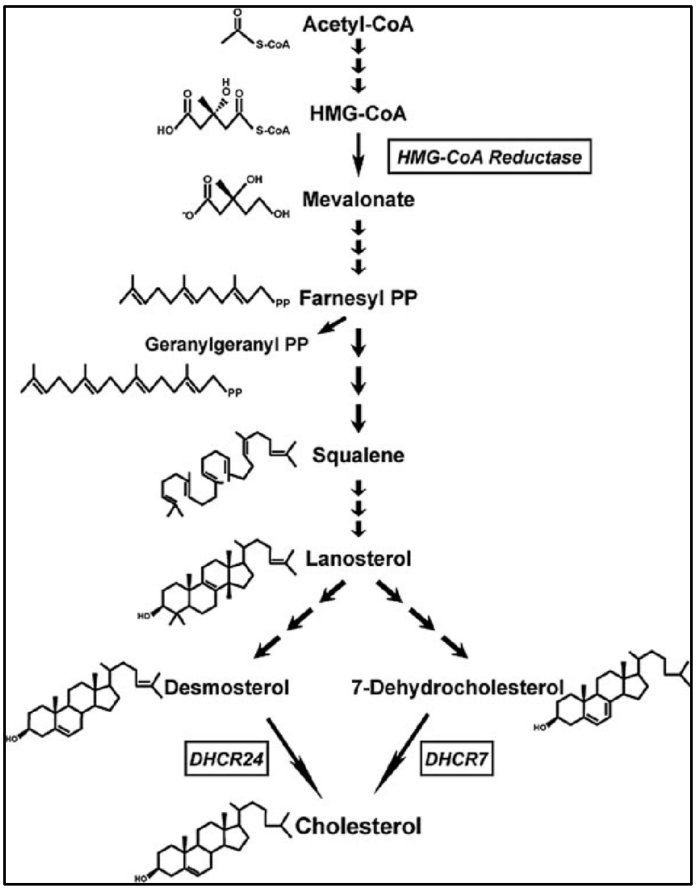


Fig. 6: The mevalonate pathway: *Acetyl-CoA is converted to HMG-CoA and further into cholesterol [Adapted from https://www.researchgate.net/figure/Cholesterol-is-the-end-product-of-the-mevalonate-pathway-The-first-step-in-cholesterol_fig1_282082147, Accessed 12.01.19.]*

2.6.2 Cellular control of cholesterol homeostasis

Under normal circumstances, the cholesterol homeostasis is a controlled process, through several intracellular (proteins and enzymes) and extracellular [lipoproteins and cholesteryl ester transfer protein (CETP)] mechanisms **(Fig. 7)** (Cruz, Mo et al. 2013). Cholesterol itself, being a lipid molecule, is only semi-soluble in aqueous environment (Hu, Zhang et al. 2010) and therefore in blood, cholesterol is transported by lipoproteins (Maxfield and Wüstner 2002; Didichenko, Navdaev et al. 2016). Lipoproteins are complex amphipathic molecules that contain hydrophilic exteriors and hydrophobic interiors allowing for the transportation of CEs internally and free cholesterol at the surface of each particle **(Fig. 7)** (Cruz, Mo et al. 2013). There are four lipoprotein cholesterol carriers: chylomicrons, LDL, VLDL and HDL (Cruz, Mo et al. 2013). LDLs are liable for transporting cholesterol from the liver to peripheral tissues. In contrast, HDLs are the key components in the removal process of excess cholesterol from tissues to the liver through reverse cholesterol transport (RCT) (Cruz, Mo et al. 2013). Additionally, several proteins assist in regulating both intracellular as well as extracellular cholesterol homeostasis **(Fig. 7)**. An important apolipoprotein involved in the assembly (45% protein mass) of HDL, used in RCT, is apolipoprotein A-1 (Apo-A1) (Zamanian-Daryoush and DiDonato 2015). The protective role of HDL and ApoA-1 has also been demonstrated against cancer (Zamanian-Daryoush and DiDonato 2015) using mouse tumour models where elevated levels of ApoA-1/HDL hindered tumour development (melanoma) and ApoA-1 supplementation demonstrated therapeutic benefits against established tumours (Zamanian-Daryoush, Lindner et al. 2013). ApoA-1 expression is known to be down-regulated in various cancers including ovarian and BC, thus explaining the over-proliferation of cancer cells (Chang, Hou et al. 2007). Furthermore, low serum ApoA-1 levels in BC are linked to increased risk of recurrence (Martin, Melnichouk et al. 2015). These observations have been linked with a number of mechanisms, which include reduction in angiogenesis and metastasis, recruitment of tumour-associated macrophages, and decreased levels of anti-apoptotic proteins (Zamanian-Daryoush, Lindner et al. 2013).

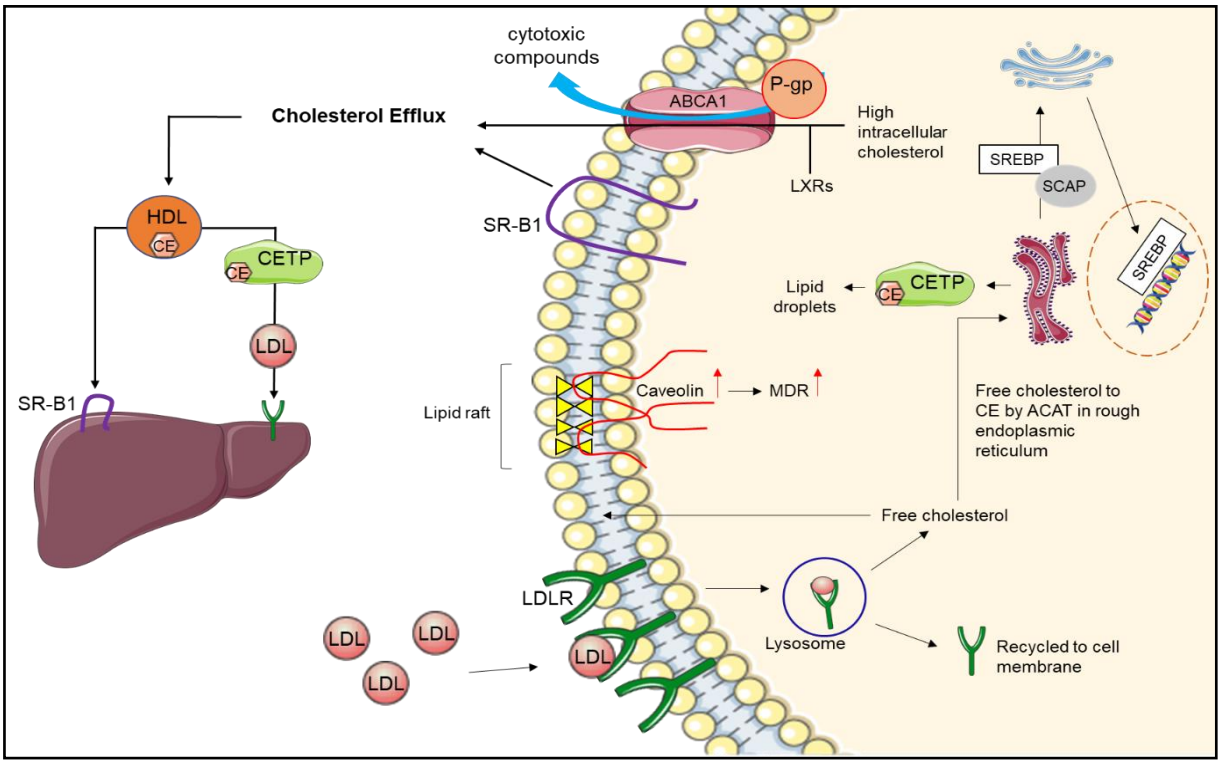


Fig. 7: Intracellular and Extracellular transportation of cholesterol.

Free cholesterol in the extracellular matrix is delivered to various cells via LDL and low-density lipoprotein receptor (LDLR) interactions. Cholesterol dissociates from the receptor in the cell lysosome. Intracellular cholesterol molecules are converted to CEs by Acetyl-coenzyme A acetyltransferase 1 (ACAT) in the endoplasmic reticulum and stored as lipid droplets mediated by CETP. Furthermore, Sterol regulatory element-binding proteins (SREBPs) regulate intracellular cholesterol synthesis and uptake between the endoplasmic reticulum and Golgi body. Intracellular cholesterol homeostasis is maintained through ATP-binding cassette transporter (ABCA1), scavenger receptor class B type 1 (SR-B1) and caveolin. The coupling of p-glycoprotein (P-gp) to ABCA1 regulates cellular toxicity by transporting cytotoxic drugs or compounds to the extracellular matrix. Therefore, ABCA1 is an important protein involved in multi-drug resistance (MDR). In addition, MDR occurs when there is an increase in caveolin (red arrow), which increases membrane cholesterol. Extracellular cholesterol homeostasis is maintained by lipoproteins; HDL and LDLs. Cholesterol is then cleared through HDLs (which interacts with SR-B1) to be excreted by the liver or shuttled by CETP from HDLs to the LDLs, which bind to LDLRs on hepatocytes for cholesterol clearance. (Gu, Saha et al. 2019 accepted in FEBS Journal) *(Source: https://smart.servier.com/)*

Despite the evidence put forward by numerous studies demonstrating the protective role of ApoA-1 in BC, contrary studies have shown a directly proportional relationship between ApoA-1 levels and BC risk (Martin, Melnichouk et al. 2015), where elevated levels of ApoA-1 increased incidence rates of BC. However the ratio of ApoB/ApoA-1 was found to be inversely associated with BC incidence (Chang, Hou et al. 2007). More research is clearly needed to establish a link between Apo-A1 levels and BC. A recently emerged new player is CETP. CETP facilitates the net transfer of CEs from HDLs to LDLs then to VLDLs to be excreted by the liver (Chirasani, Sankar et al. 2016; Millar, Lassman et al. 2017). CETP can function both intracellularly as well as extracellularly to maintain cholesterol homeostasis within the body. Intracellularly in the adipocyte, CETP translocate CEs and triglycerides (TGs) from the endoplasmic reticulum to the storage droplets (Izem and Morton 2007). Extracellularly via RCT, CEs are taken up by CETP from HDLs and transferred to the liver for cholesterol clearance through LDLR. In addition, it was found that CETP-deficient cells lead to a four-fold increase in intracellular CEs in human lipocarcinoma cells (Izem and Morton 2007). Previous studies have all looked at decreasing LDL levels and increasing HDL levels by targeting CETP as a therapeutic option for atherosclerosis and coronary heart disease (Li, Huang et al. 2014; Rashid, Sniderman et al. 2015; Chen, Sun et al. 2017; Simic, Mocharla et al. 2017). However, recently CETP has been identified as a molecular target in BC (Esau, Sagar et al. 2016). As aforementioned, BC cells accumulate cholesterol for survival, therefore, cholesterol-depleting agents such as acetyl plumbagin (AP) and methyl beta cyclodextrin (MβCD) have been successful in inducing cancer cell death (Sagar, Esau et al. 2014; Esau, Sagar et al. 2016). Previously, it was shown that AP was found to decrease or deplete membrane cholesterol levels which consequently resulted in a decrease in CETP mRNA expression and induced mitochondrial-mediated apoptosis in cancer cells (Esau, Sagar et al. 2016). In addition, the knock-down of CETP led to a substantial increase in caspase-3/7 activity in MCF7 (ER+) cells that were treated with tamoxifen (Esau, Sagar et al. 2016).

Of further importance is the fact that increasing number of studies have established links between acquired tamoxifen resistance and proteins involved in cholesterol metabolism (Pitroda, Khodarev et al. 2009; Poirot, Silvente-Poirot et al. 2012; Voisin, de Medina et al. 2017). A notable example is the mucin-1 (MUC1) protein, which is a transmembrane protein that is abnormally expressed abundantly in BC and pancreatic cancer cells (Pitroda, Khodarev et al. 2009; Poirot, Silvente-Poirot et al. 2012; Nath, Daneshvar et al. 2013). MUC1 subunit has been found to form a complex with ER and recruits coactivators and inhibits the effects of tamoxifen (Pitroda, Khodarev et al. 2009; Nath, Daneshvar et al. 2013). In addition, MUC1

induces the activation of SREBPs involved in cholesterol synthesis (Pitroda, Khodarev et al. 2009). Moreover, cell survival pathways such as extracellular signal-regulated kinase 1/2 (Erk1/2) and phosphoinositide 3-kinase/ Protein Kinase B (PI3K/Akt) pathways are enhanced with an overexpression of MUC1 (Nath, Daneshvar et al. 2013), probably contributing to drug resistance in cancer cells. ABCA1, maintains intracellular cholesterol levels (Yvan-Charvet, Wang et al. 2010; Kang, Zhang et al. 2013). A mutation in this gene results in the accumulation of excess cholesterol within the cell thereby disrupting normal cell immune response (Yvan-Charvet, Wang et al. 2010). The accumulated cholesterol binds to the P-gp and modulates its substrate recognition ability resulting in enhanced efflux of drugs from the cell **(Fig. 7)**. Therefore elevated levels of the P-gp induce MDR in cancer cells (Yvan-Charvet, Wang et al. 2010; Wu, Yang et al. 2014; Chen, Shi et al. 2016). ABCA1 and P-gp not only control intracellular cholesterol levels but also increase external transport of drugs therefore reducing intracellular toxicity resulting in drug resistance of cancer cells.

Cancer drug resistance is also contributed by increased concentration of lipid rafts in cell membranes. Caveolin-1 is a 21-24 kDa integral membrane protein that is involved in the caveolae formation (specialized lipid rafts that are rich in signalling molecules, receptors, effector proteins and transducers) of most mammalian cells (Hoque, Chen et al. 2008; Wang, He et al. 2014). Caveolin-1 protein may transport cholesterol to the plasma membrane through various mechanisms (Smart, Graf et al. 1999; Arakawa, Abe-Dohmae et al. 2000; Frank, Cheung et al. 2006). Furthermore, up-regulation of the caveolin-1 protein has also been observed to be involved in the MDR phenomenon (Lavie and Liscovitch 2000); as increased caveolae would strengthen cell membranes due to an increase in lipid rafts as well as various receptors and signalling molecules for cell proliferation and cell survival (Hoque, Chen et al. 2008). Intracellular cholesterol levels are also kept under control by transporting cholesterol in bidirectional manner by SR-B1 receptor (Rosenson, Brewer et al. 2012). More importantly, SR-B1 receptor is the mediator for the selective uptake of CEs from HDL to the liver during the RCT process (Rosenson, Brewer et al. 2012). Therefore, a mutation in this gene interrupts the RCT system, steroidogenesis and may cause cholesterol imbalance. SR-B1 has also been associated with lipid rafts and shown to have specificity to apolipoproteins, but interacts randomly with HDL, LDL, phospholipids and other ligands (Hu, Zhang et al. 2010). It has been shown that a deletion of the SR-B1 gene in mice resulted in an increase in HDL-cholesterol and halted the consumption of cholesterol by steroid-hormone producing cells (Hu, Zhang et al. 2010).

2.6.3 Cellular regulation of cholesterol content

At transcription level there are two key regulators of cholesterol homeostasis, the first being the SREBPs and the second is the LXRs (Ikonen 2008; Gabitova, Gorin et al. 2014; Nelson, Chang et al. 2014). The SREBPs are located on the membranes of endoplasmic reticulum and golgi bodies (Ikonen 2008) and are important transcription regulators encoded by Sterol Regulatory Element Binding Transcription Factor 1 (SREBF1) and Sterol Regulatory Element Binding Transcription Factor 2 (SREBF2) genes involved in the synthesis of cholesterol and cholesterol uptake (Ikonen 2008). In the absence of sufficient cholesterol content, SREBP is translocated from the endoplasmic reticulum to the golgi body with the aid of the chaperone; SREBP cleavage-activating protein (SCAP) **(Fig.7)** (Ikonen 2008; Nelson, Chang et al. 2014). The activation of SREBP through proteolytic processing signals for cholesterol synthesis (Ikonen 2008; Nelson, Chang et al. 2014). Under cholesterol-rich environment, the excess cholesterol inhibits the movement of SREBP from endoplasmic reticulum to golgi body by disrupting the SCAP chaperone (Ikonen 2008). In contrast, although LXRs also play a vital role in intracellular cholesterol homeostasis, but they are activated via oxysterol ligands (Zhao and Dahlman-Wright 2010; Nelson, Chang et al. 2014). In an elevated cholesterol environment, oxysterols, like 27 HC signal LXRs to activate genes involved in transporting cholesterol outside of the cell (such as the ABCA1) and aid in the RCT and bile acid synthesis (Schroepfer Jr 2000; Zhao and Dahlman-Wright 2010). In addition, LXRs possess anti-proliferative properties, independent of lipid synthesis, by suppressing mRNA expression of various proteins involved in cell cycle progression and reduced expression of ER mRNA and protein, thus attenuates estrogen-induced proliferation (Vedin, Lewandowski et al. 2009). A detailed biological understanding of cross-talk between cholesterol and various signalling pathways is important to utilise them as possible therapeutic tools for cancer.

Cholesterol is an essential component for the function of GPCRs (G-protein coupled receptors, classical biological targets of many known drugs) either through a direct molecular interaction or through physical modifications of the membrane proteins (Pucadyil and Chattopadhyay 2006), thereby affecting the downstream pathways involved in cancer. Furthermore, recent research has shown that cholesterol also activates the Sonic Hedgehog (SHH) pathway, an important pathway for cell differentiation, regeneration as well as cancer development **(Fig. 8)** (Luchetti, Sircar et al. 2016). Cholesterol is able to activate the SHH pathway by directly activating Smoothened (SMO; a GPCR), through its cysteine-rich domain, which is able to convey the hedgehog (HH) signal across the plasma membrane. The changes in cholesterol

concentrations could thereby regulate SMO activity (Luchetti, Sircar et al. 2016). SMO is also activated when HH proteins bind to protein patched homolog 1 (PTCH1) thus signalling an increase in cell proliferation **(Fig. 8)** (Quijada, Callejo et al. 2007). It is well known that excessive HH signalling can lead to different cancer types (Skoda, Simovic et al. 2018). With an excess of cholesterol fuelling BC, it is suggested that the SHH pathway may be triggered as more cholesterol is able to bind SMO thereby allowing for the growth of the BC. Similarly cholesterol binds with a protein known as Dishevelled, which is involved in both canonical and non-canonical Wnt signalling **(Fig. 8)** (Sheng, Kim et al. 2014), thereby promoting BC development and may in addition influence BC relapse. Transformations in the PI3K pathway are very common in BC malignancy, making cells resistant to endocrine therapy (Paplomata and O'Regan 2014).

Various PI3K inhibitors are presently under development as anti-cancer agents which include PI3K inhibitors, compounds that block mTOR (mammalian target of rapamycin) and PI3K (dual inhibitors), catalytic mTOR inhibitors and inhibitors that block Akt (Liu, Cheng et al. 2009). Akt/PI3K pathways may be involved in accumulation of cholesterol amongst several tumours (Porstmann, Griffiths et al. 2005). When Akt is activated, it in turn induces the binding of the SREBP-1 and SREBP-2 proteins with simultaneous expression of fatty acid synthase (FAS), thereby increasing the concentration of the components of cellular membranes; phosphoglycerides as well as cellular fatty acids, along with triggering the SREBP pathway involved in the regulation of cholesterol (Chang, Wang et al. 2005).

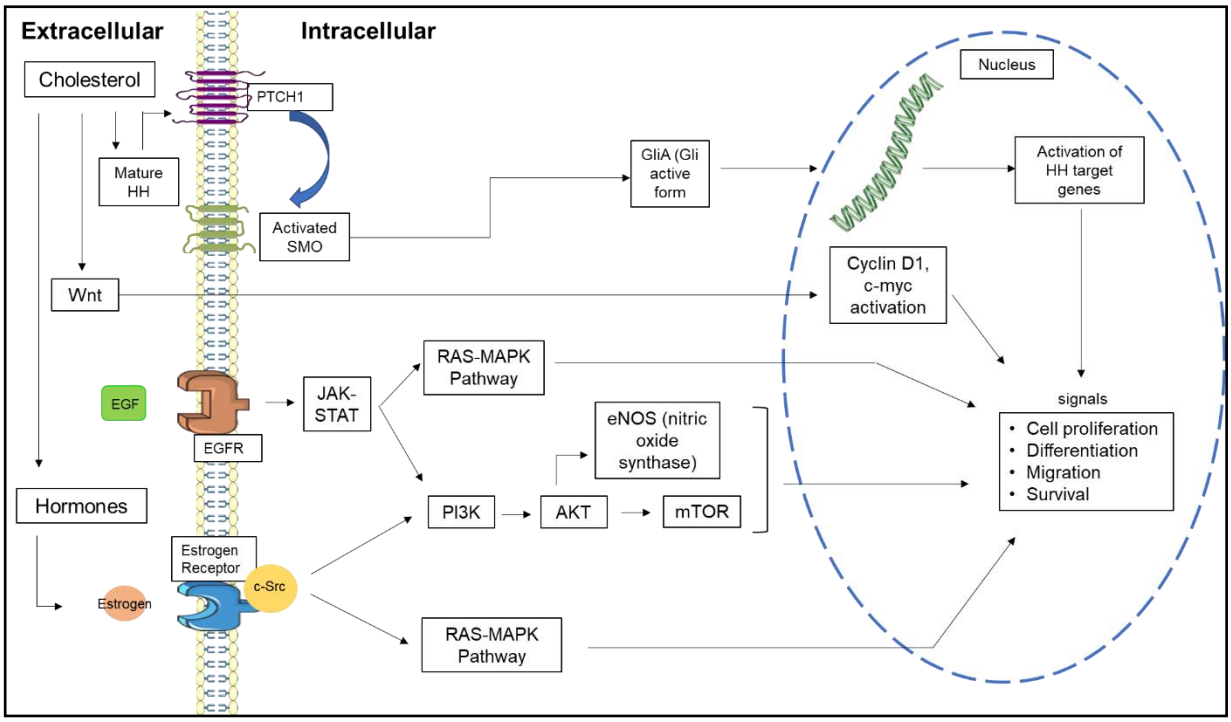


Fig. 8: Cholesterol is involved in stimulation of various BC signalling pathways.

The figure summarises complex interconnections among cholesterol, hormones and BC signalling pathways influencing cell proliferation, differentiation, migration and survival. Cholesterol activates the Wnt pathway, which activates cyclin D1 (cell cycle) and c-myc, for cell proliferation and differentiation. In addition, cholesterol is the key component in the biosynthesis of various hormones. Estrogen, specifically binds to ER for cell growth. Estrogen is an essential hormone that maintains the female reproductive tissues such as the breasts. Cholesterol results in the production of E_2, which can regulate the activity of SMO. Cholesterol leads to maturation of HH and binds to PTCH1 membrane protein and activates SMO. Activation of SMO signals for cell proliferation. In BC, E_2 is overproduced and thus increases the activity of SMO, which activates the SHH signalling pathway within the nucleus. Subsequently, this excess HH signalling results in over-proliferation of cells thereby causing various cancers such as; skin, brain and most importantly BC. Furthermore, the activation of the ER through the binding of estrogen signals for downstream growth signalling pathway; RAS-MAPK pathway. In TNBC cells, epidermal growth factors (produced in the presence of testosterone) bind to EGFR (Epidermal growth factor receptor) or HER2 receptors, which lead to a number of downstream intracellular signalling pathways that are all involved in BC cell growth. (Gu, Saha et al. 2019 accepted in FEBS Journal) *(Source: https://smart.servier.com/)*

From metastasis point of view, cellular migration and invasion involves cytokines like transforming growth factor β (TGF-β), which is a regulator of cellular events including the stimulation of MAPK (mitogen-activated protein kinase) pathway (Chapnick, Warner et al. 2011; Gui, Sun et al. 2012), and induction of Epithelial-mesenchymal transition (EMT), which is characterized by increased cellular mobility, a key aspect of tumour pathogenesis and invasion (Derynck and Akhurst 2007; Johansson, Tabor et al. 2015). What is important to understand is that the MAPK activation is highly dependent on the integrity of lipid rafts. Moreover, receptors for TGF-β are predominantly found embedded in lipid rafts and this specific localization is crucial for TGF-β-induced MAPK activation (Zuo and Chen 2009). The discovery that cholesterol-depletion in lipid rafts as a result of impaired MAPK activation disrupts EMT and cellular migration substantiates cholesterol's role in metastatic processes (Zuo and Chen 2009). Furthermore, lipid rafts were found to be a vital requirement in MAPK activation (He, Kole et al. 2003; Limpert, Karlo et al. 2007). It is thus fair to hypothesise that increase in cholesterol synthesis and thereby lipid raft formation, like in BC cells, would lead to an increase in TGF-β signalling and a surge in MAPK activation, thus increasing cell proliferation, migration and survival; critical factors for cancer progression **(Fig. 8)**. The fundamental role of cholesterol in TGF-β–induced cell migration thus proposes cholesterol-depletion as a prospective therapeutic approach against pathologically detrimental EMT during carcinogenesis (Zhao and Chen 2014).

Interestingly, JAK-STAT (Janus kinases - Signal Transducer and Activator of Transcription proteins) is best known for its interactions with both the PI3K and the MAPK pathway thus initiating downstream cascades leading to cell survival, proliferation, differentiation and migration (Yamada and Kawauchi 2013). It is worth mentioning that the activation of JAK-STAT, through a myriad of cytokines and hormones, also plays a crucial role in lipid metabolism in adipocytes (Xu, Yin et al. 2013). The adipocytes interact with BC cells to mediate BC progression in obese individuals (Picon-Ruiz, Pan et al. 2016). This complex interconnections of different pathways involved in cancer progression and invasion is dependent on lipid rafts and the lipid metabolism, therefore strengthening the hypothesis that depriving cells of the cholesterol and lipids may prove to be a viable strategy to disrupt the complex interactions of cancer related pathways, thus forcing a cancer cell to die.

A natural way to reduce access of cancer cells to cholesterol can be achieved by modulating the AMPK (AMP-activated protein kinase) pathway, which is a natural pathway that blocks cholesterol synthesis by inhibiting mevalonate pathway. HMG-CoA reductase is phosphorylated by AMPK. The phosphorylation ($^{+}$P) of AMPK is catalysed by two proteins: LKB1 (raises 5' adenosine monophosphate-activated protein (AMP) levels) and AMPK phosphorylating catalyst calmodulin-subordinate protein kinase-beta (CaMKKβ) (Mihaylova and Shaw 2011). Phosphorylated AMPK inhibits HMG-CoA reductase thus reducing cholesterol levels (Motoshima, Goldstein et al. 2006). Thus, activating AMPK may have anti-cancer effects. The proposed association of AMPK with tumour suppressive drugs like metformin, which inhibits complex I of the mitochondrial electron-transport chain and in turn increases the intracellular AMP/ADP (adenosine 5'-diphosphate protein) proportion thereby activating AMPK, is indicative of the fact that therapeutic control of this pathway utilizing established cancer drugs warrants further examination in cancer patients (Choi and Park 2013).

Many small molecules and antibodies have been developed that specifically target a particular cancer signalling pathway. Many more are under investigation such as cholesterol-lowering agents that can impact the cancer signalling pathways by altering cholesterol content in the cells. It is therefore highly likely that combining specific pathway inhibitors with cholesterol-lowering agents can possibly be envisaged as a viable therapeutic strategy for cancer treatment as opposed to blocking the synthesis of cholesterol using statins. This brings us to an important question, which strategy can produce long-term beneficial effects for cancer patients? "Cholesterol synthesis blocking or depletion of excess cholesterol?"

2.7 Ceasing cholesterol synthesis vs depletion of excess cholesterol

Considering the increase in synthesis of cholesterol in BC, drugs inhibiting lipid synthesis or having cholesterol-lowering properties present a unique opportunity to fight cancer (Vallianou, Kostantinou et al. 2014) and considering the significant role cholesterol plays in BC progression, there are currently two therapeutic strategies that may be employed to target cholesterol for developing successful therapies in the treatment of BC.

The first being cholesterol synthesis inhibitory drugs that involves the stunting of cholesterol synthesis and the second strategy is to decrease membrane cholesterol content by using cholesterol-depleting agents. The anti-cancer activity can be attributed to their ability to reduce cellular proliferation, migration and to stimulate apoptosis in a number of cancerous cell lines (Simigdala, Gao et al. 2016).

2.7.1 Cholesterol-synthesis blocking as anti-cancer therapy

Over the couple of decades several agents have been found to have cholesterol-depleting properties. These incorporate statins, isoprenoids, cyclodextrins (CyDs) and others. Statins act by inhibition of the mevalonate pathway resulting in reduced tumour development and proliferation (Clendening and Penn 2012; Matusewicz, Meissner et al. 2015). Predominantly known as HMG-CoA reductase inhibitors, statins actively impede the core enzyme HMG-CoA reductase **(Fig. 9)** that plays a critical role in the regulation of cholesterol synthesis. A variety of compounds belonging to the statin class of drugs have been developed: lovastatin (Mevacor), mevastatin (Compactin), atorvastatin (Lipitor), uvastatin (Lescol), rosuvastatin (Crestor), pitavastatin (Livalo), simvas- tatin (Zocor) and pravastatin (Pravachol or Selektine) (Simon and Butt 2015). According to experimental and epidemiological data, statins readily reduce the viability of cancer cells as well as incidence of certain types of cancers including BC (Hoque, Chen et al. 2008). Mechanistically, statins are able to actively inhibit cholesterol synthesis thereby attenuating cell proliferation (Warita, Warita et al. 2014). In addition, statins induce cellular senescence by down-regulating growth-promoting signals involving RAS, PI3K/AKT and Wnt/β-catenin signalling cascades (Tsubaki, Yamazoe et al. 2011; Ampuero and Romero-Gomez 2015). Furthermore, statins are able to induce pro-apoptotic signals in various cancers and interactively augment the apoptotic potential of several cytotoxic agents (Matusewicz, Meissner et al. 2015).

Despite their significant anti-cancer potential, associated adverse side effects of statins need reviewing. These side effects may range from mild to severe muscle pains, liver damage (which is a crucial organ for lipid metabolism), raising blood sugar levels and thus increasing risk of developing diabetes or cardiovascular diseases and possible neurological decline (Sinzinger, Wolfram et al. 2002; Ramsunder 2015; Strom, Schinnar et al. 2015). The recent proposed use of Proprotein convertase subtilisin/kextin type- 9 (PCSK9) inhibitors potentially might also cause diabetes by increasing the inflow of cholesterol and consequently damage pancreatic cells (Besseling, Kastelein et al. 2015). Memory loss has been an apparent symptom of statin use as UK Medicines & Healthcare products Regulatory Agency (MHRA) recommended listing memory-loss as one of the side-effects in product label, which was followed by label changes recommendations by US Food and Drug Administration (FDA) in https://www.fda.gov/Drugs/DrugSafety/ucm293101.htm, therefore it is crucial to develop alternate cholesterol-lowering agents that are not only more potent but also have minimal side effects. Alternative agents targeting key enzymes in sterol biosynthesis or mevalonate pathway

include lonafarnib and tipifarnib, which inhibit farnesyltransferase (Marcuzzi, De Leo et al. 2011) and certain bisphosphonates, which have the potential to inhibit farnesyl-diphosphate (an intermediate in mevalonate pathway) synthase (Tsoumpra, Muniz et al. 2015). Other molecules like Terbinane (Lamisil) potentially inhibit squalene epoxidase (a rate-limiting enzyme in sterol biosynthesis pathway) or 2, 3- oxidosqualene cyclase (Nowosielski, Hoffmann et al. 2011) and TAK-475 (Lapaquistat) inhibit squalene synthase. All these aforesaid agents are currently undergoing clinical trials, which will establish their efficacy and long-term benefits in patients.

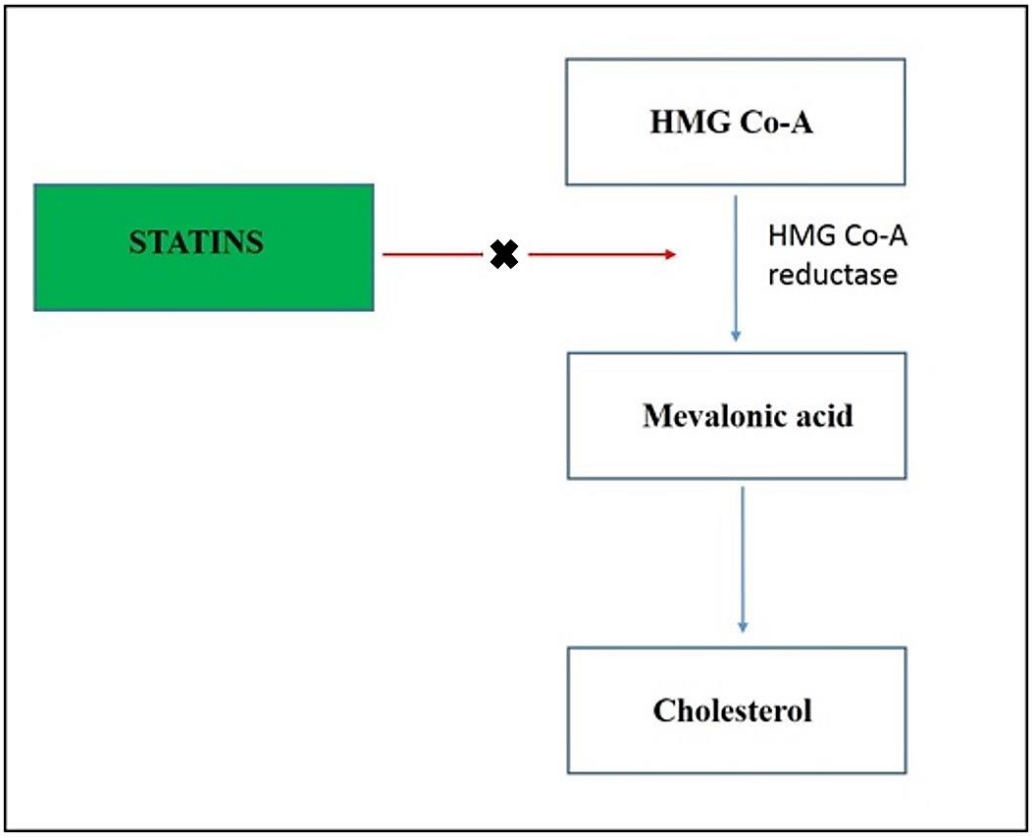


Fig. 9: Mode of action for statins: *Statins act by competitively inhibiting the key rate-limiting enzyme of the cholesterol biosynthetic pathway, HMG-CoA reductase. They mimic HMG-CoA, and subsequently competes for binding to the HMGCR enzyme.*

2.7.2 Cholesterol-depletors as anti-cancer agents

Since cholesterol is a precursor for the synthesis of steroid hormones, therefore the mevalonate pathway is currently being targeted for anti-cancer drug development by inhibiting HMG-CoA (blocking cholesterol production) using statins (Hoque, Chen et al. 2008; Warita, Warita et al. 2014; Simon and Butt 2015). Superior anti-cancer effects are obtained from molecular-targeted drugs as compared to conventional chemotherapeutic agents and they also have less adverse effects (http://www.cancer.gov). Recent work in this direction, a novel cholesterol-depleting agent, AP has been identified and it has been established that AP has selective apoptotic activity against MCF7 (ER+ BC cells) as compared to normal skin fibroblasts (BJ) and TNBC (BT20 cells) (Sagar, Esau et al. 2014). AP is a derivative of a natural product, Plumbagin (PL), and the observed selective anti-cancer activity of AP against cholesterol rich ER+ BC cells shows that plants harbor cholesterol-depleting agents.

Similar to statins, isoprenoids (Mo and Elson 2004) and tocotrienols stifle tumour development *in vitro* and *in vivo* resulting from deprivation of mevalonate. On similar lines, a drug named ezitimibe was shown to interfere with carcinogenesis (Solomon, Pelton et al. 2009). In Ms. Liang Gu's (Lab colleague) dissertation work it was seen that both *in vitro* and *in vivo* assays on BC cells showed depletion of cholesterol using AP and led to significantly decreased CETP expression in BC cells, which sensitized cancer cells to apoptosis. Moreover *in silico* analysis of BC samples showed that the overall survival, with reduced relapse, of BC patients was improved and this is correlated with low level expression of CETP. In addition, knocking-down CETP in BC cells resulted in several fold increase in caspase-3/7 activity in tamoxifen treated cells and also reduced resistance of BC cells towards tamoxifen thereby making the cells more susceptible to intrinsic apoptosis (Esau, Sagar et al. 2016). The fact that cholesterol homeostasis is derailed in cancer cells and there are demarcated differences in BC and normal cells, provides basis for testing cholesterol-lowering as a viable approach to develop treatments for BC.

CyDs is one such cholesterol-depleting group of compounds. They are effective due to the presence of relatively hydrophobic cavity and can be utilised to solubilize cholesterol (Zidovetzki and Levitan 2007; Hinzey, Kline et al. 2012). They were first isolated by Villiers in 1891 from *Bacillus amylobacter* grown on a medium containing starch. The external environment of CyDs is hydrophilic whereas the internal is hydrophobic. CyDs are essentially cyclic amylose oligomers composed of a-1-4-linked glucose units. The glucose chains rearrange to a conical indentation where molecules or compounds may insert and thereby becomes a water soluble complex. This in turn changes the medication's intrinsic and extrinsic properties. The number of units pertains to the measure of the conical indentation and its analogous name (Szejtli 1998; Uekama, Hirayama et al. 1998). The interior cavity of CyDs can epitomize lipophilic compounds, for example, cholesterol and improve the solubility in aqueous solutions (Davis and Brewster 2004) **(Fig. 11)**. They have been shown to act as medication transporters/drug carriers (Challa, Ahuja et al. 2005; Arun, Ashok Kumar et al. 2008). The most widely recognized CyDs utilised are a, b and c-CyDs. All of them are utilised effectively for drug fusion into aqueous vehicles (Antlsperger and Schmid 1996) and their toxicity profiles has also been extensively researched (WHO, 1993). These molecules, albeit comparative in their unit make-up, have diverse absorption rates, conceivably because of the difference in the degradation processes (Antlsperger and Schmid 1996). CyDs have also been shown to associate with cholesterol and phospholipids and causing hemolysis (Motoyama, Toyodome et al. 2009). Over the years, CyDs have been widely used as a complexation with other drugs to improve drug efficacy **(Table 1.)**. The mechanism of action of CyDs has been shown in **Fig. 10**.

The main advantages of CyDs over other cholesterol depletors are:

a) *Enhancement of solubility*
b) *Enhancement of bioavailability*
c) *Improvement of stability*
d) *Reduction of irritation*
e) *Prevention of incompatibility*:
f) *Odour and taste masking*
g) *Material handling benefits*

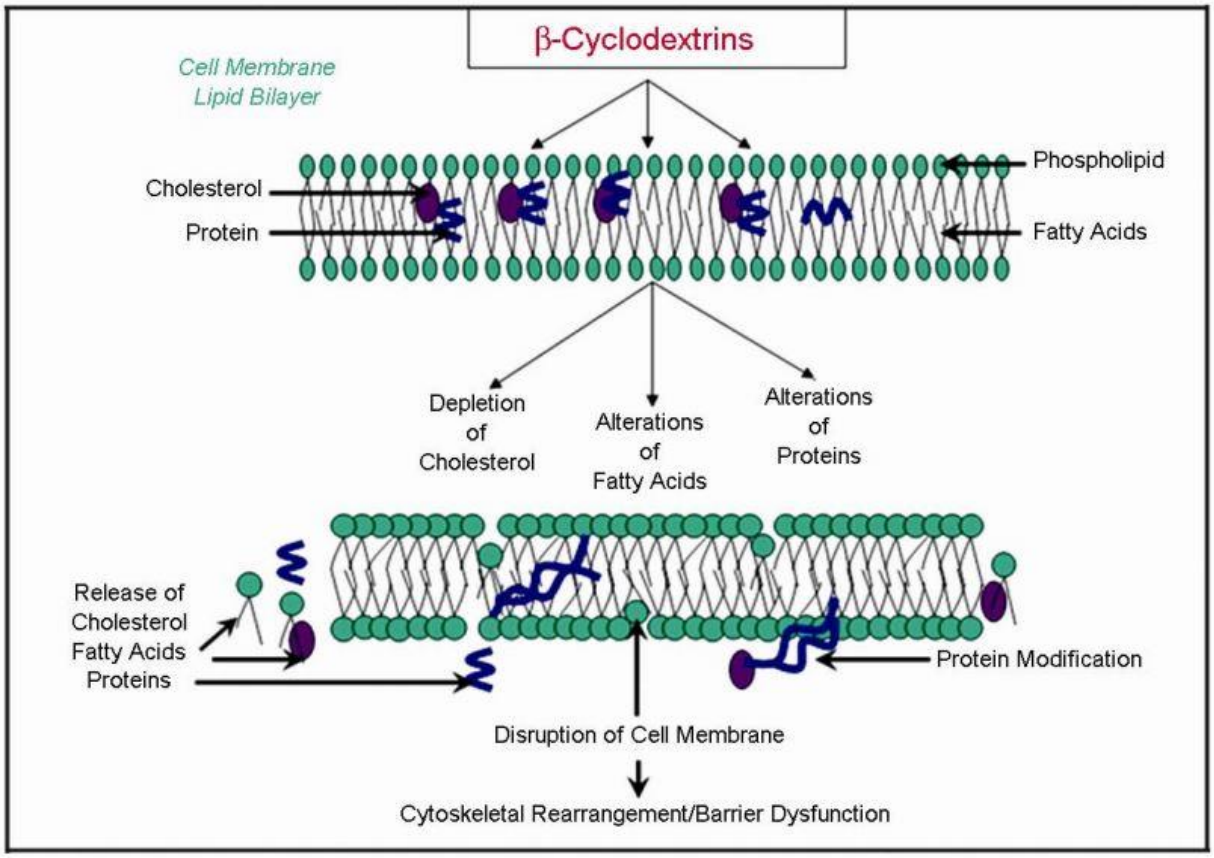


Fig. 10: Proposed Mechanism of β CyD induced cholesterol-depletion: *β CyD leading to alterations in cell morphology, loss of ability to proliferate (apoptosis) [Image adopted from (Hinzey, Kline et al. 2012), Accessed on: 12.01.19]*.

A variant of CyDs, known as methyl-β-cyclodextrin (MβCD) has been significantly utilised as a disrupting agent for lipid rafts through extraction of cholesterol (Simons and Ehehalt 2002; George and Wu 2012). Several *in vitro* studies have exhibited that MβCD prompts apoptosis of different cancer cells (Park, Park et al. 2009; Yan, Li et al. 2012; Onodera, Motoyama et al. 2013). MβCD is amongst the most extensively studied cholesterol-depleting agents, which has shown significant anti-cancer activity in a number of cancers including BC (Mohammad, Malvi et al. 2014), by effectively decreasing membrane cholesterol through lipid raft disruption (Li, Park et al. 2006). The Akt protein, which is anchored into the lipid raft, when activated contributes to tumour development and invasiveness, and this activity is associated with an increase in lipid rafts (Courtney, Corcoran et al. 2010). As a consequence, lipid raft disruption actively inhibits Akt activation thereby reducing tumour development and progression (Zhuang, Kim et al. 2005). Consequently, cholesterol-depletion by MβCD induced apoptosis in BC cells through downregulating Bcl-xL and Akt, and by activating caspase-3 (Li, Park et

al. 2006). Additionally, MβCD was shown to increase the efficacy of tamoxifen treatment by increasing its cellular uptake as cholesterol-depletion in the membrane disrupts lipid raft integrity and simultaneously increases membrane permeability for drug passage (Mohammad, Malvi et al. 2014). Therefore, current cancer drugs can be used in conjunction with cholesterol-depletors such as MβCD to enhance their uptake and efficacy (Mohammad, Malvi et al. 2014). This is a relatively new concept under exploration and therefore, further research in this direction is needed to discover new biological targets in the cell so that targeted cholesterol-depleting agents can be identified and developed. 2-hydroxylpropyl- β -cyclodextrin (HPβCD) is quite a contrast as compared to the above mentioned CyDs, with enhanced solubility properties (Yoshida, Yamamoto et al. 1988) and is more toxicologically benign. Recently there was a study which showed that upon treatment with HPβCD, there was a reduction in the murine atherosclerosis with reduced plaque size and cholesterol crystals load (Zimmer, Grebe et al. 2016) **(Table 2.)**. Other studies have shown that HPβCD treatment led to reduced cholesterol intracellularly resulting in reduction of leukemic cell development through G2/M cell-cycle mitotic arrest and apoptosis (Yokoo, Kubota et al. 2015) **(Table 2.)**. Furthermore, HPβCD showed no toxicity, contingent upon the dosage in several species (Gould and Scott 2005).

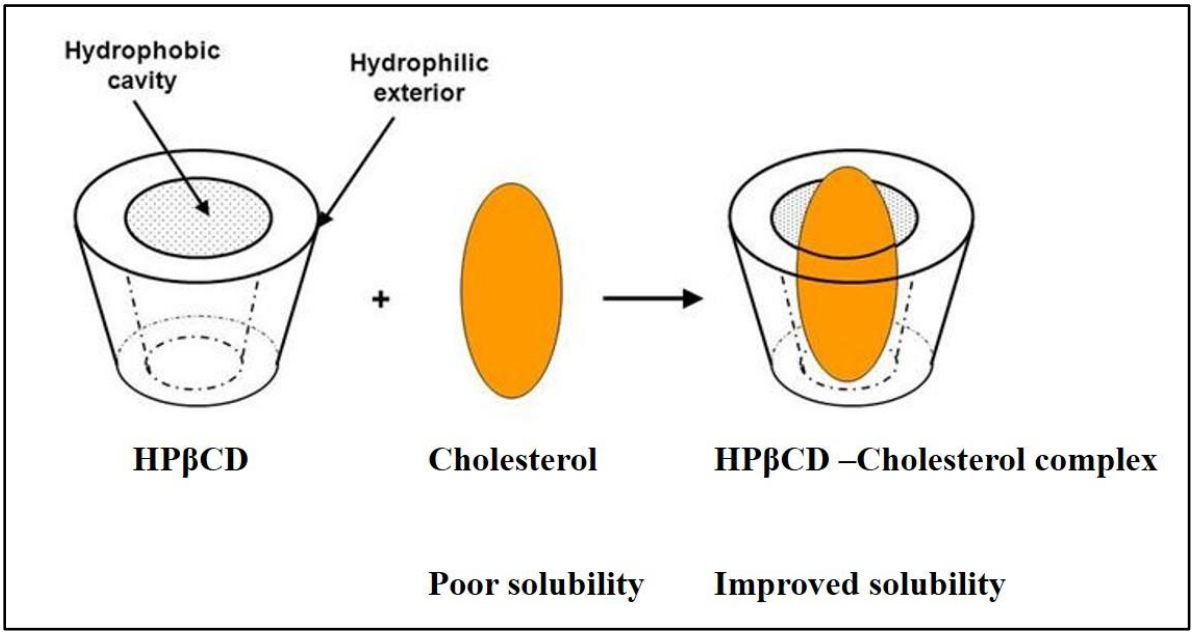


Fig 11: Proposed mode of action of HPβCD: HPβCD *has better solubility because of the hydrophilic exterior, cholesterol is lipophilic and gets engulfed in the conical indentation thereby forming* HPβCD-*Cholesterol complex with improved solubility (Image adapted from: http://slideplayer.com/slide/9337618 Accessed on: 12.01.19).*

A number of clinical studies have likewise reported that HPβCD was tolerated in the majority of human trials done at daily oral dosages for no less than 2 weeks (Irie et al. 1997). HPβCD has additionally been appeared to be far less cytotoxic when contrasted with MβCD while effectively removing the cellular cholesterol (Hinzey, Kline et al. 2012). A recently concluded clinical trial with HPβCD done by Therapeutics for Rare and Neglected Diseases (TRND), an NIH (National Institutes of Health, USA) initiative for Niemann-Pick disease type C1 **(Table 2.)** which is an autosomal recessive lysosomal storage disorder due to the accumulation of unesterified cholesterol, yielded promising results and the Phase 1 trial was concluded successfully and currently, the drug is being tested in a multicentre, multinational Phase 2b/3 clinical efficacy trial https://clinicaltrials.gov/ct2/show/NCT02534844.

Table 1: List of anti-cancer drugs complexed with CyDs for enhanced efficacy.

Serial No.	Drug	Type of CD	Disease	Results	Refs.
1.	9-Nitro camptothecin	HPβCD	Pancreatic cancer	Significant improvement in antitumour activity and reduction in toxicity	(Jiang, Jiang et al. 2011)
2.	Methotrexate	HPβCD	Melanoma	Enhancement of aqueous solubility and bioavailability	(Singh, Aithal et al. 1997)
3.	Lonidamine	MβCD	Prostate cancer	Enhancement of solubility	(Lahiani-Skiba, Bounoure et al. 2011)
4.	Exemestane	MβCD	BC	Enhanced solubility and better bioavailability	(Yavuz, Bilensoy et al. 2010)
5.	Vorinostat	HPβCD, MβCD	Lymphoma	Enhancement of bioavailability	(Cai, Yap et al. 2010)

6.	Imatinib	MβCD	Chronic leukemia	Enhancement of solubility	(Béni, Szakács et al. 2007)
7.	Doxorubicin	HPβCD	Lymphoma and leukemia	Increased stability to photodegradation and acid hydrolysis	(Peng, Liu et al. 2010)
8.	Cisplatin	HPβCD	Testicular, ovarian, and cervical carcinoma	Reduced toxicity, enhanced solubility, better dissolution rate	(Balaji, Pandey et al. 2009)
9.	Flutamide	HPβCD	Prostatic carcinoma	Enhancement of solubility and dissolution	(Elgindy, Elkhodairy et al. 2010)
10.	Zerumbone	HPβCD	Colon and skin cancer	Better bioavailability, stability and solubility	(Eid, Abdul et al. 2011)
11.	Melphalan	HPβCD	Multiple myeloma and ovarian cancer	Stability against hydrolysis, solubility enhancement	(Ma, Rajewski et al. 1999)
12.	Oridonin	MβCD	Oesophageal and cardiac cancer	Enhancement of bioavailability	(Li, Li et al. 2012)
13.	5-Fluorouracil	HPβCD	Cervical cancer	Enhancement of solubility	(Bilensoy, Cırpanlı et al. 2007)

Table 2: List of diseases till date responsive to direct HPβCD treatment without complexation.

Serial No.	Disease	Results	Refs.
1.	Niemann Pick Type C	Phase 1 successfully complete ,Phase 2b/3 clinical efficacy trial currently being done	(Tanaka, Yamada et al. 2015)
2.	Atherosclerosis	Regression via macrophage reprogramming	(Sagar, Esau et al. 2014)
3.	Chronic myeloid leukemia	Disturbs leukemic cell cholesterol homeostasis via apoptosis	(Perelman, Wachtel et al. 2012)

Treatment with HPβCD for BC has never been investigated before and therefore it led us to hypothesize and investigate HPβCD as a stand-alone compound without any complexation, and delving into the possibility to use it as a potential and novel therapeutic agent for BC.

3. AIM and OBJECTIVES

3.1 Aim

To test 2-hydroxypropyl-β-cyclodextrin (HPβCD) as a novel therapeutic agent for BC.

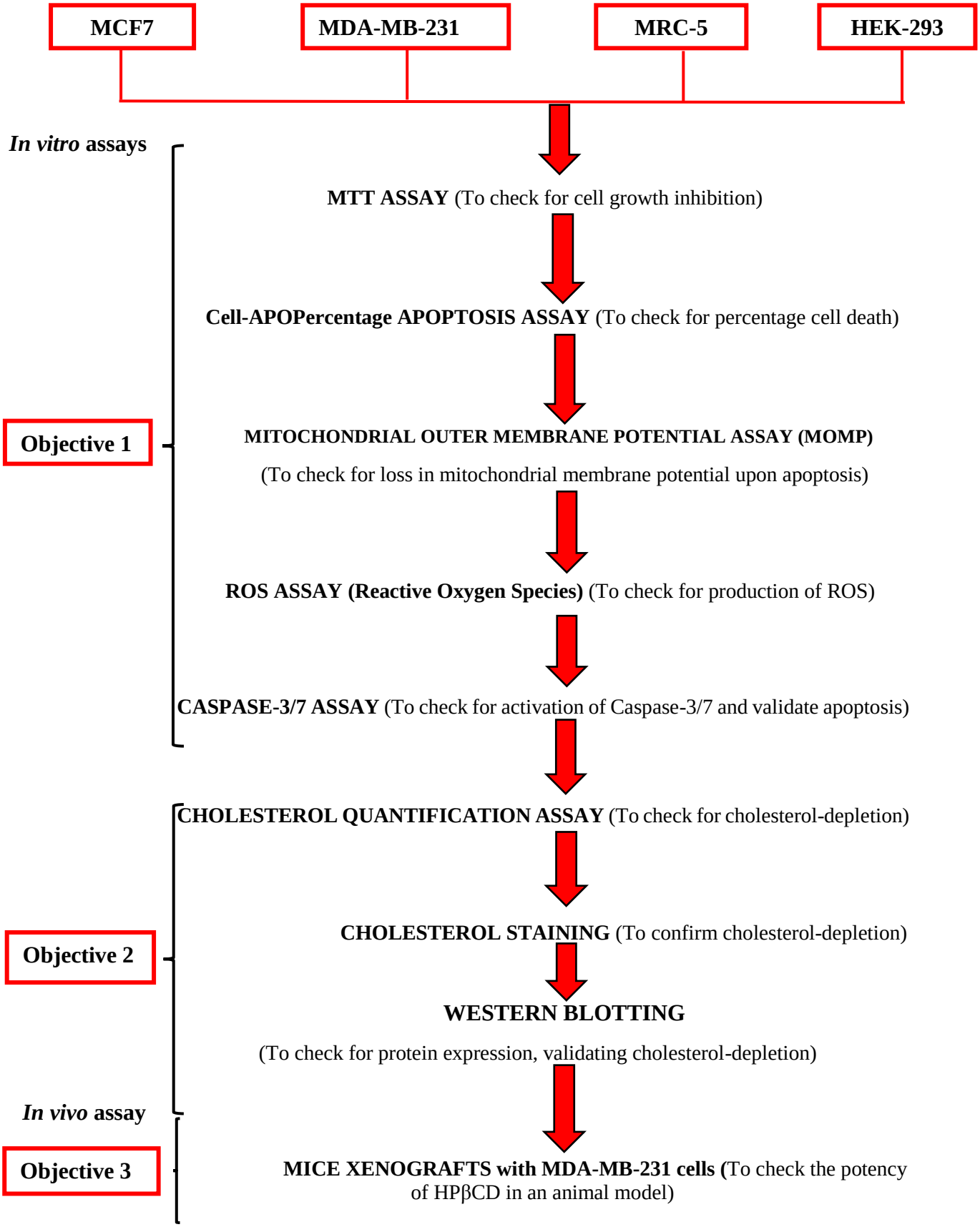
3.2 Objectives

1) To investigate apoptosis inducing potential of HPβCD *in vitro* in BC cell lines.

2) To elucidate HPβCD's molecular mechanism of action in cancer cells.

3) To test the tumour inhibition properties of HPβCD in mouse model (*in vivo*).

4. WORKFLOW


MCF7
MDA-MB-231
MRC-5
HEK-293
In vitro assays
MTT ASSAY (To check for cell growth inhibition)
Cell-APOPercentage APOPTOSIS ASSAY (To check for percentage cell death)
Objective 1
MITOCHONDRIAL OUTER MEMBRANE POTENTIAL ASSAY (MOMP)
(To check for loss in mitochondrial membrane potential upon apoptosis)
ROS ASSAY (Reactive Oxygen Species) (To check for production of ROS)
CASPASE-3/7 ASSAY (To check for activation of Caspase-3/7 and validate apoptosis)
CHOLESTEROL QUANTIFICATION ASSAY (To check for cholesterol-depletion)
Objective 2
CHOLESTEROL STAINING (To confirm cholesterol-depletion)
WESTERN BLOTTING
(To check for protein expression, validating cholesterol-depletion)
In vivo assay
Objective 3
MICE XENOGRAFTS with MDA-MB-231 cells (To check the potency of HPβCD in an animal model)

5. MATERIALS AND METHODS

5.1 CELL CULTURING

The proposed work done using MCF7, MDA-MB-231, MRC-5 and HEK-293. Authentication was done by STR profiling and mycoplasma-free cell lines were procured from The European Collection of Authenticated Cell Cultures (ECACC).

Table 3: Cell lines used for the study.

Cell Line	Abbreviation	Full name	Morphology	Media
Human Breast Cancer (ER+)	MCF7	Michigan Cancer Foundation-7	Epithelial	DMEM +10% FBS+ 1% Penicillin-Streptomycin
Human Breast Cancer (TNBC)	MDA-MB-231	M.D. Anderson Metastatic Breast Adenocarcinoma	Epithelial	3:1(DMEM: Ham's F12) +10% FBS+ 1% Penicillin-Streptomycin
Lung fibroblasts (Control)	MRC-5	Medical Research Council Cell strain 5	Fibroblasts	DMEM +10% FBS+ 1% Penicillin-Streptomycin
Embryonic kidney (Control)	HEK-293	Human Embryonic Kidney	Epithelial	DMEM +10% FBS+ 1% Penicillin-Streptomycin

5.1.1 MCF7 cell line

Cells were cultured in Dulbecco's modified Eagles medium (DMEM) containing 4.5g/L D-Glucose-Glutamine, Pyruvate (Gibco, UK).The media was supplemented with 10% fetal bovine serum (FBS,100U/ml) (biowest, France), 1% Penicillin/Streptomycin (100 µg/ml) (Merck, USA) **(Table 3)**. The cells were incubated in 25 cm^2 and 75 cm^2 Corning® cell culture flasks (Merck, USA) for 24 hours (hrs), 48 hrs and 72 hrs at 37 ^oC in an incubator (ThermoFischer Scientific, USA) under a 5% CO_2 humidified atmosphere.

5.1.2 MDA-MB-231 cell line

Cells were cultured in DMEM medium containing 4.5g/L D-Glucose-Glutamine, Pyruvate (Gibco, UK).The media was supplemented with 10% fetal bovine serum (FBS, 100U/ml) (biowest, France), 1% Penicillin/Streptomycin (100 µg/ml, Merck, USA) and Ham's F12 (biowest, France) in a ratio 3:1 (DMEM: Ham's F12) **(Table 3)**. The cells were incubated in 25 cm² and 75 cm² Corning® cell culture flasks (Merck, USA) for 24 hrs, 48 hrs and 72 hrs at 37 ºC in an incubator (ThermoFischer SCIENTIFIC, USA) under a 5% CO_2 humidified atmosphere.

5.1.3 MRC-5 cell line

Cells were cultured in DMEM containing 4.5g/L D-Glucose-Glutamine, Pyruvate (Gibco, UK). The media was supplemented with 10% fetal bovine serum (FBS, 100U/ml) (biowest, France), 1% Penicillin/Streptomycin (100 µg/ml) (Merck, USA) **(Table 3)**. The cells were incubated in 25 cm² and 75 cm² Corning® cell culture flasks (Merck, USA) for 24 hrs, 48 hrs and 72 hrs at 37 ºC in an incubator (ThermoFischer SCIENTIFIC, USA) under a 5% CO_2 humidified atmosphere.

5.1.4 HEK-293 cell line

Cells were cultured in DMEM containing 4.5g/L D-Glucose-Glutamine, Pyruvate (Gibco, UK). The media was supplemented with 10% fetal bovine serum (FBS, 100U/ml) (biowest, France), 1% Penicillin/Streptomycin (100 µg/ml) (Merck, USA) **(Table 3)**. The cells were incubated in 25 cm² and 75 cm² Corning® cell culture flasks (Merck, USA) for 24 hrs, 48 hrs and 72 hrs at 37 ºC in an incubator (ThermoFischer SCIENTIFIC, USA) under a 5% CO_2 humidified atmosphere.

5.2 SUB-CULTURING OF CELLS

5.2.1 MCF7, MDA-MB-231, MRC-5 and HEK-293 cell lines

The cells were washed once with 2 ml Phosphate buffer Saline (PBS) (Merck, USA). Two millilitres (ml) of 1% (v/v) Trypsin-EDTA (biowest, France) was added to the flasks and incubated for 5-10 minutes (mins). After incubation, the flasks were agitated to loosen the cells from the surface. This was then followed by the addition of 4 ml supplemented DMEM to inactivate the trypsin. The cells were then transferred to new flasks and the amount of transfer was dependent on the confluency needed. The cells were passaged every 48 hrs.

5.3 CELL STOCKS

Cells were removed and collected as described above. Cells were then centrifuged using eppendorf Centrifuge MiniSpin® at 4000 x *g* for 4 mins. The pellet was resuspended in 70% (v/v) DMEM, 20 % FBS and 10 % DMSO to a total volume of 1 ml. The cell stocks were stored in cryogenic vials at -80 ºC and few in liquid nitrogen until needed.

5.3.1 Revival of stocks

Cells were taken out of stocks and thawed in a preheated (37 ºC) water bath. The thawed cells containing a total volume of 1 ml were added to respective 25 cm² and 75 cm² Corning® cell culture flasks (Merck, USA) containing 4 ml DMEM for 25 cm² and 7 ml DMEM for 75 cm² culture flasks followed by incubation. After 24 hrs, the media was replaced with new supplemented media (5 ml or 7 ml respectively) and the cells were further incubated until confluence.

5.4 CELL COUNTING WITH TRYPAN BLUE EXCLUSION ASSAY

Media was removed and 2 ml of 1 X trypsin/EDTA (biowest, France) was added into the flask and incubated at 37 °C for to allow cells to be detached. The pellet was resuspended in 2 ml media to inactivate trypsin. Trypan blue (Merck, USA) is a widely used dye that only stains the dead cells. This is due to the disruption of the plasma membrane which renders the cells susceptible to dye uptake. The live cells do not take up the dye due to the intact cell membrane. The cell suspension was then mixed (10 µl) to 10 µl of 0.4 % trypan blue dye (1:1). The suspension was mixed on a Para film and 10 µl of the stained suspension were added to a Neubauer haemocytometer. The cellular viability was determined using the following formula:

$$\% \text{ Cell viability} = \frac{\text{No. of live cells (unstained)}}{\text{Total no. of counted cells (dead and live)}} \times 100$$

For all experiments, only cells at a viability of over 90 % were used.

5.5 PL ATING OF CELLS

5.5.1 MCF7, MDA-MB-231, MRC-5 and HEK-293 cell lines

Cells were collected and counted as described in sections 5.2.1 and 5.4. 5000 cells were seeded in a final volume of 45 µl DMEM to 96 well plates (Nunc-Immuno™ MicroWell™, USA). Plating was done in triplicates and were incubated for 24 hrs for optimal adhesion prior to treatments. The outer wells of the plate were filled with autoclaved H_2O to avoid media evaporation in the CO_2 incubator.

Cells were then seeded at a desired density as follows:

45 µl ×total no. of wells =total volume of media required (**a**)

5000 cells/well× total no. of wells =total no. of cells required

$$\frac{\text{Total volume in flask (µl)} \times \text{total no. of cells required}}{\text{Total no. of cells counted in flask}} = \text{volume of cells required from flask (}\mathbf{b}\text{)}$$

a -b =volume of media to be added to cells

45 µl was then pipetted into each well with 5000 cells per well.

5.6 *IN VITRO* AND *IN VIVO* TREATMENTS

All *in vitro* treatments were carried for 24 hrs, 48 hrs and 72 hrs depending on the assay performed. All *in vivo* treatments were carried for maximum 2-3 weeks maintaining a 10 dose approach.

5.6.1 MCF7, MDA-MB-231, MRC-5 and HEK-293 cell lines

Cells were plated as described in section 5.5.1. 5 µl of different treatments were added to the already existing 45 µl DMEM to make the final volume upto 50 µl. PL (Merck, USA), MβCD (Merck, USA), Hydrogen peroxide (H_2O_2) (Merck, USA) and HPβCD (Merck, USA) were used at concentrations of 10 µM and 40 µM for PL, 5 mM for MβCD, 10 mM for H_2O_2 and 10 mM for HPβCD. PL, H_2O_2, MβCD were used as positive controls. Stocks of all the treatments were made prior to the required concentrations.

5.7 GROWTH INHIBITION ASSAYS

5.7.1 MTT (3-(4, 5-dimethylthiazol-2-yl)-2, 5-diphenyltetrazolium bromide) ASSAY

Principle:

This is a colorimetric assay that measures the cleavage of tetrazolium ring of the yellow MTT by mitochondrial succinate dehydrogenase in active mitochondria of living cells. The MTT enters the cells and goes into the mitochondria and is reduced to dark purple formazan crystals. These crystals are then solubilized with an organic solvent and the solubilized product is quantified spectrophotometrically. MTT is reduced, and it only occurs in cells that are metabolically active and therefore the activity level is directly proportional to the viability of the cells. This assay can also calculate the reduction in cell viability, when in case of apoptosis (Sylvester 2011). The background absorbance of MTT dye is very less when cells are absent.

Protocol:

5000 cells were plated as mentioned in section 5.5.1 in 96 well plates. After 24 hrs of cell adhesion, HPβCD and PL were added in a desired volume so that the final concentration in the wells were 10 mM and 40 µM for HPβCD and PL respectively. The treatment was done for further 24 hrs as mentioned in section 5.6.1. 40 µM PL was used as a positive control. For untreated sample, only cells containing media were used. Post treatment, the MTT dye (Merck, USA) was added for 4 hrs and once the formazan crystals were formed, they were solubilized using 10% SDS (Merck, USA) solution in 0.01 M HCl (Merck, USA) and incubated for 16-24 hrs for complete dissolution of the crystals. The absorbance was then read at 570 nm using a microtiter plate reader Multiskan GO Microplate Reader (Thermo Fisher Scientific, SkanIt™ software). The percentage cell inhibition/viability was determined and graphs were generated using GraphPad Prism5®.

5.7.2 Cell-APOPercentage APOPTOSIS ASSAY

Principle:

Initiation of the final execution phase of apoptosis is correlated to the translocation of phosphatidylserine (PS) from the interior of the cell membrane to the exterior. In most laboratory experiments this is usually supported by the binding of annexin V to PS. PS transmembrane movement is carried by phospholipid transportation enzymes like scramblases (floppase) and flippases **(Fig. 12)** which results in the uptake of the APOPercentage Dye by apoptotic or unhealthy cells. The dye uptake is continuous till “blebbing” (protrusion of the

plasma membrane) occurs (Sagar, Esau et al. 2014). There is no release of the dye at this point from the inoperative cell except for the blebbed ones.

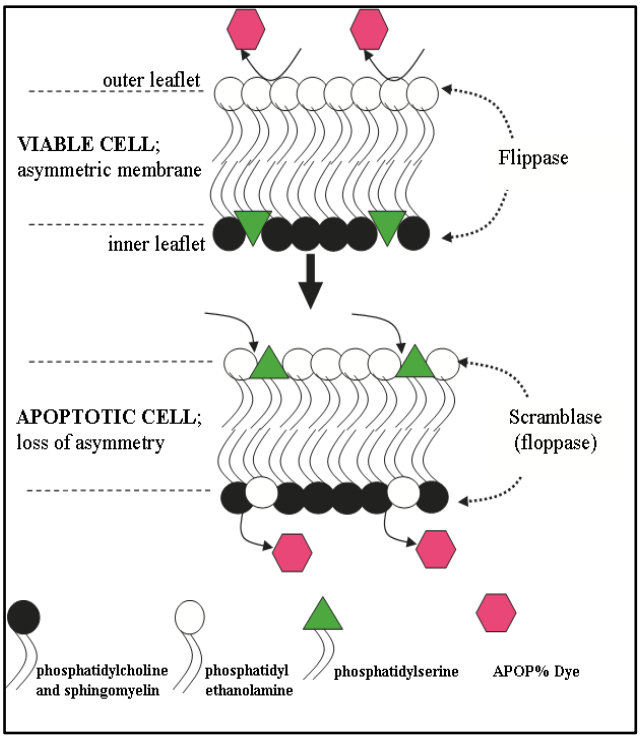


Fig. 12: The mode of action of the Cell-APOPercentage dye. *The dye binds to the externally exposed PS and then taken up into the cell via the PS transmembrane movement. [Image adopted from: www.biocolor.co.uk, Accessed 12.01.19]*

Protocol:

5000 cells were plated as mentioned in section 5.5.1 in 96 well plates. After 24 hrs of cell adhesion, HPβCD and PL were added in a desired volume so that the final concentration in the wells were 10 mM and 10 µM for HPβCD and PL respectively. 10 µM PL was used as a positive control. The treatment was done for further 24 hrs (as mentioned in section 5.6.1). For untreated sample, only cells containing media were used. After 24 hrs of treatment, the entire 50 µl of media was removed and the wells were washed with 1X PBS. Next, 64.5 µl of 1X PBS was mixed with 0.5 µl of the APOPercentage dye (Biocolor, UK) and incubated for 15 mins in the CO_2 incubator at 37 ºC keeping the plate foiled up because the dye is extremely sensitive to light. After 15 mins the constituents from wells were removed and washed with 100 µl of 1X PBS twice. Finally 100 µl of 1 X PBS was added again and absorbance was then read at 550 nm using a microtiter plate reader Multiskan GO Microplate Reader (Thermo Fisher Scientific, SkanIt™ software). The percentage cell death was determined and graphs were generated using GraphPad Prism5®.

5.7.3. MITOCHONDRIAL OUTER MEMBRANE POTENTIAL (MOMP) ASSAY

Principle:

The MOMP assay uses a cyanine dye, JC-1. This dye is positively charged and has high membrane permeability potential. It accumulates in the electronegative interior of the mitochondrion resulting in the formation of J-aggregates (Perelman, Wachtel et al. 2012). These aggregates emit red fluorescence at 580-590 nm and can be captured in the FL-2 channel. When apoptosis is initiated, MOMP gets disrupted and JC-1 cannot aggregate, therefore it stays in a monomeric form. The accumulation in mitochondria is indicated by a fluorescence emission shift from green (~529 nm) to red (~590 nm) **(Fig. 13)**. This particular characteristic feature of JC-1 is beneficial to identify cells with disrupted mitochondria which is linked with early stage apoptosis. When mitochondrial membrane potential depolarizes, and cells become unhealthy, the red/green fluorescence ratio can then be utilised to determine the mitochondrial function. The ratio of green to red fluorescence is solely dependent on the mitochondrial membrane potential and is independent of mitochondrial density, shape or size.

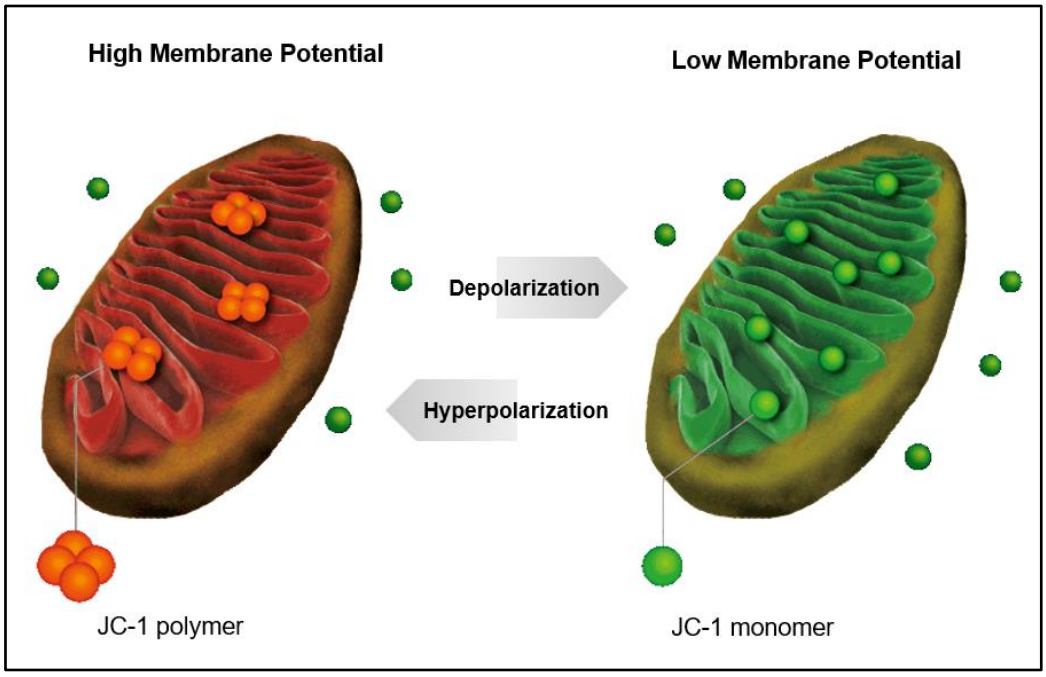


Fig. 13: The mechanism of action of the JC-1 dye. *JC-1 forms aggregate (in healthy mitochondria) producing red fluorescence. With the gradual decrease in membrane potential, JC-1 stays as monomers and shows green fluorescence [Image adopted from: [www.dojindo.com, Accessed 12.01.19].*

Protocol:

5000 cells were plated as mentioned in section 5.5.1 in 96 well plates. After 24 hrs of cell adhesion, HPβCD and H_2O_2 were added in a desired volume so that the final concentration in the wells are 10 mM for both HPβCD and H_2O_2. Treatment was done for another 24 hrs (as mentioned in section 5.6.1). 10 mM H_2O_2 was used as a positive control. For untreated sample, only cells containing media were used but was stained with the dye. An additional sample was plated which was used as unstained cells, this contained just cells and media like the untreated. After 24 hrs of treatment, 12 µl of 15 mM EDTA was added to the existing 50 µl to make the final volume to 62 µl. The 96 well plate was then shook on a plate shaker for 15 seconds and incubated for 40 mins at 37ºC in the CO_2 incubator. This was done to detach the cells. Following this, 15 µl of JC-1 dye (Merck, USA) was added to all wells except the unstained wells (15 µl of serum free media was added here to maintain similar volumes) to make the final concentration of the dye to 2 µM (made in serum free media) from a stock of 2 mM in a final volume of 77 µl). The plate was then covered with foil because JC-1 is light sensitive and incubated for 30 mins in the CO_2 incubator at 37 ºC. After 30 mins, the entire constituents from the wells were carefully transferred in separate vials (each vial for each sample) and foiled individually (Kaur and Esau 2015). The vials were then kept on ice for 5 mins to stop the reaction and then analysed in a 2D plot using BD Accuri™ C6 Flow Cytometer (BD Biosciences, USA).

5.7.4. REACTIVE OXYGEN SPECIES (ROS) ASSAY

Principle:

The ROS assay or DCFDA assay utilises the cell permeant reagent 2', 7' –dichlorofluorescin diacetate (DCFDA or H_2DCFDA) (Wang and Roper 2014), which is a fluorogenic dye capable of measuring the ROS production within the cell. Once inside the cell, DCFDA is deacetylated via cleavage of the acetate groups by intracellular esterases to a non-fluorescent compound H_2DCFDA which is then subsequently oxidized by ROS into 2', 7' –dichlorofluorescein (DCF). DCF can emit extremely high fluorescence and can be detected by flow cytometry with excitation / emission at 495 nm / 529 nm **(Fig. 14)**.

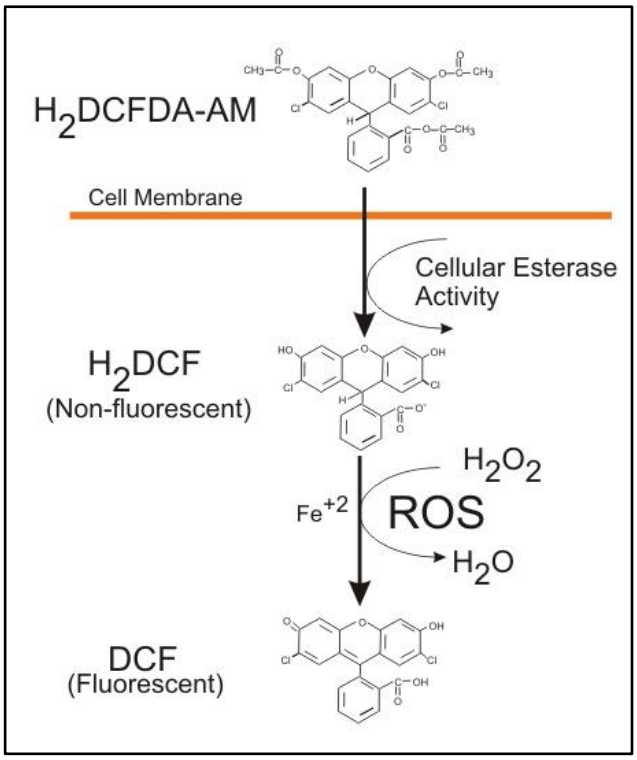


Fig. 14: The mechanism of ROS. *DCF is formed due to the action of esterases and production of ROS via the oxidation of H_2DCF. [Image adopted from: www. biotek.com, Accessed 12.01.19].*

Protocol:

5000 cells were plated as mentioned in section 5.5.1 in 96 well plates. After 24 hrs of cell adhesion, HPβCD and PL were added in a desired volume so that the final concentration in the wells are 10 mM for both HPβCD and H_2O_2. 10 mM H_2O_2 was used as a positive control. The treatment was done for another 24 hrs (as mentioned in section 5.6.1). 10 mM HPβCD and 10 mM H_2O_2 treatments were added in a volume of 3 µl for further 24 hrs to make the final volume per well up to 48 µl. 10 mM H_2O_2 was used as a positive control. For untreated sample, only cells containing media were used. An additional sample was plated which was used as unstained cells, this contained just cells and media like the untreated. After 24 hrs, 2 µl DCFDA was added so that the final concentration is 10 µM in a total volume of 50 µl from a stock of 2 mM. The plate was then shaken on a plate shaker for 20 seconds and incubated at 37 ^{o}C in the CO_2 incubator for 1 hr. After an hour, 12 µl of 15 mM EDTA per well was added, shaken on a plate shaker for 20 seconds and incubated at 37 ^{o}C in the CO_2 incubator until cells lift (usually 40-45 mins) (Kaur and Esau 2015). Once the cells are lifted 15 µl of serum free media was added to all wells and incubated for 5-10 mins. This was done to keep consistency with total

volume of 77 µl (as described in section 5.7.3) and allows the use of consistent settings on flow cytometer instruments. After ~10 mins, the entire constituents from the wells were carefully transferred in separate vials (each vial for each sample) and foiled individually and then analysed in a 1D plot of the FL1 channel using BD Accuri™ C6 Flow Cytometer.

5.7.5 CASPASE-3/7 ASSAY

Principle:

The Caspase-3/7 Assay (Muse® Caspase-3/7 Assay Kit), enables concurrent measurement of caspase-3/7 activity and cell death together. The assay gives a measure of the percentage of cells in all the stages of apoptosis based on caspase-3/7 activity in conjugation with a dead cell dye. The Caspase-3/7 reagent is fluorogenic and measures the caspase-3/7 activity. The Assay also uses a cell death dye, 7-AAD which provides knowledge on membrane integrity. The Caspase-3/7 reagent contains a DNA-binding dye, conjugated to a tetrapeptide sequence of DEVD substrate **(Fig. 15)**. The reagent is non-fluorescent by itself when it is still conjugated to DEVD, because the DEVD peptide impedes the DNA binding capacity of the dye. When caspase-3/7 is activated in unhealthy cells, the peptide gets cleaved following which, the dye is released enabling binding to DNA and produce a high fluorescence. 7-AAD (The dead cell marker) is not included in the live and early apoptotic cells, but enters the late stage apoptotic and dead cells since their membranes are compromised. These cells thus show enhanced fluorescence. The fluorescence of the dye when bound to DNA is ~530 nm and can be analysed using a standard FITC filter set.

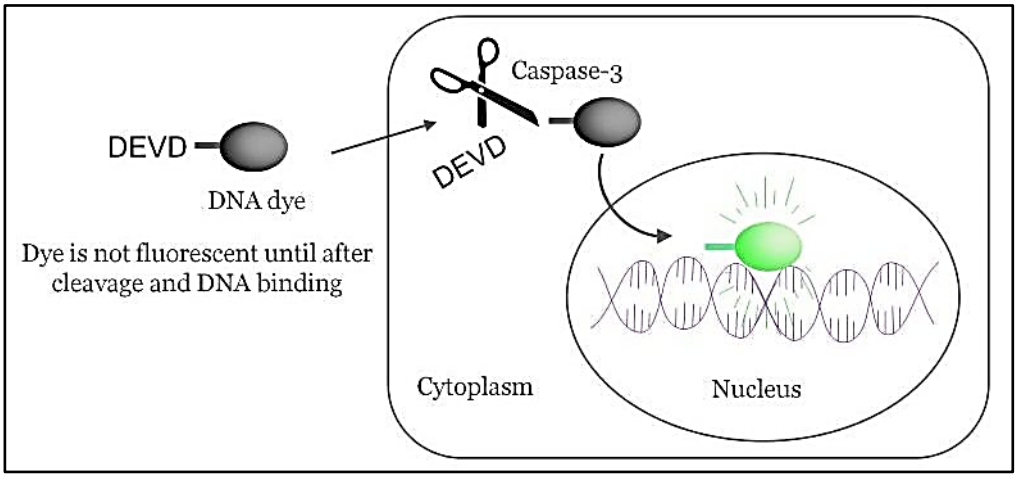


Fig. 15: The mechanism of Caspase-3/7 assay. *DNA does not bind to the non-fluorescent substrate. The high-affinity DNA dye is released to bind DNA after the enzyme is cleaved and become fluorescent [Image adopted from: [www. biotium.com, Accessed 12.01.19].*

Protocol:

50,000 cells were plated as mentioned in section 5.5.1 in 6 well plates at a volume of 3 ml. After 24 hrs of cell adhesion, 10 mM HPβCD, 10 µM or 40 µM PL treatments were done for another 24 hrs (as mentioned in section 5.6.1). 10 µM PL was used as a positive control for MCF7 only (because at higher concentrations apoptosis could not be captured) and 40 µM PL was used as a positive control for MDA-MB-231 and HEK-293 cells. For untreated sample, only cells containing media were used. After trypsinization, the cells were pelleted at 4000 x g for 4 mins. The pellets were then re-suspended in 50 µl of 1 X Assay Buffer BA (Merck, USA). The Muse™ Caspase-3/7 Reagent (Merck, USA) working solution was prepared by diluting the stock solution in 1:8 ratio with 1 X PBS in the dark. 5 µl of the working solution was then added to each 50 µl sample and incubated at 37 °C for 30 mins in an incubator (ThermoFischer SCIENTIFIC, USA). Finally, the Muse™ Caspase-7-AAD working solution (Merck, USA) was prepared by adding 2 µl of the stock solution to 148 µl of 1 X Assay Buffer (BA) for each sample. Following the 30 mins incubation, 140 µl of the Caspase-7-AAD working (Merck, USA) solution was added to each sample and incubated at room temperature (RT) in the dark for 5 mins. The samples were then analysed using the Muse™ Cell Analyser (Merck, USA) with appropriate gates to eliminate cell debris.

5.8 CHOLESTEROL ASSAYS

5.8.1 CHOLESTEROL QUANTIFICATION ASSAY

Principle:

The test is a catalyst (enzyme) driven response which evaluates and quantifies both free cholesterol and CE's. The assay gives an estimation of the cholesterol content mass in micrograms (µg). CE's are hydrolyzed by cholesterol esterase into cholesterol, and then oxidized by cholesterol oxidase into ketone cholest-4-en-3-one and H_2O_2 **(Fig. 16)**. H_2O_2 is then recognized by an extremely specific probe (Ampliflu™ Red - Merck, USA). Horseradish peroxidase (HRP) is responsible for the catalysis of the reaction between the probe and H_2O_2 in a 1:1 ratio. This reaction leads to the development of a pink colour, which is read at 570 nm using a microtiter plate reader.

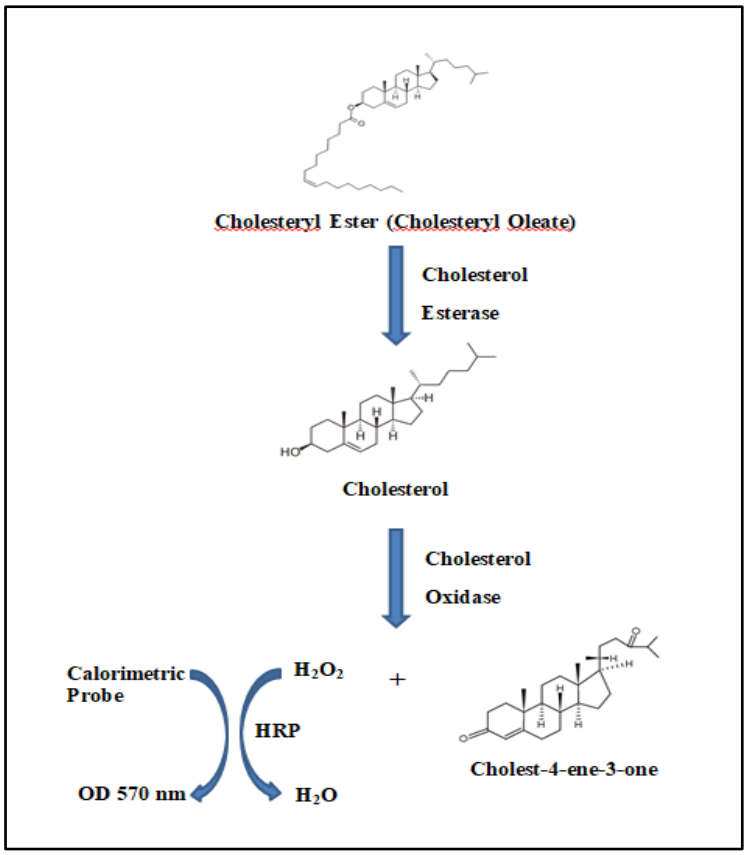


Fig. 16: Principle of cholesterol quantification assay. *CE's are hydrolyzed and eventually HRP catalyses the reaction. Image adopted from: www.bioscience.co.uk/userfiles/pdf/STA-384-total-cholesterol-colorimetric-assay-kit.pdf, Accessed: 12.01.19)*

Protocol:

5000 cells were plated as mentioned in section 5.5.1 in 96 well plates. After 24 hrs of cell adhesion, HPβCD and PL were added in a desired volume so that the final concentration in the wells are 10 mM and 40 µM for HPβCD and PL respectively where 40 µM PL was used as a positive control. The treatment was done for further 24 hrs (as mentioned in section 5.6.1). For untreated sample, only cells in media were used. Cells were plated in duplicates and in two sets. Duplicates were preferred over triplicates in order to make the assay cost-effective because the probe is highly expensive. One set was used to test for total cholesterol in the presence of cholesterol esterase and the other for free cholesterol. 10 µl of 100 U/mL catalase (Merck, USA) was then added to each well and incubated for 15 mins at 37 °C. Catalase was added in order to reduce the background absorbance. Reagent A was prepared and then added to each well as per **Table 4** below.

Table 4: Components comprising Reagent A added per well

	Total Cholesterol (with esterase) (µl/well)	Free Cholesterol (without esterase) (µl/well)
1 M Potassium phosphate buffer (KPO_4) (Merck, USA)	2.5	2.5
1 M Sodium chloride (NaCl) (Merck, USA)	6.25	6.25
100 mM Cholic acid (Merck, USA)	1.25	1.25
100% Triton-X-100 (Merck, USA)	0.25	0.25
20 U/mL cholesterol oxidase (Merck, USA)	2.5	2.5
150 U/mL HRP (Merck, USA)	1.44	1.44
25 U/mL cholesterol esterase (Inqaba Biotec™, SA)	3.33	-
Isopropanol: NP-40 (Nonident-P40) (9:1) (Merck, USA)	6.48	9.81
10 mM Ampliflu™ Red (Merck, USA)	1	1

After 15 mins of incubation with the catalase, 25 µl of Reagent A (with esterase and without esterase, respectively) was added to the each well and incubated in the dark for 30 min at 37 °C. The OD of each well was subsequently measured at 570 nm using a microtiter plate reader Multiskan GO Microplate Reader (Thermo Fisher Scientific, SkanIt™ software). The cholesterol concentration was calculated in comparison to the known cholesterol standards (0, 5, 10, 15, and 20 µg/ml) **(Fig. 17)**.

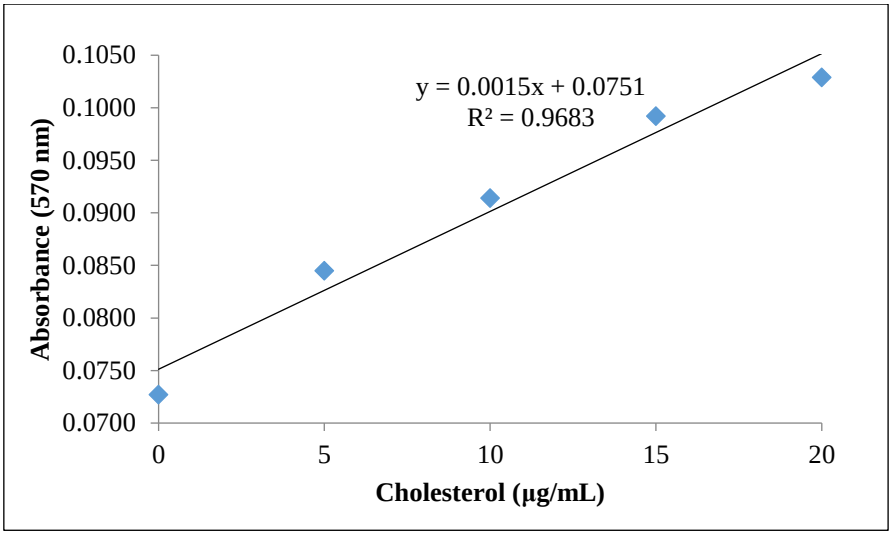


Fig. 17: A representative cholesterol standard curve.

Calculating CE's:

Average of samples -Average of blanks =(**a**)

Substituted y-value with (**a**) in y= mx + c formula in standard curve above
∴ x-value=cholesterol concentration (µg/ml)
µg/ml converted to µg/µl

x-value ÷1000 ×total volume in well=cholesterol concentration (µg/µl)

Total cholesterol-Free cholesterol=Cholesterol esters

5.8.2 CHOLESTEROL STAINING WITH FILIPIN

Principle:

Filipin is a sterol-binding molecule and was isolated from cultures of *Streptomyces filipinensis*. It is a fluorescent dye which allows visualization of sterols with a fluorescence microscope. Sterols are integral components of lipid rafts and Filipin can be used to detect areas in the cell, which are enriched with sterols and also correlates to areas rich in lipid rafts. Filipin is anti-fungal and this mechanism of action is due to the alterations in membrane permeability and other functions by conjugating to membrane sterols. Filipin III (Surls, Nazarov-Stoica et al. 2012) is the major component in Filipin dye. Interaction with cholesterol alters its fluorescence and absorption spectra allowing visualization using fluorescence microscopy.

Protocol:

Filipin stock was made at a concentration of 25 mg/ml in DMSO (Merck, USA), which was diluted to 0.05 mg/ml in PBS to make the working solution. 50,000 cells were plated (as mentioned in section 5.5.1) in 6 well plates containing cover slips (cells were grown on cover slips) at a volume of 3 ml. After 24 hrs of cell adhesion, 10 mM HPβCD and 5 mM MβCD treatments were done for further 24 hrs (as mentioned in section 5.6.1). 5 mM MβCD was used as a positive control. For untreated sample, only cells containing media and the Filipin dye were used. Cells were then washed 3 times with PBS and fixed with 10% formalin (Merck, USA) for 10 mins. After 10 mins, cells were rinsed again 3 times with PBS. 1 ml of Filipin working solution was then added and cells were stained for 2 hrs at RT. Cells were then given a final wash 3 times with PBS and the cover slips (containing cells) were then transferred onto microscopy slides to be viewed by a fluorescence microscope (390-446 nm) using FLoid™ Cell Imaging Station (ThermoFischer Scientific, USA).

5.8.3 WESTERN BLOTTING and SDS-PAGE

Principle:

Western blotting is a fast and extremely sensitive assay to characterize proteins. The proteins are separated via a polyacrylamide gel based on their molecular weight**.** It is widely used to identify a particular protein of interest from a mixture of proteins.

Protocol (preparation of lysates):

Treated and non-treated MCF, MDA-MB-231and MRC-5 cells were harvested (10^6 cells/well) and pelleted at 4000 x *g* for 5 mins. To prepare the cell lysates, the supernatant was removed and pellets were re-suspended in 1 X RIPA or lysis buffer (prepared according to **Table 5** below) (100 µl/10^6 cells) on ice for 30 mins. Lysis buffer disrupts the cell membrane thus releasing the internal proteins and components of the cell. It solubilizes the cell membrane by interacting with the integral membrane proteins and thereby disrupting them. The protein concentrations of each cell sample were calculated using a bicinchoninic acid (BCA) assay.

Table 5: Lysis buffer components.

	Components for 100 mL
1 X RIPA/Lysis buffer	• 300 mM NaCl = 0.876 g • 1% Triton-X-100 = 1 mL • 1% Deoxycholate = 1 g • 0.1% SDS (1 mL of 10% SDS) • 50 mM Tris = 1.21 g • 10 mM EDTA = 1 mL (All reagents from Merck, USA)

5.8.3.1 Protein quantification: BCA assay

Principle and protocol:

Under alkaline conditions, there is formation of a Cu^{2+}-protein complex which is then followed by reduction of the Cu^{2+} to Cu^{1+}. The extent of reduction directly corresponds to the measure of protein present. A purple-blue complex is formed when BCA interacts with Cu^{1+} in alkaline conditions and the reduction of alkaline Cu^{2+} by the proteins is estimated. The coloured reaction can then be quantified spectrophotometrically (Walker 2002). The protein content of unknown samples can be estimated by comparing with a known protein standard (Smith, Krohn et al. 1985). Quantifying proteins prior to sodium dodecyl sulfate polyacrylamide gel electrophoresis (SDS-PAGE) is essential to ensure equal loading of protein concentrations in order to interpret the expression levels. A bovine serum albumin (BSA) (Amresco; Inqaba Biotec™, SA) standard curve was generated **(Fig. 18)** using the following BSA concentrations; 1, 0.8, 0.6, 0.4, 0.2 and 0 mg/ml. 25 µl of each standard concentration was added into a 96 well plate in triplicates. The protein concentration of each lysate was evaluated by adding 5 µl of protein lysate and 20 µl of 1 X lysis buffer into each well in triplicates. This was then followed with the addition of 200 µl of BCA reagent mix (196 µl of BCA (Merck, USA) and 4 µl of Cu^{2+} (Merck, USA) was added into each well and the plate was incubated at 37 °C for 30 min. The OD of each well was then measured at 562 nm using a microtiter plate reader Multiskan GO Microplate Reader (Thermo Fisher Scientific, SkanIt™ software). The protein concentration of each lysate was calculated using Microsoft Office Excel©.

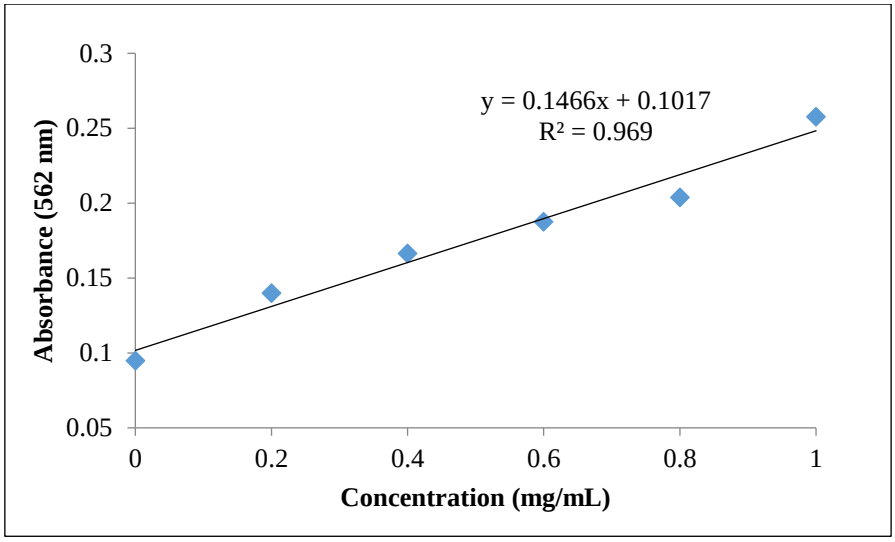


Fig. 18: A representative BSA protein standard curve.

Calculating protein lysate concentrations:

Average of samples-Average of blank=(**a**)

Substituted y-value with (**a**) in y= mx+ c formula in standard curve above

∴x-value ×5 (dilution factor)=protein lysate concentration (mg/ml)

5.8.3.2 SDS-PAGE

Principle:

The standard curve above **(Fig. 18)** allowed calculations to be made in order to determine the amount of 2 x Laemmli sample buffer (Bio-Rad, USA), which contained β-mercaptoethanol and SDS, to be added to the samples. Protein samples were then loaded into wells in the gel and electric voltage was connected. β-mercaptoethanol separates the disulfide bonds involved in protein folding and SDS imparts negative charge to the proteins and subsequently linearizing them. The proteins keep running towards the anode through the gel when electric field is connected.

Protocol:

The samples were boiled at 85 °C for 5 mins and placed on ice immediately. 20 µl of the normalized sample with a total protein concentration of 20 µg was loaded per well in the gel (as per **Table 6**) for analysis and the gel was run at 120 volts (V) for 1 hr. A protein molecular weight marker (Precision Plus Protein™ unstained standards (Bio-Rad, USA) was included for size estimation. Buffers, Bis-acrylamide, APS (Ammonium per sulphate) were prepared as per **Table 7**.

Table 6: SDS-PAGE gel (10%, 1 mm) components.

Components	Resolving gel	Stacking gel
Resolving gel buffer with SDS (Merck, USA)	3 ml	-
Stacking gel buffer with SDS	-	750 µl
30% Bis-acrylamide (Merck, USA)	3 ml	500 µl
Distilled water (dH_2O)	3 ml	1.75 ml
10% Ammonium persulfate (APS) (Merck, USA)	100 µl	30 µl
Tetramethylethylenediamine (TEMED) (Merck, USA)	10 µl	3 µl

Table 7: SDS-PAGE buffer components.

	Components
Resolving gel buffer	• 36.2 g Tris • 0.8 g SDS • Dissolve in 150 ml dH_2O • pH to 8.9 • Make up to 200 ml with dH_2O
Stacking gel buffer	• 5.9 g Tris • 0.4 g SDS • Dissolve in 70 ml dH_2O • pH to 6.8 • Make up to 100 ml with dH_2O

30% Bis-acrylamide	• 30 g Acrylamide • 0.8 g Bis-acrylamide • 0.1 g SDS • Make up to 100 ml dH_2O
10% APS	• 100 mg APS in 1 ml dH_2O

5.8.3.3 Western blot

Resolved proteins were then transferred onto a 0.22 3M polyvinylidene fluoride (PVDF) membrane for 30 mins using the Trans-Blot®Turbo™ Transfer System (Bio-Rad, USA). The PVDF membrane was used as opposed to a nitrocellulose membrane as it is generally used for high molecular weight proteins ($\geq$20 kDa) and has higher binding capacity which allows enhanced sensitivity in the detection of lowly expressed proteins.

The membrane was then blocked in a 5% BSA *(*Amresco; Inqaba Biotec™, SA) made in Tris-buffered saline (TBS) (50 mM Tris-Cl, pH 7.5 and 150 mM NaCl) with 0.1% Tween-20 (Merck, USA) for 1 hr to prevent non-specific binding. Incubation of the membrane with relevant primary antibodies (anti-SREBP1 or anti-β-tubulin; loading control) (1:1000) was performed overnight at 4 °C. Thereafter, 5 x 5 mins of 1 X Tris-Buffered saline with Tween-20 (TBST) washes were performed to wash off unbound antibodies followed by the addition of specific secondary antibodies (1:2000) incubated for 1 hr at RT. Subsequent 1 X TBST washes were performed for 5 x 5 mins.

Chemiluminescence was performed by using Clarity™ Western ECL Substrates (Bio-Rad, USA). The membrane was incubated in equal volumes of Peroxidase solution and Luminol/enhancer solution for 2 mins in the dark before viewing on the ChemiDoc (Bio-Rad, USA). Densitometry was performed using the Image Lab™ 4.0 Software (Bio-Rad, USA).

5.9 XENOGRAFT STUDY

Principle:

MF-1 Nude mice were chosen for this study as these mice are immunodeficient therefore permit transplantation of tumour cell xenografts without showing any graft versus host response. Novel investigations, are considered inappropriate to directly test it on humans without preliminary investigations in animal model. Animal studies need short amount of time

and allow easier data acquisition. Additionally, animal studies can provide a firm basis for possible future testing in humans.

Ethical approval

The study was approved by the Animal Research Ethics Committee (AREC), WITS and the approval certificate number is 2017/10 69/B.

Protocol:

The non-blinded study was performed at animal facility located at the Central Animal Services (CAS) Unit, Wits Medical Campus, Parktown, Johannesburg. The approvals were obtained from the ethics committee of WITS. 14 MF-1 female nude mice were used for the study and the animals were acclimatized for one week and had access to free food and water during the study.

This study was an intervention study as we were testing the effects of HPβCD on BC development and treatment. The study was sub-divided into 4 groups as mentioned below and **Fig. 19**:

1. Mice injected with MDA-MB-231 cells (4 mice) but not treated with HPβCD to serve as control. (Tumour size ~13000 mm^3).
2. Mice injected with MDA-MB-231 cells (4 mice) and treated with HPβCD (Late stage, tumour size ~3500 mm^3).
3. Mice injected with MDA-MB-231 cells (3 mice) and treated with HPβCD (Intermediate stage, tumour size ~800 mm^3).
4. Mice injected with MDA-MB-231 cells (3 mice) and treated with HPβCD (early stage, tumour size ~20 mm^3).

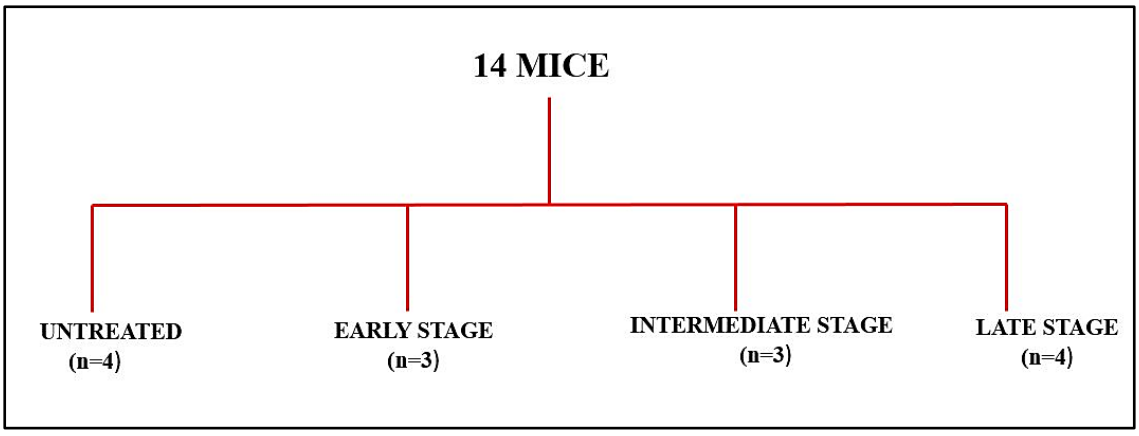


Fig. 19: Groups of mice used in the study.

MDA-MB-231 cancer cell lines were injected subcutaneously into the left flank of the MF-1 Nude mice thereby resulting in tumour growth. Tumour xenografts were measured by calliper in two dimensions (2D) thrice a week until the tumours reach a certain size and the response to HPβCD were studied *in vivo*. A maximum of 3000 mg/kg body weight of HPβCD, were injected as an intraperitoneal (IP) injection upto a maximum of 3 weeks for a maximum amount of 10 doses. The response to therapy was evaluated by investigating the effects of HPβCD on the weight of mouse, growth rate and shrinkage/regression of the tumour (Liu, Hung et al. 2014).

The total duration of the study was approximately 14 weeks. Mice tumours for MDA-MB-231 induced tumours reached ~18000 mm^3 in **5 weeks**. Then treatments with HPβCD were done for **2-3 weeks**. Here is the breakdown of time:
Acclimatization of mice: 1 week
MDA-MB-231 injected: 1 week
Tumour growth: **5 weeks**
Drug treatment: **2-3 weeks**
Relapse test: 4 weeks
Total approximate duration of the study: 13 weeks (excluding 1 week acclimatization)

The weight chart **(Fig. 56)** has been shown for 12 weeks [5 weeks (tumour growth) +2-3 weeks (treatment) +4 weeks (relapse for early stage)]. Weight for late and intermediate stage could not be documented after 8 weeks because mice were euthanized at this point to meet humane end points.

5.9.1 Inoculation

Using 28-gauge ½-in. insulin syringes (Monoject™, USA) the mice were injected with MCF7 or MDA-MB-231 cancer cells in PBS (100 µl). Cells were inoculated subcutaneously into the left flank of each mice for MDA-MB-231 cells.

5.9.2 Anaesthetization

The mice were anaesthetized using 2 % Isoflurane [Bayer (Pty) Ltd Animal Health Div., South Africa]. The mice were briefly anaesthetized in order to keep them motionless.

5.9.3 Measurements and observations made on animals

The response to therapy can be evaluated by investigating the effect of the drug on the growth rate, shrinkage/regression of the tumour (Kelland 2004). Tumour size were determined by

calliper in two dimensions (2D), thrice a week during the 2-3 weeks of treatment and weight measurements were done. Photographs of the mice were also taken.

5.9.4 Terminal procedures

After the mice have received all their treatments, they were euthanised using Eutha-naze (Bayer (Pty) Ltd Animal Health Div., South Africa) containing Sodium Pentobarbitone. At termination, mice were necropsied; blood were collected for alanine aminotransferase (ALT) and aspartate aminotransferase (AST) measurements. Tumour size was expressed in mm^3 using the formula: $V = 1/2 \times a \times b^2$ where 'a' and 'b' represent the long and short diameters of the tumour respectively. The tumour mass was weighed and photographed at the end of the experiment after being harvested. The tumour mass were cut into small pieces and snap frozen in liquid nitrogen for RNA extraction. Tumour inhibition rate was calculated as Inhibition rate (%) = (average tumour volume of control group-average tumour volume of test group)/ average tumour volume of control group×100%.

5.9.5 Alanine transaminase/aspartate transaminase (ALT/AST) tests

Blood was collected post euthanisation of mice and serum was separated. The serum was then tested for ALT/AST liver toxicity using IDEXX Catalyst Dx Chemistry Analyzer with individual ALT/AST cartridges.

5.9.6 Surgical procedures with recovery

To avoid unnecessary suffering, mice were euthanised when the size of the tumours reached ~13000 mm^3 (Late stage, untreated), ~3500 mm^3 (Late stage, treated), ~750 mm^3 (Intermediate stage, treated), ~25 mm^3 (Early stage, treated) or when animals showed distress. At the termination of the experiment, the whole tumour mass was harvested and weighed. The tissue biopsies were fixed in 10% formalin (Merck, USA) and embedded in paraffin before they are to be processed for histological analysis. Tumours and organs (heart, kidneys, liver, ovaries, brain, lungs and lymphs) were explanted, imaged, and immediately placed in 10% formalin (Merck, USA).

5.9.7 Body fluid sampling

The blood samples were collected at the end of the study when mice were euthanised. The controls sufficed for the study and there was no need to get baseline blood sample values prior to treatments. Blood sample was collected at the end of the study when mice were euthanised. The preferable methods for blood collection from mice are single-stick caudal vena cava method and intracardiac method because of consistency as determined by lower standard deviations (S.D.) and tighter ranges (Schnell, Hardy et al. 2002). We used intracardiac method to draw 1-2 ml of blood using 25- gauge 5/ 8-inch needle (Monoject™, USA).

5.9.8 Biochemistry

Blood samples were taken to measure serum levels AST and ALT measurements to estimate liver toxicity induced by HPβCD treatment. Tissues will be used for RNA extraction for further studies. The tumours will be homogenized and will be used for molecular biology techniques (Western/ Immuno-blotting, flow cytometry, ELISAs, RT-PCR) to test protein expression levels and other changes, to further discern the molecular effects of HPβCD. This will also help to understand the molecular mechanisms linking cholesterol with cancer.

5.9.10 Animal welfare and reduction of suffering, if any

Proper handling and restraint of the mice is pivotal for correct administration of anaesthesia or the test substance (Shimizu 2004) and appropriate care was taken during this procedure. HPβCD and cells were administered in water and PBS respectively which are widely accepted (Liu, Hung et al. 2014) and did not induce pain and tissue damage. The volume of injections is usually calculated based on the size and weight of the mouse and is kept as low as possible. The most commonly used routes for administration of injectables to mice are subcutaneous, IP or intravenous. Subcutaneous administrations are easy and rarely painful (Wolfensohn and Lloyd 2008) and IP injection is the most common route because it is technically simple (Shimizu 2004). The maximal administration volumes for subcutaneous and IP injection are 2-3 ml and intravenous is 200 µl (Shimizu 2004). In this study volumes of less than or equal to 200 µl were used. Usually, 26–27-G needles are permissible for injections. When a small volume (less than 100 µl, as is the case in this study) is administered, an insulin syringe plus needle (27–30-G) is convenient. A complete 'welfare score sheet' for each animal under study was maintained during the course of the study. The animals were also continuously monitored using several 'Humane End-points' as per the score sheet. Following clinical/behavioural

indicators were closely monitored and were used to euthanise animals even before the completion of the study:

1. Weight loss of 15% as compared to control group.
2. Redness in nose or eyes (a sign of stress).
3. A rough coat with fur standing on end
4. If colour of the ears and feet is not pink.
5. If animal is not Bright, Alert, and Responsive.
6. Decreased food and water intake.

Signs of pain to give analgesics:

1. Back arch, belly press, writhe, stagger, twitch and fall.

The animals were closely monitored every day for signs of distress.

5.9.11 Housing conditions

Animals were individually housed (1 mouse/cage) under 12 h light cycle at 22-25 °C temperature and relative humidity of 40-70 %. Food and water was available *ad libitum*.

Environmental friendly cages were used and they had the following:

1. Daily cleaning of cages (additional cleaning of the cages were done whenever animals urinated more frequently).
2. Transfer nest to clean cage with animals during cage change, adding extra bedding or providing new shelter if necessary.
3. Providing nesting material (shredded paper, hay or paper towels)
4. Unlimited water and food supply.

5.9.12 Transport of animals

The mice were bought locally and therefore no permits were required to transport animals to the animal facility. The mice were sourced from University of Cape Town and were transported according to approved transport regulations.

5.10 Statistical analysis

A Z-factor of ≥0.6 was recorded for each assay performed in 96 well plate, indicating good to excellent robustness (Zhang, Chung et al. 1999). One-way Anova test was done followed by a student's *t*-test to determine statistical significance, where $p<0.05$ was used to estimate the significance of the observations. Effect size (ES) was calculated using Cohen's d where 0.2, 0.5, 0.8 and 1.30 represent small, medium, large and very large effect size respectively. All statistics including mean and S.D. calculations were performed using Microsoft Office Excel© or GraphPad Prism5®. The results of each assay were confirmed using technical and biological repeats.

6. RESULTS

6.1 GROWTH INHIBITION ASSAYS

Four different cell lines were used MCF7 (ER+), MDA-MB-231 (TNBC), MRC-5 (Lung Fibroblasts) and HEK-293 (Embryonic kidney). MRC-5 and/or HEK-293 were used as control cell lines depending on availability.

6.1.1 MTT ASSAY

In order to determine whether HPβCD has the ability to induce cancer cell death a primary screening using an MTT assay was performed. Three different time points 24 hrs, 48 hrs & 72 hrs treatment were selected in order to establish the potency of HPβCD. This is in accordance to recent papers published for leukemia (Yokoo, Kubota et al. 2015) and atherosclerosis (Zimmer, Grebe et al. 2016). 40 µM PL was used as a positive control and showed almost 80%, 90% & 100 % growth inhibition at 24 hrs, 48 hrs & 72 hrs respectively. PL is a well-known compound proven to inhibit cancer cell growth (Li, Shen et al. 2012; Eldhose, Gunawan et al. 2014).

Results obtained for MCF7's, showed ~ 45% growth inhibition at 10 mM concentration of HPβCD. Subsequently, the percentage growth inhibition kept on increasing with an increase in concentrations of HPβCD. The results were consistent for all the three time points, thus indicating its potential ability to disrupt the mitochondrial processes and its probable slow action (Fig. 20). The statistically significant difference between groups was determined by one-way ANOVA ($F(4,10)= 1528.5$, $p= 6.95E-14$ (24 hrs), ANOVA ($F(4,10)=544.34$, $p= 1.32E-12$ (48 hrs), ANOVA ($F(4,10)=823.4$, $p= 3.32E-11$ (72 hrs). ES – 2.68, 31.23, 36.84, 39.22, 84.5 for 1 mM, 5 mM, 10 mM, 20 mM, 50 mM (24 hrs) respectively. ES – 28.65, 46.49, 41.32, 86.43, 145.21 (48 hrs) respectively. ES – 18.21, 33.51, 31.43, 76.43, 91.23 (72 hrs) respectively.

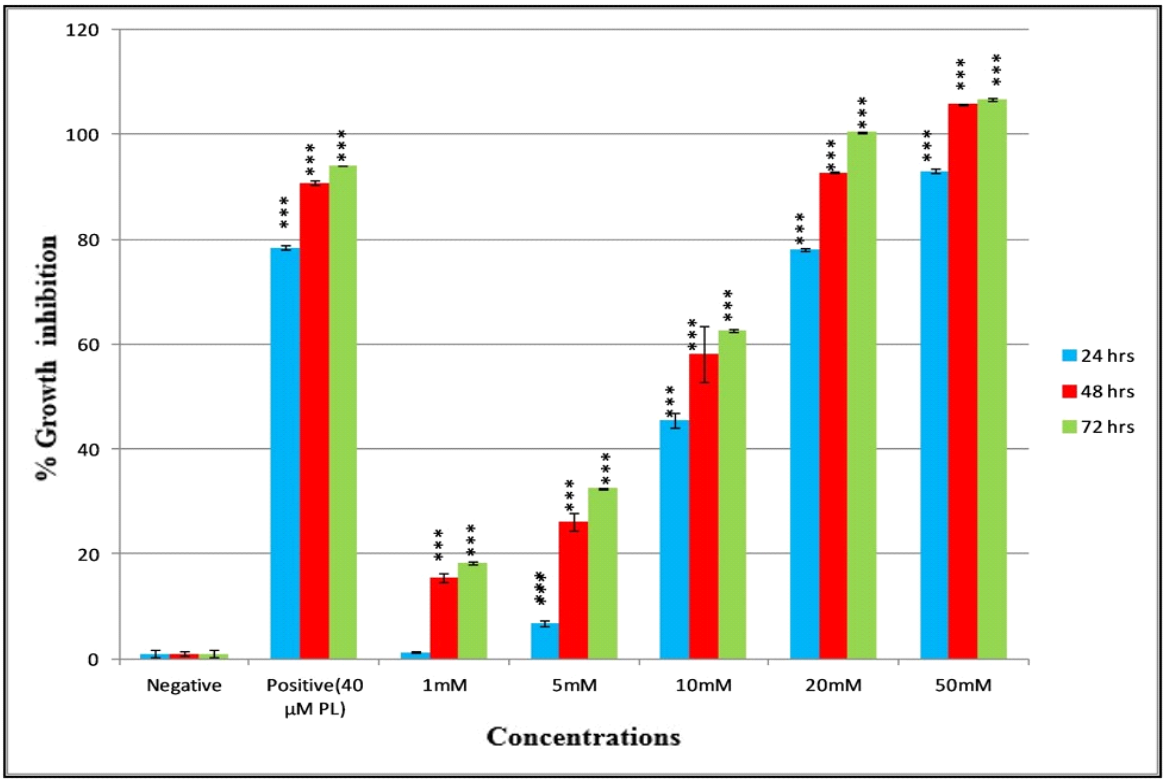


Fig. 20: Graph comparing the percentage growth inhibition of MCF7 cells at selected concentrations of HPβCD *at 1 mM, 5 mM, 10 mM, 20 mM and 50 mM. PL (40 µM) was used as a positive control. Data are mean ± S.D. (n=3) from raw data, where *p<0.05, **p<0.01 and ***p<0.001 significant difference to untreated control. Independent experiments were run at least 3 times.*

Like MCF7s three different time points 24 hrs, 48 hrs & 72 hrs were selected for MDA-MB-231 cells. Results obtained, showed ~ 45% growth inhibition at 10 mM concentration of HPβCD and again, there was a gradual increase in the percentage growth inhibition as the concentrations of HPβCD increased. The results were similar for all the three time points, thus indicating the fact that HPβCD is effective across different breast cancer cells **(Fig. 21).**

PL was used as a positive control and showed almost 85%, 92% & 95 % growth inhibition at 24 hrs, 48 hrs & 72 hrs respectively. The statistically significant difference between groups was determined by one-way ANOVA (F(4,10)= 268.7, p= 3.96E-10 (24 hrs), ANOVA (F(4,10)=1788.88, p= 3.17E-14 (48 hrs), ANOVA (F(4,10)=447.8, p= 3.15E-11 (72 hrs) ES – 1.98, 26.07, 26.67, 19.13, 76.7 for 1 mM, 5 mM, 10 mM, 20 mM, 50 mM respectively. ES- 18.33, 44.17, 21.39, 91.66, 131.95 (48 hrs) respectively. ES- 14.48, 37.55, 10.88, 79.89, 89.28 (72 hrs) respectively.

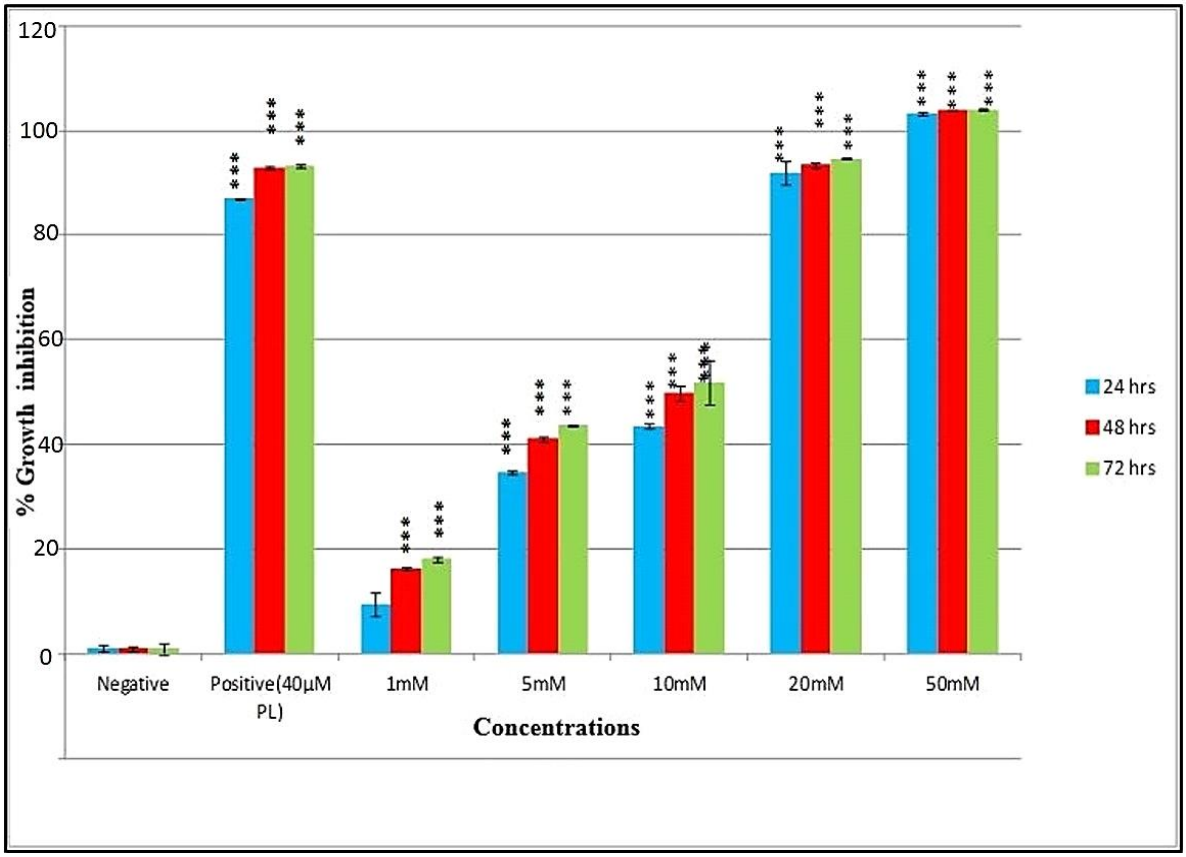


Fig. 21: Graph comparing the percentage growth inhibition of MDA-MB-231 cells at selected concentrations of HPβCD *at 1 mM, 5 mM, 10 mM, 20 mM and 50 mM. PL (40 µM) was used as a positive control. Data are mean ± S.D. (n=3) from raw data, where *p<0.05, **p<0.01 and ***p<0.001 significant difference to untreated control. Independent experiments were run at least 3 times.*

For the control cell lines, MRC-5 and HEK-293 similar time points were selected (24 hrs, 48 hrs, 72 hrs) to maintain consistency. Results obtained, showed absolutely zero growth inhibition till 10 mM concentration of HPβCD. The results hold true for two time points (24 hrs and 48 hrs). Interestingly at 72 hrs **(Black box in Fig. 22 & Fig. 23)**, even 20 mM became

non-toxic to the cells, thus indicating that HPβCD is actually assisting the cells to survive and all the unhealthy cells are now reprogramming themselves and behaving normally. 50 mM was seen to be very toxic for the cells **(Fig. 22 & Fig. 23)** because the dosage was too high. Every cell has a threshold value for a particular drug concentration beyond which it becomes toxic and every drug follows a dose-response approach (Snyder 1984).

The statistically significant difference between groups for MRC-5 and HEK-293 was determined by one-way ANOVA (F(4,10)= 1657.5, p= 4.6E-14 (24 hrs), ANOVA (F(4,10)=1032.6, p= 4.9E-13 (48 hrs), ANOVA (F(4,10)=218.6, p= 1.1E-09 (72 hrs). ES – 11.51, 6.72, 3.66, 13.72, 24.29 for 1 mM, 5 mM, 10 mM, 20 mM, 50 mM (24 hrs) respectively. ES- 5.66, 13.59, 15.93, 66.78, 74.66 (48 hrs) respectively. ES- 150.37, 14.68, 27.24, 5.73, 29.96 (72 hrs) respectively for MRC-5 and ANOVA (F(4,10)= 263.9, p= 4.6E-10 (24 hrs), ANOVA (F(4,10)=823.3, p= 1.52E-12 (48 hrs), ANOVA (F(4,10)=542.3, p= 1.1E-11 (72 hrs). ES – 0.92, 0.83, 1.30, 6.85, 19.42 for 1 mM, 5 mM, 10 mM, 20 mM, 50 mM (24 hrs) respectively. ES- 1.83, 0.28, 4.45, 28.66, 42.91 (48 hrs) respectively. ES- 7.77, 7.96, 2.30, 27.44, 46.74 (72 hrs) respectively for HEK-293.

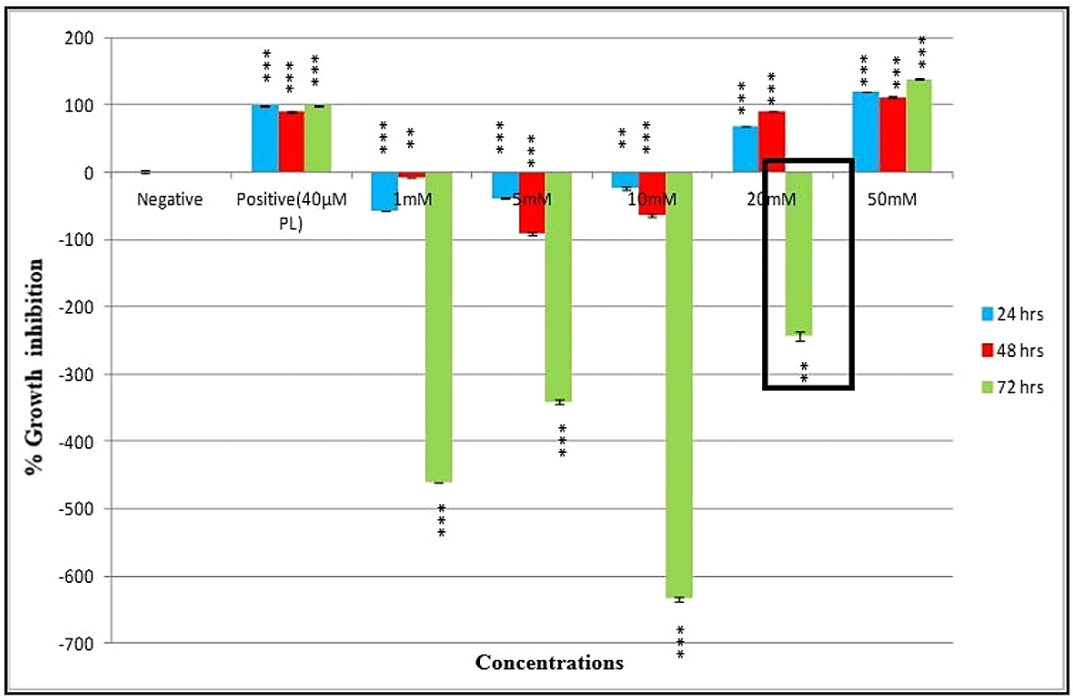


Fig. 22: Graph comparing the percentage growth inhibition of MRC-5 cells at selected concentrations of HPβCD *at 1 mM, 5 mM, 10 mM, 20 mM and 50 mM. PL (40 µM) was used as a positive control. Data are mean ± S.D. (n=3) from raw data, where *p<0.05, **p<0.01 and ***p<0.001 significant difference to untreated control. Independent experiments were run at least 3 times.*

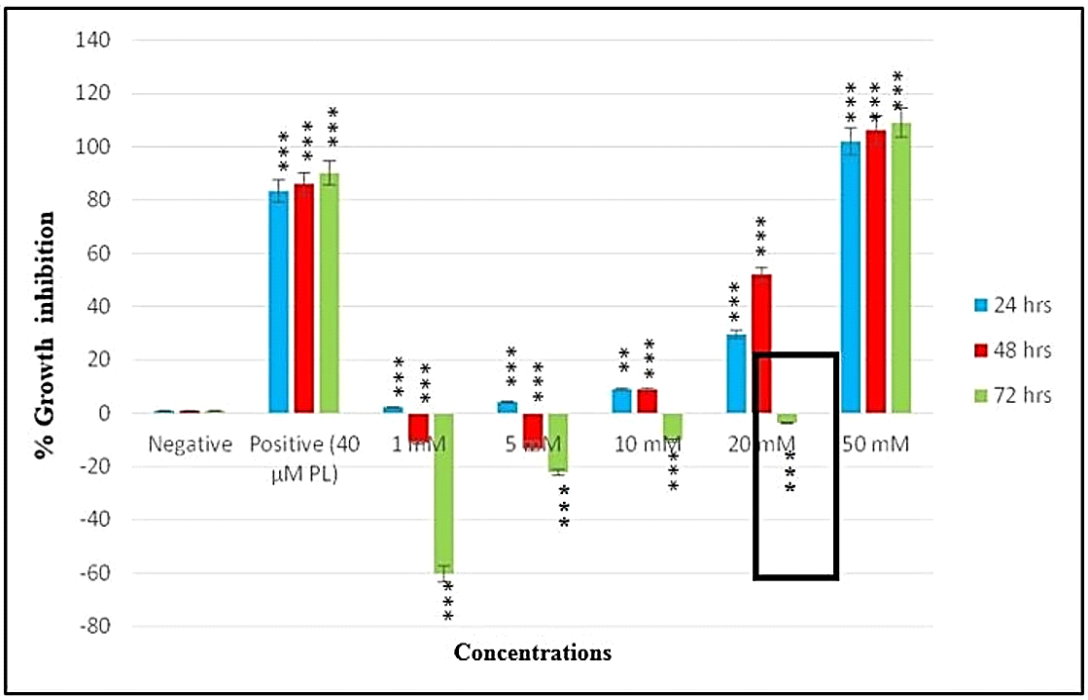


Fig. 23: Graph comparing the percentage growth inhibition of HEK-293 cells at selected concentrations of HPβCD *at 1 mM, 5 mM, 10 mM, 20 mM and 50 mM. PL (40 µM) was used as a positive control. Data are mean ± S.D. (n=3) from raw data, where *p<0.05, **p<0.01 and ***p<0.001 significant difference to untreated control. Independent experiments were run at least 3 times.*

Upon calculating the IC_{50} values which is the concentration required to cause 50% growth inhibition, it was seen that almost double the concentration of HPβCD was required to cause 50% growth inhibition in both the cell lines at 24 hrs **(Table 8)** and at 72 hrs the concentration went up to almost five times as compared to the cancerous cells, thus indicating that HPβCD is specifically toxic to cancerous cells.

Table 8: Shows IC_{50} values for MCF7, MDA-MB-231, MRC-5 and HEK-293 cells.

	IC_{50} Values (mM)		
Cell Line	**24 hrs**	**48 hrs**	**72 hrs**
MCF7	11.11	9.82	7.45
MDA-MB-231	12.34	11.22	8.56
MRC-5	20.67	19.89	41.69
HEK-293	22.81	26.53	50.26

6.1.2 Cell-APOPercentage APOPTOSIS ASSAY

As mentioned in 5.7.2, APO-Percentage assay gives a measure of overall apoptosis in the cell. Apoptosis is an early event and therefore just one time point (24 hrs) was selected and tested on four cell lines MCF7, MDA-MB-231, MRC-5 & HEK-293 cells. 10 µM PL was used as a positive control as opposed to 40 µM from MTT because higher concentrations of PL was way too toxic for the cells and to capture the early activity, optimal dosage was required. This assay was performed to check if the growth inhibition obtained from the MTT assay was actually due to apoptosis. The APOPercentage apoptosis assay is a robust assay and quite recently has been gaining popularity amongst researchers (Sagar, Esau et al. 2014; Omoyeni, Hussein et al. 2015). Results for MCF7 showed 45 % cell death at 10 mM concentration of HPβCD. The cell death percentage was proportional to an increase in concentration of HPβCD across all the treatments (Fig. 24). 10 µM PL was used as a positive control and yielded almost 90% apoptosis.

Pictures **(Fig. 25)** taken under a light microscope post staining with the APOPercentage dye validates our graphical data, where it is clear that as the concentration of HPβCD increases the number of cells taking up pink dye increase, thus indicating an increase in apoptosis. The statistically significant difference between groups was determined by one-way ANOVA ($F(4,10)= 2231.56$, $p= 2.4E-10$. ES – 43.21, 66.22, 56.89, 121.76, 136.72 (for 1 mM, 5 mM, 10 mM, 20 mM, 50 mM respectively.

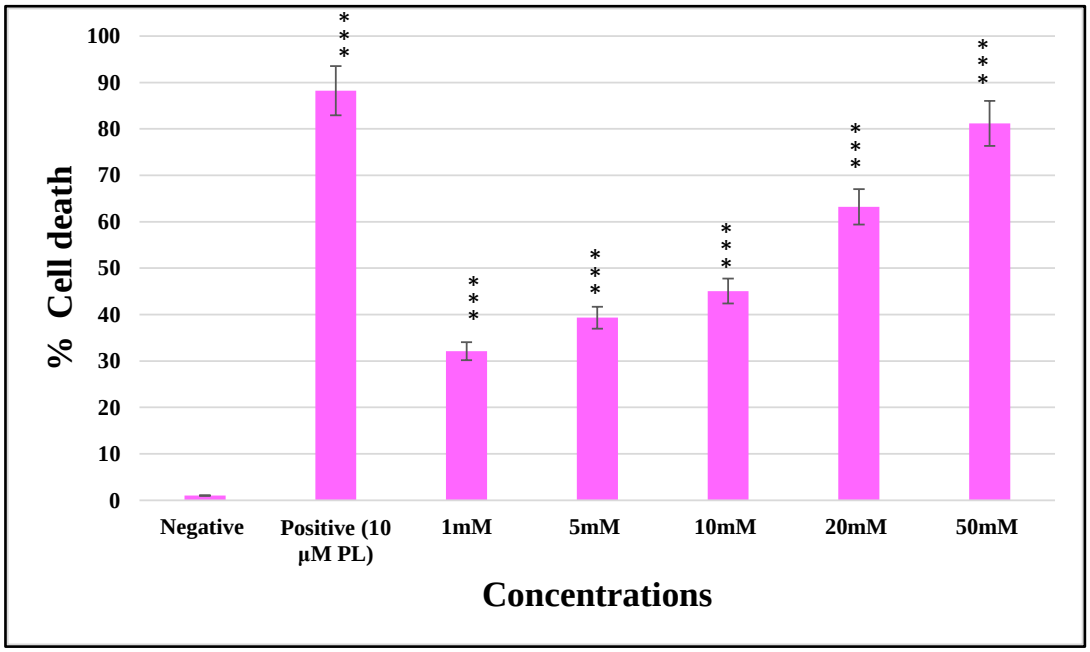


Fig. 24: Graph comparing the percentage of apoptosis in MCF7 cells at selected concentrations of HPβCD *at 1 mM, 5 mM, 10 mM, 20 mM, 50 mM and negative samples. PL (10µM) was used as a positive control. Data are mean ± S.D. (n=3) from raw data, where *p<0.05, **p<0.01 and ***p<0.001 significant difference to untreated control. Independent experiments were run at least 3 times.*

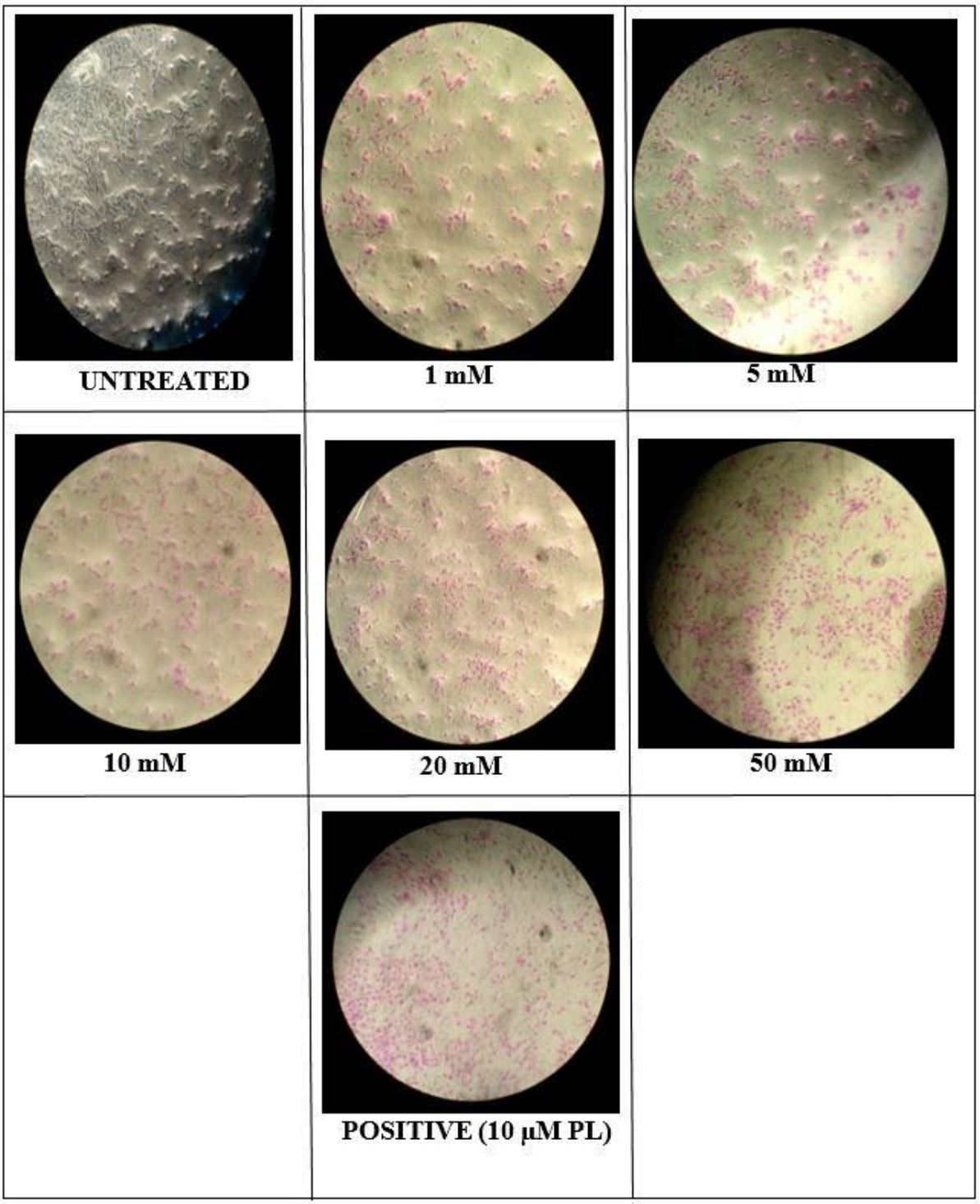


Fig. 25: Light microscope images showing the amount of apoptosis in MCF7 cells *at selected concentrations of HPβCD at 1 mM, 5 mM, 10 mM, 20 mM ,50 mM and untreated samples. PL was used as a positive control.*

MDA-MB-231 cells showed 40 % cell death (lesser than MCF7) at 10 mM concentration of HPβCD **(Fig. 26)**. Like MCF7's, the cell death percentage kept increasing at all the higher concentrations of HPβCD and the maximum cell death achieved was ~ 70 % at 50 mM HPβCD. 10 µM PL was used as a positive control and the percentage of apoptosis observed was almost 90 %. Pictures taken under a light microscope post staining with the APO Percentage dye validates our graphical data **(Fig. 27)** where, like MCF7's it is clear that as the concentration of HPβCD increases the number of cells taking up pink dye increase, thus indicating a gradual progression in apoptosis. The statistically significant difference between groups was determined by one-way ANOVA (F(4,10)= 954.2, p= 1.5E-11. ES – 31.25, 43.55, 86.54, 126.44, 151.43 for 1 mM, 5 mM, 10 mM, 20 mM, 50 mM respectively.

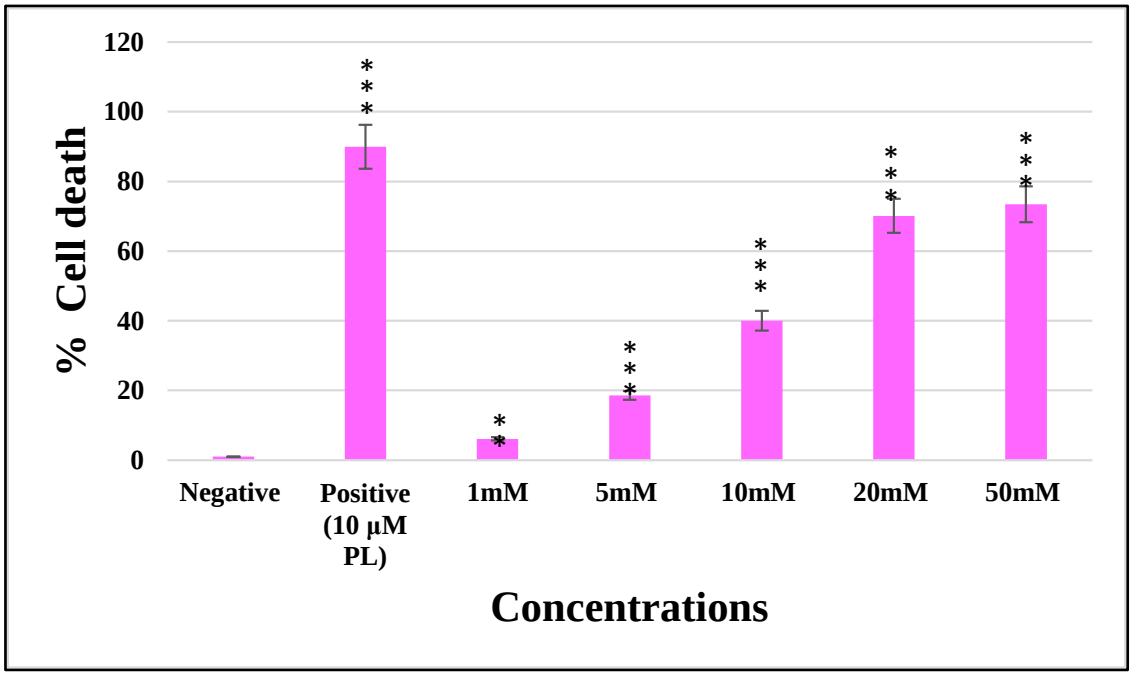


Fig. 26: Graph comparing the percentage of apoptosis in MDA-MB-231 cells at selected concentrations HPβCD *at 1 mM, 5 mM, 10 mM, 20 mM, 50 mM and negative samples. PL (10µM) was used as a positive control. Data are mean ± S.D. (n=3) from raw data, where *p<0.05, **p<0.01 and ***p<0.001 significant difference to untreated control. Independent experiments were run at least 3 times.*

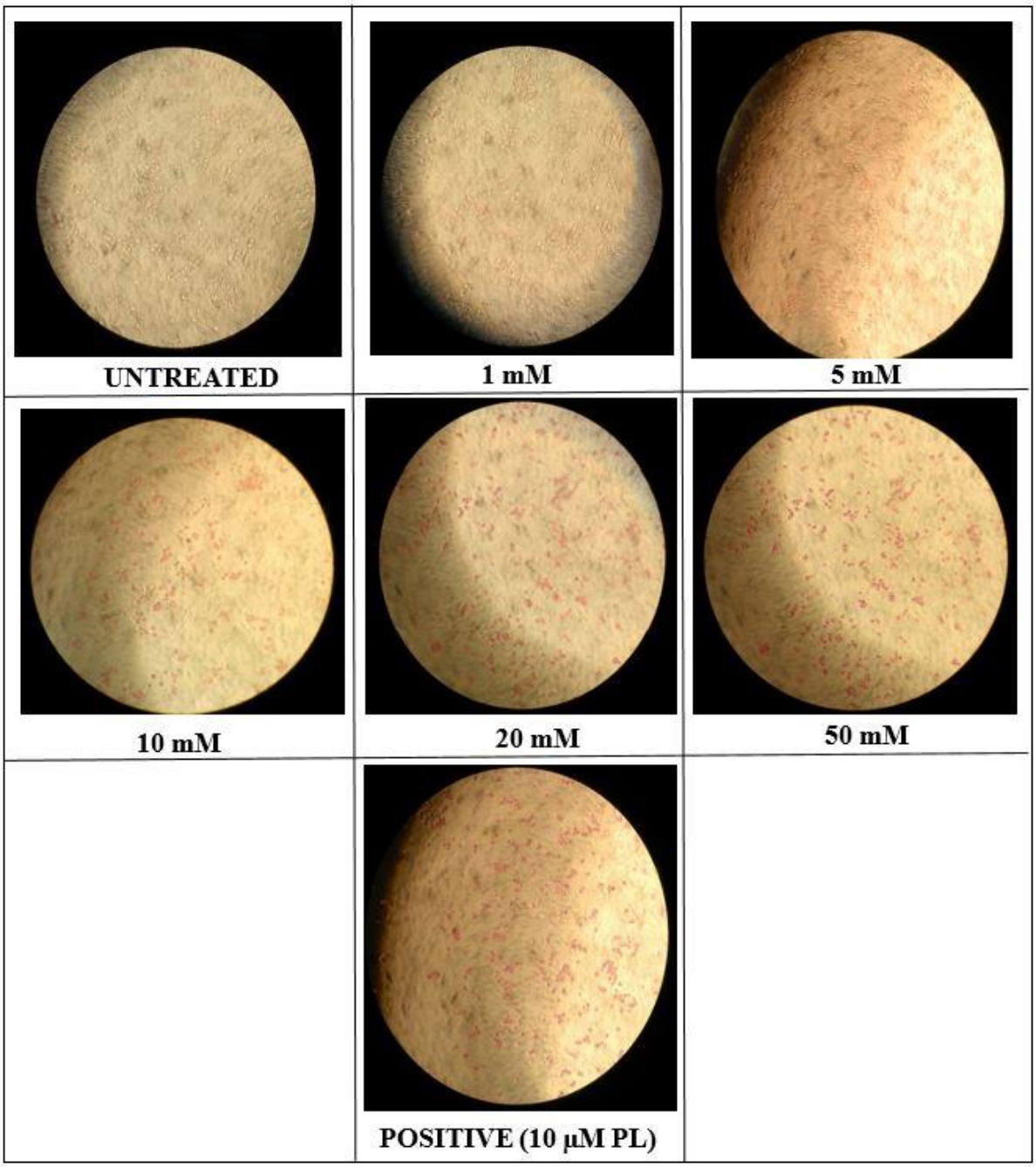


Fig. 27: Light microscope images showing the amount of apoptosis in MDA-MB-231cells at selected concentrations of HPβCD *at 1 mM, 5 mM, 10 mM, 20 mM ,50 mM and untreated samples. PL was used as a positive control.*

Finally, for the normal cells (MRC-5 and HEK-293), the results obtained demonstrated negligible cell death till 10 mM concentration of HPβCD (Fig. 28 & Fig. 30). 20 mM & 50 mM resulted in ~ 19% and ~20% cell death respectively for both the cell lines. Pictures taken under a light microscope post staining with the APO Percentage dye validated our graphical data (Fig. 29 & Fig. 31) and it is quite evident that there was no dye uptake by the cells till the concentration of 10 mM HPβCD. At higher concentrations, very little pink intensity was seen which corroborates with the graphical data and therefore confirms the fact that HPβCD is indeed toxicologically benign to normal cells. The statistically significant difference between groups was determined by one-way ANOVA (F(4,10)= 1134.7, p= 1.1E-14. ES – 1.11 , 4.23, 11.32, 23.48, 42.34 (for 1 mM, 5 mM, 10 mM, 20 mM, 50 mM respectively for MRC-5 and ANOVA (F(4,10)= 521.6, p= 1.1E-11. ES – 0.73, 2.27, 16.22, 21.23, 28.44 for 1 mM, 5 mM, 10 mM, 20 mM, 50 mM respectively for HEK-293.

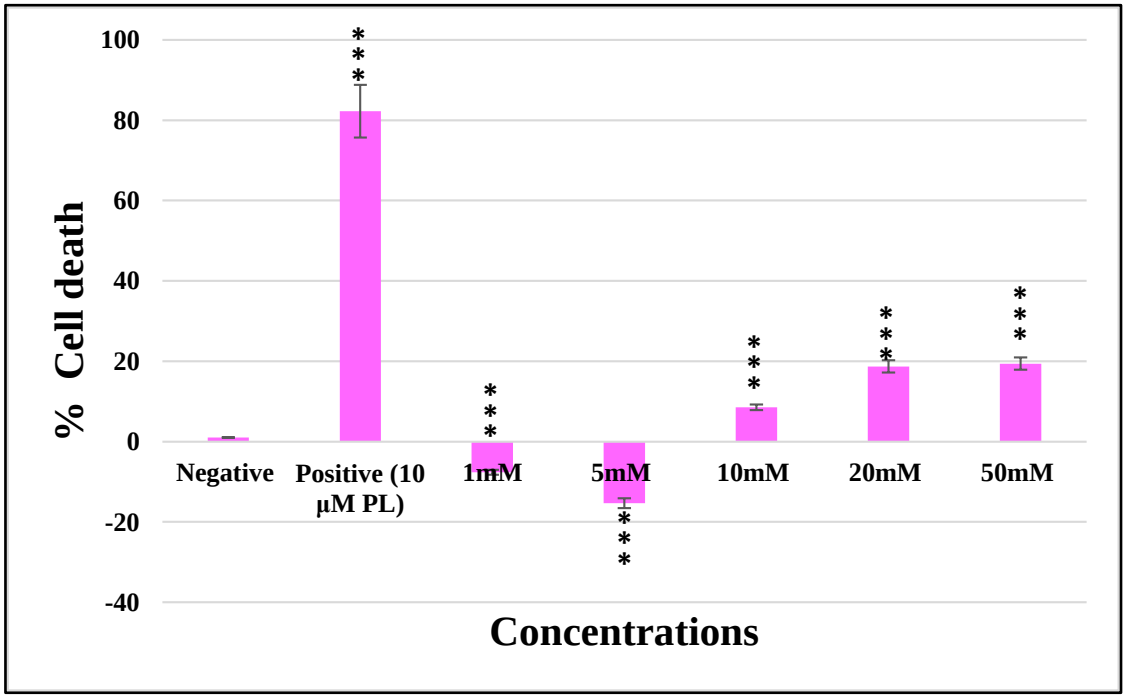


Fig. 28: Graph comparing the percentage of apoptosis in MRC-5 cells at selected concentrations of HPβCD *at 1 mM, 5 mM, 10 mM, 20 mM, 50 mM and negative samples. PL (10µM) was used as a positive control. Data are mean ± S.D. (n=3) from raw data, where *p<0.05, **p<0.01 and ***p<0.001 significant difference to untreated control. Independent experiments were run at least 3 times.*

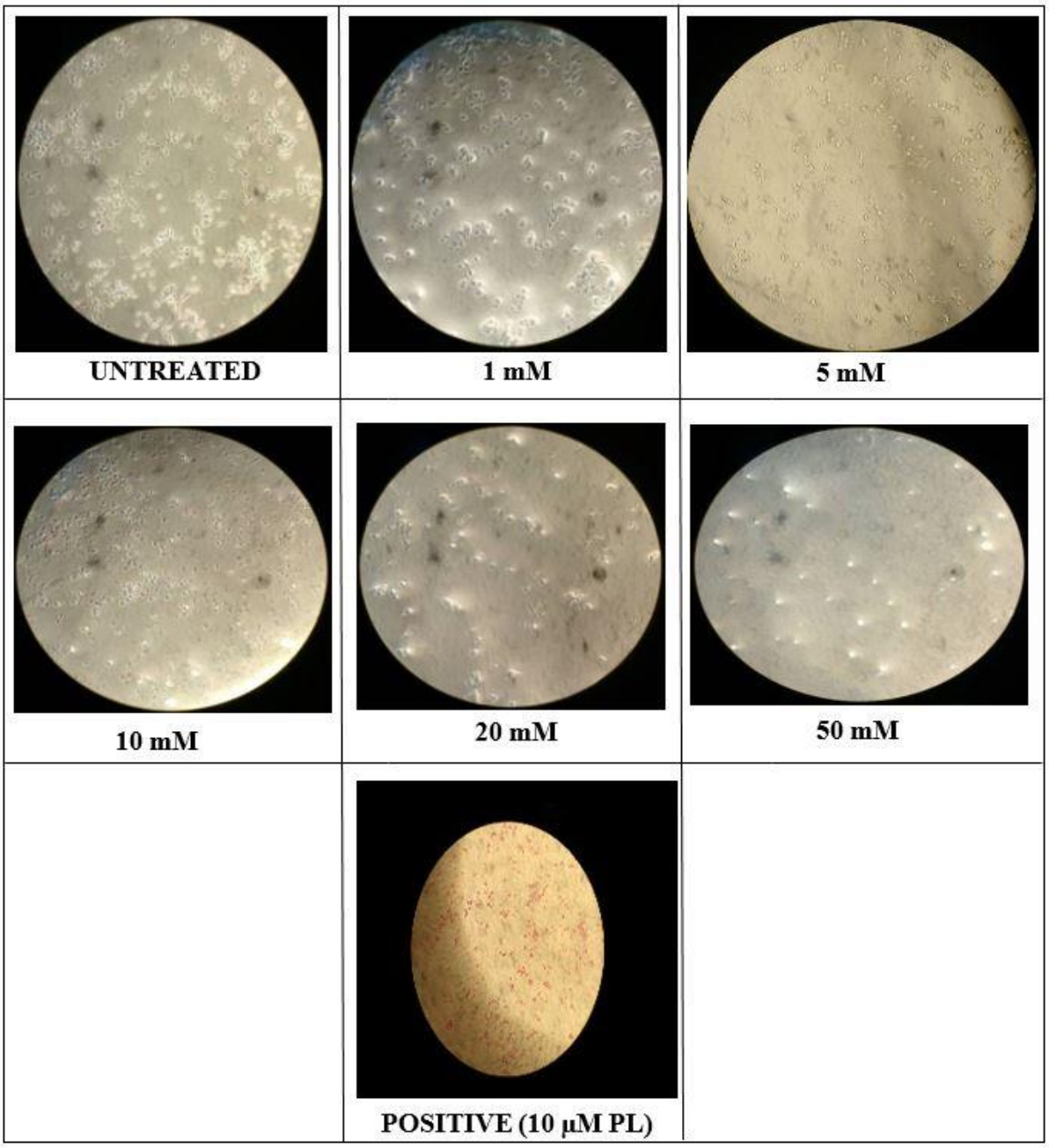


Fig. 29: Light microscope images showing the amount of apoptosis in MRC-5 cells at selected concentrations of HPβCD *at 1 mM, 5 mM, 10 mM, 20 mM ,50 mM and untreated samples. PL was used as a positive control.*

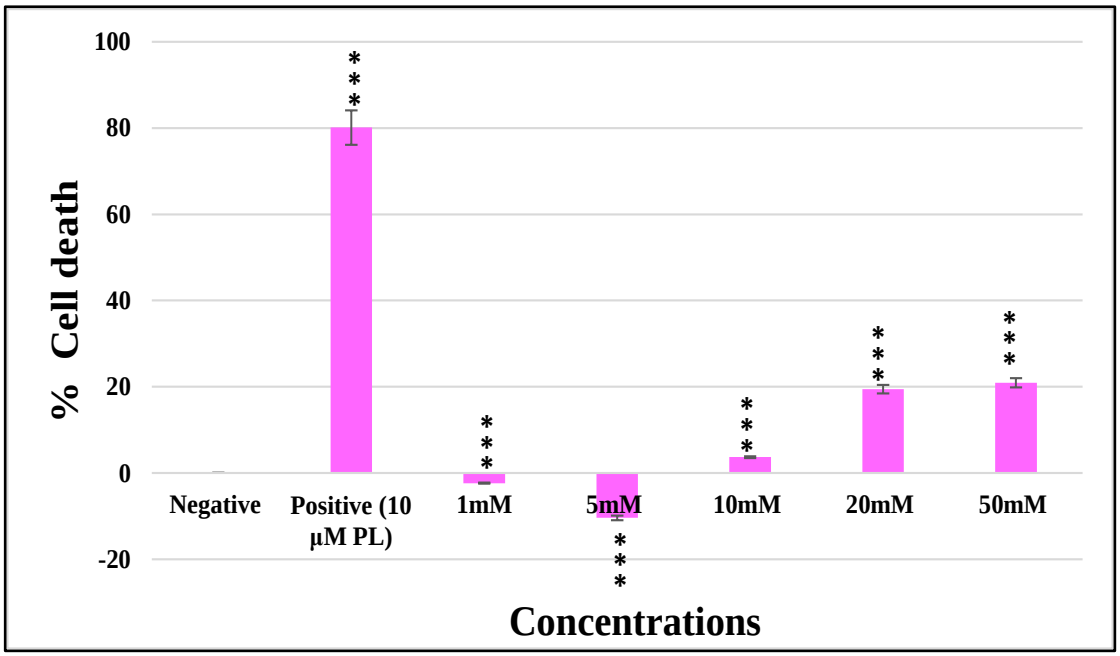


Fig. 30: Graph comparing the percentage of apoptosis in HEK-293 cells at selected concentrations of HPβCD *at 1 mM, 5 mM, 10 mM, 20 mM, 50 mM and negative samples. PL (10µM) was used as a positive control. Data are mean ± S.D. (n=3) from raw data, where *p<0.05, **p<0.01 and ***p<0.001 significant difference to untreated control. Independent experiments were run at least 3 times.*

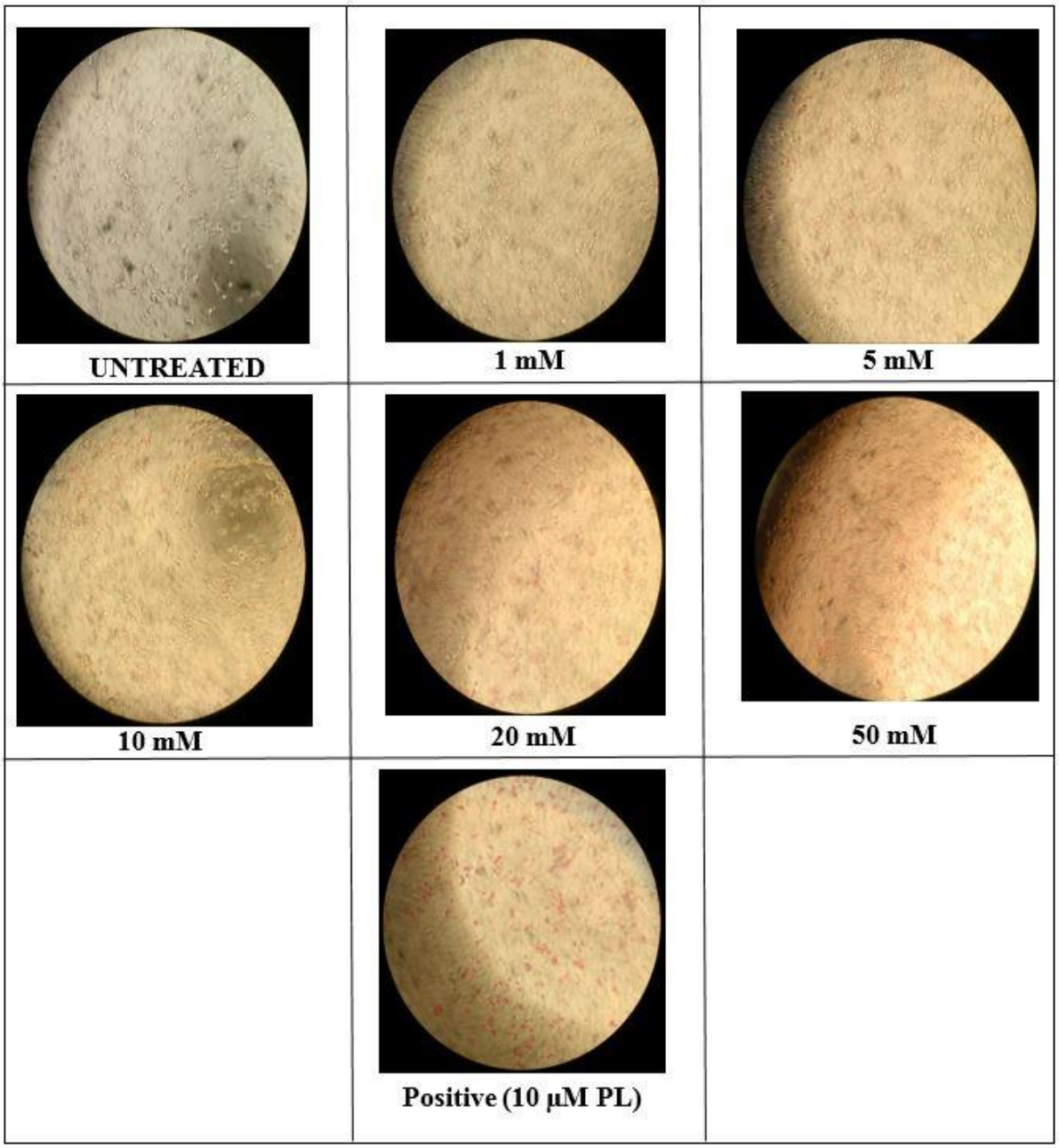


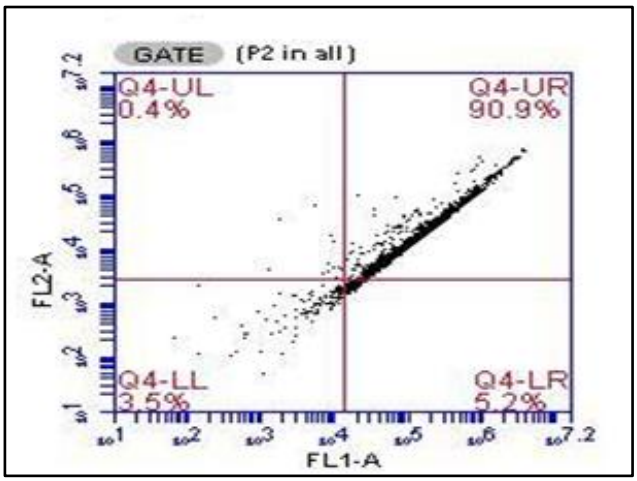
Fig. 31: Light microscope images showing the amount of apoptosis in HEK-293 cells at selected concentrations of HPβCD *at 1 mM, 5 mM, 10 mM, 20 mM ,50 mM and untreated samples. PL was used as a positive control.*

6.1.3 MITOCHONDRIAL OUTER MEMBRANE POTENTIAL ASSAY (MOMP)

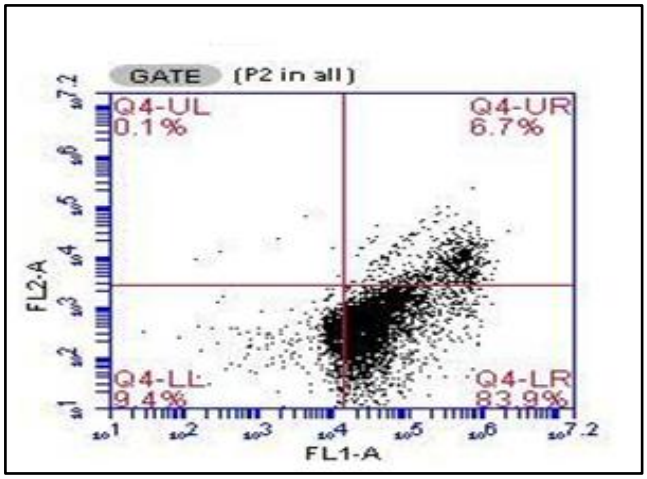
One of the key hallmarks of apoptosis is the loss of mitochondrial membrane potential or MOMP (Elmore 2007). To investigate whether MOMP is the basis of the observed apoptosis in cancer cells, a MOMP assay was performed using JC-1 dye. This assay was done on three cell lines MCF7, MDA-MB-231 & MRC-5.The top **right** and **bottom** hand quadrants of each plot represents healthy (FL2-A) and apoptotic (FL1-A) cells respectively.

From the results obtained from MTT (IC_{50} values) and APOPercentage assays it was quite evident that ~10 mM HPβCD caused cellular growth inhibition through apoptosis in cancer cells and had little or no effect in normal cells. Therefore, we selected 10 mM HPβCD going forward as the only working concentration for HPβCD treatment. 24 hrs time point was selected (HPβCD & 10 mM H_2O_2) because mitochondrial membrane potential loss is an early cellular event.

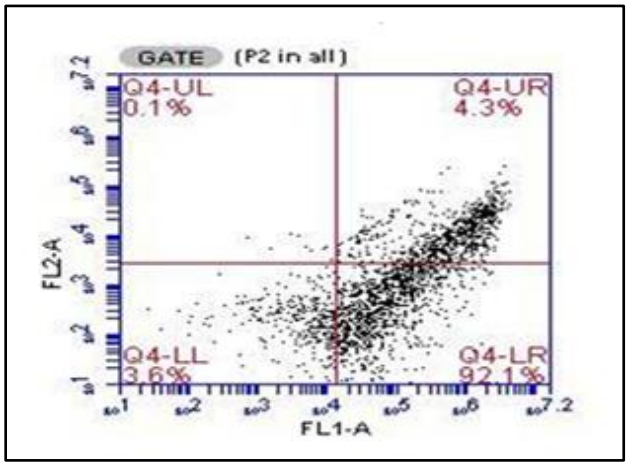
Results obtained for MCF7 **(Fig. 32 C)** showed 92.1% apoptotic population at 10 mM concentration of HPβCD (treated), whereas the healthy population in untreated cells was 90.0%. The percentage of apoptotic cells in the positive sample (10 mM H_2O_2) was 92.1%. H_2O_2, like PL is an agent well-known to cause apoptosis (Xiang, Wan et al. 2016).



(A) UNTREATED



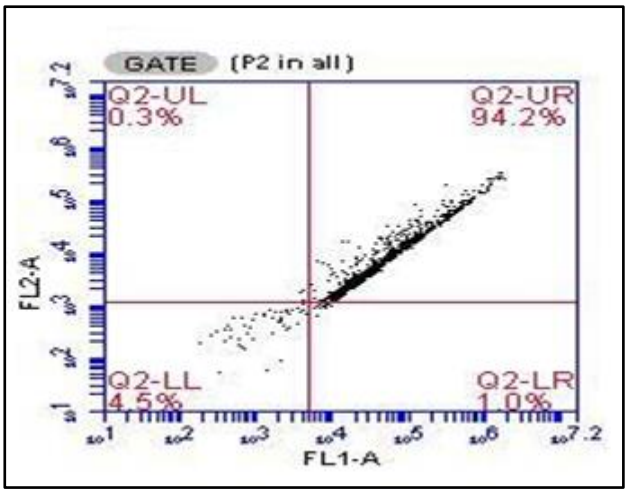
(B) POSITIVE (10 mM H_2O_2)



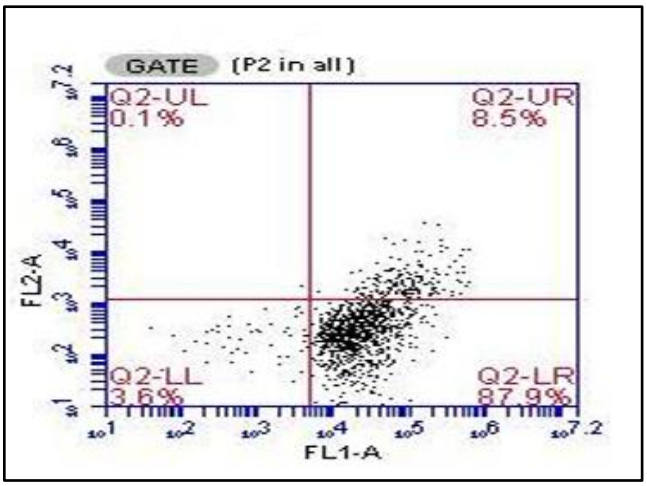
(C) TREATED (10 mM HPβCD)

Fig. 32: MOMP plots for MCF7 cells. ***(A):*** *Loss of mitochondrial membrane potential in untreated cells,* ***(B):*** *Loss of mitochondrial membrane potential in positive sample (10 mM H_2O_2) and* ***(C):*** *Loss of mitochondrial membrane potential at 10 mM HPβCD. Independent experiments were run at least 3 times.*

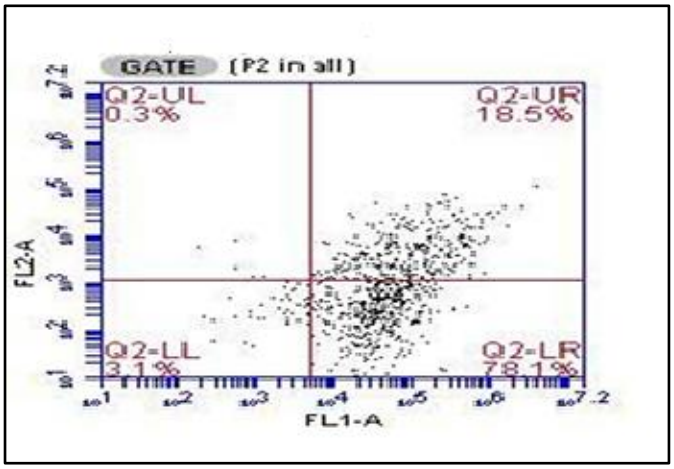
MDA-MB-231 cells gave a 78.1% cell death at 10 mM concentration of HPβCD **(Fig. 33 C)**, whereas the healthy the population in untreated was still quite high at 94.2%. The positive sample (10 mM H_2O_2) as expected yielded a very high 92.4% apoptotic cells.



(A) UNTREATED



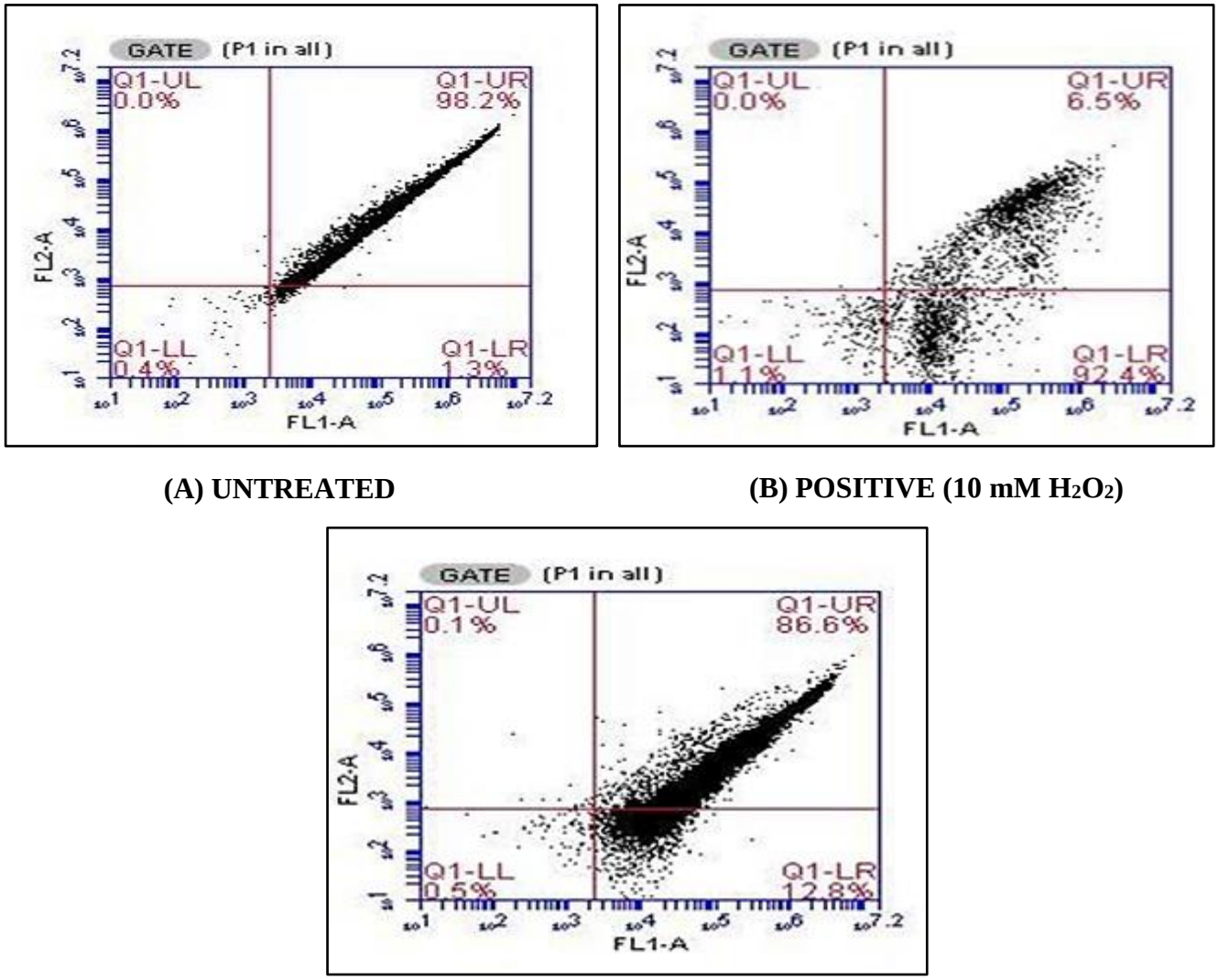
(B) POSITIVE (10 mM H_2O_2)



(C) TREATED (10 mM HPβCD)

Fig. 33: MOMP plots for MDA-MB-231 cells. ***(A):*** *Loss of mitochondrial membrane potential in untreated cells,* ***(B):*** *Loss of mitochondrial membrane potential in positive sample (10 mM H_2O_2) and* ***(C):*** *Loss of mitochondrial membrane potential at 10 mM HPβCD. Independent experiments were run at least 3 times.*

For the normal cells (MRC-5), results obtained gave us 98.2% non-apoptotic/healthy population **(Fig. 34 A)** and 12.8 % apoptotic cells at 10 mM concentration of HPβCD **(Fig. 34 C)**. This confirms that HPβCD is non-toxic to normal cells, while it is significantly apoptotic to cancerous cells via the intrinsic apoptosis pathway and causes loss in mitochondrial membrane potential. This is possibly due to the nature of CyDs in general as cholesterol chelators and their ability to deplete mitochondrial cholesterol content as demonstrated for MβCD (Ziolkowski, Szkatula et al. 2010).



(A) UNTREATED **(B) POSITIVE (10 mM H_2O_2)**

(C) TREATED (10 mM HPβCD)

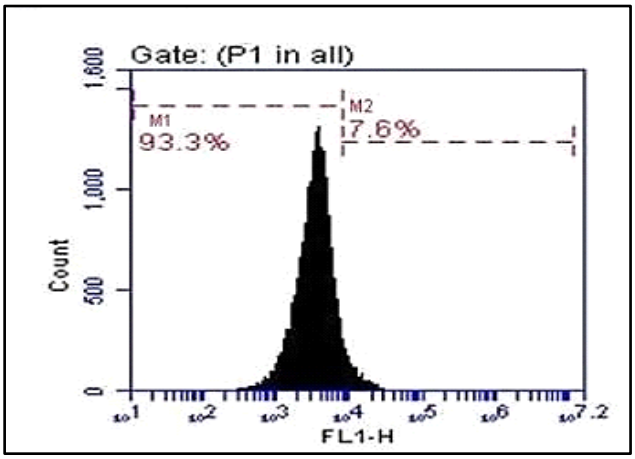
Fig. 34: MOMP plots for MRC-5 cells. ***(A)****: Loss of mitochondrial membrane potential in untreated cells,* ***(B):*** *Loss of mitochondrial membrane potential in positive sample (10 mM H_2O_2) and* ***(C):*** *Loss of mitochondrial membrane potential at 10 mM HPβCD. Independent experiments were run at least 3 times.*

6.1.4 ROS ASSAY (Reactive Oxygen Species)

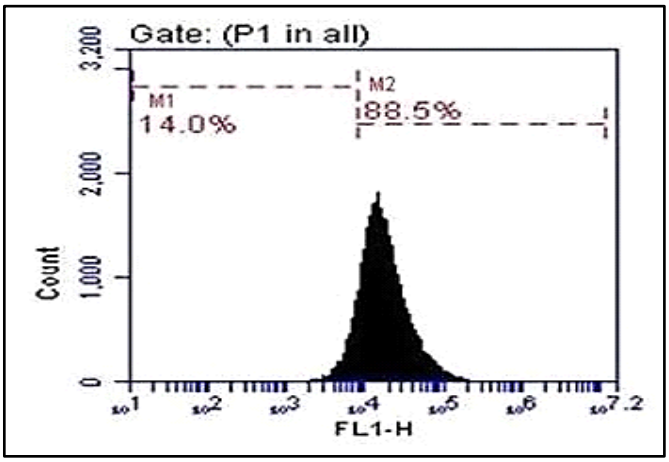
To further validate the incurrence of apoptosis and to investigate the exact mechanisms of apoptosis in this study, a ROS assay to capture the production of ROS, because generation of ROS has also been shown to be a characteristic feature in apoptosis (Redza-Dutordoir and Averill-Bates 2016). In order to be in solidarity with this fact, a ROS assay was performed in three cell lines: MCF7, MDA-MB-231 & MRC-5. HPβCD and the positive (10 mM H_2O_2) were treated for 24 hrs. The **right hand section** in each plot represents the production of ROS.

Cancer cells in general have enhanced metabolism due to the fact that they divide rapidly as compared to normal cells thereby leading to an abundant generation of ROS (Nogueira and Hay 2013).

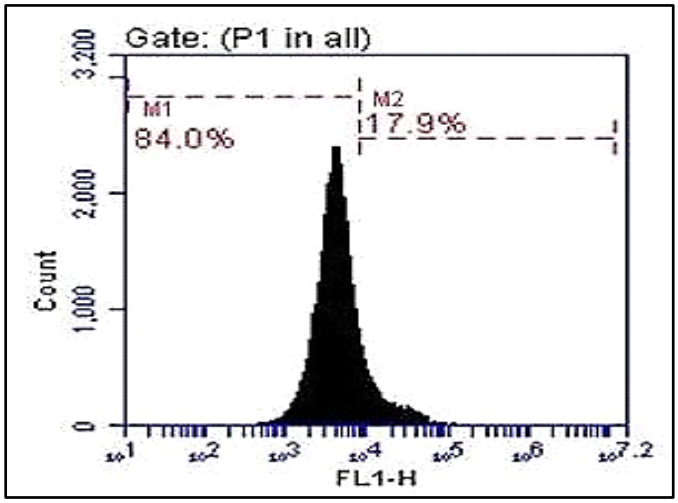
From **Fig. 35 C**, it can be seen that the percentage of ROS production in MCF7 cells for 10 mM HPβCD treatment was 17.9% whereas in the untreated it was 7.6% (**Fig. 35 A)**. Although this was about 2.5 fold more as compared to the untreated sample but was not too significant especially if we look at the levels of ROS generation in normal cells (MRC-5) which showed 10.8% ROS activity at 10 mM HPβCD treatment **(Fig. 37 C)**. The ROS production in the positive sample however, had a very high 88.5 %.



(A) UNTREATED



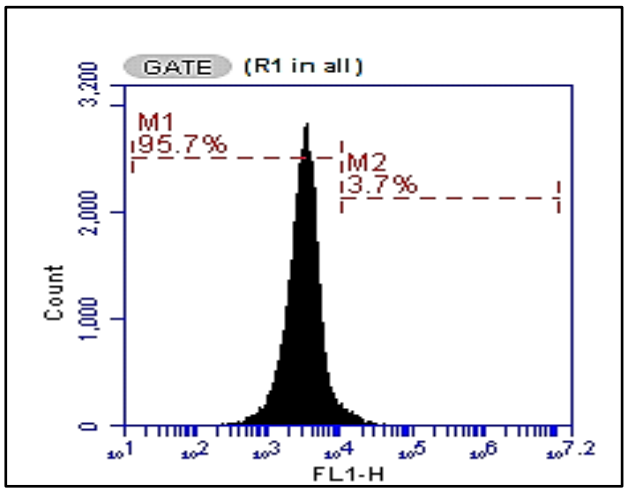
(B) POSITIVE (10 mM H_2O_2)



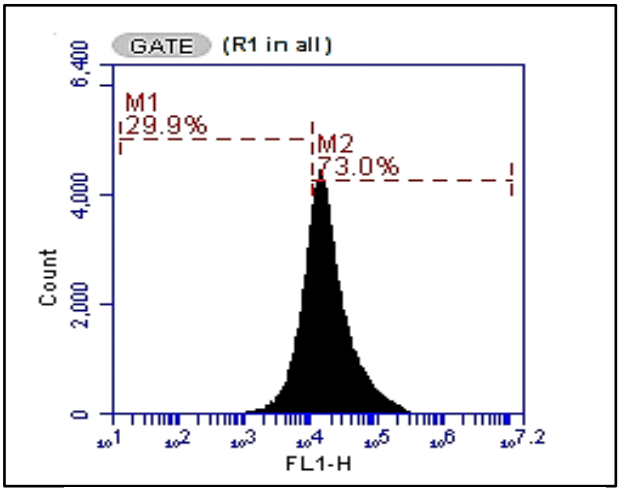
(C) TREATED (10 mM HPβCD)

Fig. 35: ROS generation in MCF7 cells. ***(A):*** *ROS generation in untreated cells (7.6 %)* ***(B):*** *ROS generation in positive sample (10 mM H_2O_2) (88.5 %) and* ***(C):*** *ROS generation at 10 mM HPβCD (17.9%). Independent experiments were run at least 3 times.*

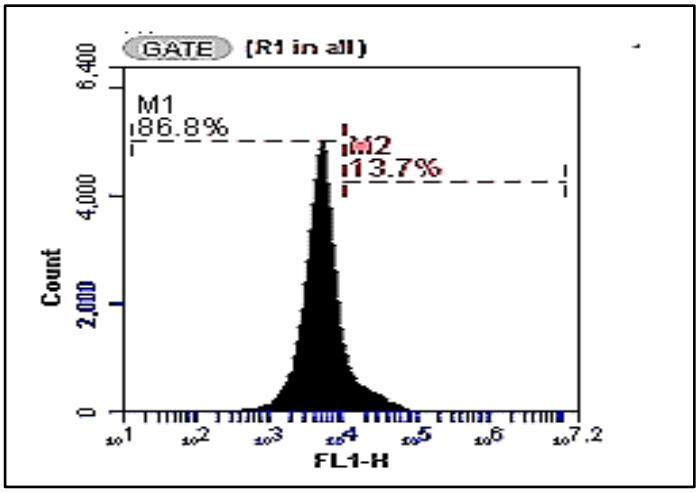
MDA-MB-231 cells gave similar results like MCF7 and the percentage of ROS production for 10 mM HPβCD treatment was 13.7 % **(Fig. 36 C)** whereas in the untreated it was 3.7% **(Fig. 36 A)**. Again, this was about 4 fold more as compared to the untreated cells but not too staggering when we look at the ROS production in normal cells where 10.8 % ROS production was seen at 10 mM HPβCD treatment **(Fig. 37 C)**. The positive sample showed 73% ROS activity.



(A) UNTREATED



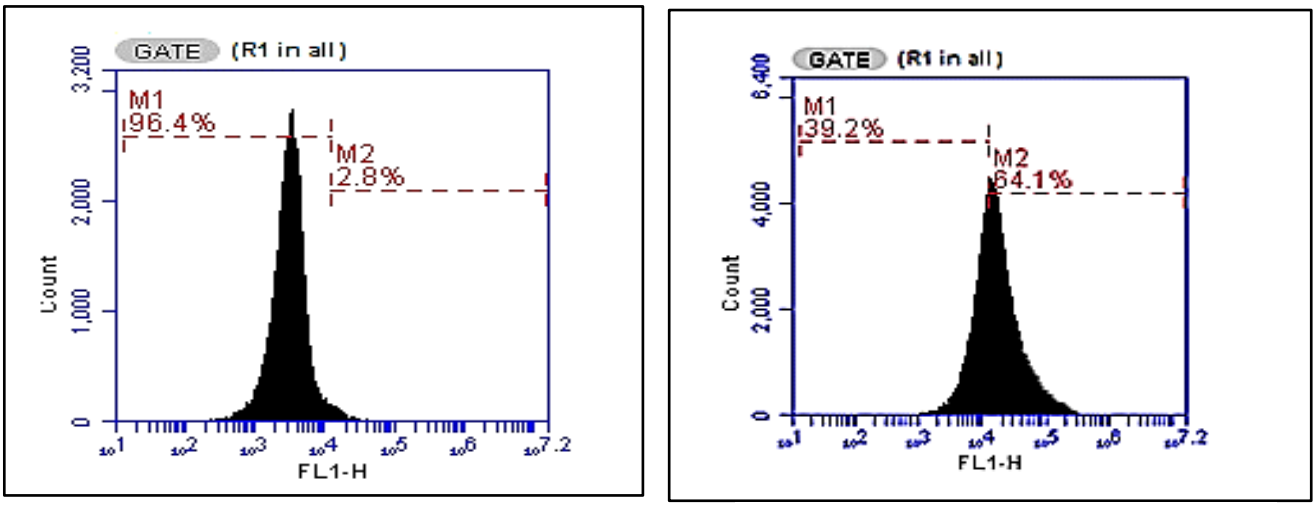
(B) POSITIVE (10 mM H_2O_2)



(C) TREATED (10 mM HPβCD)

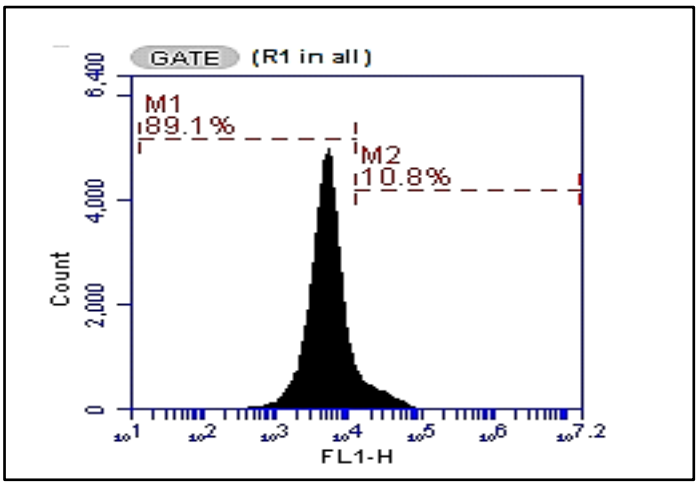
Fig. 36: ROS generation in MDA-MB-231 cells. ***(A):*** *ROS generation in untreated cells (3.7 %),* ***(B):*** *ROS generation in positive sample (10 mM H_2O_2) (73 %) and* ***(C):*** *ROS generation at 10 mM HPβCD (13.7 %). Independent experiments were run at least 3 times.*

MRC-5 cells in general showed 2.8 % ROS activity in untreated cells **(Fig. 37 A)** and like MCF and MDA-MB-231 cells the ROS production went up to almost 4 folds at 10 mM HPβCD treatment (10.8%) **(Fig. 37 C)**. Thus, it was inferred that although HPβCD does cause apoptosis but it doesn't do so via enormous production of ROS. Downregulation of ROS in apoptosis has often been observed and it can happen considering that ROS has significant roles in physiological processes (Jeong and Joo 2016). It is quite possible there is an over expression of detoxifying enzymes like catalase and glutathione reductase, which are responsible for the maintenance of free radicals.



(A) UNTREATED

(B) POSITIVE (10 mM H_2O_2)



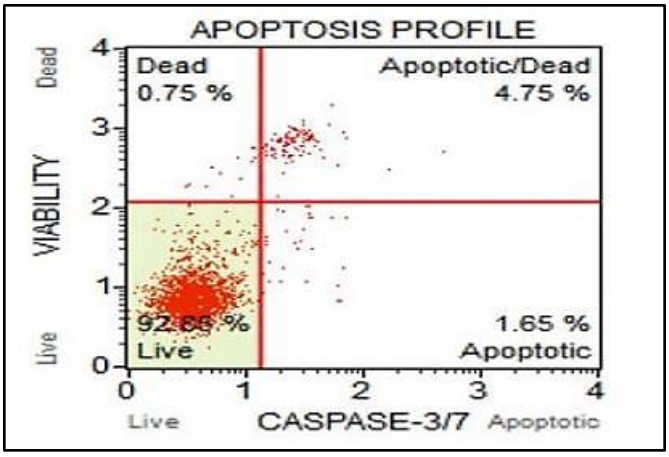
(C) TREATED (10 mM HPβCD)

Fig. 37: ROS generation in MRC-5 cells. ***(A):*** *ROS generation in untreated cells (2.8 %),* ***(B):*** *ROS generation in positive sample (10 mM H_2O_2) (64.1 %) and* ***(C):*** *ROS generation at 10 mM HPβCD (10.8 %). Independent experiments were run at least 3 times.*

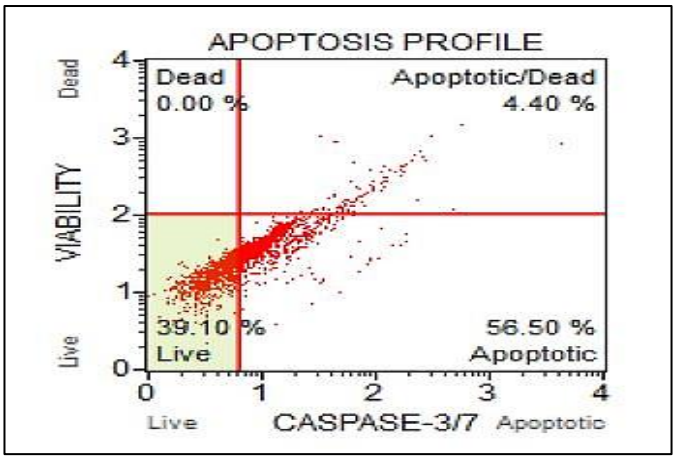
6.1.5 CASPASE-3/7 ASSAY

The final step in apoptosis following the intrinsic pathway is the activation of executioner caspases like caspase-3 and caspase-7 (Brentnall, Rodriguez-Menocal et al. 2013) which leads to the release of cytochrome c. Therefore, to confirm if the cell death observed was due to the apoptosis, a Caspase-3/7 assay was performed. Caspases are activated in response to a myriad of cellular death stimuli and they dismantle the cell. Caspase-3 and caspase-7 contribute to the majority of proteolytic cleavage occurring in apoptosis (Walsh, Cullen et al. 2008). CyDs have been previously seen to be involved in activating caspases (Hipler, Schönfelder et al. 2007). As a final step to confirm and validate apoptosis via the mitochondrial intrinsic pathway, the caspase-3/7 assay was performed on three cell lines: MCF7, MDA-MB-231 & HEK-293. HPβCD and positive (10 µM PL or 40 µM PL) were treated for 24 hrs. The percentage of dead/apoptotic cells are clearly indicated in specific corners of each quadrants in the above plots.

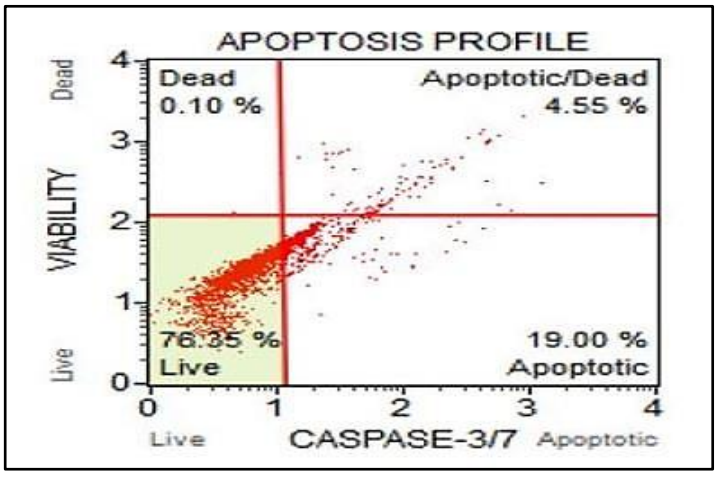
For MCF7 cells, the total apoptosis observed in untreated cells was 6.4% **(Fig. 38 A)** whereas in the treated cells (10 mM HPβCD) it went up to 23.55 % **(Fig. 38 C)** which was almost four times more as compared to the untreated sample. For the positive sample (10 µM PL), the total apoptotic population was 60.90 % **(Fig. 38 B)**. 10 µM PL was used as opposed to 40 µM PL to capture maximum caspase-3/7 activity because 40 µM PL was too toxic. The overall low caspase-3/7 activity was because MCF7 cells do not express caspase-3 activity in general (Jänicke 2009). Because this particular assay gives a measure of both caspase-3 and 7 therefore, the cell death activity in MCF7 was solely due to caspase-7 and quite possibly, caspase-7 activity in MCF7 cells was low overall.



(A) UNTREATED



(B) POSITIVE (10 µM PL)

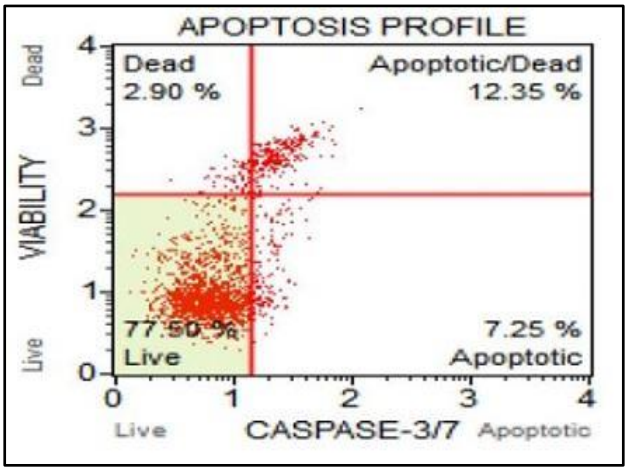


(C) TREATED (10 mM HPβCD)

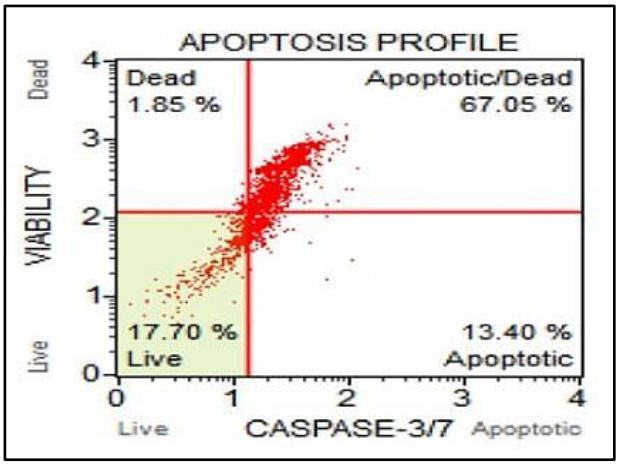
Fig. 38: Caspase-3/7 profile in MCF cells. ***(A):*** *Total apoptotic/live cells generation in untreated cells, Total Apoptotic – 6.4%,* ***(B):*** *Total apoptotic/live cells generation in positive sample (10 µM PL), Total Apoptotic – 60.90 % and* ***(C):*** *Total apoptotic/live cells in treated (10 mM HPβCD) cells, Total Apoptotic- 23.55 %. Independent experiments were run at least 3 times.*

MDA-MB-231 cells on the other hand showed a better activity of caspase-3/7. In the untreated cells the total apoptotic population was found to be 19.6% **(Fig. 39 A)** which went up to 48.75% in 10 mM HPβCD treated sample **(Fig. 39 C).** Thus confirming that in MDA-MB-231 cells, HPβCD acts via the intrinsic pathway and causes a disruption in the mitochondria thereby activating the executioner caspases-3 and caspase-7. In the positive sample (40 µM PL), the total apoptotic population was 80.45 % **(Fig. 39 B).**

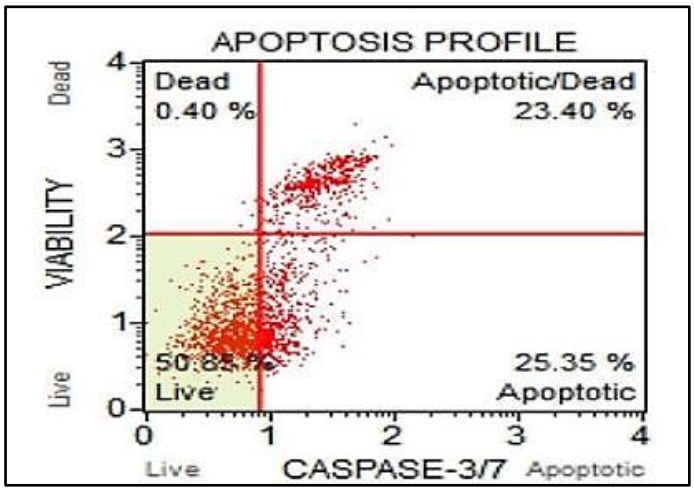
MDA-MB-231 cells on the other hand showed a better activity of caspase-3/7. In the untreated cells the total apoptotic population was found to be 19.6% **(Fig. 39 A)** which went up to 48.75% in 10 mM HPβCD treated sample **(Fig. 39 C).** Thus confirming that in MDA-MB-231 cells, HPβCD acts via the intrinsic pathway and causes a disruption in the mitochondria thereby activating the executioner caspases-3 and caspase-7. In the positive sample (40 µM PL), the total apoptotic population was 80.45 % **(Fig. 39 B).**



(A) UNTREATED



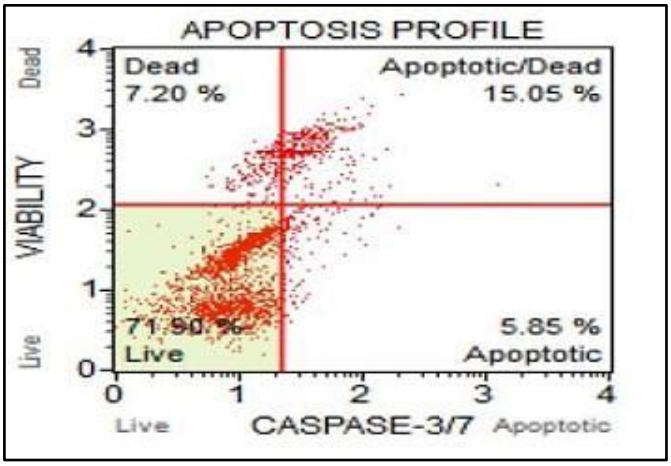
(B) POSITIVE (40 µM PL)



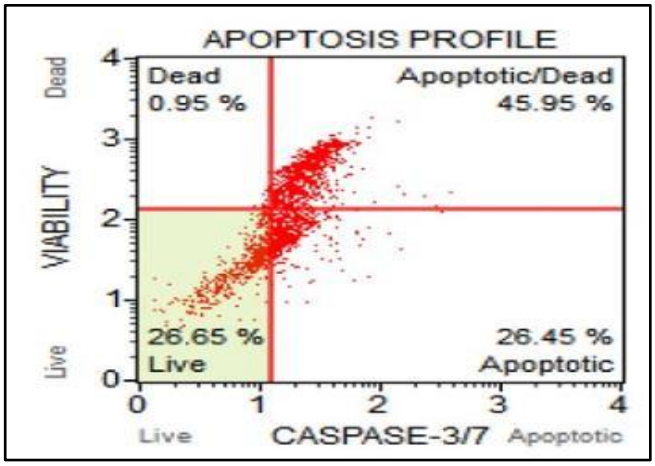
(C) TREATED (10 mM HPβCD)

Fig. 39: Caspase-3/7 profile in MDA-MB-231 cells. ***(A):*** *Total apoptotic/live cells generation in untreated cells (Total Apoptotic – 19.6%),* ***(B):*** *Total apoptotic/live cells generation in positive sample (40 µM PL), Total Apoptotic – 80.45 % and* ***(C):*** *Total apoptotic/live cells generation in treated (10 mM HPβCD) cells, Total Apoptotic- 48.75%. Independent experiments were run at least 3 times.*

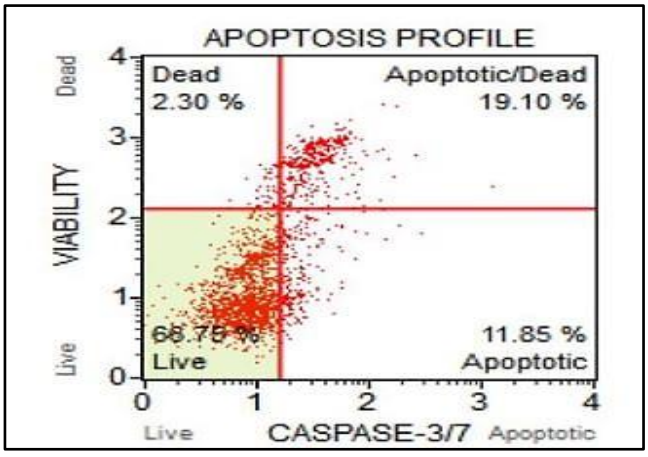
In the normal cells (HEK-293), the total healthy population in the untreated cells was 71.90% **(Fig. 40 A)**, which decreased only partially in the 10 mM HPβCD treated sample **(Fig. 40 C)** and went down to 66.75%. In the positive sample (40 µM PL), the total apoptotic population was 72.4 % **(Fig. 40 B).** This further warrants that HPβCD is non-toxic to normal cells. HPβCD's non-toxicity was later further validated in an *in vivo* study.



(A) UNTREATED



(B) POSITIVE (40 µM PL)



(C) TREATED (10 mM HPβCD)

Fig. 40: Caspase-3/7 profile in HEK-293 cells. ***(A):*** *Total apoptotic/live cells generation in untreated cells, Total Live – 71.90 %,* ***(B):*** *Total apoptotic/live cells generation in positive sample (40 µM PL), Total Apoptotic – 72.40 % and* ***(C):*** *Total apoptotic/live cells generation in treated (10 mM HPβCD) cells, Total Live- 66.75%. Independent experiments were run at least 3 times.*

6.2 CHOLESTEROL ASSAYS

6.2.1 CHOLESTEROL QUANTIFICATION ASSAY

To investigate if the apoptosis observed from all the above assays was due to cholesterol-depletion, a cholesterol assay was performed on all three cell lines: MCF7, MDA-MB-231 and MRC-5. HPβCD and the positive PL, a known cholesterol depletor (Esau, Sagar et al. 2016) were treated for 24 hrs. It is a well-known fact that cancer cells, have elevated levels of cholesterol (Llaverias, Danilo et al. 2011; Radwan and Alanazi 2014) because cholesterol is an integral part of the cell membrane (de Oliveira Andrade 2016) and is recruited by the cancer cells for rapid division. As mentioned before, HPβCD extracts the excess cholesterol (Hinzey, Kline et al. 2012) and can be utilised to extract excess cholesterol from cell membranes. HPβCD and the positive (40 µM PL) were used for treatment of cancer cells for 24 hrs. This assay provided an estimate of total cholesterol, CE and free cholesterol and showed similar results as obtained for leukemia (Yokoo, Kubota et al. 2015) and atherosclerosis (Zimmer, Grebe et al. 2016).

Results for MCF7 **(Fig. 41)** clearly showed that, as compared to untreated, the HPβCD treated cells had reduced total cholesterol content at all concentrations starting from 1 mM, 5 mM, 10 mM, 20 mM, and 50 mM . At 10 mM, which is the concentration selected based on previous assays, the total cholesterol levels were reduced to more than 75 % as compared to the untreated sample.

The statistically significant difference between groups was determined by one-way ANOVA ($F(4,10)= 442.2$ $p= 1.2E-11$. ES – 23.34, 45.65, 57.93, 132.54, 135.43 for 1 mM, 5 mM, 10 mM, 20 mM, 50 mM respectively.

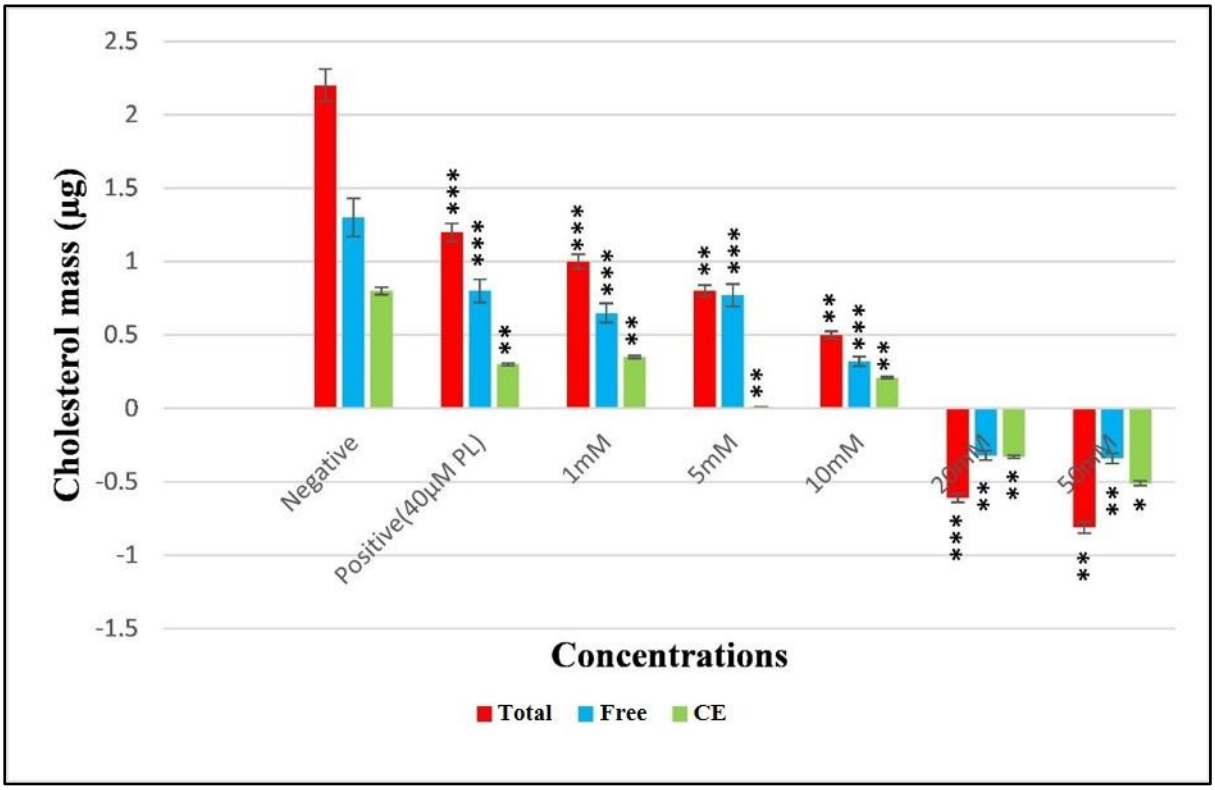


Fig. 41: Graph comparing the total, free and esterified cholesterol levels in MCF7 cells at selected concentrations of HPβCD *at 1 mM, 5 mM, 10 mM, 20 mM, 50 mM and negative samples. PL was used as a positive control. Data are mean ± S.D. (n=3) from raw data, where *p<0.05, **p<0.01 and ***p<0.001 significant difference to untreated control. Independent experiments were run at least 3 times.*

MDA-MB-231 cells had lesser levels of cholesterol compared to MCF7 **(Fig. 42)**. Results clearly showed that, as compared to untreated, the HPβCD treated cells had reduced total cholesterol content at all concentrations of HPβCD starting from 1 mM, 5 mM, 10 mM, 20 mM and 50 mM. At 10 mM the total cholesterol levels were reduced to more than 50 % as compared to the untreated sample like MCF7 cells.

The statistically significant difference between groups was determined by one-way ANOVA (F(4,10)= 5174.2, p= 3.2E-15. ES – 12.45, 32.19, 47.56, 122.43, 142.56 for 1 mM, 5 mM, 10 mM, 20 mM, 50 mM respectively.

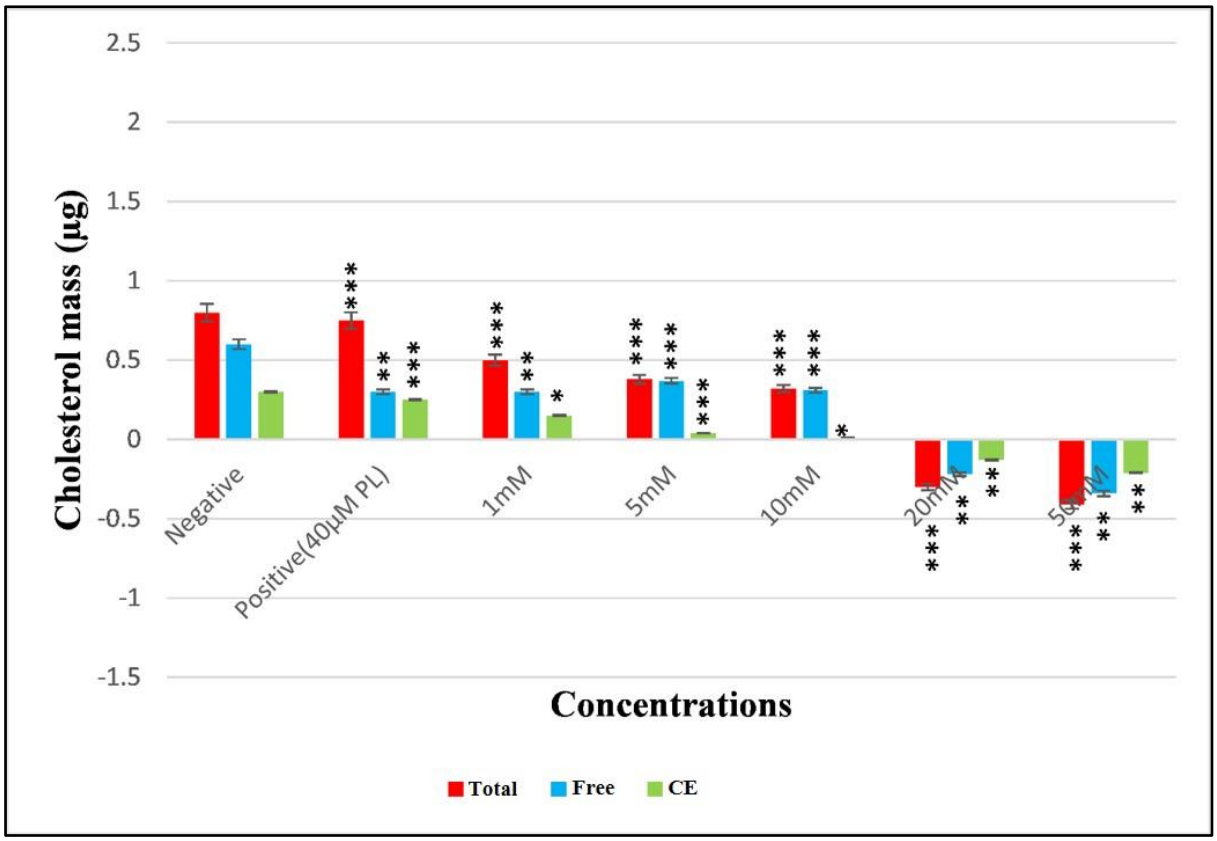


Fig. 42: Graph comparing the total, free and esterified cholesterol levels in MDA-MB-231 cells at selected concentrations of HPβCD *at 1 mM, 5 mM, 10 mM, 20 mM, 50 mM and negative samples. PL was used as a positive control. Data are mean ± S.D. (n=3) from raw data, where *p<0.05, **p<0.01 and ***p<0.001 significant difference to untreated control. Independent experiments were run at least 3 times.*

MRC-5 cells, being non-cancerous has lower levels of cholesterol compared to both MCF7 and MDA-MB-231 cells because they do not divide aggressively and therefore needs less cholesterol. Results clearly showed that, as compared to untreated, the HPβCD treated cells had reduced total cholesterol content at all concentrations starting from 1 mM, 5 mM, 10 mM, 20 mM, and 50 mM **(Fig. 43)**. In MRC-5 cells at 10 mM the total cholesterol levels were reduced to more than 50 % as compared to the untreated sample similar to MCF7 and MDA-MB-231 cells but this depletion was enough to actually kill the cells as observed from our earlier assays. Upon quantifying the total cholesterol content it was seen that MCF7 and MDA-MB-231 cells has approximately 7.7 and 2.7 times more cholesterol as compared to the normal MRC-5 cells. The statistically significant difference between groups was determined by one-way ANOVA ($F(4,10)= 3258.4$, $p= 3.5E-15$. ES – 0.92, 0.43, 1.21, 12.32, 73.83 for 1 mM, 5 mM, 10 mM, 20 mM, 50 mM respectively.

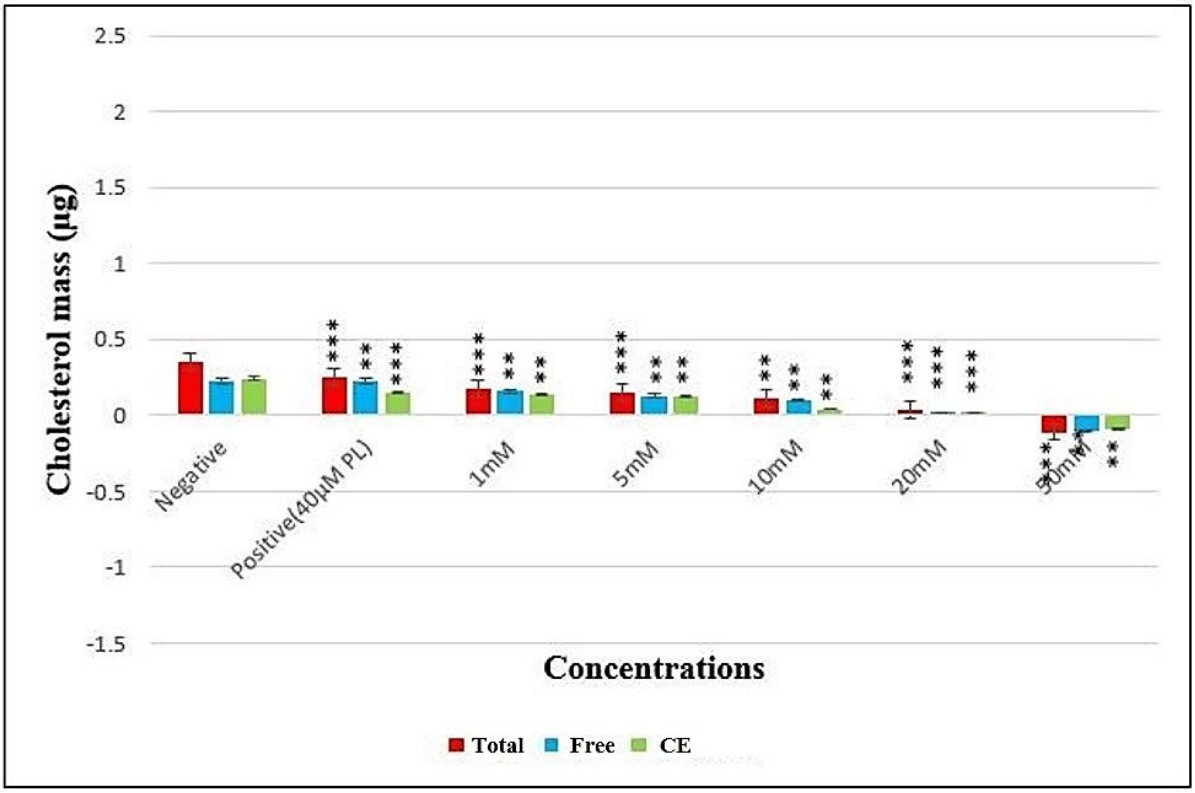
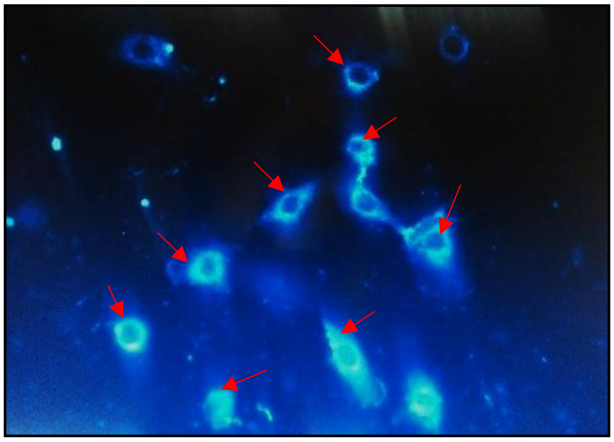


Fig. 43: Graph comparing the total, free and esterified cholesterol levels in MRC-5 cells at selected concentrations of HPβCD *at 1 mM, 5 mM, 10 mM, 20 mM, 50 mM and negative samples. PL was used as a positive control. Data are mean ± S.D. (n=3) from raw data, where *p<0.05, **p<0.01 and ***p<0.001 significant difference to untreated control. Independent experiments were run at least 3 times.*

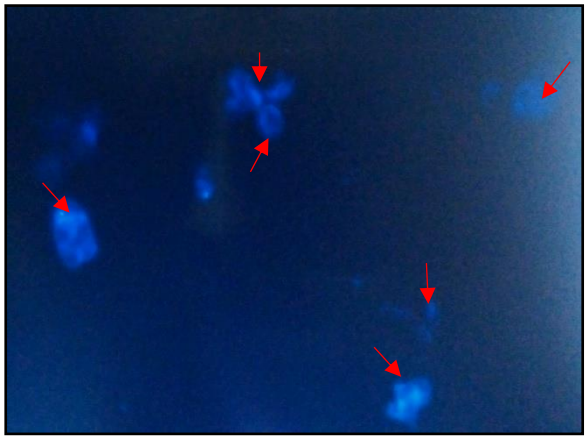
6.2.2 CHOLESTEROL STAINING

To further validate cholesterol-depletion as observed from the cholesterol assay above, a Filipin based cholesterol staining was performed. MCF7 and MDA-MB-231 cells were used. HEK-293 cells couldn't be used due to their unavailability at the moment. HPβCD and the positive (5 mM MβCD) were treated for 24 hrs. Like PL, MβCD is also a well know cholesterol depletor (Mahammad and Parmryd 2015). Fluorescence microscopy has been a robust tool for investigating the intracellular transport of proteins. Filipin specifically binds to cholesterol and can give an overall quantification and has been more recently been clinically used in the diagnosis of Type C Niemann-Pick disease (Vanier and Latour 2015), which has significantly higher levels of cholesterol.

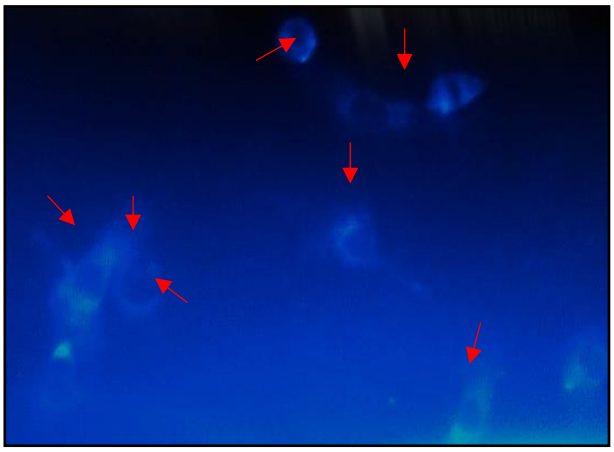
For MCF7 cells post-staining with Filipin, the untreated sample **(Fig. 44 A)** and the 10 mM HPβCD treated sample **(Fig. 44 C)** showed significant difference in terms of FU which was measured using NIH's ImageJ software. The treated cells had four times less fluorescence **(Fig. 46)** as compared to the untreated ones. This is in accordance to our cholesterol quantification assay where 10 mM HPβCD treatment caused almost 75% cholesterol-depletion. The positive (5 mM MβCD) had almost three times less fluorescence as compared to the untreated after quantification **(Fig. 44 B)**.



(A) UNTREATED



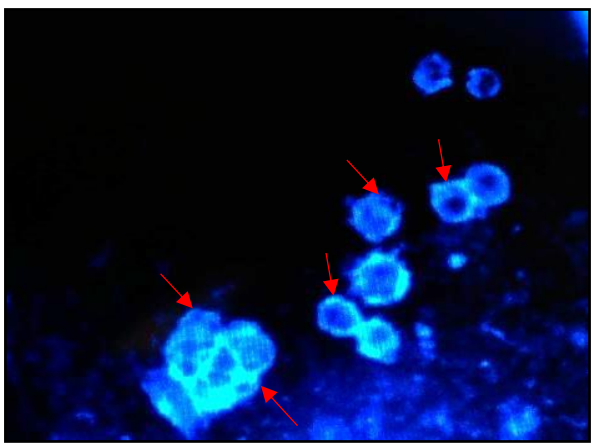
(B) POSITIVE (5 mM MβCD)



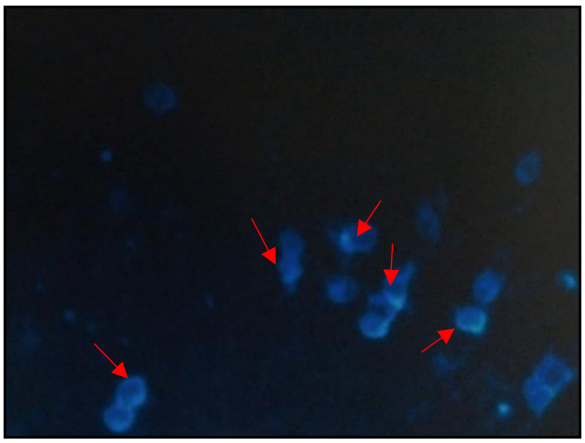
(C) TREATED (10 mM HPβCD)

Fig. 44: Pictures taken on fluorescent microscope (The FLoid® cell imaging station) after Filipin staining, comparing the overall cholesterol levels in MCF7 cells. *Prominent cells are marked with red arrows.* ***(A):*** *Fluorescence in untreated cells,* ***(B):*** *Fluorescence in positive sample (5 mM MβCD) and* ***(C):*** *Fluorescence in 10 mM HPβCD treated cells. All settings were kept at default settings. Independent experiments were run at least 2 times.*

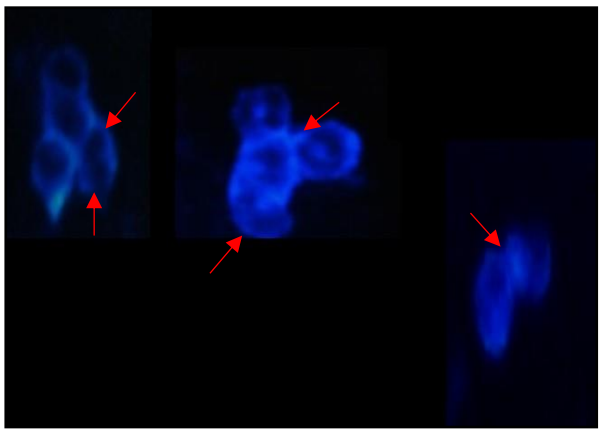
Similarly for MDA-MB-231 cells there was a remarkable difference in the FU between the untreated **(Fig. 45 A)** and 10 mM HPβCD treated cells **(Fig. 45 C)**. After quantification with ImageJ, the treated cells had six times less fluorescence **(Fig. 46)** as compared to the untreated ones. This again, correlates with our data from cholesterol quantification assay where at 10 mM HPβCD, almost 50% total cholesterol was seen to be depleted. The positive (5 mM MβCD) had almost eight times less fluorescence as compared to the untreated after quantification **(Fig. 45 B)**. Thus, it can be affirmed that the apoptosis caused my HPβCD is indeed due to the overall depletion of cholesterol.



(A) UNTREATED



(B) POSITIVE (5 mM MβCD)



(C) TREATED (10 mM HPβCD)

Fig. 45: Pictures taken on fluorescent microscope (The FLoid® cell imaging station) after Filipin staining, comparing the overall cholesterol levels in MDA-MB-231 cells. *Prominent cells are marked with red arrows.* ***(A):*** *Fluorescence in untreated cells,* ***(B):*** *Fluorescence in positive sample (5 mM MβCD) and* ***(C):*** *Fluorescence in 10 mM HPβCD treated cells. All settings were kept at default settings. Independent experiments were run at least 2 times.*

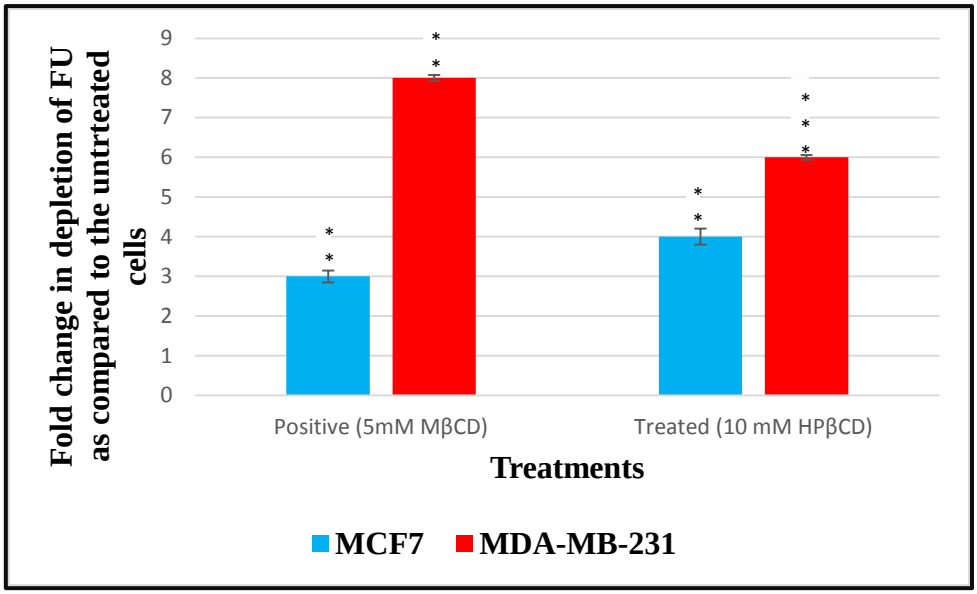


Fig. 46: Graph comparing fold change in depletion of fluorescence intensity (FU) as compared to untreated cells. *Results from two independent experiments were combined to calculate S.D. ES- 0.73 (MCF7), ES- 0.88 (MDA-MB-231).*

Although studies couldn't be done on normal cells, but it is quite adequately known that they do have lesser cholesterol levels as compared to cancerous cells like mentioned before and therefore will show significantly lesser florescence. A similar study done in 2015 (Maekawa and Fairn 2015) confirms this fact.

6.2.3 WESTERN BLOTTING

In order to delve in to more detailed mechanisms of cholesterol-depletion we did a western blotting analysis for SREBP-1 protein, which is a known transcription factor involved in cholesterol homeostasis (Nakakuki, Shimano et al. 2007; Shao and Espenshade 2012). Lysates from MCF7, MDA-MB-231 and MRC-5 cells were used. 10 mM HPβCD was treated for 24 hrs.

SREBP's are key elements responsible for the gene expression of vital enzymes involved in fatty acid synthesis (Nakakuki, Shimano et al. 2007) which includes SREBP-1 and SREBP-2. Down regulation of SREBP's potentially correlates to regression in cell growth and migration and has also been shown to cause apoptosis in several cancers (Nie, Lu et al. 2013; Sun, He et al. 2015). In order to investigate this characteristic feature of SREBP's, a western blot analysis was performed to observe if HPβCD treatment does alter SREBP levels.

For MCF7's, after quantification using the Image Lab™ Software, it was seen that the treated (10 mM HPβCD) protein sample **(Fig. 47 B)** had about five times less activity of SREBP-1 as compared to the untreated lysate **(Fig. 47 A)** after equal loading of the respective samples. Thus indicating that SREBP-1 is significantly downregulated upon HPβCD treatment.

In MDA-MB-231, a similar observation was made. Post quantification using the Image Lab™ Software, it was seen that the treated (10 mM HPβCD) protein sample **(Fig. 48 B)** had about two and a half times less activity of SREBP-1 as compared to the untreated lysate **(Fig. 48 A)** after equal loading of the respective samples. This was expected, considering the relatively lower cholesterol levels in MDA-MB-231 cells as observed from our cholesterol quantification assay (6.2.1) which again emphasizes that like in MCF7, SREBP-1 is also downregulated upon HPβCD treatment in MDA-MB-231 cells.

Interestingly, in the normal MRC-5 cells, after quantification it was observed that SREBP-1 activity remained equal and stayed at basal levels both in the untreated **(Fig. 49 A)** and treated lysates **(Fig. 49 B)**. In a very recent study, HPβCD was reported to cause a downregulation in SREBP thereby providing significant insights on its mode of action (Gaspar, Mathieu et al. 2017). Our western blotting analysis is a confirmation and proves that HPβCD treatment knocks down SREBP-1 activity in cancer cells whereas in normal cells it stays the same and doesn't affect cholesterol biosynthesis.

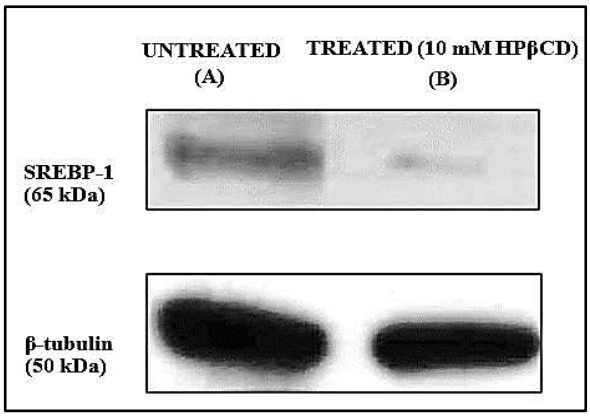


Fig. 47: Western blot assay to detect protein expression of SREBP-1 in MCF7 cells. ***(A):*** *Protein levels in untreated cells,* ***(B):*** *Protein levels in HPβCD treated cells (10 mM HPβCD). β-tubulin was used as a loading control. Independent experiments were run at least 3 times.*

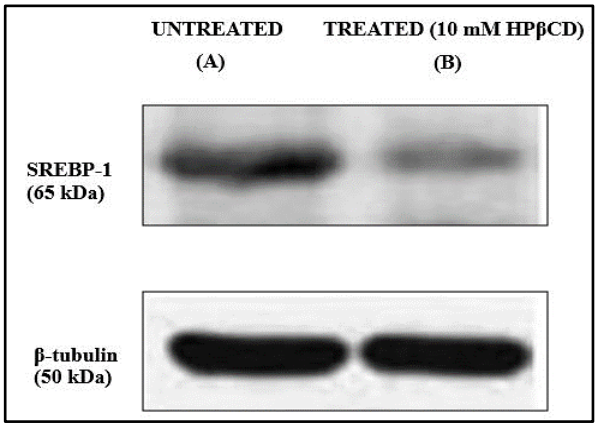


Fig. 48: Western blot assay to detect protein expression of SREBP-1 in MDA-MB-231 cells. ***(A):*** *Protein levels in untreated cells,* ***(B):*** *Protein levels in HPβCD treated cells (10 mM HPβCD). β-tubulin was used as a loading control. Independent experiments were run at least 3 times.*

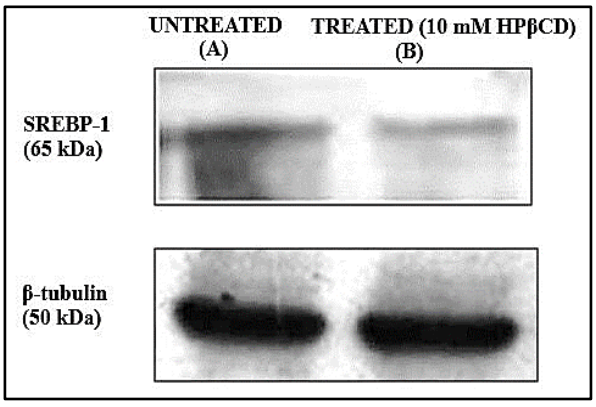


Fig. 49: Western blot assay to detect protein expression of SREBP-1 in MRC-5 cells. ***(A):*** *Protein levels in untreated cells,* ***(B):*** *Protein levels in HPβCD treated cells (10 mM HPβCD). β-tubulin was used as a loading control. Independent experiments were run at least 3 times.*

6.3 *IN VIVO* STUDIES (MICE XENOGRAFTS)

Since the potency of HPβCD against breast cancer was established in our *in vitro* assays, we took the study further and did a thorough investigation in a mice model (MF-1 Nude Mice). MDA-MB-231 cells were injected in 14 mice and after tumour development, was treated with HPβCD (3000 mg/kg b.w.). A maximum of 10 doses treatment plan was followed throughout the study.

Mice models are generally preferred for medical testing because of their biological and genetic makeup which are closely related to humans (Perlman 2016). They also tend to exhibit similar disease patterns and have been widely used to investigate potential drugs. To examine if HPβCD can be used a future anti-breast cancer drug, mice xenografts were prepared.

The study for TNBC (MDA-MB-231) is complete. The mice were subdivided into various groups namely: Late stage, intermediate stage and early stage estrogen negative cancer. 4 mice were grouped as untreated (not receiving HPβCD), 4 for treated (late stage), 3 for treated (intermediate stage) and 3 for treated (early stage).

After about 5 weeks post cells injection, we started observing tumours in the untreated group (n=4) and the average size went up to 13178.12 mm^3 in two weeks' time **(Fig. 50 A, B, C)**. This is because MDA-MB-231 cells are extremely aggressive in nature (Gozgit, Pentecost et al. 2006) and that is the reason we still don't have any adequate treatments except the side effects prone chemotherapy. These 4 mice had to be euthanised at this point because of humane end points. In the late stage treated group, the treatment commenced when the size of the tumour was in between 900 mm^3 to 1350 mm^3 **(Fig. 51 A, B, C)**. After following a strict 10 dose approach where HPβCD was administered via IP, 10 times, (once each day) for a period of 2-3 weeks, we saw significant reduction in the progression of tumours and the average size of the tumours reduced to a significant **73.9 % (Fig. 51 C)** compared to the untreated group.

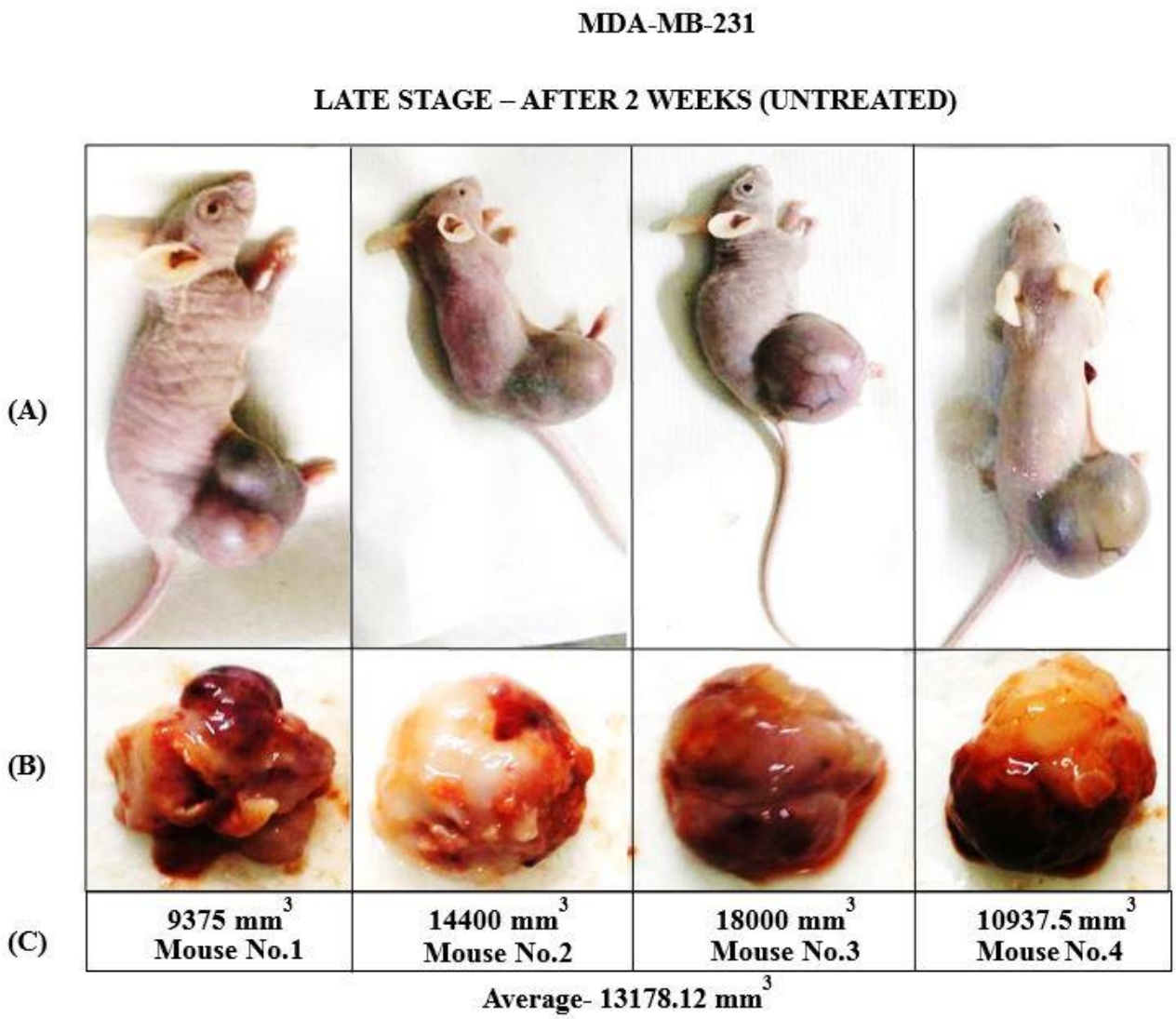


Fig. 50: Mice images post euthanisation showing tumour sizes in untreated group at a late stage, injected with MDA-MB-231 cells. ***(A):*** *Mice post euthanisation,* ***(B):*** *Harvested tumours and* ***(C):*** *Tumour sizes.*

LATE STAGE – AFTER 10 doses of HPβCD (TREATED) (3000 mg/kg b.w.)

(Treatment commenced at 950-1300 mm^3)

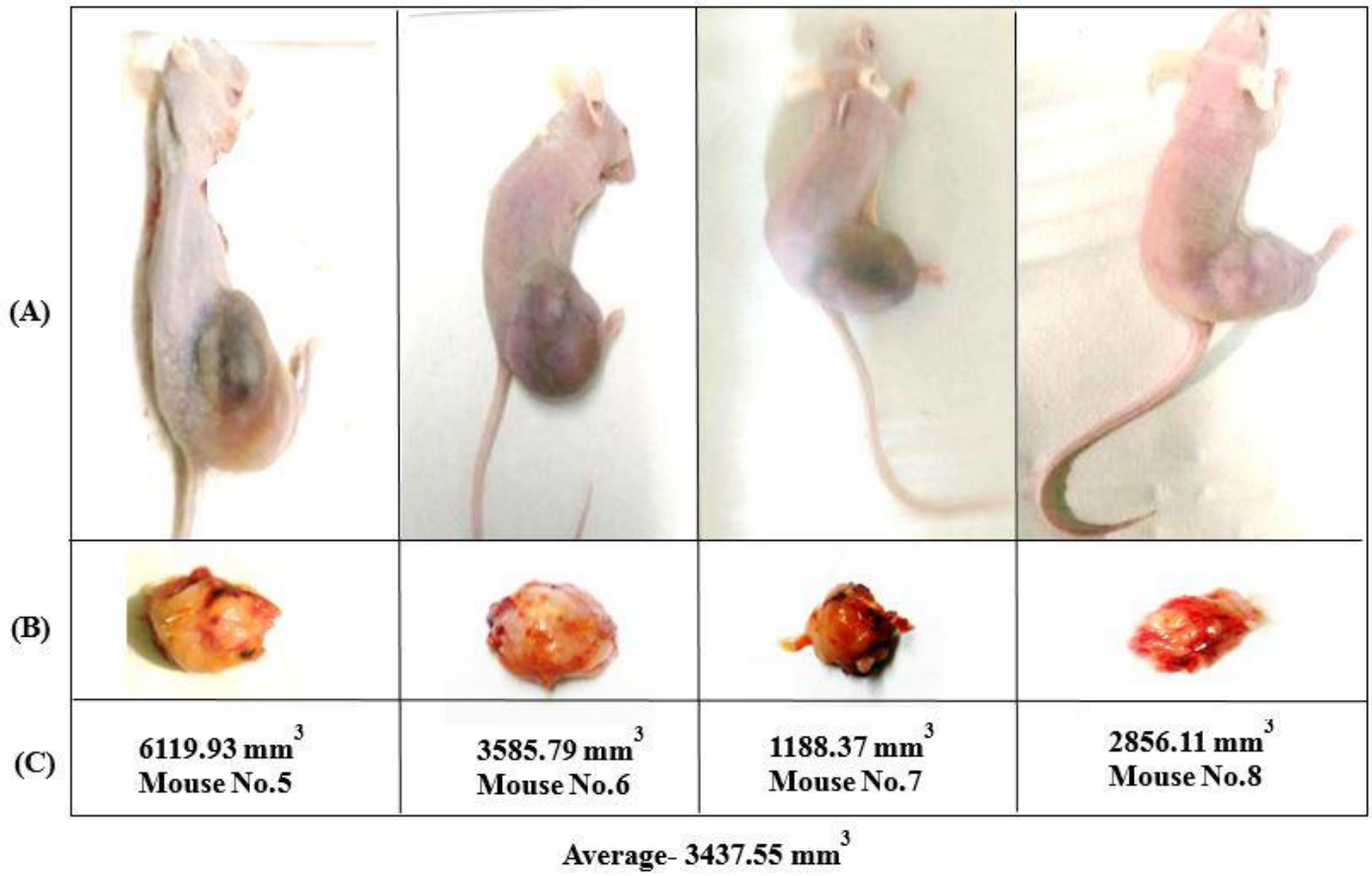


Fig. 51: Mice images post euthanisation showing tumour sizes in treated group at a late stage, injected with MDA-MB-231 cells and treated with HPβCD (3000 mg/kg b.w.) for 10 doses. ***(A):*** *Mice post euthanisation,* ***(B):*** *Harvested tumours and* ***(C):*** *Tumour sizes. Results show tumour reduction by 73.9 % compared to the untreated group.*

In the intermediate stage group (n=3), the treatment commenced when the size of the tumours reached ~250 mm^3. Again, after 10 doses of HPβCD treatment (once each day) for a period of two weeks, we saw the average size of the tumours went down to 784.18 mm3 which is a staggering **94%** decrease **(Fig. 52 B, C)** as compared to the untreated group. This was remarkable considering the invasiveness of MDA-MB-231 cells.

INTERMEDIATE STAGE - AFTER 10 doses of HPβCD (TREATED) (3000 mg/kg b.w.)
Treatment commenced at ~250 mm^3

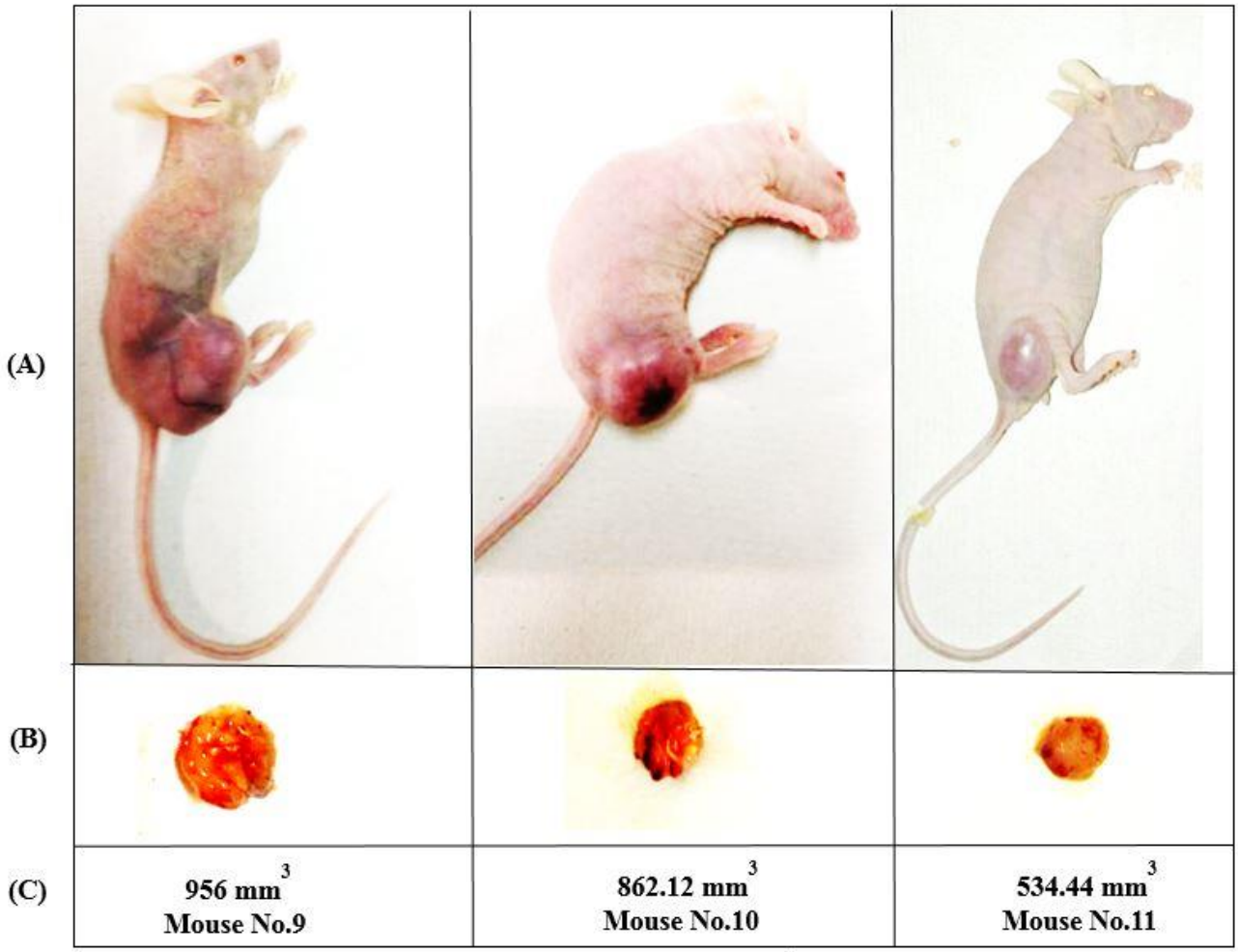


Fig. 52: Mice images post euthanisation showing tumour sizes in treated group at an intermediate stage, injected with MDA-MB-231 cells and treated with HPβCD (3000 mg/kg b.w.) for 10 doses. ***(A):*** *Mice post euthanisation,* ***(B):*** *Harvested tumours and* ***(C):*** *Tumour size. Results show tumour reduction by 94 % compared to the untreated group.*

Finally, in the early stage group (n=3), the treatment commenced when the tumour size was ~ 20 mm^3 **(Fig. 53 A, B)**. HPβCD was administered for 10 dosages (once each day) and after about a period of one and a half weeks, the tumours were completely healed **(Fig. 54 A, B)**. These 3 mice were then kept for a period of 4 weeks to check for relapse of tumour because estrogen negative tumours have an extreme propensity to recur (Fisher, Redmond et al. 1988). After 4 weeks of the relapse test **(Fig. 55)** it was clearly observed that there was no recurrence of the tumour. These mice could not be kept for longer periods due to financial and technical constraints.

EARLY STAGE – AFTER 1 WEEK (UNTREATED)

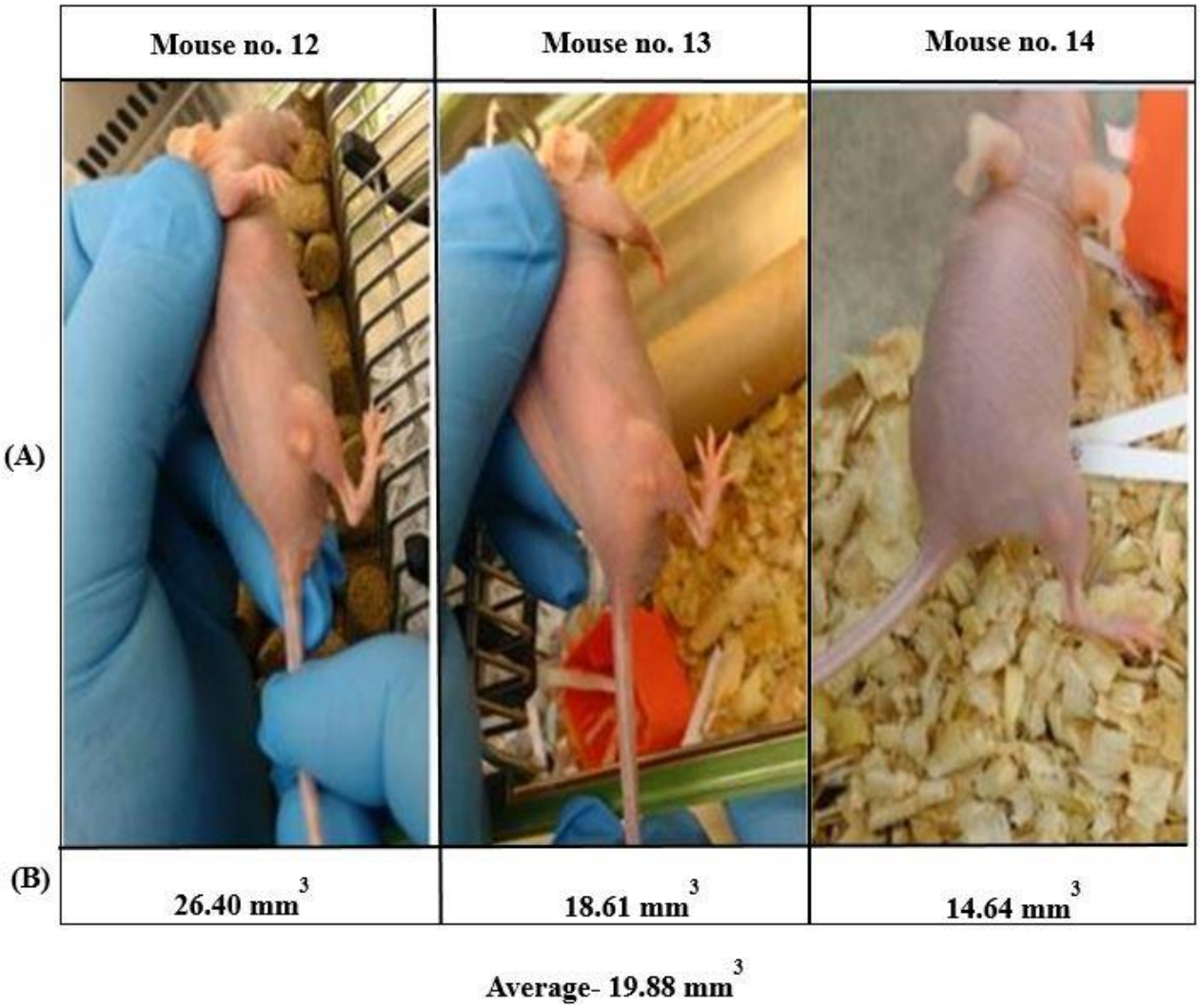


Fig. 53: Mice images showing tumour sizes in untreated group at an early stage, injected with MDA-MB-231 cells. ***(A):*** *Initiation of tumour and* ***(B):*** *Tumour sizes*

EARLY STAGE – AFTER 10 doses of HPβCD (TREATED) (3000 mg/kg b.w.)
Treatment commenced at ~20 mm^3

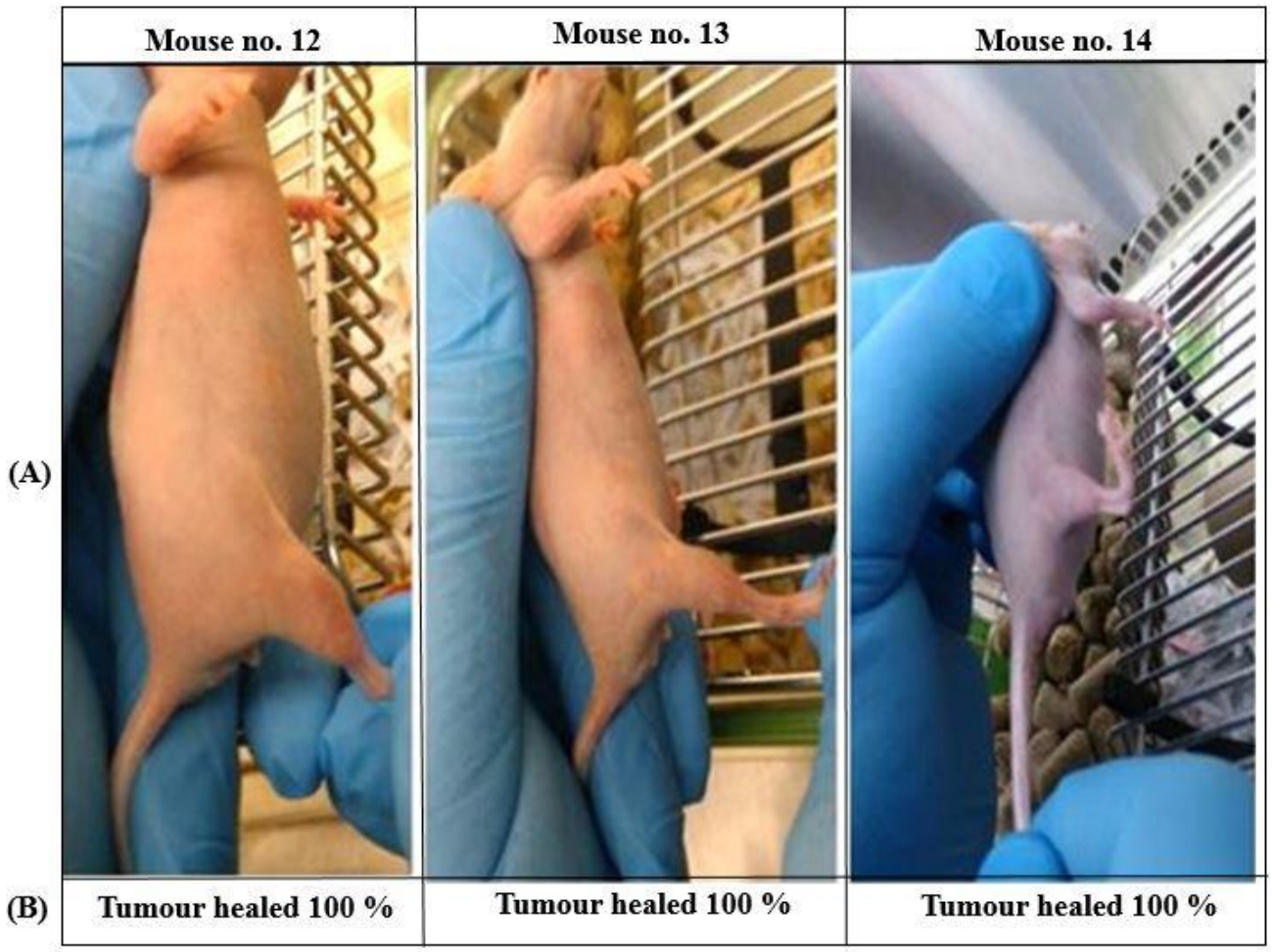


Fig. 54: Mice images showing tumour sizes in treated group at an early stage, injected with MDA-MB-231 cells and treated with HPβCD (3000 mg/kg b.w.) for 10 doses. ***(A):*** *Termination of tumour and* ***(B):*** *Complete healing of tumour.*

RELAPSE TEST FOR 4 WEEKS (Early stage)

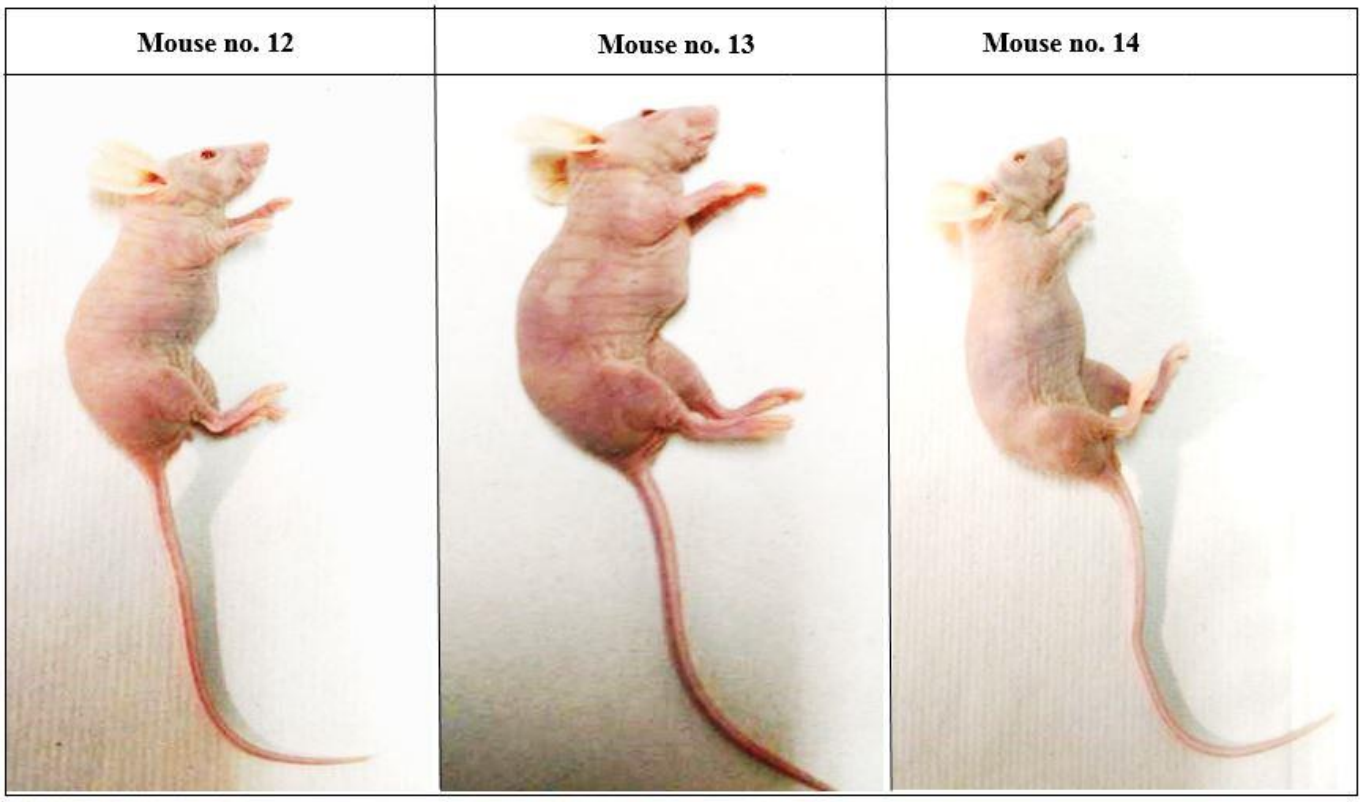


Fig. 55: All three healed mice (No. 12, 13 and 14) tested for relapse of TNBC tumour for a period of 4 weeks. *Results show no relapse at all.*

The weights of all the mice were monitored throughout the study in order to check if HPβCD treatment is affecting mice health (Fig. 56). No abnormal weight change was observed throughout thus indicating that HPβCD has little or no side-effects. Post-euthanisation, the mice serum was analysed for ALT/AST levels in order to observe if HPβCD treatment had any toxicity (Fig. 57). The ALT/AST ratio gives an estimate of liver toxicity or damage. The tests revealed that HPβCD didn't have any toxic effects on the mice. The ALT/AST ratio for all the mice were under the recommended ratio of 2 and the values were in between the reference range. The levels of ALT/AST in the late, intermediate and early stage mice were not significant as compared to the untreated group. Thus indicating that there was little or no toxicity when HPβCD was administered to the mice. The statistically significant difference between groups was determined by one-way ANOVA ($F(3,16)= 1.74$, $p= 0.19$ (Late), ES- 0.32, ANOVA ($F(2,12)= 1.87$, $p= 0.19$ (Intermediate), ES- 0.34, ANOVA ($F(2,12)= 4.85$, $p= 0.02$ (Early), ES- 0.44.

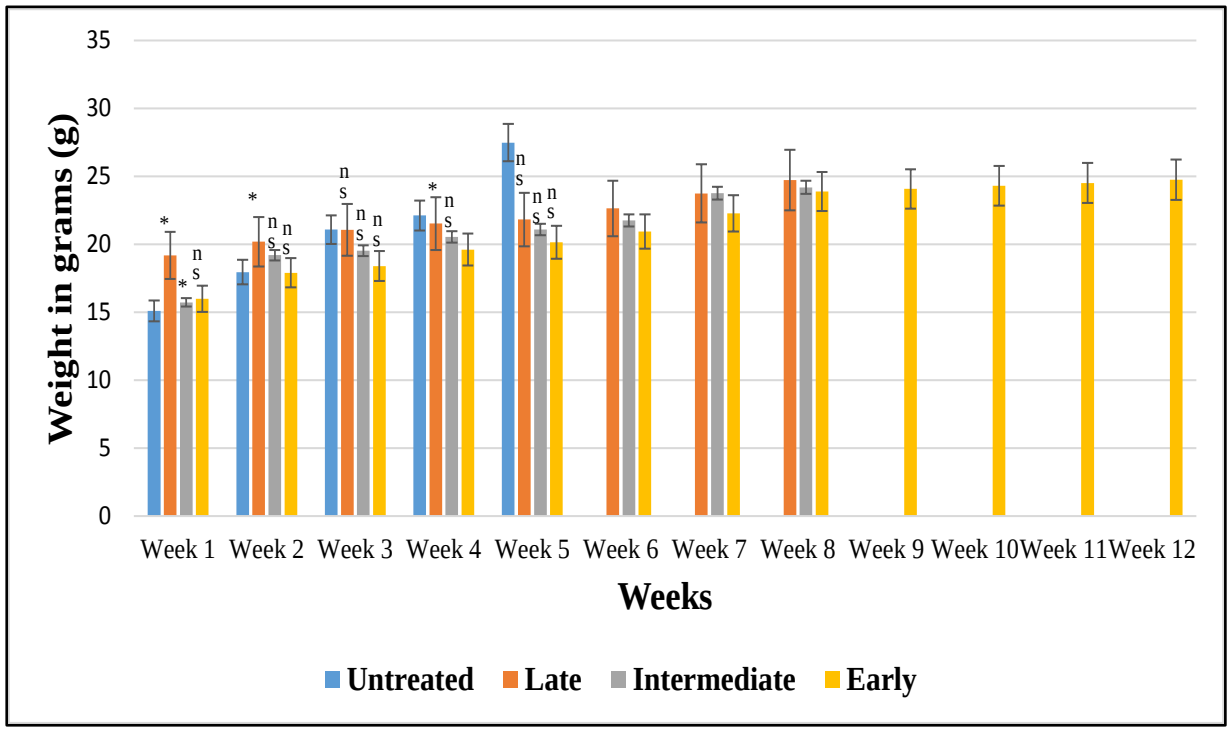


Fig. 56: Weight change in all 14 mice across the study. *Data are mean ± S.D. (n=3 or n=4) from raw data, where *p<0.05, **p<0.01 and ***p<0.00, and 'ns' corresponds to not significant difference to untreated control. Significance was only calculated for five weeks because the untreated group had to be euthanised at this point.*

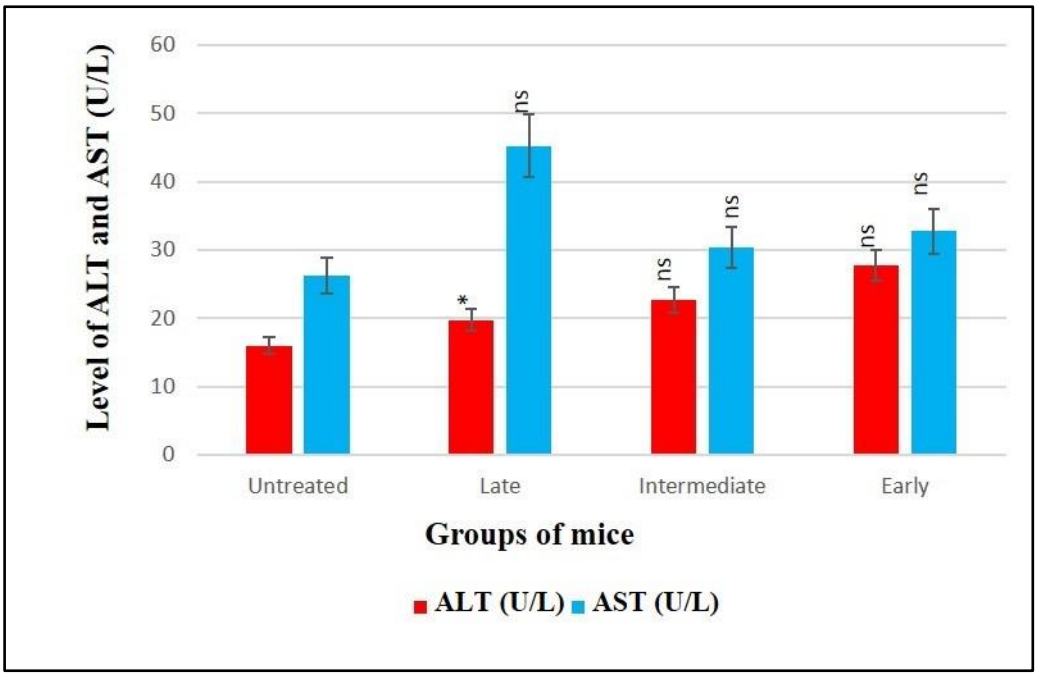


Fig. 57: Graphical representation of ALT/AST levels in all 14 mice across the study. *Permissible range in mice, for ALT is 28-132 U/L and AST is 59-247 U/L. Data are mean ± S.D. (n=3 or n=4) from raw data, where *p<0.05, and 'ns' corresponds to not significant difference to untreated control.*

The statistically significant difference between groups was determined by one-way ANOVA ($F(2,7)= 1.65$, $p= 0.25$ (ALT), ES- 0.34, ANOVA ($F(2,7)= 0.28$, $p= 0.75$ (AST), ES- 0.65.

7. DISCUSSION

The present study aimed to investigate the potential of HPβCD as an anti-breast cancer agent. Historically, it has predominantly been used as a carrier to solubilize poorly soluble drugs **(Table 1)** owing to its hydrophilic exterior which leads to enhanced absorption in the body. Investigating HPβCD without any complex and as a stand-alone agent for diseases has recently garnered attention. HPβCD is being investigated currently as a strategy to treat Niemann-Pick disease type C. It has successfully passed Phase 1 clinical trials in 2013 and received the FDA's Breakthrough Therapy Designation. Phase 2b/3 clinical trial efficacy tests are currently underway. But the studies in cancer are relatively scarce. To address this caveat and to explore the potential of HPβCD as an anti-breast cancer agent, the present study was conducted in two phases. In the first part, the efficacy of HPβCD against BC was tested using primary screening assays in order to determine the cell growth inhibition and cell death. The mechanism of cell death was then elucidated with cholesterol based assays. In the second part, HPβCD was tested in mice xenografts to validate its efficacy against TNBC tumours. Recent studies with leukemia (Yokoo, Kubota et al. 2015) and atherosclerosis (Zimmer, Grebe et al. 2016) has shown the potential use of HPβCD as a future drug.

Yokoo et al., tested HPβCD across different leukemia cells and the IC_{50} values ranged from ~4 mM to ~10 mM across different time points upto 72 hrs whereas Zimmer et al. reported using similar concentrations, that cholesterol homeostasis was disturbed upon treatment with HPβCD which resulted in a decrease in the overall cholesterol content following a dose-dependent response in atherosclerosis. Varying concentrations were tested in the present study at three different time points 24 hrs, 48 hrs and 72 hrs. Both MCF7 and MDA-MB-231 cells had IC_{50} values of 11.11 mM and 12.34 mM respectively **(Table 8)** thus confirming cell growth inhibition. The statistically significant difference between groups was determined for both MCF7 and MDA-MB-231 cells by one-way ANOVA. For MCF7, (F(4,10)= 1528.5, p= 6.95E-14 (24 hrs), ANOVA (F(4,10)=544.34, p= 1.32E-12 (48 hrs), ANOVA (F(4,10)=823.4, p= 3.32E-11 (72 hrs). ES – 2.68, 31.23, 36.84, 39.22, 84.5 for 1 mM, 5 mM, 10 mM, 20 mM, 50 mM (24 hrs) respectively. ES – 28.65, 46.49, 41.32, 86.43, 145.21 (48 hrs) respectively. ES – 18.21, 33.51, 31.43, 76.43, 91.23 (72 hrs) respectively. For MDA-MB-231, (F(4,10)= 268.7, p= 3.96E-10 (24 hrs), ANOVA (F(4,10)=1788.88, p= 3.17E-14 (48 hrs), ANOVA (F(4,10)=447.8, p= 3.15E-11 (72 hrs) ES – 1.98, 26.07, 26.67, 19.13, 76.7 for 1 mM, 5 mM, 10 mM, 20 mM, 50 mM respectively. ES- 18.33, 44.17, 21.39, 91.66, 131.95 (48 hrs) respectively. ES- 14.48, 37.55, 10.88, 79.89, 89.28 (72 hrs) respectively.

A very low "p" value was observed between groups along with high ES thus suggesting a large significance. In similar studies on leukemia (Yokoo, Kubota et al. 2015), investigations with HPβCD have shown its inhibitory effects on cell growth through apoptosis and G_2/M mitotic cell-cycle arrest.

The mechanism of growth inhibition is usually through cell death due to apoptosis (Elmore 2007). Over the years many agents have been researched for apoptotic potential against BC like quercetin (Choi, Kim et al. 2001), vernodalin (Looi, Arya et al. 2013), lycorine hydrochloride (Ji, Yu et al. 2017), statins (Garwood, Kumar et al. 2010) etc. The major shortcomings of all the agents were toxicity in normal cells. The use of CyDs against BC has shown promising results in multiple studies with limited or no toxicity. But studies with HPβCD are still quite limited. A latest study has reported a variant of CyDs, hydroxypropyl-alpha CyD (HPαCD) to be quite effective in BC *in vitro*, but studies in an animal model was not done (Wittkowski, Dadurian et al. 2018). The most well researched and popular amongst all CyDs however is MβCD. It has been extensively used over the years both as a complex and *per se* as a treatment in several diseases and because HPβCD and MβCD are structurally quite similar it is hypothesized that the mechanism of action for both are comparable. Very recently, MβCD was used to investigate effects on Equine metabolic syndrome (EMS) where a steady level of Bcl-2/Bax expression was captured thus indicating its role in apoptosis (Szydlarska, Weiss et al. 2018). In this study, treatment with MβCD on the control cells led to a significant increase in the DNA fragmentation as compared to cells without MβCD. Further studies showed that CyDs have the potential to initiate cell death, but the extent of cell death depends on the final concentration of MβCD and also the type of cell. The nature of the cell death is apoptotic but is independent of caspase-3 activity and leads to elevated levels of Bax protein (Wood and Newcomb 2000). Bax and Bcl-X_L play crucial roles in the nervous system (Motoyama, Wang et al. 1995). They have also been reported to play critical roles in the survival of cells (Gross, Pilcher et al. 2000). Moreover, overexpression studies conducted on Bcl-X_L, was seen to have an inhibitory response to apoptosis induced by Bax (Finucane, Bossy-Wetzel et al. 1999). High levels of PC12 cells (derived from pheochromocytoma of the rat adrenal medulla) death was also observed as a response to MβCD treatment if the levels of Bcl-X_L protein are kept high (Ulloth, Almaguel et al. 2007). Possible explanations for such a phenomenon could be firstly, Bax and Bcl-X_L levels of elevation are not affected at all in the MβCD-induced apoptosis and secondly, Bax has the potential to bypass the effects of Bcl-X_L.

Bax cleavage induced by MβCD may give an imperative piece of information in recognizing these two potential outcomes.

HPβCD have very recently been a molecule of interest due to its low toxicity. In 2017, a study was conducted using Dentatin (DEN). DEN is a hydrophobic compound and occurs naturally in *Clausena excavata*. It has been reported to cause apoptosis on liver (Andas, Abdul et al. 2015), breast (Arbab, Abdul et al. 2013) and prostate cancer cells (Arbab, Looi et al. 2012). In several human cancer cells, DEN has shown to cause apoptosis by the upregulation of apoptotic protease-activating factor 1 and pro-apoptotic proteins like Bax and Bak which leads to caspase activation and down regulation of the anti-apoptotic gene poly ADP-ribose polymerase (PARP). This eventually leads to the release of cytochrome c from mitochondria to the cytosol. The anti-cancer effects of DEN are quite selective, it is seen to be non-toxic to normal cells (Arbab, Looi et al. 2012; Andas, Abdul et al. 2015; Ashwaq, Al-Qubaisi et al. 2016). However, DEN when complexed with HPβCD (DEN-HPβCD) caused increased growth inhibition in MDA-MB-231, HGT (Human Gastric Cancer) and LNCaP cells (human prostate carcinoma) (Ashwaq, Rasedee et al. 2017). DEN-HPβCD showed an overexpression of the Bax proteins (Ashwaq, Al-Qubaisi et al. 2016). If lipophilic compounds like cholesterol are incorporated into the HPβCD cavity, it was shown to improve their solubility in water and moreover it enhanced the therapeutic potential (Davis and Brewster 2004). Even though this study showed that DEN, irrespective of being free or complexed in HPβCD induces apoptosis and thereby cancer cell death, the molecular mechanisms related with their anti-cancer activities are still not understood. Translocation of PS during apoptosis was detected in a study by Keichii et al 2009. Both these reports support the results of the present study where significant apoptosis, 45% and 40% **(Fig. 24 and Fig. 26)** was observed via translocation of PS in MCF7 and MDA-MB-231 cells respectively. The statistically significant difference between groups was determined for both MCF7 and MDA-MB-231 cells by one-way ANOVA. For MCF7, ($F(4,10)= 2231.56$, $p= 2.4E-10$. ES – 43.21, 66.22, 56.89, 121.76, 136.72 (for 1 mM, 5 mM, 10 mM, 20 mM, 50 mM respectively. For MDA-MB-231, ($F(4,10)= 954.2$, $p= 1.5E-11$. ES – 31.25, 43.55, 86.54, 126.44, 151.43 for 1 mM, 5 mM, 10 mM, 20 mM, 50 mM respectively. "p" value was seen to be quite low along with a high ES like MTT assay thus suggesting a very high significance.

CyDs have been accounted for interactions with components of the cell membrane, mostly phospholipids and cholesterol , leading to the disruption of the red blood cells in humans and rabbits (Irie, Otagiri et al. 1982; Ohtani, Irie et al. 1989; Fauvelle, Debouzy et al. 1997). A myriad of studies have reported that CyDs have the ability to disrupt the lipid rafts (Kabouridis, Janzen et al. 2000; Parpal, Karlsson et al. 2001). It is now a well-documented fact that MβCD in particular, disrupts lipid rafts by extracting cholesterol from the cell membranes thereby altering cell signalling (Hueber, Bernard et al. 2002; Gniadecki 2004). In another study, it was reported that MβCD initiated a change in the morphology of rabbit red blood cells from discocyte (8 μm in diameter) to echinocyte (> 9 μm in diameter) via extracting cholesterol from the lipid rafts (Motoyama, Toyodome et al. 2009), whereas 2,6-di-*O*-methyl-α-cyclodextrin (MαCD) which is another variant of CyDs, leads to morphological changes from discocyte to stomatocyte by extracting sphingomyelin and not cholesterol from the lipid rafts. These lines of proof make it interesting to hypothesise that MβCD and MαCD demonstrate different kinds of cell death, because they have the ability to extract membrane constituents from separate lipid microdomains on cell membranes. Inspite of all the on-going research, ambiguity still remains to the fact that whether these CyDs induce apoptosis or not via the interaction with membrane components in different types of cells. As previously mentioned, MβCD has the potential to extract cholesterol from lipid microdomains in rabbit red blood cells. Therefore, it's a pertinent question if MβCD induced apoptosis is responsible for its ability to extract cholesterol. In fact, it has been shown in KB cells (Keratin-forming tumour cell line HeLa) that MβCD can release cholesterol from lipid rafts into the culture medium. Additionally, the cytotoxic ability of MβCD can be significantly inhibited if cholesterol is supplemented in the culture medium. Therefore, the results strongly indicates that MβCD induced apoptosis is due to the depletion of cholesterol in lipid rafts. Further studies on the levels of cholesterol after MβCD treatment in cell membranes with its correlation to cell death and the extracted cholesterol are however warranted (Motoyama, Toyodome et al. 2009).

One of the key steps in apoptosis is the loss of MOMP. Mitochondria plays a crucial role in the signal transduction during apoptosis, it incites activation of the caspase family via the reduction of mitochondrial transmembrane potential ($\Delta\psi_m$) which leads to the release of cytochrome *c* prior to the initiation of apoptosis. CyDs have been reported to lower $\Delta\psi_m$ leading to the release of cytochrome *c* in NR8383 cells (derived from rat macrophages) (Motoyama, Toyodome et al. 2009), which initiates apoptosis by Bad and contributes to the binding of Bad/Bcl- x_L on the mitochondrial membrane. Subsequently, the phosphorylation of Bad is inhibited by CyDs and this results in the collapse of $\Delta\psi_m$ and releases cytochrome *c* from mitochondria. Therefore, it is quite evident that CyDs induce the mitochondria-dependent pathway mediated apoptosis (intrinsic pathway). Bax/Bak induces MOMP and other "sensitizers" like Bik, Bmf, Bad, Hrk, Puma and Noxa, which are not directly responsible for Bax/Bak activation but instead inhibit anti-apoptotic proteins. Present study also demonstrated similar results where MOMP mediated apoptosis by HPβCD was established for MCF7 and MDA-MB-231 cells at 92.1% and 78.1% respectively **(Fig. 32 and Fig. 33)**.

It is a well-known fact that reduction in MOMP leads to the release of cytochrome *c* from mitochondria leading to the activation of caspase-3 and caspase-7 via the formation of apoptosome (Wang 2001). Activation of caspases-3 upon treatment with CyDs have been reported in 2009 in NR8383 cells (Motoyama, Kameyama et al. 2009). Caspases are inactive zymogens, when activated, initiator caspases like caspase-8 and 10 cleaves downstream effector caspases like caspase-3 and caspase-7, which are responsible in metabolizing specific substrates that causes cell death. Following this convention the current investigations with the caspase-3/7 assay yielded elevated levels (4 folds and 2.5 folds) of caspase activity both in MCF7 and MDA-MDA-231 cells respectively **(Fig. 38 and Fig. 39)** thus confirming apoptosis via the mitochondrial-mediated (intrinsic) pathway.

Another hallmark of apoptosis is the production of ROS (Redza-Dutordoir and Averill-Bates 2016). ROS are small molecules, highly reactive and very short-lived (Halliwell 2011; Winterbourn 2015). They are either non-radical molecules like H_2O_2 or free radicals like superoxide anion ($O_2^{\bullet-}$) and the hydroxyl radical ($OH^{\bullet}$). The production of ROS in cells co-exists with an array of anti-oxidant defences like peroxiredoxins, superoxide dismutases (SOD), glutathione peroxidase and catalase along with carotenoids, vitamins C and E, lipoic acid, glutathione (GSH) and iron chelators (Halliwell 2011), which are non-enzymatic. ROS generation have been widely implicated in the initiation of various transcription factors and

cell signalling pathways which include nuclear factor (erythroid-derived 2)-like 2 (Nrf2)/Kelch like-ECH-associated protein 1 (Keap1), PI3K/Akt, MAPK, tumour suppressor p53 and the nuclear factor-κB (NF-κB) which are known to mediate cell survival and the cell death mechanisms such as apoptosis and autophagy (Covarrubias, Hernández-García et al. 2008; Zhang, Wang et al. 2016). In most cases, an increase of ROS has a positive correlation with the levels of apoptosis. However, there are several reports of downregulation in ROS production in apoptosis. Although this is perplexing, but is possible considering the essential roles of ROS in maintaining the physiological balance in the body. Several studies have shown the use of apoptotic agents such as metformin and quercetin subsequently downregulated ROS production. Metformin, at levels of $\sim 10^{-5}$ mol/L was shown to lower ROS levels in endothelial cells (Ouslimani, Peynet et al. 2005). The ROS assay performed in the present research observed a parallel result where the levels of ROS production were not elevated drastically as compared to the untreated samples and control cell line **(Fig. 35, Fig. 36 and Fig. 37)**. It has also been reported that the decrease in ROS could potentially inhibit DNA damage and thereby reducing the risk of cancer (Algire, Moiseeva et al. 2012). Some clinically relevant functions of quercetin are hypocholesterolaemic, anti-tumour and antihypertensive activity. Studies have reported the downregulation of ROS by a quercetin glycoside known as rutin, which was used in H_2O_2 induced apoptosis of human endothelial cells (Gong, Qin et al. 2010).

Over the past decade, numerous studies have shown that CyDs remove cellular cholesterol when introduced to different cholesterol rich cells. The level of cholesterol-depletion is however dependant on several factors like the type of CyD derivative, type of cells, temperature, the concentration and the incubation time of treatment. Another important point that needs to be considered is how CyDs affect the cholesterol distribution between different cell membranes. Studies have implicated that compared to the intracellular membranes, plasma membranes have significantly higher cholesterol levels (Davis and Poznansky 1987; Slotte and Bierman 1988; Lange, Swaisgood et al. 1989; Lange 1991). Quite specifically, approximately 90% of free cholesterol was observed to be residing in the plasma membrane in different cell types (Lange, Swaisgood et al. 1989; Kim, Maxwell et al. 1991; Lange 1991). In 1989, however the levels of cholesterol in the plasma membrane was quantified to be about 25–40% of total cellular cholesterol (van Meer 1989). Therefore, when cells are treated with CyDs, the intracellular membrane cholesterol levels are affected, which were found to be responsible for the constitution of the cholesterol kinetic pool as analysed by CyD-induced cholesterol efflux (Hao, Lin et al. 2002). In fact, it has been shown that the cholesterol levels in the intracellular

membranes are positively regulated by the cholesterol levels in the plasma membrane (Lange, Ye et al. 1999; Lange, Ye et al. 2004). Moreover, even subtle changes in the plasma membrane cholesterol initiates extensive changes in the intracellular membranes cholesterol levels. One such example is the study with fibroblasts and HPβCD which resulted in approximately 25% depletion of cholesterol level in the plasma and intracellular membrane thus resulting in an 80% depletion of the cholesterol levels in the endoplasmic reticulum (Lange, Ye et al. 1999). Low-density membrane fractions have been classically identified as membrane rafts. These fractions were seen to contain approximately 30%–50% of total (Brown and Rose 1992; Larbi, Douziech et al. 2004; Rouquette-Jazdanian, Pelassy et al. 2006) or cell membrane (Gaus, Kritharides et al. 2004; Gaus, Rodriguez et al. 2005) cholesterol in diverse cell types. Lipid rafts contain unesterified cholesterol as a major component and it is regulated by the circulating LDL via extracellular uptake from blood (Ho, Brown et al. 1976; Verhoeye, Descamps et al. 1996) and *de novo* intracellular synthesis (Lehoux, Kandalaft et al. 1985).

CyDs ability to deplete cholesterol and CE from phospholipid bilayers in cell membranes has now been established. A group of researchers (Stelzl, Nielsen et al. 2015) showed that in giant unilamellar vesicles (GUV) composing of cholesterol, when lipid bilayers were exposed to HPβCD and MβCD in a water environment, the cholesterol-depletion was a favourable process and took place spontaneously. A similar study (Litz, Thakkar et al. 2016) using fluorescence spectroscopy showed that the cholesterol removal from GUVs was very fast (milliseconds), and there was a formation of extended holes in the lipid bilayers (composed of unsaturated and saturated phospholipids).

Breast and prostate cancer cells have elevated levels of cholesterol (Li, Park et al. 2006) than normal cells. Therefore treatment with cholesterol-depleting agents like CyDs elicits an overall depletion in cholesterol levels and inhibit growth of cells via apoptosis. The initiation of apoptosis is limited to only cholesterol-extracting CyDs like MβCD and HPβCD, it is quite likely that the disruption of cholesterol-rich microdomains is due to the depletion of cholesterol from cellular membranes. There is a plethora of evidences that lipid rafts play extremely crucial roles in the signal transduction pathways along with receptor tyrosine kinases and glycosylphosphatidylinisotol (GPI)-anchored proteins (Simons and Toomre 2000; Pike 2003; Fielding and Fielding 2004). Moreover, lipid rafts involvement in the signalling pathways following the activation of death receptor in mouse thymocytes and human lymphoid cells has been shown (Hueber, Bernard et al. 2002; Eramo, Sargiacomo et al. 2004). Quantification via

the cholesterol assay **(Fig. 41 and Fig. 42)** in our study showed an overall cholesterol-depletion across different concentrations of HPβCD thus indicating the involvement of lipid rafts mediated cholesterol-depletion as well as esterified cholesterol. The statistically significant difference between groups was determined for both MCF7 and MDA-MB-231 cells by one-way ANOVA. For MCF7, ($F(4,10)= 442.2$ $p= 1.2E-11$. ES – 23.34, 45.65, 57.93, 132.54, 135.43 for 1 mM, 5 mM, 10 mM, 20 mM, 50 mM respectively. For MDA-MB-231, ($F(4,10)= 5174.2$, $p= 3.2E-15$. ES – 12.45, 32.19, 47.56, 122.43, 142.56 for 1 mM, 5 mM, 10 mM, 20 mM, 50 mM respectively. Like MTT and APOPercentage assays, a very low "p" value and a high ES was observed which suggests a very large significance. This was further supported by the cholesterol staining assay **(Fig. 44 and Fig. 45)** where 50-75% cholesterol-depletion was achieved as detected by Filipin staining. Similarly, in K562 cells (erythroleukemic cell line), upon HPβCD treatment, p-Lyn (known to reside in lipid rafts) levels were greatly reduced (Tilbrook, Palmer et al. 2001). Thus establishing a positive correlation between HPβCD and cholesterol-depletion in lipid rafts.

Several transcription factors have been implicated to play a crucial role in fatty acid and cholesterol synthesis as well as in lipid rafts (Pertusa, Morenilla-Palao et al. 2007). The most common being SREBPs, such as SREBP-1a, SREBP-1c and SREBP-2 (Tontonoz, Kim et al. 1993). These consists of leucine zipper transcription factors having a basic-helix-loop-helix structure and regulates the uptake and synthesis of two of the most important building blocks of cell membranes, cholesterol and fatty acids. The activation and expression of genes such as mevalonate kinase, HMG-CoA reductase and HMG-CoA synthase are involved in cholesterol biosynthesis whereas, SREBPs activate LDL receptor expression (Sato, Inoue et al. 1996) for cholesterol uptake and for fatty acid synthesis and initiates the expression of acetyl-CoA carboxylase and FAS.

SREBPs are usually tightly regulated due to their essential role in cholesterol and triglycerides. As of now, more than 30 genes are known to be controlled by SREBPs which are directly involved in transcription, phospholipids, fatty acids, triglycerides and uptake and synthesis of cholesterol (Horton, Shah et al. 2003). Although SREBPs act in diverse biosynthetic pathways, the activity of each of its isoform is regulated by SCAP and sterols (Matsuda, Korn et al. 2001). SREBP-1 has now been identified as a predominant regulator in TGF-β signalling due to its role as a TβRI cell surface retention factor. The inhibition and downregulation of SREBP-1 has shown to cause secretion in exosomes resulting in its loss from the cell surface mediated by the

lipid rafts. This ultimately leads to reduced levels of TβRI expression on the cell surface receptor available for signalling. (Huang and Chen 2012). Studies demonstrating additional findings on the extent of SREBP-1's involvement in the regulation of TGF-β1 signalling underlines the potential significance of targeting SREBP-1 (Chen, Wang et al. 2014). It is envisaged that SREBP-2 has no role in fatty acid synthesis and is mostly responsible for activation of genes involved in cholesterol synthesis. Conversely, SREBP-1c is responsible to drive fatty acid synthesis functions primarily in the liver. On the other hand, SREBP-1a has the ability to drive both pathways. However, understanding specificity in tissues and the differential genetic potential for every SREBP isoform is still ambiguous.

The central role of SREBPs in controlling lipid synthesis is accentuated by their several interactions with other signalling pathways. In order to increase the supply of unsaturated fatty acids for cholesterol esterification and storage, the nuclear hormone receptors LXR and RXR (retinoid X receptor) function as a heterodimer and upregulate SREBP-1c as a response to cholesterol overloading (Repa, Liang et al. 2000). The transcription of both SREBP-1c and SREBP-2 occurs in the liver and is stimulated by SREBPs which utilise SRE sequences in the promoters of these genes (Horton, Goldstein et al. 2002). The liver converts excess carbohydrates to fatty acids and stores it as triglycerides. Excess carbohydrate leads to the activation of insulin leading to fatty acid synthesis (Horton, Goldstein et al. 2002). SREBP-1c mediates these *de novo* effects of insulin in the liver (Eberle, Hegarty et al. 2004). Insulin is also known to elevate levels of SREBP-1c target gene expression and SREBP-1c mRNA and in the liver and tissue culture cells (Foretz, Guichard et al. 1999; Shimomura, Bashmakov et al. 1999). It has been reported (Chen, Liang et al. 2004) that RXR-LXR mediates the control of SREBP-1c transcription by insulin even though a complete description of insulin action on SREBP-1c requires further validation.

SREBPs also control the genes required for cholesterol and fatty acid synthesis and the transcription of LDL receptor (Horton, Goldstein et al. 2002). In normal conditions, SREBP is located in the endoplasmic reticulum and forms a complex with SCAP, which is complexed to insulin-induced genes. When cellular cholesterol levels are reduced, it leads to a sub-sequential release of the SREBP-SCAP complex and ultimately leads to the translocation to the golgi body where cleavage occurs by site 1 and site 2 proteases at the N-terminus. The active (cleaved) SREBP then translocates to the nucleus where SREBP-1 upregulates enzyme

expression involved in *de novo* synthesis and SREBP-2 modulates the upregulation of the cholesterol biosynthetic genes (Espenshade 2006).

However, an overexpression of SREBP-1 leads to cellular lipotoxicity which contributes to several metabolic disorders and anomalous lipid synthesis (Musso, Gambino et al. 2009). Therefore, SREBP-1 is thought to be an important target to investigate metabolic disorders due to abnormal lipid accumulation. Interestingly, SREBP-1 activation can either be cholesterol-independent or dependent. SREBP-1a can be regulated through SCAP (Espenshade 2006) whereas SREBP-1c through insulin (Sheng, Otani et al. 1995). Studies however have shown that SREBP-1 caused a depletion in HDL levels when cellular cholesterol is elevated. But when treated with CyDs, the depletion of cellular cholesterol abrogated the effect of HDL, thus giving an indication that elevated cellular cholesterol levels are involved in the inhibition of SREBP-1 and is mediated by HDL (Rinninger, Brundert et al. 2001; Brundert, Heeren et al. 2003).

Limited studies showing link between HPβCD and SREBP-1 have been conducted till date. A recent study in 2017 (Gaspar, Mathieu et al. 2017) showed that in cholesterol-loaded cells, HPβCD has the potential to expand the active cholesterol pool and this was the first report to show that SREBP1 levels were reduced with HPβCD treatment. This interestingly, now demands more investigations into explanations pertaining to exactly how HPβCD modifies the composition of the lysosome membrane, especially when it's a known fact that lipid composition affects autophagy (Koga, Kaushik et al. 2010; Rodriguez-Navarro, Kaushik et al. 2012). In our experiments with SREBP-1 upon treatment with HPβCD, a 2.5 to 5 fold decrease in SREBP-1 levels were observed in MCF7 and MDA-MB-231 cells respectively, thus drawing similar conclusions to the above results **(Fig. 47 and Fig. 48)** and indicating that HPβCD treatment leads to a decrease in sterol biosynthesis. Further protein expression studies with cholesterol-mediated genes would help us decipher the exact upregulation or downregulation precisely. To elucidate the exact pathways affecting HPβCD treatment, future studies would be done with RT^2 Profiler PCR Arrays using Human Breast Cancer and Lipoprotein Signalling & Cholesterol Metabolism arrays (Qiagen, Germany).

In vivo studies with CyDs have not been done extensively till date. The first used of MβCD in mice was reported way back in 1998 (Grosse, Bressolle et al. 1998). In this study athymic nude mice were induced with MCF7 cells and treated every week with MβCD for 5 weeks. Following the treatment, tumour volume in MβCD treated mice was statistically reduced in

comparison to the control and after eight doses, this reduction was about 50 %. No lethality was observed in the mice. At the end of the study, autopsied xenografts and organ samples revealed no macroscopic anomalies. During the course of the study all the MβCD treated mice as well as the controls showed no changes in behaviour also no physical changes like loss in body weight was observed. Recent studies with HPβCD for leukemia (Yokoo, Kubota et al. 2015) and atherosclerosis (Zimmer, Grebe et al. 2016) gave us valuable insights about the dosage concentrations and also the mode of administration. IP injections of HPβCD was seen to significantly improve the survival in leukemia mouse models and administration of HPβCD was seen to prolong their survival (Yokoo, Kubota et al. 2015). It was also observed in this study that HPβCD treated mice survived longer than vehicle-treated mice and the overall survival of mice that received 695.5 mg/kg - 2086.5 mg/kg HPβCD was substantially higher than that of vehicle-treated mice. Thus suggesting HPβCD is quite non-toxic to the normal physiology of alive animals. In studies with atherosclerosis, HPβCD treatment caused significant atherosclerosis regression. $ApoE^{-/-}$ mice were used in this study which are hypercholesterolemic. These mice were kept on a high cholesterol diet for eight weeks in order to induce advanced lesions. They were then switched to a normal diet for four weeks, during which treatment commenced with HPβCD or vehicle control. Results showed significant plasma cholesterol-depletion. No effect on atherosclerotic lesion size was observed upon switching to a normal diet and HPβCD treatment resulted in a reduction of atherosclerotic plaques by approximately 45% (Zimmer, Grebe et al. 2016).

For Niemann Type C disease, HPβCD is already under clinical trials as mentioned before. In a base-line study, here one patient was treated with approximately 2,500 mg/kg of HPβCD (intravenously administered for 8 hrs) (García-Robles, Megías-Vericat et al. 2016). Similar concentrations (3000 mg/kg) were used in our *in vivo* experiments.

All these studies formed the basis of our *in vivo* study and we successfully achieved comparable regression in tumour sizes **(Fig. 51, Fig. 52 and Fig. 54)**. It can also be hypothesized that prolonged treatment with HPβCD might infact heal intermediate and late stage cancer. Our results highlight HPβCD as a promising anti-breast cancer agent with no side-effects and can be taken forward for clinical trials.

8. CONCLUSIONS

The purpose of this study was to investigate a cholesterol-depleting compound which has little or no side effects to the normal cells. Since BC has high levels of cholesterol, cholesterol-depletion could therefore be a way to counteract the malignancy. HPβCD is an orphan molecule approved for testing by both FDA and European Medicines Agency (EMA) for the treatment of Niemann Pick type C (NPC) disease, which is a fatal cholesterol metabolism disorder [ClinicalTrials.gov Identifier: NCT01747135, (Tanaka, Yamada et al. 2015)]. There are hundreds of sub-types of different cancers and it is not easy to predict the use of a particular compound for the treatment of a specific sub-type of a cancer. The work presented here is particularly of high importance for women of Arab (Chouchane, Boussen et al. 2013) and African descent (Stead, Lash et al. 2009) as they present cancer at an earlier age, have more aggressive tumour types and have a high prevalence of TNBC (absence of ER, PR and HER2 receptors) type. Even penta-negative tumours (i.e., negative for the estrogen and progesterone receptors, HER2, EGFR, and cytokeratin 5/6) have also been reported in Saudi women (Al Tamimi, Shawarby et al. 2010).

In conclusion, this study proposes an innovative strategy never tried before for ER + and TNBC. We have successfully depleted cholesterol in TNBC and ER+ BC cells, thereby causing cell death via apoptosis. Our work provides experimental evidences to support this hypothesis. We identified the potency of HPβCD *in vitro* against two BC cell lines: MCF7 (ER+), MDA-MB-231(TNBC) and compared the results against two normal cell lines: MRC-5 (Normal Human Lung Fibroblasts) and HEK-293 (Human embryonic kidney) using cytotoxic, apoptosis and cholesterol based assays. We have also tested HPβCD *in vivo* in MF-1 Nude mice and obtained 73.9%, 94% and 100% reduction in tumour size for late stage, intermediate stage and early stage TNBC respectively **(Fig. 51, Fig. 52 and Fig. 54)**. For early stage TNBC, no signs of relapse was observed even after a period of one month. These data suggests that HPβCD can prevent cholesterol accumulation in BC cells and is a promising anti- breast cancer agent. The study has been provisionally patented by our group **(Patent no. P1194P)** on 31st January, 2019.

Therefore, in conclusion to our mice studies it can be inferred that possibly in humans, if the tumour is diagnosed at a late stage or intermediate stage, HPβCD treatment might slow the progression of the cancer and thereby improve human life expectancy and if the cancer is detected at an early stage, we might be able to cure the cancer completely without any severe side-effects of the therapy.

9. FUTURE STUDIES

Currently HPβCD is being tested *in vivo* for MCF7 (Estrogen positive) induced BC in 14 mice. Organs explanted from the MDA-MB-231 induced mice have been fixed in 10% buffered formalin. These will be sectioned and stained with hematoxylin and eosin (H&E).

Additionally, RT^2 Profiler PCR Arrays are currently being used after RNA extraction and retro-transcribed by an RT-PCR kit (Qiagen, Germany). Human Breast Cancer, Cancer Drug Resistance, and Lipoprotein Signalling & Cholesterol Metabolism RT^2 Profiler PCR Arrays (Qiagen, Germany) will be run on all samples isolated from all MCF7 and MDA-MB-231 treated (10 mM HPβCD) and untreated cells. The arrays will be run in duplicates at least.

Further studies with Surface Plasmon Resonance Biosensor based ProteOn™ XPR36 protein interaction array system will be used to identify interaction of HPβCD with differentially expressed proteins as selected from PCR arrays. Above system can analyse up to 36 different protein interactions in a single run on a single chip. We will run it in duplicates on untreated (both for MCF7 and MDA-MB-231) cells and for HPβCD treated (10 mM) MCF7 and MDA-MB-231 cells. In total 6 protein arrays will be run. The experiments and analysis of data using ProteOn™ Manager Software will be performed by Dr Gavin Owen (Lecturer and Researcher, Department of Molecular Medicine and Haematology, University of the Witwatersrand, Johannesburg, South Africa).

Western blots will also be done do check the expression of several apoptotic and cholesterol mediated genes from the tumours collected.

The fact that HPβCD has no side-effects makes it an ideal candidate to skip pre-clinical trials and instead taking it forward to clinical trials. This work is being planned to be done in 2020.

10. TROUBLESHOOTING

Several challenges were faced throughout this study and has been enlisted below:

IN VITRO

1) New laboratory- All the basic cell culture techniques and assays had to be standardized.

2) APOPercentage Assay- The volume of the APOPercentage dye and PBS had to be standardized. We tried different range of volumes and finally 0.5µl of dye +64.5 µl of PBS was established to make a total volume of 65 µl per well.

3) MOMP ASSAY- Trypsin was first tried to detach cells which led to unwanted cell death. This was carried for different time points with no success. Several concentrations of EDTA was then tried as an alternative to trypsin and finally 15 mM EDTA was seen to be most effective to detach cells and not cause cell death.

4) CHOLESTEROL QUANTIFICATION ASSAY- Due to the high costs involved with the kits, we decided to make our own Reagent A and added individual chemicals to make final reagent. This led to several permutations and combinations in terms of concentrations and volumes until finally a standard technique was established.

IN VIVO

The main challenge was the aggressiveness of MDA-MB-231 induced tumours. MDA-MB-231's aggressiveness is a well-known fact which leads to metastasis. Tumours grew at a rapid pace and it was extremely challenging to keep the untreated group of mice alive because as explained in the results section the tumour size went up extremely high and due to humane-end points they had to be euthanised.

The mode of administering HPβCD was first tried via oral gavage for enhanced bioavailability but no significant tumour reduction was observed, so we started the treatment via IP which resulted in remarkable tumour shrinkage.

11. REFERENCES

Adams, J. M. and S. Cory (2007). "The Bcl-2 apoptotic switch in cancer development and therapy." Oncogene 26(9): 1324.

Adeloye, D., O. Y. Sowunmi, et al. (2018). "Estimating the incidence of breast cancer in Africa: a systematic review and meta-analysis." Journal of global health 8(1).

Al Tamimi, D. M., M. A. Shawarby, et al. (2010). "Protein expression profile and prevalence pattern of the molecular classes of breast cancer a Saudi population based study." BMC cancer 10(1): 223.

Albanito, L., R. Lappano, et al. (2008). "Retracted: G-Protein–Coupled Receptor 30 and Estrogen Receptor-α Are Involved in the Proliferative Effects Induced by Atrazine in Ovarian Cancer Cells." Environmental health perspectives 116(12): 1648-1655.

Algire, C., O. Moiseeva, et al. (2012). "Metformin reduces endogenous reactive oxygen species and associated DNA damage." Cancer Prevention Research 5(4): 536-543.

Ali, S. and R. C. Coombes (2000). "Estrogen receptor alpha in human breast cancer: occurrence and significance." Journal of mammary gland biology and neoplasia 5(3): 271-281.

Ampuero, J. and M. Romero-Gomez (2015). "Prevention of hepatocellular carcinoma by correction of metabolic abnormalities: Role of statins and metformin." World journal of hepatology 7(8): 1105-1111.

Andas, A., A. B. Abdul, et al. (2015). "Dentatin from clausena excavata induces apoptosis in HEPG2 cells via mitochondrial mediated signaling." Asian Pac. J. Cancer Prev 16: 4311-4316.

Antlsperger, G. and G. Schmid (1996). Toxicological comparison of cyclodextrins. Proceedings of the eighth international symposium on cyclodextrins, Springer.

Arakawa, R., S. Abe-Dohmae, et al. (2000). "Involvement of caveolin-1 in cholesterol enrichment of high density lipoprotein during its assembly by apolipoprotein and THP-1 cells." Journal of lipid research 41(12): 1952-1962.

Arbab, I. A., A. B. Abdul, et al. (2013). "Dentatin isolated from Clausena excavata induces apoptosis in MCF-7 cells through the intrinsic pathway with involvement of NF-κB signalling and G0/G1 cell cycle arrest: a bioassay-guided approach." Journal of ethnopharmacology 145(1): 343-354.

Arbab, I. A., C. Y. Looi, et al. (2012). "Dentatin induces apoptosis in prostate cancer cells via Bcl-2, Bcl-xL, Survivin downregulation, caspase-9,-3/7 activation, and NF-κB inhibition." Evidence-Based Complementary and Alternative Medicine 2012.

Arbab, I. A., C. Y. Looi, et al. (2012). "Dentatin induces apoptosis in prostate cancer cells via Bcl-2, Bcl-xL, Survivin downregulation, caspase-9,-3/7 activation, and NF-κB inhibition." Evidence-Based Complementary and Alternative Medicine 2012.

Arpino, G., H. Weiss, et al. (2005). "Estrogen receptor–positive, progesterone receptor–negative breast cancer: association with growth factor receptor expression and tamoxifen resistance." Journal of the National Cancer Institute 97(17): 1254-1261.

Arun, R., C. Ashok Kumar, et al. (2008). "Cyclodextrins as drug carrier molecule: a review." Scientia Pharmaceutica 76(4): 567-598.

Ashkenazi, A. and V. M. Dixit (1998). "Death receptors: signaling and modulation." Science 281(5381): 1305-1308.

Ashwaq, A.-A., M. Al-Qubaisi, et al. (2016). "Inducing G2/M cell cycle arrest and apoptosis through generation reactive oxygen species (ROS)-mediated mitochondria pathway in HT-29 cells by dentatin (DEN) and dentatin incorporated in hydroxypropyl-β-cyclodextrin (DEN-HPβCD)." International journal of molecular sciences 17(10): 1653.

Ashwaq, A.-A. S., A. Rasedee, et al. (2017). "Characterization, drug release profile and cytotoxicity of Dentatin-Hydroxypropyl-β-Cyclodextrin complex." Journal of Inclusion Phenomena and Macrocyclic Chemistry 87(1-2): 167-178.

Balaji, A., V. Pandey, et al. (2009). "Synthesis and characterization studies of cisplatin/hydroxypropyl-β-cyclodextrin complex." Pharmacologyonline 1: 1135-1143.

Béni, S., Z. Szakács, et al. (2007). "Cyclodextrin/imatinib complexation: binding mode and charge dependent stabilities." European Journal of Pharmaceutical Sciences 30(2): 167-174.

Besseling, J., J. J. Kastelein, et al. (2015). "Association between familial hypercholesterolemia and prevalence of type 2 diabetes mellitus." Jama 313(10): 1029-1036.

Bilensoy, E., Y. Cırpanlı, et al. (2007). "Thermosensitive mucoadhesive gel formulation loaded with 5-Fu: cyclodextrin complex for HPV-induced cervical cancer." Journal of Inclusion Phenomena and Macrocyclic Chemistry 57(1-4): 363-370.

Bjornstrom, L. and M. Sjoberg (2005). "Mechanisms of estrogen receptor signaling: convergence of genomic and nongenomic actions on target genes." Molecular endocrinology 19(4): 833-842.

Brentnall, M., L. Rodriguez-Menocal, et al. (2013). "Caspase-9, caspase-3 and caspase-7 have distinct roles during intrinsic apoptosis." BMC cell biology 14(1): 32.

Brown, D. A. and J. K. Rose (1992). "Sorting of GPI-anchored proteins to glycolipid-enriched membrane subdomains during transport to the apical cell surface." Cell 68(3): 533-544.

Brueggemeier, R. W., A. L. Quinn, et al. (1999). "Correlation of aromatase and cyclooxygenase gene expression in human breast cancer specimens." Cancer letters 140(1): 27-35.

Brundert, M., J. Heeren, et al. (2003). "Hepatic lipase mediates an increase in selective uptake of HDL-associated cholesteryl esters by cells in culture independent from SR-BI." Journal of lipid research 44(5): 1020-1032.

Buhaescu, I. and H. Izzedine (2007). "Mevalonate pathway: a review of clinical and therapeutical implications." Clinical biochemistry 40(9): 575-584.

Cai, Y., C. Yap, et al. (2010). "Solubilization of vorinostat by cyclodextrins." Journal of clinical pharmacy and therapeutics 35(5): 521-526.

Campoy, E. M., S. R. Laurito, et al. (2016). "Asymmetric cancer hallmarks in breast tumors on different sides of the body." PloS one 11(7): e0157416.

Carmeci, C., D. A. Thompson, et al. (1997). "Identification of a gene (GPR30) with homology to the G-protein-coupled receptor superfamily associated with estrogen receptor expression in breast cancer." Genomics 45(3): 607-617.

Challa, R., A. Ahuja, et al. (2005). "Cyclodextrins in drug delivery: an updated review." Aaps Pharmscitech 6(2): E329-E357.

Chang, S.-J., M.-F. Hou, et al. (2007). "The association between lipid profiles and breast cancer among Taiwanese women." Clinical Chemical Laboratory Medicine 45(9): 1219-1223.

Chang, Y., J. Wang, et al. (2005). "KGF induces lipogenic genes through a PI3K and JNK/SREBP-1 pathway in H292 cells." Journal of lipid research 46(12): 2624-2635.

Chapnick, D. A., L. Warner, et al. (2011). "Partners in crime: the TGFbeta and MAPK pathways in cancer progression." Cell Biosci 1(42): 1-8.

Chen, G., G. Liang, et al. (2004). "Central role for liver X receptor in insulin-mediated activation of Srebp-1c transcription and stimulation of fatty acid synthesis in liver." Proceedings of the National Academy of Sciences 101(31): 11245-11250.

Chen, G., T. Wang, et al. (2014). "SREBP-1 is a novel mediator of TGF β 1 signaling in mesangial cells." Journal of molecular cell biology 6(6): 516-530.

Chen, T., M. Sun, et al. (2017). "A novel swine model for evaluation of dyslipidemia and atherosclerosis induced by human CETP overexpression." Lipids in health and disease 16(169): 1-8.

Chen, Z., T. Shi, et al. (2016). "Mammalian drug efflux transporters of the ATP binding cassette (ABC) family in multidrug resistance: A review of the past decade." Cancer letters 370(1): 153-164.

Chicheportiche, Y., P. R. Bourdon, et al. (1997). "TWEAK, a new secreted ligand in the tumor necrosis factor family that weakly induces apoptosis." Journal of Biological Chemistry 272(51): 32401-32410.

Chirasani, V. R., R. Sankar, et al. (2016). "Mechanism of inhibition of cholesteryl ester transfer protein by small molecule inhibitors." J. Phys. Chem. B 120(33): 8254-8263.

Choi, J.-A., J.-Y. Kim, et al. (2001). "Induction of cell cycle arrest and apoptosis in human breast cancer cells by quercetin." International journal of oncology 19(4): 837-844.

Choi, Y. K. and K.-G. Park (2013). "Metabolic roles of AMPK and metformin in cancer cells." Molecules and cells 36(4): 279-287.

Chouchane, L., H. Boussen, et al. (2013). "Breast cancer in Arab populations: molecular characteristics and disease management implications." The lancet oncology 14(10): e417-e424.

Clendening, J. and L. Penn (2012). "Targeting tumor cell metabolism with statins." Oncogene 31(48): 4967.

Courtney, K. D., R. B. Corcoran, et al. (2010). "The PI3K pathway as drug target in human cancer." Journal of Clinical Oncology 28(6): 1075-1083.

Covarrubias, L., D. Hernández-García, et al. (2008). "Function of reactive oxygen species during animal development: passive or active?" Developmental biology 320(1): 1-11.

Cruz, P. M., H. Mo, et al. (2013). "The role of cholesterol metabolism and cholesterol transport in carcinogenesis: a review of scientific findings, relevant to future cancer therapeutics." Frontiers in pharmacology 4(119): 1-7.

Cui, Y. and T. E. Rohan (2006). "Vitamin D, calcium, and breast cancer risk: a review." Cancer Epidemiology and Prevention Biomarkers 15(8): 1427-1437.

Dai, X., L. Xiang, et al. (2016). "Cancer hallmarks, biomarkers and breast cancer molecular subtypes." Journal of cancer 7(10): 1281.

Danilo, C. and P. G. Frank (2012). "Cholesterol and breast cancer development." Current opinion in pharmacology 12(6): 677-682.

Davis, M. E. and M. E. Brewster (2004). "Cyclodextrin-based pharmaceutics: past, present and future." Nature reviews Drug discovery 3(12): 1023.

Davis, P. J. and M. J. Poznansky (1987). "Modulation of 3-hydroxy-3-methylglutaryl-CoA reductase by changes in microsomal cholesterol content or phospholipid composition." Proceedings of the National Academy of Sciences 84(1): 118-121.

de Oliveira Andrade, L. (2016). "Understanding the role of cholesterol in cellular biomechanics and regulation of vesicular trafficking: The power of imaging." Biomedical Spectroscopy and Imaging 5(s1): S101-S117.

Debry, P., E. A. Nash, et al. (1997). "Role of multidrug resistance P-glycoproteins in cholesterol esterification." Journal of Biological Chemistry 272(2): 1026-1031.

Dent, S., B. Oyan, et al. (2013). "HER2-targeted therapy in breast cancer: a systematic review of neoadjuvant trials." Cancer treatment reviews 39(6): 622-631.

Derynck, R. and R. J. Akhurst (2007). "Differentiation plasticity regulated by TGF-β family proteins in development and disease." Nature cell biology 9(9): 1000-1004.

Devitt, J. (1967). "The clinical stages of breast cancer-what do they mean?" Canadian Medical Association Journal 97(21): 1257.

Díaz-Cruz, E. S., C. L. Shapiro, et al. (2005). "Cyclooxygenase inhibitors suppress aromatase expression and activity in breast cancer cells." The Journal of Clinical Endocrinology & Metabolism 90(5): 2563-2570.

Didichenko, S. A., A. Navdaev, et al. (2016). "Enhanced HDL functionality in small HDL species produced upon remodeling of HDL by reconstituted HDL, CSL112: effects on cholesterol efflux, anti-inflammatory and antioxidative activity." Circulation research: 1-49.

Dillard, P. R., M.-F. Lin, et al. (2008). "Androgen-independent prostate cancer cells acquire the complete steroidogenic potential of synthesizing testosterone from cholesterol." Molecular and cellular endocrinology 295(1-2): 115-120.

Doisneau-Sixou, S., C. Sergio, et al. (2003). "Estrogen and antiestrogen regulation of cell cycle progression in breast cancer cells." Endocrine-related cancer 10(2): 179-186.

dos Santos, C. R., G. Domingues, et al. (2014). "LDL-cholesterol signaling induces breast cancer proliferation and invasion." Lipids in health and disease 13(1): 16.

Dufour, J., E. Viennois, et al. (2012). "Oxysterol receptors, AKT and prostate cancer." Current opinion in pharmacology 12(6): 724-728.

Eberle, D., B. Hegarty, et al. (2004). "SREBP transcription factors: master regulators of lipid homeostasis." Biochimie 86(11): 839-848.

Eid, E. E., A. B. Abdul, et al. (2011). "Characterization of the inclusion complex of zerumbone with hydroxypropyl-β-cyclodextrin." Carbohydrate Polymers 83(4): 1707-1714.

Eldhose, B., M. Gunawan, et al. (2014). "Plumbagin reduces human colon cancer cell survival by inducing cell cycle arrest and mitochondria-mediated apoptosis." International journal of oncology 45(5): 1913-1920.

Elgindy, N., K. Elkhodairy, et al. (2010). "Lyophilization monophase solution technique for improvement of the physicochemical properties of an anticancer drug, flutamide." European Journal of Pharmaceutics and Biopharmaceutics 74(2): 397-405.

Elmore, S. (2007). "Apoptosis: a review of programmed cell death." Toxicologic pathology 35(4): 495-516.

Eramo, A., M. Sargiacomo, et al. (2004). "CD95 death-inducing signaling complex formation and internalization occur in lipid rafts of type I and type II cells." European journal of immunology 34(7): 1930-1940.

Esau, L., S. Sagar, et al. (2016). "Identification of CETP as a molecular target for estrogen positive breast cancer cell death by cholesterol-depleting agents." Genes & cancer 7(9-10): 309.

Espenshade, P. J. (2006). "SREBPs: sterol-regulated transcription factors." Journal of cell science 119(6): 973-976.

Fauvelle, F., J. Debouzy, et al. (1997). "Mechanism of α-cyclodextrin-lnduced hemolysis. 1. The two-step extraction of phosphatidylinositol from the membrane." Journal of pharmaceutical sciences 86(8): 935-943.

Ferlay, J., I. Soerjomataram, et al. (2015). "Cancer incidence and mortality worldwide: sources, methods and major patterns in GLOBOCAN 2012." International journal of cancer 136(5): E359-E386.

Fielding, C. and P. Fielding (2004). Membrane cholesterol and the regulation of signal transduction, Portland Press Limited.

Filardo, E. J., J. A. Quinn, et al. (2002). "Estrogen action via the G protein-coupled receptor, GPR30: stimulation of adenylyl cyclase and cAMP-mediated attenuation of the epidermal growth factor receptor-to-MAPK signaling axis." Molecular endocrinology 16(1): 70-84.

Filardo, E. J. and P. Thomas (2005). "GPR30: a seven-transmembrane-spanning estrogen receptor that triggers EGF release." Trends in Endocrinology & Metabolism 16(8): 362-367.

Finucane, D. M., E. Bossy-Wetzel, et al. (1999). "Bax-induced caspase activation and apoptosis via cytochromec release from mitochondria is inhibitable by Bcl-xL." Journal of Biological Chemistry 274(4): 2225-2233.

Fisher, B., C. Redmond, et al. (1988). "Relative worth of estrogen or progesterone receptor and pathologic characteristics of differentiation as indicators of prognosis in node negative breast cancer patients: findings from National Surgical Adjuvant Breast and Bowel Project Protocol B-06." Journal of Clinical Oncology 6(7): 1076-1087.

Foretz, M., C. Guichard, et al. (1999). "Sterol regulatory element binding protein-1c is a major mediator of insulin action on the hepatic expression of glucokinase and lipogenesis-related genes." Proceedings of the National Academy of Sciences 96(22): 12737-12742.

Fox, E. M., J. Andrade, et al. (2009). "Novel actions of estrogen to promote proliferation: integration of cytoplasmic and nuclear pathways." Steroids 74(7): 622-627.

Frank, P. G., M. W.-C. Cheung, et al. (2006). "Caveolin-1 and regulation of cellular cholesterol homeostasis." American Journal of Physiology-Heart and Circulatory Physiology 291(2): H677-H686.

Frasor, J., J. M. Danes, et al. (2003). "Profiling of estrogen up-and down-regulated gene expression in human breast cancer cells: insights into gene networks and pathways underlying estrogenic control of proliferation and cell phenotype." Endocrinology 144(10): 4562-4574.

Friedberg, E. C. (2003). "DNA damage and repair." Nature 421(6921): 436.

Furberg, A.-S., G. Jasienska, et al. (2005). "Metabolic and hormonal profiles: HDL cholesterol as a plausible biomarker of breast cancer risk. The Norwegian EBBA Study." Cancer Epidemiology and Prevention Biomarkers 14(1): 33-40.

Gabitova, L., A. Gorin, et al. (2014). "Molecular pathways: sterols and receptor signaling in cancer." Clinical Cancer Research 20(1): 28-34.

García-Robles, A. A., J. E. Megías-Vericat, et al. (2016). "Use of 2 hydroxypropyl-beta-cyclodextrin therapy in two adult Niemann Pick Type C patients." Journal of the neurological sciences 366: 65-67.

Garrigues, A., A. E. Escargueil, et al. (2002). "The multidrug transporter, P-glycoprotein, actively mediates cholesterol redistribution in the cell membrane." Proceedings of the National Academy of Sciences 99(16): 10347-10352.

Garwood, E. R., A. S. Kumar, et al. (2010). "Fluvastatin reduces proliferation and increases apoptosis in women with high grade breast cancer." Breast cancer research and treatment 119(1): 137-144.

Gaspar, J., J. Mathieu, et al. (2017). "2-Hydroxypropyl-beta-cyclodextrin (HPβCD) reduces age-related lipofuscin accumulation through a cholesterol-associated pathway." Scientific reports 7(1): 2197.

Gaus, K., L. Kritharides, et al. (2004). "Apolipoprotein A-1 interaction with plasma membrane lipid rafts controls cholesterol export from macrophages." The FASEB journal 18(3): 574-576.

Gaus, K., M. Rodriguez, et al. (2005). "Domain-specific lipid distribution in macrophage plasma membranes." Journal of lipid research 46(7): 1526-1538.

George, K. S. and S. Wu (2012). "Lipid raft: A floating island of death or survival." Toxicology and applied pharmacology 259(3): 311-319.

Ginestier, C., F. Monville, et al. (2012). "Mevalonate metabolism regulates Basal breast cancer stem cells and is a potential therapeutic target." Stem cells 30(7): 1327-1337.

Gniadecki, R. (2004). "Depletion of membrane cholesterol causes ligand-independent activation of Fas and apoptosis." Biochemical and biophysical research communications 320(1): 165-169.

Gompel, A., S. Somaï, et al. (2000). "Hormonal regulation of apoptosis in breast cells and tissues." Steroids 65(10-11): 593-598.

Gong, G., Y. Qin, et al. (2010). "Rutin inhibits hydrogen peroxide-induced apoptosis through regulating reactive oxygen species mediated mitochondrial dysfunction pathway in human umbilical vein endothelial cells." European journal of pharmacology 628(1-3): 27-35.

Gould, S. and R. C. Scott (2005). "2-Hydroxypropyl-β-cyclodextrin (HP-β-CD): a toxicology review." Food and Chemical Toxicology 43(10): 1451-1459.

Gozgit, J. M., B. T. Pentecost, et al. (2006). "Use of an aggressive MCF-7 cell line variant, TMX2-28, to study cell invasion in breast cancer." Molecular Cancer Research 4(12): 905-913.

Gralow, J. R. (2006). "Breast cancer 2004: Progress and promise on the clinical front." Physica Medica 21: 2.

Gross, A., K. Pilcher, et al. (2000). "Biochemical and genetic analysis of the mitochondrial response of yeast to BAX and BCL-XL." Molecular and cellular biology 20(9): 3125-3136.

Grosse, P., F. Bressolle, et al. (1998). "Antiproliferative effect of methyl-m-cyclodextrin in vitro and in human tumour xenografted athymic nude mice."

Gui, T., Y. Sun, et al. (2012). "The Roles of Mitogen-Activated Protein Kinase Pathways in TGF-beta-Induced Epithelial-Mesenchymal Transition." J Signal Transduct 2012: 1-10.

Hager, M. H., K. R. Solomon, et al. (2006). "The role of cholesterol in prostate cancer." Current Opinion in Clinical Nutrition & Metabolic Care 9(4): 379-385.

Halliwell, B. (2011). "Free radicals and antioxidants–quo vadis?" Trends in pharmacological sciences 32(3): 125-130.

Hanahan, D. and R. A. Weinberg (2000). "The hallmarks of cancer." Cell 100(1): 57-70.

Hao, M., S. X. Lin, et al. (2002). "Vesicular and non-vesicular sterol transport in living cells The endocytic recycling compartment is a major sterol storage organelle." Journal of Biological Chemistry 277(1): 609-617.

Harkin, D. P. (2000). "Uncovering functionally relevant signaling pathways using microarray-based expression profiling." The Oncologist 5(6): 501-507.

Hart, C. D., I. Migliaccio, et al. (2015). "Challenges in the management of advanced, ER-positive, HER2-negative breast cancer." Nature reviews Clinical oncology 12(9): 541.

He, H.-J., S. Kole, et al. (2003). "Interaction of filamin A with the insulin receptor alters insulin-dependent activation of the mitogen-activated protein kinase pathway." Journal of Biological Chemistry 278(29): 27096-27104.

Hess, K. R., L. Pusztai, et al. (2003). "Estrogen receptors and distinct patterns of breast cancer relapse." Breast cancer research and treatment 78(1): 105-118.

Hewitt, S. C. and K. S. Korach (2000). "Progesterone action and responses in the αERKO mouse." Steroids 65(10-11): 551-557.

Hewitt, S. C. and K. S. Korach (2002). "Estrogen receptors: structure, mechanisms and function." Reviews in Endocrine and Metabolic Disorders 3(3): 193-200.

Hinzey, A. H., M. A. Kline, et al. (2012). "Choice of cyclodextrin for cellular cholesterol depletion for vascular endothelial cell lipid raft studies: cell membrane alterations, cytoskeletal reorganization and cytotoxicity."

Hipler, U., U. Schönfelder, et al. (2007). "Influence of cyclodextrins on the proliferation of HaCaT keratinocytes in vitro." Journal of Biomedical Materials Research Part A: An Official Journal of The Society for Biomaterials, The Japanese Society for Biomaterials, and The Australian Society for Biomaterials and the Korean Society for Biomaterials 83(1): 70-79.

Ho, Y., S. Brown, et al. (1976). "Regulation of low density lipoprotein receptor activity in freshly isolated human lymphocytes." The Journal of clinical investigation 58(6): 1465-1474.

Hoque, A., H. Chen, et al. (2008). "Statin induces apoptosis and cell growth arrest in prostate cancer cells." Cancer Epidemiol Biomarkers Prev 17(1): 88-94.

Horton, J. D., J. L. Goldstein, et al. (2002). "SREBPs: activators of the complete program of cholesterol and fatty acid synthesis in the liver." The Journal of clinical investigation 109(9): 1125-1131.

Horton, J. D., N. A. Shah, et al. (2003). "Combined analysis of oligonucleotide microarray data from transgenic and knockout mice identifies direct SREBP target genes." Proceedings of the National Academy of Sciences 100(21): 12027-12032.

Hu, J., Z. Zhang, et al. (2010). "Cellular cholesterol delivery, intracellular processing and utilization for biosynthesis of steroid hormones." Nutrition & metabolism 7(47): 1-25.

Huang, F. and Y.-G. Chen (2012). "Regulation of TGF-β receptor activity." Cell & bioscience 2(1): 9.

Hudis, C. A. and L. Gianni (2011). "Triple-negative breast cancer: an unmet medical need." The Oncologist 16(Supplement 1): 1-11.

Hueber, A. O., A. M. Bernard, et al. (2002). "An essential role for membrane rafts in the initiation of Fas/CD95-triggered cell death in mouse thymocytes." EMBO reports 3(2): 190-196.

Ikonen, E. (2008). "Cellular cholesterol trafficking and compartmentalization." Nature reviews Molecular cell biology 9(2): 125-138.

Ingvarsson, S. (1999). Molecular genetics of breast cancer progression. Seminars in cancer biology, Elsevier.

Irie, T., M. Otagiri, et al. (1982). "Cyclodextrin-induced hemolysis and shape changes of human erythrocytes in vitro." Journal of Pharmacobio-dynamics 5(9): 741-744.

Izem, L. and R. E. Morton (2007). "Possible role for intracellular cholesteryl ester transfer protein in adipocyte lipid metabolism and storage." Journal of Biological Chemistry 282(30): 21856-21865.

Jackson, S. P. and J. Bartek (2009). "The DNA-damage response in human biology and disease." Nature 461(7267): 1071.

Jänicke, R. U. (2009). "MCF-7 breast carcinoma cells do not express caspase-3." Breast cancer research and treatment 117(1): 219-221.

Jensen, E. V. and V. C. Jordan (2003). "The estrogen receptor: a model for molecular medicine." Clinical Cancer Research 9(6): 1980-1989.

Jeong, C.-H. and S. H. Joo (2016). "Downregulation of reactive oxygen species in apoptosis." Journal of cancer prevention 21(1): 13.

Ji, Y., M. Yu, et al. (2017). "Study on apoptosis effect of human breast cancer cell MCF-7 induced by lycorine hydrochloride via death receptor pathway." Saudi Pharmaceutical Journal 25(4): 633-637.

Jiang, Y., X. Jiang, et al. (2011). "Enhanced anti-tumor effect of 9-nitro-camptothecin complexed by hydroxypropyl-β-cyclodextrin and safety evaluation." International journal of pharmaceutics 415(1-2): 252-258.

Johansson, J., V. Tabor, et al. (2015). "TGF-β1-induced epithelial–mesenchymal transition promotes monocyte/macrophage properties in breast cancer cells." Frontiers in oncology 5(3): 1-9.

Junttila, M. R. and G. I. Evan (2009). "p53—a Jack of all trades but master of none." Nature reviews Cancer 9(11): 821.

Kabouridis, P. S., J. Janzen, et al. (2000). "Cholesterol depletion disrupts lipid rafts and modulates the activity of multiple signaling pathways in T lymphocytes." European journal of immunology 30(3): 954-963.

Kang, M. H., L.-H. Zhang, et al. (2013). "Regulation of ABCA1 protein expression and function in hepatic and pancreatic islet cells by miR-145." Arterioscler Thromb Vasc Biol 33(12): 2724-2732.

Kaur, M. and L. Esau (2015). "Two-step protocol for preparing adherent cells for high-throughput flow cytometry." BioTechniques 59(3): 119-126.

Kelland, L. (2004). "“Of mice and men”: values and liabilities of the athymic nude mouse model in anticancer drug development." European Journal of Cancer 40(6): 827-836.

Kennedy, R. D., J. E. Quinn, et al. (2004). "The role of BRCA1 in the cellular response to chemotherapy." Journal of the National Cancer Institute 96(22): 1659-1668.

Kim, J., K. Maxwell, et al. (1991). "Beta-VLDL increases endothelial cell plasma membrane cholesterol." Journal of lipid research 32(7): 1125-1131.

Kim, Y., S. K. Park, et al. (2009). "Serum high-density lipoprotein cholesterol and breast cancer risk by menopausal status, body mass index, and hormonal receptor in Korea." Cancer Epidemiology and Prevention Biomarkers 18(2): 508-515.

Koga, H., S. Kaushik, et al. (2010). "Altered lipid content inhibits autophagic vesicular fusion." The FASEB journal 24(8): 3052-3065.

Lahiani-Skiba, M., F. Bounoure, et al. (2011). "Effect of cyclodextrins on lonidamine release and in-vitro cytotoxicity." Journal of Inclusion Phenomena and Macrocyclic Chemistry 69(3-4): 481-485.

Lange, C. A. and D. Yee (2008). "Progesterone and breast cancer." Women's Health 4(2): 151-162.

Lange, Y. (1991). "Disposition of intracellular cholesterol in human fibroblasts." Journal of lipid research 32(2): 329-339.

Lange, Y., M. Swaisgood, et al. (1989). "Plasma membranes contain half the phospholipid and 90% of the cholesterol and sphingomyelin in cultured human fibroblasts." Journal of Biological Chemistry 264(7): 3786-3793.

Lange, Y., J. Ye, et al. (1999). "Regulation of endoplasmic reticulum cholesterol by plasma membrane cholesterol." Journal of lipid research 40(12): 2264-2270.

Lange, Y., J. Ye, et al. (2004). "How cholesterol homeostasis is regulated by plasma membrane cholesterol in excess of phospholipids." Proceedings of the National Academy of Sciences 101(32): 11664-11667.

Larbi, A., N. Douziech, et al. (2004). "Effects of methyl-β-cyclodextrin on T lymphocytes lipid rafts with aging." Experimental gerontology 39(4): 551-558.

Lavie, Y. and M. Liscovitch (2000). "Changes in lipid and protein constituents of rafts and caveolae in multidrug resistant cancer cells and their functional consequences." Glycoconjugate journal 17(3): 253-259.

Lehoux, J.-G., N. Kandalaft, et al. (1985). "Characterization of 3-hydroxy-3-methylglutaryl coenzyme A reductase in human adrenal cortex." Endocrinology 117(4): 1462-1468.

Leung, Y.-K., P. Mak, et al. (2006). "Estrogen receptor (ER)-β isoforms: a key to understanding ER-β signaling." Proceedings of the National Academy of Sciences 103(35): 13162-13167.

Leygue, E. and L. C. Murphy (2013). "A bi-faceted role of estrogen receptor β in breast cancer." Endocrine-related cancer 20(3): R127-R139.

Li, B.-q., N. Li, et al. (2012). "Pharmacokinetics of injectable beta-cyclodextrin-oridonin inclusion complex, a novel formulation of oridonin in Wistar rats." National Journal of Physiology, Pharmacy and Pharmacology 2(1): 52.

Li, J., L. Shen, et al. (2012). "Plumbagin inhibits cell growth and potentiates apoptosis in human gastric cancer cells in vitro through the NF-κB signaling pathway." Acta Pharmacologica Sinica 33(2): 242.

Li, Q., P. Huang, et al. (2014). "Association between the CETP polymorphisms and the risk of Alzheimer's disease, carotid atherosclerosis, longevity, and the efficacy of statin therapy." Neurobiology of aging 35(6): 1-11.

Li, Y. C., M. J. Park, et al. (2006). "Elevated levels of cholesterol-rich lipid rafts in cancer cells are correlated with apoptosis sensitivity induced by cholesterol-depleting agents." The American journal of pathology 168(4): 1107-1118.

Limpert, A. S., J. C. Karlo, et al. (2007). "Nerve growth factor stimulates the concentration of TrkA within lipid rafts and extracellular signal-regulated kinase activation through c-Cbl-associated protein." Molecular and cellular biology 27(16): 5686-5698.

Lin, C.-Y., C. Huo, et al. (2013). "Cholestane-3β, 5α, 6β-triol suppresses proliferation, migration, and invasion of human prostate cancer cells." PloS one 8(6): e65734.

Litz, J. P., N. Thakkar, et al. (2016). "Depletion with cyclodextrin reveals two populations of cholesterol in model lipid membranes." Biophysical journal 110(3): 635-645.

Liu, C.-Y., M.-H. Hung, et al. (2014). "Tamoxifen induces apoptosis through cancerous inhibitor of protein phosphatase 2A–dependent phospho-Akt inactivation in estrogen receptor–negative human breast cancer cells." Breast Cancer Research 16(5): 431.

Liu, P., H. Cheng, et al. (2009). "Targeting the phosphoinositide 3-kinase pathway in cancer." Nature reviews Drug discovery 8(8): 627-644.

Liu, Y.-L., H.-X. Qian, et al. (2011). "Serum LDL-C and LDL-C/HDL-C ratio are positively correlated to lymph node stages in males with colorectal cancer." Hepato-gastroenterology 58(106): 383-387.

Llaverias, G., C. Danilo, et al. (2011). "Role of cholesterol in the development and progression of breast cancer." The American journal of pathology 178(1): 402-412.

Locksley, R. M., N. Killeen, et al. (2001). "The TNF and TNF receptor superfamilies: integrating mammalian biology." Cell 104(4): 487-501.

Lonning, P. (2004). "Aromatase inhibitors in breast cancer." Endocrine Related Cancer 11(2): 179-189.

Looi, C. Y., A. Arya, et al. (2013). "Induction of apoptosis in human breast cancer cells via caspase pathway by vernodalin isolated from Centratherum anthelminticum (L.) seeds." PloS one 8(2): e56643.

Loreto, C., G. La Rocca, et al. (2014). "The role of intrinsic pathway in apoptosis activation and progression in Peyronie's disease." BioMed research international 2014.

Lowe, S. W., E. Cepero, et al. (2004). "Intrinsic tumour suppression." Nature 432: 307.

Luchetti, G., R. Sircar, et al. (2016). "Cholesterol activates the G-protein coupled receptor Smoothened to promote Hedgehog signaling." eLife 5: 1-22.

Ma, D. Q., R. A. Rajewski, et al. (1999). "New injectable melphalan formulations utilizing (SBE) 7m-β-CD or HP-β-CD." International journal of pharmaceutics 189(2): 227-234.

Macedo, L. F., G. Sabnis, et al. (2009). "Aromatase inhibitors and breast cancer." Annals of the New York Academy of Sciences 1155(1): 162-173.

Maekawa, M. and G. D. Fairn (2015). "Complementary probes reveal that phosphatidylserine is required for the proper transbilayer distribution of cholesterol." J Cell Sci 128(7): 1422-1433.

Mahammad, S. and I. Parmryd (2015). Cholesterol depletion using methyl-β-cyclodextrin. Methods in Membrane Lipids, Springer: 91-102.

Marcuzzi, A., L. De Leo, et al. (2011). "The farnesyltransferase inhibitors tipifarnib and lonafarnib inhibit cytokines secretion in a cellular model of mevalonate kinase deficiency." Pediatr Res 70(1): 78-82.

Markov, G. V., J. Gutierrez-Mazariegos, et al. (2017). "Origin of an ancient hormone/receptor couple revealed by resurrection of an ancestral estrogen." Science Advances 3(3): 1-14.

Martin, L. J., O. Melnichouk, et al. (2015). "Serum lipids, lipoproteins, and risk of breast cancer: a nested case-control study using multiple time points." Journal of the National Cancer Institute 107(5): 1-9.

Martín, M. G., F. Pfrieger, et al. (2014). "Cholesterol in brain disease: sometimes determinant and frequently implicated." EMBO reports: 1-17.

Matsuda, M., B. S. Korn, et al. (2001). "SREBP cleavage-activating protein (SCAP) is required for increased lipid synthesis in liver induced by cholesterol deprivation and insulin elevation." Genes & development 15(10): 1206-1216.

Matusewicz, L., J. Meissner, et al. (2015). "The effect of statins on cancer cells." Tumor Biology 36(7): 4889-4904.

Maughan, K. L., M. A. Lutterbie, et al. (2010). "Treatment of breast cancer." Chemotherapy 51: 53.

Maxfield, F. R. and D. Wüstner (2002). "Intracellular cholesterol transport." The Journal of clinical investigation 110(7): 891-898.

McDonnell, D. P., S. Park, et al. (2014). "Obesity, cholesterol metabolism, and breast cancer pathogenesis." Cancer research 74(18): 4976-4982.

Mehta, R. G., M. Hawthorne, et al. (2014). "Differential roles of ERα and ERβ in normal and neoplastic development in the mouse mammary gland." PloS one 9(11): e113175.

Mihaylova, M. M. and R. J. Shaw (2011). "The AMPK signalling pathway coordinates cell growth, autophagy and metabolism." Nature cell biology 13(9): 1016-1023.

Miki, Y., J. Swensen, et al. (1994). "A strong candidate for the breast and ovarian cancer susceptibility gene BRCA1." Science 266(5182): 66-71.

Millar, J. S., M. E. Lassman, et al. (2017). "Effects of CETP inhibition with anacetrapib on metabolism of VLDL-TG and plasma apolipoproteins C-II, C-III, and E." Journal of lipid research 58(6): 1214-1220.

Mirmalek, S. A., M. Hajilou, et al. (2014). "Prevalence of HER2 and hormone receptors and P53 mutations in the pathologic specimens of breast cancer patients." International journal of breast cancer 2014.

Mo, H. and C. E. Elson (2004). "Studies of the isoprenoid-mediated inhibition of mevalonate synthesis applied to cancer chemotherapy and chemoprevention." Experimental biology and medicine 229(7): 567-585.

Mohammad, N., P. Malvi, et al. (2014). "Cholesterol depletion by methyl-β-cyclodextrin augments tamoxifen induced cell death by enhancing its uptake in melanoma." Molecular cancer 13(1): 204.

Moore, J. T., D. D. McKee, et al. (1998). "Cloning and characterization of human estrogen receptor β isoforms." Biochemical and biophysical research communications 247(1): 75-78.

Morhason-Bello, I. O., F. Odedina, et al. (2013). "Challenges and opportunities in cancer control in Africa: a perspective from the African Organisation for Research and Training in Cancer." The lancet oncology 14(4): e142-e151.

Mostaghel, E. A., K. R. Solomon, et al. (2012). "Impact of circulating cholesterol levels on growth and intratumoral androgen concentration of prostate tumors." PloS one 7(1): e30062.

Motoshima, H., B. J. Goldstein, et al. (2006). "AMPK and cell proliferation--AMPK as a therapeutic target for atherosclerosis and cancer." J Physiol 574(Pt 1): 63-71.

Motoyama, K., K. Kameyama, et al. (2009). "Involvement of PI3K-Akt-Bad pathway in apoptosis induced by 2, 6-di-O-methyl-β-cyclodextrin, not 2, 6-di-O-methyl-α-cyclodextrin, through cholesterol depletion from lipid rafts on plasma membranes in cells." European Journal of Pharmaceutical Sciences 38(3): 249-261.

Motoyama, K., H. Toyodome, et al. (2009). "Involvement of lipid rafts of rabbit red blood cells in morphological changes induced by methylated β-cyclodextrins." Biological and Pharmaceutical Bulletin 32(4): 700-705.

Motoyama, N., F. Wang, et al. (1995). "Massive cell death of immature hematopoietic cells and neurons in Bcl-x-deficient mice." Science 267(5203): 1506-1510.

Mullan, P. B., J. E. Quinn, et al. (2001). "BRCA1 and GADD45 mediated G2/M cell cycle arrest in response to antimicrotubule agents." Oncogene 20(43): 6123.

Murai, T. (2012). "The role of lipid rafts in cancer cell adhesion and migration." International journal of cell biology 2012.

Murtola, T. J., H. Syvälä, et al. (2012). "The importance of LDL and cholesterol metabolism for prostate epithelial cell growth." PloS one 7(6): e39445.

Musso, G., R. Gambino, et al. (2009). "Recent insights into hepatic lipid metabolism in non-alcoholic fatty liver disease (NAFLD)." Progress in lipid research 48(1): 1-26.

Nakakuki, M., H. Shimano, et al. (2007). "A transcription factor of lipid synthesis, sterol regulatory element-binding protein (SREBP)-1a causes G1 cell-cycle arrest after accumulation of cyclin-dependent kinase (cdk) inhibitors." The FEBS journal 274(17): 4440-4452.

Nath, S., K. Daneshvar, et al. (2013). "MUC1 induces drug resistance in pancreatic cancer cells via upregulation of multidrug resistance genes." Oncogenesis 2(6): 1-9.

Nelson, E. R., C.-y. Chang, et al. (2014). "Cholesterol and breast cancer pathophysiology." Trends in Endocrinology & Metabolism 25(12): 649-655.

Nelson, E. R., S. E. Wardell, et al. (2013). "27-Hydroxycholesterol links hypercholesterolemia and breast cancer pathophysiology." Science 342(6162): 1094-1098.

Nie, L.-Y., Q.-T. Lu, et al. (2013). "Sterol regulatory element-binding protein 1 is required for ovarian tumor growth." Oncology reports 30(3): 1346-1354.

Nogueira, V. and N. Hay (2013). "Molecular pathways: reactive oxygen species homeostasis in cancer cells and implications for cancer therapy." Clinical Cancer Research 19(16): 4309-4314.

Nowosielski, M., M. Hoffmann, et al. (2011). "Detailed mechanism of squalene epoxidase inhibition by terbinafine." J Chem Inf Model 51(2): 455-462.

O'Malley, B. W. and S. Khan (2013). "Elwood V. Jensen (1920–2012): Father of the nuclear receptors." Proceedings of the National Academy of Sciences 110(10): 3707-3708.

Ogawa, S., S. Inoue, et al. (1998). "Molecular cloning and characterization of human estrogen receptor βcx: a potential inhibitor of estrogen action in human." Nucleic acids research 26(15): 3505-3512.

O'hare, T., M. S. Zabriskie, et al. (2012). "Pushing the limits of targeted therapy in chronic myeloid leukaemia." Nature reviews Cancer 12(8): 513.

Ohtani, Y., T. Irie, et al. (1989). "Differential effects of α-, β-and γ-cyclodextrins on human erythrocytes." European Journal of Biochemistry 186(1-2): 17-22.

Omoto, Y., H. Eguchi, et al. (2003). "Estrogen receptor (ER) β1 and ERβcx/β2 inhibit ERα function differently in breast cancer cell line MCF7." Oncogene 22(32): 5011.

Omoyeni, O. A., A. Hussein, et al. (2015). "Pleiocarpa pycnantha leaves and its triterpenes induce apoptotic cell death in Caco-2 cells in vitro." BMC complementary and alternative medicine 15(1): 224.

Onodera, R., K. Motoyama, et al. (2013). "Involvement of cholesterol depletion from lipid rafts in apoptosis induced by methyl-β-cyclodextrin." International journal of pharmaceutics 452(1-2): 116-123.

Ou, J., H. Tu, et al. (2001). "Unsaturated fatty acids inhibit transcription of the sterol regulatory element-binding protein-1c (SREBP-1c) gene by antagonizing ligand-dependent activation of the LXR." Proceedings of the National Academy of Sciences 98(11): 6027-6032.

Ouslimani, N., J. Peynet, et al. (2005). "Metformin decreases intracellular production of reactive oxygen species in aortic endothelial cells." Metabolism 54(6): 829-834.

Paplomata, E. and R. O'Regan (2014). "The PI3K/AKT/mTOR pathway in breast cancer: targets, trials and biomarkers." Therapeutic advances in medical oncology 6(4): 154-166.

Park, E. K., M. J. Park, et al. (2009). "Cholesterol depletion induces anoikis-like apoptosis via FAK down-regulation and caveolae internalization." The Journal of pathology 218(3): 337-349.

Parpal, S., M. Karlsson, et al. (2001). "Cholesterol depletion disrupts caveolae and insulin receptor signaling for metabolic control via insulin receptor substrate-1, but not for mitogen-activated protein kinase control." Journal of Biological Chemistry 276(13): 9670-9678.

Peng, M., Y. Liu, et al. (2010). "Photostability Study of Doxorubicin Aqueous Solution Enhanced by Inclusion Interaction between Doxorubicin and Hydroxypropyl-β-cyclodextrin." Chinese Journal of Chemistry 28(7): 1291-1295.

Perelman, A., C. Wachtel, et al. (2012). "JC-1: alternative excitation wavelengths facilitate mitochondrial membrane potential cytometry." Cell death & disease 3(11): e430.

Perl, A. and M. Carroll (2011). "BCR-ABL kinase is dead; long live the CML stem cell." The Journal of clinical investigation 121(1): 22-25.

Perlman, R. L. (2016). "Mouse models of human diseaseAn evolutionary perspective." Evolution, medicine, and public health 2016(1): 170-176.

Pertusa, M., C. Morenilla-Palao, et al. (2007). "Transcriptional control of cholesterol biosynthesis in Schwann cells by axonal neuregulin 1." Journal of Biological Chemistry 282(39): 28768-28778.

Picon-Ruiz, M., C. Pan, et al. (2016). "Interactions between adipocytes and breast cancer cells stimulate cytokine production and drive Src/Sox2/miR-302b–mediated malignant progression." Cancer research 76(2): 491-504.

Pike, L. J. (2003). "Lipid rafts bringing order to chaos." Journal of lipid research 44(4): 655-667.

Pitroda, S. P., N. N. Khodarev, et al. (2009). "MUC1-induced alterations in a lipid metabolic gene network predict response of human breast cancers to tamoxifen treatment." Proceedings of the National Academy of Sciences 106(14): 5837-5841.

Platet, N., A. M. Cathiard, et al. (2004). "Estrogens and their receptors in breast cancer progression: a dual role in cancer proliferation and invasion." Critical reviews in oncology/hematology 51(1): 55-67.

Poirot, M., S. Silvente-Poirot, et al. (2012). "Cholesterol metabolism and resistance to tamoxifen." Current opinion in pharmacology 12(6): 683-689.

Poola, I., J. Abraham, et al. (2005). "Estrogen receptors beta4 and beta5 are full length functionally distinct ERβ isoforms." Endocrine 27(3): 227-238.

Porstmann, T., B. Griffiths, et al. (2005). "PKB/Akt induces transcription of enzymes involved in cholesterol and fatty acid biosynthesis via activation of SREBP." Oncogene 24(43): 6465-6481.

Prossnitz, E. R., J. B. Arterburn, et al. (2008). "Estrogen signaling through the transmembrane G protein–coupled receptor GPR30." Annu. Rev. Physiol. 70: 165-190.

Prossnitz, E. R., T. I. Oprea, et al. (2008). "The ins and outs of GPR30: a transmembrane estrogen receptor." The Journal of steroid biochemistry and molecular biology 109(3-5): 350-353.

Pucadyil, T. J. and A. Chattopadhyay (2006). "Role of cholesterol in the function and organization of G-protein coupled receptors." Progress in lipid research 45(4): 295-333.

Quijada, L., A. Callejo, et al. (2007). "The patched receptor: Switching on/off the Hedgehog signaling pathway." Hedgehog-Gli Signaling in Human Disease: 23-33.

Radwan, A. A. and F. K. Alanazi (2014). "Targeting cancer using cholesterol conjugates." Saudi Pharmaceutical Journal 22(1): 3-16.

Ramsunder, N. (2015). "Side effects of statins." South African Journal of Diabetes and Vascular Disease 12(2): 48-50.

Rashid, S., A. Sniderman, et al. (2015). "Elevated cholesteryl ester transfer protein (CETP) activity, a major determinant of the atherogenic dyslipidemia, and atherosclerotic cardiovascular disease in South Asians." European journal of preventive cardiology 22(4): 468-477.

Redza-Dutordoir, M. and D. A. Averill-Bates (2016). "Activation of apoptosis signalling pathways by reactive oxygen species." Biochimica et Biophysica Acta (BBA)-Molecular Cell Research 1863(12): 2977-2992.

Repa, J. J., G. Liang, et al. (2000). "Regulation of mouse sterol regulatory element-binding protein-1c gene (SREBP-1c) by oxysterol receptors, LXRα and LXRβ." Genes & development 14(22): 2819-2830.

Rinninger, F., M. Brundert, et al. (2001). "Lipoprotein lipase mediates an increase in selective uptake of HDL-associated cholesteryl esters by cells in culture independent of scavenger receptor BI." Journal of lipid research 42(11): 1740-1751.

Rodriguez-Navarro, J. A., S. Kaushik, et al. (2012). "Inhibitory effect of dietary lipids on chaperone-mediated autophagy." Proceedings of the National Academy of Sciences 109(12): E705-E714.

Rosenson, R. S., H. B. Brewer, et al. (2012). "Cholesterol efflux and atheroprotection." Circulation 125(15): 1905-1919.

Rouquette-Jazdanian, A. K., C. Pelassy, et al. (2006). "Revaluation of the role of cholesterol in stabilizing rafts implicated in T cell receptor signaling." Cellular signalling 18(1): 105-122.

Saelens, X., N. Festjens, et al. (2004). "Toxic proteins released from mitochondria in cell death." Oncogene 23(16): 2861.

Sagar, S., L. Esau, et al. (2014). "Cytotoxicity and apoptosis induced by a plumbagin derivative in estrogen positive MCF-7 breast cancer cells." Anti-Cancer Agents in Medicinal Chemistry (Formerly Current Medicinal Chemistry-Anti-Cancer Agents) 14(1): 170-180.

Saji, S., E. V. Jensen, et al. (2000). "Estrogen receptors α and β in the rodent mammary gland." Breast Cancer Research 2(1): S. 11.

Sato, R., J. Inoue, et al. (1996). "Sterol-dependent transcriptional regulation of sterol regulatory element-binding protein-2." Journal of Biological Chemistry 271(43): 26461-26464.

Schnell, M. A., C. Hardy, et al. (2002). "Effect of blood collection technique in mice on clinical pathology parameters." Human gene therapy 13(1): 155-161.

Schroepfer Jr, G. J. (2000). "Oxysterols: modulators of cholesterol metabolism and other processes." Physiological reviews 80(1): 361-554.

Shao, W. and P. J. Espenshade (2012). "Expanding roles for SREBP in metabolism." Cell metabolism 16(4): 414-419.

Sharpe, L. J. and A. J. Brown (2013). "Controlling cholesterol synthesis beyond 3-hydroxy-3-methylglutaryl-CoA reductase (HMGCR)." Journal of Biological Chemistry 288(26): 18707-18715.

Sheng, R., H. Kim, et al. (2014). "Cholesterol selectively activates canonical Wnt signalling over non-canonical Wnt signalling." Nature communications 5(4393): 1-28.

Sheng, Z., H. Otani, et al. (1995). "Independent regulation of sterol regulatory element-binding proteins 1 and 2 in hamster liver." Proceedings of the National Academy of Sciences 92(4): 935-938.

Shimizu, S. (2004). "Routes of administration." The laboratory mouse: 527-541.

Shimomura, I., Y. Bashmakov, et al. (1999). "Insulin selectively increases SREBP-1c mRNA in the livers of rats with streptozotocin-induced diabetes." Proceedings of the National Academy of Sciences 96(24): 13656-13661.

Silvente-Poirot, S. and M. Poirot (2012). "Cholesterol epoxide hydrolase and cancer." Current opinion in pharmacology 12(6): 696-703.

Silvente-Poirot, S. and M. Poirot (2014). "Cholesterol and Cancer, in the Balance." Science 343: 1445-1446.

Simic, B., P. Mocharla, et al. (2017). "Anacetrapib, but not evacetrapib, impairs endothelial function in CETP-transgenic mice in spite of marked HDL-C increase." Atherosclerosis 257: 186-194.

Simigdala, N., Q. Gao, et al. (2016). "Cholesterol biosynthesis pathway as a novel mechanism of resistance to estrogen deprivation in estrogen receptor-positive breast cancer." Breast Cancer Research 18(58): 1-14.

Simon, T. G. and A. A. Butt (2015). "Lipid dysregulation in hepatitis C virus, and impact of statin therapy upon clinical outcomes." World Journal of Gastroenterology: WJG 21(27): 8293–8303.

Simons, K. and R. Ehehalt (2002). "Cholesterol, lipid rafts, and disease." The Journal of clinical investigation 110(5): 597-603.

Simons, K. and M. J. Gerl (2010). "Revitalizing membrane rafts: new tools and insights." Nature reviews Molecular cell biology 11(10): 688.

Simons, K. and E. Ikonen (2000). "How cells handle cholesterol." Science 290(5497): 1721-1726.

Simons, K. and D. Toomre (2000). "Lipid rafts and signal transduction." Nature reviews Molecular cell biology 1(1): 31.

Singh, U., K. Aithal, et al. (1997). "Physicochemical and Biological Studies of Inclusion Complex of Methotrexate with β-Cyclodextrin." Pharmacy and Pharmacology Communications 3(12): 573-577.

Sinzinger, H., R. Wolfram, et al. (2002). "Muscular side effects of statins." Journal of cardiovascular pharmacology 40(2): 163-171.

Skliris, G., E. Leygue, et al. (2006). "Expression of oestrogen receptor-β in oestrogen receptor-α negative human breast tumours." British journal of cancer 95(5): 616.

Skoda, A. M., D. Simovic, et al. (2018). "The role of the Hedgehog signaling pathway in cancer: A comprehensive review." Bosnian journal of basic medical sciences 18(1): 8-20.

Slotte, J. P. and E. L. Bierman (1988). "Depletion of plasma-membrane sphingomyelin rapidly alters the distribution of cholesterol between plasma membranes and intracellular cholesterol pools in cultured fibroblasts." Biochemical Journal 250(3): 653-658.

Smart, E. J., G. A. Graf, et al. (1999). "Caveolins, liquid-ordered domains, and signal transduction." Molecular and cellular biology 19(11): 7289-7304.

Smith, P. K., R. I. Krohn, et al. (1985). "Measurement of protein using bicinchoninic acid." Analytical Biochemistry 150(1): 76-85.

Snyder, R. (1984). Basic concepts of the dose-response relationship. ACS Symposium Series, AMER CHEMICAL SOC 1155 16TH ST, NW, WASHINGTON, DC 20036 USA.

Solomon, K. R., K. Pelton, et al. (2009). "Ezetimibe is an inhibitor of tumor angiogenesis." The American journal of pathology 174(3): 1017-1026.

Speirs, V., G. Skliris, et al. (2002). "Distinct expression patterns of ERα and ERβ in normal human mammary gland." Journal of clinical pathology 55(5): 371-374.

Stanculescu, A., L. A. Bembinster, et al. (2010). "Estrogen promotes breast cancer cell survival in an inhibitor of apoptosis (IAP)-dependent manner." Hormones and Cancer 1(3): 127-135.

Stead, L. A., T. L. Lash, et al. (2009). "Triple-negative breast cancers are increased in black women regardless of age or body mass index." Breast Cancer Research 11(2): R18.

Stelzl, D., T. T. Nielsen, et al. (2015). "β-CD-dextran polymer for efficient sequestration of cholesterol from phospholipid bilayers: mechanistic and safe-toxicity investigations." International journal of pharmaceutics 496(2): 896-902.

Stope, M. B., S. L. Popp, et al. (2010). "Estrogen receptor α attenuates transforming growth factor-β signaling in breast cancer cells independent from agonistic and antagonistic ligands." Breast cancer research and treatment 120(2): 357-367.

Strom, B. L., R. Schinnar, et al. (2015). "Statin therapy and risk of acute memory impairment." JAMA internal medicine 175(8): 1399-1405.

Sun, Y., W. He, et al. (2015). "SREBP1 regulates tumorigenesis and prognosis of pancreatic cancer through targeting lipid metabolism." Tumor Biology 36(6): 4133-4141.

Surls, J., C. Nazarov-Stoica, et al. (2012). "Increased membrane cholesterol in lymphocytes diverts T-cells toward an inflammatory response." PloS one 7(6): e38733.

Sylvester, P. W. (2011). Optimization of the tetrazolium dye (MTT) colorimetric assay for cellular growth and viability. Drug design and discovery, Springer: 157-168.

Szejtli, J. (1998). "Introduction and general overview of cyclodextrin chemistry." Chemical reviews 98(5): 1743-1754.

Szydlarska, J., C. Weiss, et al. (2018). "The Effect of Methyl-β-cyclodextrin on Apoptosis, Proliferative Activity, and Oxidative Stress in Adipose-Derived Mesenchymal Stromal Cells of Horses Suffering from Metabolic Syndrome (EMS)." Molecules 23(2): 287.

Tabe, Y., L. Jin, et al. (2012). "Role of stromal microenvironment in nonpharmacological resistance of CML to imatinib through Lyn/CXCR4 interactions in lipid rafts." Leukemia 26(5): 883.

Tanaka, Y., Y. Yamada, et al. (2015). "Efficacy of 2-hydroxypropyl-β-cyclodextrin in Niemann–Pick disease type C model mice and its pharmacokinetic analysis in a patient with the disease." Biological and Pharmaceutical Bulletin 38(6): 844-851.

Teicher, B. A., W. M. Linehan, et al. (2012). Targeting cancer metabolism, AACR.

Tilbrook, P. A., G. A. Palmer, et al. (2001). "Maturation of erythroid cells and erythroleukemia development are affected by the kinase activity of Lyn." Cancer Research 61(6): 2453-2458.

Tontonoz, P., J. Kim, et al. (1993). "ADD1: a novel helix-loop-helix transcription factor associated with adipocyte determination and differentiation." Molecular and cellular biology 13(8): 4753-4759.

Tsoumpra, M. K., J. R. Muniz, et al. (2015). "The inhibition of human farnesyl pyrophosphate synthase by nitrogen-containing bisphosphonates. Elucidating the role of active site threonine 201 and tyrosine 204 residues using enzyme mutants." Bone 81: 478-486.

Tsubaki, M., Y. Yamazoe, et al. (2011). "Blockade of the Ras/MEK/ERK and Ras/PI3K/Akt pathways by statins reduces the expression of bFGF, HGF, and TGF-β as angiogenic factors in mouse osteosarcoma." Cytokine 54(1): 100-107.

Uekama, K., F. Hirayama, et al. (1998). "Cyclodextrin drug carrier systems." Chemical reviews 98(5): 2045-2076.

Ulloth, J. E., F. G. Almaguel, et al. (2007). "Characterization of methyl-β-cyclodextrin toxicity in NGF-differentiated PC12 cell death." Neurotoxicology 28(3): 613-621.

Vallianou, N. G., A. Kostantinou, et al. (2014). "Statins and cancer." Anti-Cancer Agents in Medicinal Chemistry (Formerly Current Medicinal Chemistry-Anti-Cancer Agents) 14(5): 706-712.

van Meer, G. (1989). "Lipid traffic in animal cells." Annual review of cell biology 5(1): 247-275.

Vanier, M. T. and P. Latour (2015). Laboratory diagnosis of Niemann–Pick disease type C: The filipin staining test. Methods in cell biology, Elsevier. 126: 357-375.

Vedin, L.-L., S. A. Lewandowski, et al. (2009). "The oxysterol receptor LXR inhibits proliferation of human breast cancer cells." Carcinogenesis 30(4): 575-579.

Verhoeye, F., O. Descamps, et al. (1996). "An improved method for detection of low density lipoprotein receptor defects in human T lymphocytes." Journal of lipid research 37(6): 1377-1384.

Voisin, M., P. de Medina, et al. (2017). "Identification of a tumor-promoter cholesterol metabolite in human breast cancers acting through the glucocorticoid receptor." Proceedings of the National Academy of Sciences 114(44): E9346-E9355.

Vorobiof, D. A., F. Sitas, et al. (2001). "Breast cancer incidence in South Africa." Journal of Clinical Oncology 19(18; SUPP): 125s-125s.

Walker, J. M. (2002). The bicinchoninic acid (BCA) assay for protein quantitation. The protein protocols handbook, Springer: 11-14.

Walsh, J. G., S. P. Cullen, et al. (2008). "Executioner caspase-3 and caspase-7 are functionally distinct proteases." Proceedings of the National Academy of Sciences 105(35): 12815-12819.

Wang, R., W. He, et al. (2014). "Caveolin-1 functions as a key regulator of 17β-estradiol-mediated autophagy and apoptosis in BT474 breast cancer cells." International journal of molecular medicine 34(3): 822-827.

Wang, X. (2001). "The expanding role of mitochondria in apoptosis." Genes & development 15(22): 2922-2933.

Wang, X. and M. G. Roper (2014). "Measurement of DCF fluorescence as a measure of reactive oxygen species in murine islets of Langerhans." Analytical Methods 6(9): 3019-3024.

Warita, K., T. Warita, et al. (2014). "Statin-induced mevalonate pathway inhibition attenuates the growth of mesenchymal-like cancer cells that lack functional E-cadherin mediated cell cohesion." Scientific reports 4: 7593.

Winterbourn, C. C. (2015). "Are free radicals involved in thiol-based redox signaling?" Free Radical Biology and Medicine 80: 164-170.

Wittkowski, K. M., C. Dadurian, et al. (2018). "Complex polymorphisms in endocytosis genes suggest alpha-cyclodextrin as a treatment for breast cancer." PloS one 13(7): e0199012.

Wolfensohn, S. and M. Lloyd (2008). Handbook of laboratory animal management and welfare, John Wiley & Sons.

Wood, D. E. and E. W. Newcomb (2000). "Cleavage of Bax enhances its cell death function." Experimental cell research 256(2): 375-382.

Wooster, R., S. L. Neuhausen, et al. (1994). "Localization of a breast cancer susceptibility gene, BRCA2, to chromosome 13q12-13." Science 265(5181): 2088-2090.

Wu, Q., T. Ishikawa, et al. (2013). "27-Hydroxycholesterol promotes cell-autonomous, ER positive breast cancer growth." Cell reports 5(3): 637-645.

Wu, Q., Z. Yang, et al. (2014). "Multi-drug resistance in cancer chemotherapeutics: mechanisms and lab approaches." Cancer letters 347(2): 159-166.

Xiang, J., C. Wan, et al. (2016). "Is hydrogen peroxide a suitable apoptosis inducer for all cell types?" BioMed research international 2016.

Xu, D., C. Yin, et al. (2013). "JAK-STAT in lipid metabolism of adipocytes." Jak-Stat 2(4): 1-7.

Yamada, O. and K. Kawauchi (2013). "The role of the JAK-STAT pathway and related signal cascades in telomerase activation during the development of hematologic malignancies." Jak-Stat 2(4): 1-11.

Yan, J., Q.-F. Li, et al. (2012). "Methyl-β-cyclodextrin induces programmed cell death in chronic myeloid leukemia cells and, combined with imatinib, produces a synergistic downregulation of ERK/SPK1 signaling." Anti-cancer drugs 23(1): 22-31.

Yarden, R. I., S. Pardo-Reoyo, et al. (2002). "BRCA1 regulates the G2/M checkpoint by activating Chk1 kinase upon DNA damage." Nature genetics 30(3): 285.

Yavuz, B., E. Bilensoy, et al. (2010). "Alternative oral exemestane formulation: improved dissolution and permeation." International journal of pharmaceutics 398(1-2): 137-145.

Yokoo, M., Y. Kubota, et al. (2015). "2-Hydroxypropyl-β-cyclodextrin acts as a novel anticancer agent." PloS one 10(11): e0141946.

York, A. G. and S. J. Bensinger (2013). "Subverting sterols: rerouting an oxysterol-signaling pathway to promote tumor growth." Journal of Experimental Medicine 210(9): 1653-1656.

Yoshida, A., M. Yamamoto, et al. (1988). "Improvement of chemical instability of digitoxin in aqueous solution by complexation with β-cyclodextrin derivatives." Chemical and pharmaceutical bulletin 36(10): 4075-4080.

Yue, W., J. P. Wang, et al. (2010). "Effects of estrogen on breast cancer development: Role of estrogen receptor independent mechanisms." International journal of cancer 127(8): 1748-1757.

Yvan-Charvet, L., N. Wang, et al. (2010). "Role of HDL, ABCA1, and ABCG1 transporters in cholesterol efflux and immune responses." Arteriosclerosis, thrombosis, and vascular biology 30(2): 139-143.

Zamanian-Daryoush, M. and J. A. DiDonato (2015). "Apolipoprotein AI and Cancer." Frontiers in pharmacology 6: 1-10.

Zamanian-Daryoush, M., D. Lindner, et al. (2013). "The cardioprotective protein apolipoprotein A1 promotes potent anti-tumorigenic effects." Journal of Biological Chemistry 288(29): 21237-21252.

Zhang, J., X. Wang, et al. (2016). "ROS and ROS-mediated cellular signaling." Oxidative medicine and cellular longevity 2016.

Zhang, J. H., T. D. Chung, et al. (1999). "A Simple Statistical Parameter for Use in Evaluation and Validation of High Throughput Screening Assays." J Biomol Screen 4(2): 67-73.

Zhao, B. and Y.-G. Chen (2014). "Regulation of TGF-β signal transduction." Scientifica 2014: 1-9.

Zhao, C. and K. Dahlman-Wright (2010). "Liver X receptor in cholesterol metabolism." Journal of Endocrinology 204(3): 233-240.

Zhuang, L., J. Kim, et al. (2005). "Cholesterol targeting alters lipid raft composition and cell survival in prostate cancer cells and xenografts." The Journal of clinical investigation 115(4): 959-968.

Zhuang, L., J. Lin, et al. (2002). "Cholesterol-rich lipid rafts mediate akt-regulated survival in prostate cancer cells." Cancer research 62(8): 2227-2231.

Zidovetzki, R. and I. Levitan (2007). "Use of cyclodextrins to manipulate plasma membrane cholesterol content: evidence, misconceptions and control strategies." Biochimica et Biophysica Acta (BBA)-Biomembranes 1768(6): 1311-1324.

Zimmer, S., A. Grebe, et al. (2016). "Cyclodextrin promotes atherosclerosis regression via macrophage reprogramming." Science translational medicine 8(333): 333ra350-333ra350.

Ziolkowski, W., M. Szkatula, et al. (2010). "Methyl-beta-cyclodextrin induces mitochondrial cholesterol depletion and alters the mitochondrial structure and bioenergetics." FEBS letters 584(22): 4606-4610.

Zuo, W. and Y.-G. Chen (2009). "Specific activation of mitogen-activated protein kinase by transforming growth factor-β receptors in lipid rafts is required for epithelial cell plasticity." Molecular biology of the cell 20(3): 1020-1029.

1575707:Turnitin.docx

ORIGINALITY REPORT

10%	7%	8%	%
SIMILARITY INDEX	INTERNET SOURCES	PUBLICATIONS	STUDENT PAPERS

PRIMARY SOURCES

1	repository.tudelft.nl Internet Source	1%
2	pdfs.semanticscholar.org Internet Source	1%